



University
of Glasgow

Togneri, Peter (2015) *Characterisation and modification of a series of esterases for cold temperature applications*. PhD thesis.

<http://theses.gla.ac.uk/6242/>

Copyright and moral rights for this thesis are retained by the author

A copy can be downloaded for personal non-commercial research or study, without prior permission or charge

This thesis cannot be reproduced or quoted extensively from without first obtaining permission in writing from the Author

The content must not be changed in any way or sold commercially in any format or medium without the formal permission of the Author

When referring to this work, full bibliographic details including the author, title, awarding institution and date of the thesis must be given

Characterisation and modification of a series of esterases for cold temperature applications

Peter Daniel Togneri

Submitted in fulfilment of the requirements for the Degree of Doctor
of Philosophy (PhD)

Institute of Molecular, Cell and Systems Biology
College of Medical, Veterinary and Life Sciences

University of Glasgow

G12 8QQ

September 2014

Abstract

The purpose of this project was to generate low temperature active esterases for a constituent of laundry detergent, to permit the hydrolysis of fat and oil stains in cold water washing. To determine how well the esterase could work against substrate bound to a surface at low temperatures, it was decided to utilise the esterases as ligands in atomic force microscopy to measure affinity of said esterases against non-emulsified substrates.

Early work involved the identification and characterisation of a novel family of esterases from extremophilic origins as possible ligands for use in the method described. Additional work was performed on testing the theory behind atomic force microscopy by developing ligands from thoroughly understood lipolytic enzymes and measuring any changes in activity. Finally, work was performed on making a psychrophilic variant through mutagenesis from an esterase that had not been previously studied in this project.

Results indicated that there was one candidate from the novel family which showed great activity against long-chain substrates at the desired temperature, but experiments indicated that no member of the novel family were monomers, and were thus deemed unsuitable for use with atomic force spectroscopy.

For this reason, other psychrophilic, monomeric esterase were explored. One such candidate was found, variants were made through directed evolution which were found to have increased activity over the wild-type form.

Results from collaborators working with atomic force microscopy using ligands designed in this project indicated that it was valid as a method for analysing esterase affinity to substrate.

Table of Contents

List of Tables	9
List of Figures	10
Acknowledgements	13
Author's Declaration	14
Definitions/Abbreviations	15
Chapter 1 - Introduction	19
1.1. Industrial use of esterases	20
1.2. Examples of Industrial applications of esterases	20
1.2.1. Biosensor applications	20
1.2.2. Chiral specific-applications	21
1.2.3. Pollutant reducing applications	21
1.2.4. Food industry applications	22
1.2.5. Use of lipases and esterases in detergents	22
1.3. Background to esterases and lipases	24
1.4. The active site of lipolytic enzymes	26
1.5. Residue conservation in lipolytic enzymes	30
1.6. Classification system of lipolytic enzymes	30
1.6.1. Family I	31
1.6.2. Remaining lipolytic families	32
1.7. Differences between lipases and esterases	34
1.7.1. Features of Lipases	35
1.7.2. Features of Esterases	37
1.8. Uses of extremophilic esterases in industry	37
1.8.1. Differences and similarities between mesophilic and extremophilic esterases	38
1.9. Aims of this project	40
Chapter 2 - Materials and Methods	42
2.1. General use Media and Buffers	43
2.1.1. Growth media methodologies	43
2.1.1.1. Luria-Bertani media	43
2.1.1.2. NZY+ Broth	43
2.1.2. PAGE buffer methodologies	43
2.1.2.1. SDS-PAGE	43
2.1.2.2. Native PAGE	44

2.1.3. Other buffer methodologies	45
2.1.3.1. Universal Buffer	45
2.1.3.2. TAE gel	46
2.2. Kits used	46
2.3. Primers used	46
2.4. Bacterial strains used	48
2.5. Plasmids used	48
2.5.1. pENTR-d-TOPO	48
2.5.2. pDest17	48
2.5.3. pEXP5-CT/TOPO	49
2.5.4. pET-28a(+)	49
2.5.5. pET-30a(+)	49
2.5.6. pMAL-c2x	49
2.5.7. pQE30	49
2.6. Protocols used	50
2.6.1. Cell-specific protocols	50
2.6.1.1. Transformation protocols	50
2.6.1.1.1. BL21-AI transformation protocol	50
2.6.1.1.2. TOP10 transformation protocol	50
2.6.1.2. Expression protocols	51
2.6.1.2.1. Small-scale expression of esterases	51
2.6.1.2.2. BL21-AI expression	51
2.6.2. Protein-specific protocols	51
2.6.2.1. SDS-PAGE/non-denaturing gel technique	51
2.6.2.2. Purifying esterases through poly-His tag/Nickel immobilised metal ion affinity chromatography	52
2.6.2.3. Bradford Assay	53
2.6.5. DNA specific protocols	54
2.6.5.1. Vector isolation	54
2.6.5.2. DNA endonuclease cutting	54
2.6.5.3. DNA ligation	54
2.6.5.4. Gateway System recombination	55
2.6.5.5. PCR primer design	55
2.6.5.6. DNA Sequencing	56
2.6.5.7. PCR protocols used	56

2.6.5.7.1. Phusion High-Fidelity DNA PCR	56
2.6.5.7.2. GoTaq DNA PCR for DNA for insertion into TOPO vectors	56
2.6.5.7.3. Site-directed mutagenesis PCR	57
2.6.5.8. PCR purification protocol	57
2.6.5.9. TAE gel running procedure	58
2.6.5.10. Gel purification protocol	58
2.6.6. On-line software for predicting surface residues	58
2.6.6.1. Weighted Ensemble Solvent Accessibility	58
2.6.6.2. ASA-view	59
2.6.6.3. polyview	59
2.6.6.4. NetSurfP	59
2.7. Companies which supplied chemicals	60
Chapter 3 - Identification and characterisation of a novel family of esterases containing an OsmC domain	61
3.1. Introduction	62
3.1.1. Project aims and background	62
3.1.2. The identification of members of a novel esterase family	63
3.2. Materials and Methods	67
3.2.1. Auto-inducing media	67
3.2.2. Origins and growth temperatures of novel esterases	68
3.2.3. Assay for determining esterase activity	69
3.2.4. Determining esterase purification factor	70
3.3. Results	71
3.3.1. Purification of the esterases in this project	71
3.3.2. Purification of EstLA from expression in BL21-AI	71
3.3.3. Purification of Truncated Δ esterases	73
3.3.4. Dialysis conditions for esterases in this project	74
3.3.5. Characterisation of the Δ esterases under a range of conditions	75
3.3.5.1. Characterisation of the temperature profiles of the Δ esterases	75
3.3.5.2. Characterisation of the pH profiles of the Δ esterases	77
3.3.5.3. Characterisation of Δ esterases activities with a range of substrates of varying fatty acid chain length	79
3.3.5.4. Investigation into effects of metal ion on activity of	82

Δ esterases	
3.3.5.5. Investigation into effects of putative inhibitors on activity of Δ esterases	85
3.3.6. Multimeric state of Δ esterases	88
3.4. Discussion	89
3.4.1. Discovery of a new family of esterases	89
3.4.2. Comparison of Δ EstO with published EstO and Δ EstO activities	90
3.4.3. Comparing activities of all investigated Δ esterases	92
3.4.3.1. Comparison of all Δ esterases activities across temperature range	92
3.4.3.2. Comparison of all Δ esterases activities across pH range	94
3.4.3.3. Comparison of all Δ esterases activities against selection of substrates	95
3.4.3.4. The effect of metal ions against all Δ esterases activities	96
3.4.3.5. Comparison of effect of inhibitors on all Δ esterases activities	98
3.4.5. Comparing characterisation results to esterases used in laundry detergents	101
Chapter 4 - Assay for screening esterase affinity to fat and oil stains	103
4.1. Introduction	104
4.1.1. AFM as an assay	104
4.1.2. Attachment of the esterase to the AFM tip	108
4.2. Materials and Methods	111
4.2.1. Synthetic gene design and synthesis	110
4.2.2. PEGylation of proteins	110
4.3. Results	112
4.3.1. Esterase PA3859	112
4.3.2. PEGylation of C14S/M37C PA3859	113
4.3.3. Lipase CalB	118
4.3.4. Designing PEGylation site of CalB	120
4.3.5. Further modification of E269C CalB	124
4.4. AFM measurements obtained from collaborators	126
4.5. Discussion	129
4.5.1. Review of the choice of ligands	129
4.5.2. PEGylation for enzyme tethering	130

4.5.3. AFM substrate choice	133
4.5.4. Comparing PEGylation rates and procedures in this project to published results	134
Chapter 5 - Directed evolution of an esterase for increased activity at lower temperatures	135
5.1. Introduction	136
5.1.1. Directed evolution	136
5.1.2. Mutant library screening	139
5.1.3. Screens for esterase activity	140
5.2. Materials and Methods	141
5.2.1. Media for detecting esterase activity	141
5.2.1.1. Tributyrin agar	141
5.2.1.2. Novel soft agar overlay	141
5.2.1.3. Rhodamine B lipolytic detection agar	141
5.2.1.4. Bromocresol purple and ester substrate Tris agar	142
5.2.1.5. Fast Blue and naphthyl substrate agar	142
5.2.1.6. Tween 20 agar	142
5.2.1.7. Minimal media agar	143
5.2.2. <i>E. coli</i> M15 cell line maintenance, transformation and expression protocols	143
5.2.2.1. Production of competent <i>E. coli</i> M15 protocol	143
5.2.2.2. <i>E. coli</i> M15 transformation protocol	144
5.2.2.3. <i>E. coli</i> M15 expression	144
5.2.3. Assay methodology	145
5.2.3.1. Esterase assay Est97 variation	145
5.2.3.2. Molar extinction coefficient (ϵ) nitrophenol determination	145
5.2.4. Mutagenic PCR protocols	146
5.2.4.1. Directed Mutagenesis PCR	146
5.2.4.2. Random Mutagenic PCR	146
5.2.4.2.1. Rolling mutagenesis PCR	146
5.2.4.2.2. Mu Transposon mutagenesis	146
5.2.4.2.3. GeneMorph II EZClone Domain Mutagenesis	147
5.2.4.2.4. Low GTP nucleotide mutagenesis.	147
5.2.4.2.5. $MnCl_2$ mutagenesis.	147
5.3. Results	148

5.3.1. Analysis of a psychrophilic monomeric esterase	148
5.3.2. Purification of Est97	148
5.3.2.1. Alterations to established method for expression and purification	148
5.3.3. Measuring Est97 activity	150
5.3.4. Directed evolution and its application in this project	152
5.3.4.1. Screening techniques employed in this project	152
5.3.4.2. Mutagenic techniques employed in this project	153
5.3.4.3. Creation of mutant esterase libraries	154
5.3.5. Preliminary assay development for observation of tributyrin hydrolysis via colour change through bromocresol purple indicator dye	157
5.3.6. Novel esterase assay development	158
5.3.7. Screen of mutant library of Est97	161
5.3.7.1. Mutants of Est97 isolated and assayed	162
5.4. PEGylation of Est97	165
5.5. Discussion	170
5.5.1. Methodology employed in this project for obtaining and assaying Est97	170
5.5.2. Reviewing the generation of the mutagenic library	170
5.5.3. Reviewing the screening of the mutant library	171
5.5.4. Reasoning for the mutagenesis and alteration in residues in this project	174
Chapter 6 - Discussion	178
6.1. Introduction	179
6.2. Summarising the OsmC characterisation	179
6.3. Summarising PEGylating esterases for use in TREC	180
6.4. Summarising the development of an esterase for use in AFM	181
6.5. Were preliminary goals of project reached?	182
6.6. Future direction of work from this project	183
Appendix	186
DNA sequences	186
Amino acid sequences	195

List of Tables

2.1. Primers used in this project	47
2.2. Bacterial strains used in this project	48
3.1. Comparison of enzyme kinetics of EstLA and Δ EstLA against nitrophenyl substrates	65
3.2. Organisms OsmC esterase originate from,	68
3.3. Conditions required for OsmC immobilised metal ion affinity chromatography and dialysis	74
3.4. The chemical structure of substrates used in esterase characterisation	81
3.5. The actions of inhibition of chemicals chosen	85
4.1. Binding probability of CalB+MBP ligand against immobilised 2-acetoxypropionic acid	129
5.1. In vivo assays attempted in this project	156
5.2. Enzyme kinetics of wild-type and mutant variants of Est97 found through screen	165
5.3. Comparison kinetics of Est97 and PEGylated Est97 variants generated in this project	168

List of Figures

1.1. The canonical structure of the α/β hydrolase fold	26
1.2. Example of the nucleophilic elbow structure	28
1.3. Hydrolysis of the ester bond by an esterase	29
1.4. An example of how a lipase lid allows access to the active site	36
1.5. How mesophilic and extremophilic esterases do not differ in structure	39
3.1. Alignment of amino acid sequences of esterases identified through BLAST search	66
3.2. Hydrolysis of a nitrophenyl ester into nitrophenol and acid products	69
3.3. Structures of vectors used to express esterases	71
3.4. Expression and purification of soluble EstLA	72
3.5. Expression and purification of soluble Δ esterase	73
3.6. Effect of temperature on activity of Δ esterase	76
3.7. Effect of pH on activity of Δ esterase	78
3.8. Substrate specificity of Δ esterase	80
3.9. Effect of metal ions on activity of Δ esterase	84
3.10. Effect of putative esterase inhibitors on activity of Δ esterase	87
3.11. Native and semi-reductive gels demonstrating the multimeric states of OsmC esterases	89
3.12. Comparison of Δ esterase activity across a range of temperatures	94
3.13. Comparison of Δ esterase activity across a range of pH	95
3.14. Comparison of Δ esterase activity across a range of substrates	96
3.15. Comparison of Δ esterase activity in the presence of a selection of metal salts	97
3.16. Comparison of Δ esterase activity in the presence	99

of a selection of inhibitors	
4.1. Illustrating force curves in AFM.	106
4.2. Basic methodology behind TREC imagery using AFM	107
4.3. Chemical structures of substrates chosen for TREC theory	108
4.4. PEG and PEG maleimide	110
4.5. Expression and purification of soluble C14S/M37C PA3859	114
4.6. PEGylation of C14S/M37C PA3859	115
4.7. Methods of reduction of disulphide bridges.	116
4.8. The effect of reduction of TCEP on PEGylation of C14S/M37C PA3859	117
4.9. Assay of C14S/M37C/S113A PA3859 against C14S/M37C PA3859	118
4.10. Expression trial of CalB+MBP pMAL-c2x vector in BL21-AI expression	120
4.11. Expression and purification of soluble E269C CalB+MBP	121
4.12. SDS-PAGE analysis showing TCEP gradient against Factor Xa-treated E269C CalB	122
4.13. SDS-PAGE analysis showing effect of TCEP on PEGylation and reduction controls of E269C CalB	123
4.14. SDS-PAGE analysis showing PEGylation of E269C CalB untreated with Factor Xa	125
4.15. Effect of PEGylation and pre-PEGylating conditions on E269C CalB+MBP activity	126
4.16. Force vs. distance graph generated with E269C CalB+MBP as a ligand in QNM AFM	128
4.17. PEG molecule with mono-sulphone functional site binding to His-tag	131
5.1. A diagram illustrating the four stages of any random mutagenesis technique	137
5.2. Expression and purification of soluble Est97	149
5.3. Native gel run of Est97	150
5.4. Activity of Est97 across temperature range	152
5.5. Re-suspending induced expression vector in indicator buffer	158
5.6. Plates illustrating novel esterase assay	159
5.7. Inconsistencies with <i>in vivo</i> detection of esterase	160

activity of BL21-AI expressing C14S/M37C PA3859	
5.8. Comparing tributyrin plate assay with Tris-overlay assay	161
5.9. Comparison of the halos generated by G53A/T231I Est97 and WT Est97 on a tributyrin agar plate at 15 °C	162
5.10. Tributyrin agar used to probe <i>E. coli</i> M15 Est97/pQE30 variants	163
5.11. Expression and purification of soluble G53A/T231I Est97, G53A Est97 and T231I Est97	163
5.12. Lineweaver-Burke graphs comparing Est97 to G53A, T231I and G53A/T231I variants of Est97	164
5.13. Lineweaver-Burke graphs comparing Est97 to E40C Est97 without any modification, with pre-incubation with DMSO and when PEGylated	167
5.14. Expression and purification of soluble E40C Est97	168
5.15. The effect of a TCEP gradient on PEGylation of E40C Est97	169

Acknowledgements

There are a great number of people deserving of thanks with respect to this thesis. First and foremost; Susan Rosser for her insight, professionalism and all-round good-humour in the face of my panic as my supervisor.

Louise Horsfall, Mai Britt-Jensen, Christine Merrick, David Houston, Jill Nimmo, Femi Olorunniji, Sean Colloms, Hugh Nimmo and Liz O'Donnell for all their help in the lab with all things temporal and spiritual.

Darren Monckton and Stephen Yarwood who helped me keep calm and put my worries into perspective as additional supervisors.

Claire Osborne for all the time taken up by me wanting to double-check when forms and essays had to be handed in - her administrative skills were second-to-none.

P & G and EPSRC for providing the funding for this project.

Finally those on the non-professional level; my family, Martin Togneri, Kathleen Togneri, Michael Togneri, Hannah Togneri and wee Ada Togneri - for all the support they have given me. And Janna Östrom-Berg, who taught me more about life and myself than I could have ever anticipated.

Thank you one and all.

Author's Declaration

I hereby declare that the research presented within this thesis is my own work unless otherwise stated, and has not been submitted elsewhere for any other academic degree.

Definitions/Abbreviations

AFM = atomic force microscopy

APS = ammonium persulfate

APTES = aminopropyltriethoxysilane

BLAST = basic local alignment search tool

C. acidiphila = *Catenulispora acidiphila*

C_x (when x = a number) = linear chain of x carbon atoms

Ca²⁺ = Calcium ion

CaCl = Calcium (I) chloride

CaCl₂ = Calcium chloride

CaCl₂.2H₂O = Calcium chloride dihydrate

CalB = *Candida Antarctica* lipase B

CASP = critical assessment of protein structure prediction

CEL = human pancreatic carboxyl ester lipase

Co²⁺ = Cobalt ion

CoCl₂.(6H₂O) = Cobalt(II) chloride hexahydrate

CuSO₄.7H₂O = Copper sulphate heptahydrate

DMF = Dimethylformamide

DMSO = dimethyl sulphoxide

DSSP = define secondary structure of proteins

DNA = deoxyribonucleic acid

DSM/Z = Deutsche Sammlung von Mikroorganismen/ und Zellkulturen

DTT = Dithiothreitol

E. coli = *Escherichia coli*

E. meliloti = *Ensifer meliloti*

EDTA = ethylenediaminetetraacetic acid

EMS = ethylmethane sulphate

Fe²⁺ = Iron ion

FeCl₃.(6H₂O) = Iron(III) chloride hexahydrate

FeSO₄.7H₂O = Iron (II) sulphate heptahydrate

H₂O = Water

H₃BO₃ = Boric acid

HCl = hydrochloric acid

IMAC = immobilised metal ion affinity chromatography

IPTG = Isopropyl β-D-1-thiogalactopyranoside

K^+ = Potassium ion

kb = kilobase

k_{cat} = turnover number

KCl = potassium chloride

kDa = kiloDaltons

KH_2PO_4 = Monopotassium phosphate

K_m = concentration of substrate that leads to half-maximal velocity in enzyme activity

L = litre

L. aggregata = *Labrenzia aggregata*

LB = Luria-Bertani

Lif = Lipase-specific foldase

M = moles

MBP = maltose binding protein

Min = minute

mg = milligram

$MgSO_4$ = Magnesium sulfate

Mg^{2+} = Magnesium ion

ml = millilitre

mm (prefix) = maleimide

mM = millimole

mMol = millimolar

MNNG = N-methyl-N'-nitro-N-nitrosoguanidine

$MnCl_2 \cdot 6H_2O$ = Manganese(II) Chloride Hexahydrate

$MnSO_4 \cdot 4H_2O$ = Manganese(II) Sulphate Tetrahydrate

Mol = molar

MWCO = molecular weight cut-off

$Na_2B_4O_7 \cdot 10H_2O$ = Sodium borate decahydrate AKA Borax

Na_2EDTA = Disodium ethylenediaminetetraacetic acid

Na_2HPO_4 = Disodium hydrogen phosphate

Na_2SO_4 = Sodium sulphate

NADH = Nicotinamide adenine dinucleotide

NaH_2PO_4 = Monosodium phosphate

NaCl = sodium chloride

NaOH = sodium hydroxide

NEB = New England Biolabs
NH₄Cl = Ammonium chloride
(NH₄)₆MO₇O₂₄·4H₂O = Ammonium molybdate tetrahydrate
NiCl = nickel chloride
Ni²⁺ = Nickel ion
NHS = N-hydroxysuccinimide
nm = nanometres
NN-DMF = see DMF
np (prefix) = nitrophenyl
OD_{410/405/600} = optical density at 410/405/600nm
Ohr = organic hydroperoxide resistance
p- (suffix) = *para*
P. arctica = *Pseudoalteromonas arctica*
pARG = poly (ADP-ribose) glycohydrolase
PCR = polymerase chain reaction
PDB = protein database
PEG = polyethylene glycol
ppp = prepropeptide
QNM = quantitative nanomechanical property mapping
R. denitrificans = *Roseobacter denitrificans*
R. marinus = *Rhodothermus marinus*
RNA = ribonucleic acid
rpm = rotations per minute
RP-HPLC = Reversed phase high-performance liquid chromatography
sec = second
SDS-PAGE = sodium dodecyl sulphate polyacrylamide gel electrophoresis
SPM = scanning probe microscopy
TAE = Tris Acetate EDTA
TCEP.HCl = Tris(2-carboxyethyl)phosphine hydrochloride
TEA = Togneri esterase assay
TEMED = Tetramethylethylenediamine
TLL = *Thermomyces lanuginose* lipase
Tm = melting temperature
TREC = topography and recognition imaging
UV = ultraviolet

V_{\max} = maximum initial velocity of the enzyme catalysed reaction

v/v = volume-to-volume ratio

w/v = weight-to-volume ratio

Zn^{2+} = Zinc ion

$ZnCl_2$ = Zinc chloride

$ZnSO_4 \cdot 7H_2O$ = Zinc Sulphate Heptahydrate

$^{\circ}C$ = degrees centigrade

μg = micrograms

μl = microlitres

μM = micromoles

μMol = micromolar

Chapter 1

Introduction

1.1. Industrial use of esterases

Esterases and lipases are enzymes that are capable of hydrolysing ester bonds. The hydrolysis of ester bonds is a process utilised in many industries. The use of these enzymes in hydrolysis allows industrial reactions to occur using less energy, or more efficiently than is possible utilising alternative methods. Another feature of esterases and lipases which increases their usefulness in industrial settings is that under certain environmental conditions, they can perform dehydration synthesis, forming ester bonds instead of breaking them down (Dordick, J. S., 1989). For example, lipase R from *Penicillium roqueforti* which is normally used in the food industry for maturing Roquefort cheese (a process which requires hydrolysis), is necessary in its purified form in the manufacture of optically-pure herbicidal indanofan (Tanaka K *et al.*, 2002), a process requiring dehydration synthesis. This dual capability of these enzymes means that they are highly valued in many parts of industry beyond their uses in the making of laundry detergents which has been the main focus of this project.

1.2. Examples of Industrial applications of esterases

1.2.1. Biosensor applications

Lipase and esterase activity can be used either directly or indirectly to detect the presence of specific chemicals. For example, erythrocyte cholinesterases have been used as an indicator of exposure to nerve agents and other chemical weapons which inhibit their activity (Lefkowitz L. J, *et al.*, 2007), acetylcholinesterases being utilised to detect insecticides (Schulze H *et al.*, 2002), the exact number of individual plant cells in a culture being determined by the hydrolysis of fluorescein diacetate ester through the cells inherent esterases (Vitecek, J *et al.*, 2007). Amperometric biosensors based on esterases can be used to estimate cholesterol concentration in a patient's blood, which is an important factor in the diagnosis of heart diseases (Singh, S, *et al.*, 2004).

Some enzymes have been used to improve or modify existing probes and general sensors, e.g. labelling nucleotide probes with a lipase instead of unstable or hazardous isotopes (Kynclova E, *et al.*, 1995), using enzymes in conjunction with an ion-selective field effect transistor to detection low concentrations of triglycerides in solution (Vijayalakshmi A *et al.*, 2008), etc.

Native production and activity of lipases and esterases can be used as diagnostic tools for medical purposes - e.g. acute pancreatitis is accompanied by an increase in the level of serum lipase, peaking at approximately 24 hours after the onset of clinical symptoms, and is more sensitive and specific than the traditional amylase measurement (Munoz, A and Katerndahl D A, 2000). A further example is provided by lipoprotein-associated phospholipase A2 (Lp-PLA2), a native human enzyme found in the bloodstream bound to LDL cholesterol. In ischemic stroke victims the activity of Lp-PLA2 is greater than in members of a healthy control group; detection of this increase in activity can be used as a predictor for coronary heart disease (Oei H H, et al., 2005).

1.2.2. Chiral specific-applications

Certain esterases are sought after for the manufacture of desired product chirality or the degradation of one type of substrate chirality. Esterases can produce optically pure chemical compounds for use in synthesising anti-inflammatories and other drugs, e.g. hydrolysing *rac*-ketoprofen ethyl ester into the nonsteroidal anti-inflammatory drug (*S*)-ketoprofen (Kim G J, et al., 2002, Shen D, et al., 2002) or producing (*S*)-IPG, a precursor of β -blockers, prostaglandins, and leukotrienes (Godinho L F, et al., 2011). Esterases can also target specific chiralities of substrates for similar purposes, e.g. designing an esterase that breaks down (*S*)-ketoprofen ethyl ester only (Choi G-S *et al.*, 2003). The same principle is true for lipases as well, e.g. resolving chiral aryltrimethylsilyl alcohols and racemic 4-nitrophenyl 2-phenylpropionate (Palmeira DJ, et al., 2011, Jung H C *et al.*, 2006). The demand for such esterases and optically pure products is high, especially in the drug industries (Matsumae H, et al., 1993).

1.2.3. Pollutant reducing applications

Lipases and esterases can reduce pollution in some industrial processes. For example, *Aspergillus niger* feruloyl esterase is used as an alternative to chemical degradation of lignin in pulp, thus removing the requirement for environmentally dangerous chemicals in paper bleaching, e.g. hydrogen peroxide, sodium hydroxide and sulphuric acid salts (Record, E, et al., 2003). Lipases and esterases can also be used to break down pollutants such as fats generated from making leather products (Muthukumaran N and Dhar S C, 1982).

Lipases and esterases can be used for direct bioremediation in polluted environments, e.g. cholesterol esterases breaking down polyurethanes present in thermoset polymers (Jahangir, R *et al.*, 2003), prokaryotic isoesterase breaking down dimethylphthalate, a pollutant by-product of paper and plastic industries, in water bodies (Niazi, J H, *et al.*, 2001) and the use of purified lipase or the organisms from which they originate to treat lipid-rich wastewater (Dharmsthiti S and Kuhasuntisuk B, 1998, Cammarota M C *et al.*, 2013).

1.2.4. Food industry applications

Esterases and lipases are commonly used in making cheese and other soured milk derivatives, most importantly in improving their tastes, aromas and textures (Athawale V *et al.*, 2001, Choi Y J and Lee B H, 2001, Dherbécourt J *et al.*, 2010, Martínez-Cuesta M C, *et al.*, 2001, Kilcawley, K N *et al.*, 1998, Barron LJ *et al.*, 2004, Aydemir S *et al.*, 2007, Yilmaz G *et al.*, 2005, Güler, Z, 2007), but they have other applications in the food industry as well. The release of cinnamic acids, used in food flavourings, from raw materials, e.g. cereals, sugar beets, bamboos. etc., is promoted by the use of *Aspergillus niger* (*A. niger*) feruloyl or cinnamoyl esterases (Asther M, *et al.*, 2002). Cinnamic acid can also be treated using esterase activity to produce further food flavourings and additives, e.g. being dehydrated with methanol to form methyl cinnamate to provide a strawberry aroma (Guglielmetti, S, *et al.*, 2007). Methyl cinnamate can also be used to increase the free radical scavenging of flaxseed oil (Choo, W. S, *et al.*, 2009).

Esterases are also widely used in the spirits, wine and beer industries (Uno, T *et al.*, 2012). Furthermore, both lipases and esterases are essential in the manufacture of teas (Wright A J and Fishwick M J, 1978, Thomas R L and Murtagh K, 2006).

1.2.5. Use of lipases and esterases in laundry detergents

Washing clothes is a necessity for basic human hygiene and disease-prevention; but it is also more labour and resource-intensive than necessary if it is undertaken using laundry detergents working under sub-optimal conditions. This project deals with the removal of fat and oil stains from clothing at low temperatures by degrading triglyceride components of said stains so as to lower

the man-hours required to clean clothes in non-warmed water. There are two major reasons why this is desirable.

Firstly, for people living in poverty, especially in countries where universal affordable electric power is unavailable, the only water available for cleaning clothes is often in natural water bodies at ambient temperature. In such circumstances, even when washing water can be put into suitable washing vessels, the water can only be heated to a level that can be tolerated by human hands. Examples include the Dhobi Ghat washers in India who use the Pavana river, the residents of San Carlos in Ecuador who use the Basura, Iniap, Huamayalu or Parker rivers, the people of Matlab in Bangladesh using tube-well water, (Imandoust S B and Gadam S N, 2007, San Sebastián M, et al., 2001, Sack R B, et al., 2003). Under such conditions, any laundry detergents used to help clean clothes are often used at sub-optimal temperatures for degrading fats and oil stains; that is to say, triglycerides used in cooking. Esterases and lipases only break down fats with the highest levels of efficiency when used at the correct temperature. Therefore more human labour is required to clean the clothing successfully than would be needed at optimal temperature. A laundry detergent capable of breaking down fat and oil stains at a low temperature would help reduce the time and the effort required, which would free human labour for more productive uses, helping improve the living standards of the people involved, who are primarily women and young children (Simister J, 2012). It must be pointed out that neither esterases or lipases on their own would be capable of cleaning the stain; fatty acids (either present naturally in the actual fat itself or resulting from the hydrolysis of the fat) are insoluble in water; laundry detergents require amphiphilic components to remove them entirely.

Secondly, even for people who have ready access to modern washing machines and heated water for cleaning clothes, such options consume considerable amounts of energy and are expensive. It has been calculated that heating the required water accounts for 80-85% of the energy consumption of top-loading washing machines and that washing clothes with a washing machine accounts to 36% of American household hot water use (Petkewich, R., 2005), which produces 34 million tonnes of carbon dioxide per annum to heat (Nidumolu, R, et al., 2009). Automated machines which work at lower temperatures, such as Japanese impeller washing machines, typically use 1/10th the amount of energy as is required by hot-wash, drum-type washing machines

(Pakula C and Stamminger R, 2010), but consume up to twice as much water to clean equivalent loads, resulting in environmental concerns over excessive water consumption (Lin J and Iyer M, 2007).

If one could develop a laundry detergent capable of breaking down fats and oils at an optimal temperature of 20°C, heating water would no longer be a requirement and low temperature automated washing would not require as much water. Because both of these problems would be dealt with simultaneously, the cost of washing clothes, the carbon footprint and the amount of water used by automated methods would be reduced.

The research undertaken in this project aims to lay the groundwork for developing a biological laundry detergent constituent that is capable of cleaning fats and oils at low temperatures, for the dual purposes of reducing third-world labour requirements for the hand cleaning of clothes and more generally for reducing the energy required to clean clothes. With this in mind, a detailed analysis of what esterases actually are is needed so as to justify which enzymes were used in the project and why.

1.3. Background to esterases and lipases

Lipolytic enzymes consist of lipases and esterases - enzymes with an active site consisting of a triad of serine, histidine and aspartic/glutamic acid residues (except family VIII, see under section 1.6.1.) which act as a 'charge relay system' in conjunction with an immediate oxyanion environment to render the serine a powerful nucleophile (Blow D M *et al.*, 1969) specifically for degrading ester bonds.

This triad can be positioned in two different ways; either it is found towards the centre of the protein (lipolytic enzymes of this form are said to belong in the GX SXG family - so called due to the active site serine being present in a highly conserved pentapeptide), or an active serine residue with glycine, aspartic acid, serine and leucine residues in close proximity, closer to the N-terminal of the protein (enzymes containing this identifying feature belong to the GD SL/SGNH family) (Upton C and Buckley J T, 1995), (see Table 1.1 for a list of examples of GD SL and GX SXG enzymes). These active sites cannot be altered without severely affecting activity of the enzyme against its substrates.

Species of origin	Type	Name/function	Accession no.
<i>Aeromonas hydrophila</i>	GDSL	GCAT/Lipase and acetyltransferase	P10480
<i>Vibrio mimicus</i>	GDSL	<i>V. mimicus</i> esterase/Arylesterase	Q07792
<i>Streptomyces rimosus</i>	GDSL	Srimo/Lipase	Q93MW7
<i>Neocallimastix patricarium</i>	GDSL	BnaA-C/Aceylxylan esterase	U66251-66253
<i>Streptomyces scabies</i>	GDSL	SsEst/Suberin esterase	1ESC
<i>Escherichia coli</i>	GDSL	TAP/thioesterase	P77125
<i>Pseudomonas aeruginosa</i>	GXSXG	lipA/Lipid degradation	D50587/P95419
<i>Pseudomonas fragi</i>	GXSXG	Triacylglycerol lipase/Lipid degradation	X14033/P08658
<i>Moraxella sp.</i>	GXSXG	Lipase 1/Lipid degradation	X53053/P19833
<i>Psychobacter immobilis</i>	GXSXG	Lipase 1/Lipid degradation	X67712/Q02104
<i>Arthrobacter oxydans</i>	GXSXG	pcd/Phenylcarbamate hydrolase	Q01470
<i>Streptomyces chrysomallus</i>	GXSXG	estA/Cell-bound esterase	AAA994/O87861

Table 1.1. Examples of GDSL/SGNH and GXSXG lipolytic enzymes

(Robertson D L *et al.*, 1994, Shaw J F *et al.*, 1994, Dalrymple BP *et al.*, 1997, Arpigny J L and Jaeger K E, 1999, Vujaklija D *et al.*, 2002, Akoh C C *et al.*, 2004)

The GXSXG pentapeptide is not found solely in lipolytic enzymes; it has also been found with exfoliative toxin B and others (Vath G M, *et al.*, 1999). Also, there are some esterase variants which do not follow either expected common lipolytic active sites, e.g. *Streptomyces scabies* (*S. scabies*) esterase active site consisting of an active dyad of serine and histidine, where the imidazole group of the histidine is hydrogen-bound to a tryptophan residue instead of carboxylic acid (Wei Y *et al.*, 1995) and *Erwinia chrysanthemi* (*E. chrysanthemi*) pectin methylesterase's catalytic triad consisting of two aspartate and a single arginine residue (Jenkins J *et al.*, 2001). So, while active sites

associated with GXSXG and GDLSL conserved regions are common in lipolytic enzymes, not all lipolytic enzymes belong to these families.

1.4. The active site of lipolytic enzymes

The active site of GXSXG esterases/lipases is topologically preserved by a distinct protein fold called the α/β hydrolase fold, where at least eight β -sheets are connected (primarily parallel to each other) through alpha helices to form a sheet structure (see Figure 1.1.).

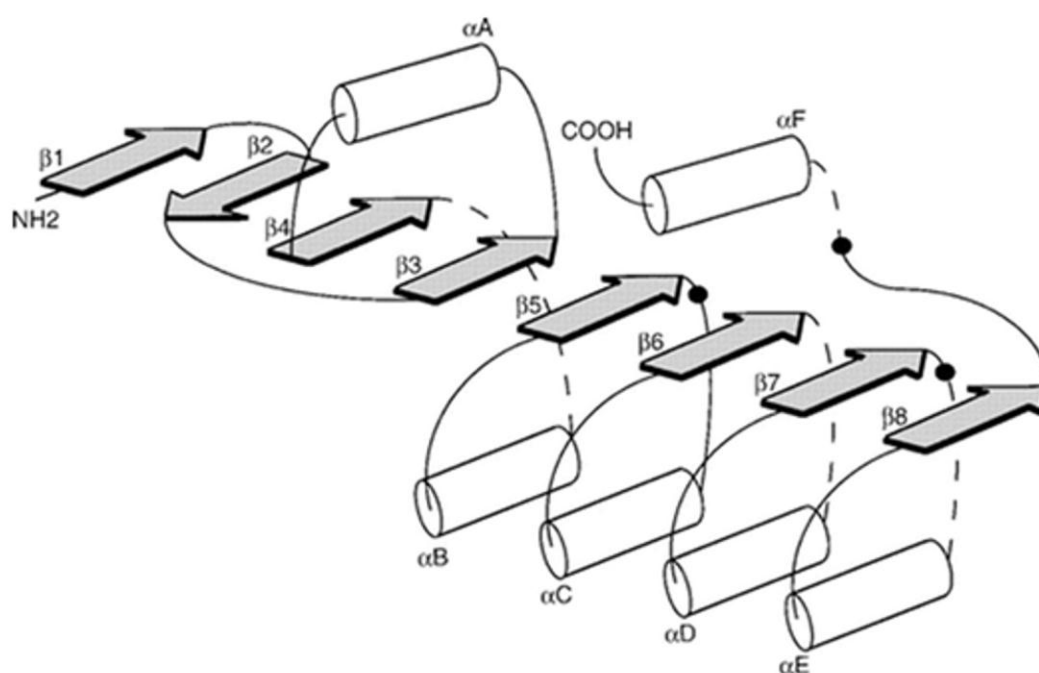


Figure 1.1. The canonical structure of the α/β hydrolase fold.

α -helices are represented by white cylinders and β -sheets by shaded arrows indicating order of protein. Solid circles in the structure indicate the position of the triad of active-site residues - the nucleophile being immediately after β -sheet 5, while the aspartic/glutamic acid and histidine residues are after β -sheet 7 and β -sheet 8 respectively (Ollis D L *et al.*, 1992, Jaeger K E *et al.*, 1999)

This structure is found in a variety of other hydrolytic but non-lipolytic enzymes so it, like a GXSXG motif and a catalytic triad, is not an instant indicator of a lipolytic enzyme (Jaeger K E *et al.*, 1999).

In the immediate vicinity of the serine residue, there is an oxyanion hole, providing an electrophilic environment for the hydrolytic activity (Mandrigh L, *et al.*, 2008). The active site residues are positioned in a highly conserved structure termed a nucleophilic elbow loop at whose apex the nucleophilic residue

involved in catalysis (see Fig 1.2.) resides. This structure is not unique to lipases/esterases, but is found in other enzymes as well, e.g. carboxylpeptidase, dehalogenase and dienelacetone hydrolase, indicating a common evolutionary ancestry (Ollis D L, et al., 1992).

The oxyanion hole has two residues that donate backbone amide protons to stabilise the transition state of the substrate in the enzyme. The other residue is not located within the conserved sequence, but is instead found in a loop in the central β -strand 3.

There are two main types of oxyanion hole, *GX* and *GGGX*, which differ from each other in the manner in which the nucleophilic elbow of the lipolytic enzyme is formed. The *GX* type has the oxyanion X residue at the elbow flanked by a conserved, neighbouring N-terminal glycine. The *GGGX* type has the oxyanionic residue flanked by a conserved, hydrophobic, C-terminal X residue and on the N-terminal side by two glycine residues. In most cases, the X residue is phenylalanine, leucine, or tyrosine, and has a role in stabilising the oxyanionic hole. In lipases, activation of the enzyme either has the *GG* dipeptide stabilising the oxyanion hole through hydrogen bonding or orientating away from the substrate.

There is also a Y variant, where the oxyanion hole is formed through the hydroxyl group on a tyrosine residue (Fischer M *et al.*, 2006).

Although *GX* and *GGGX* oxyanion holes differ in structure, the position of the hydrogen atom used to stabilise the transition state is similar, so its function is conserved in both variants.

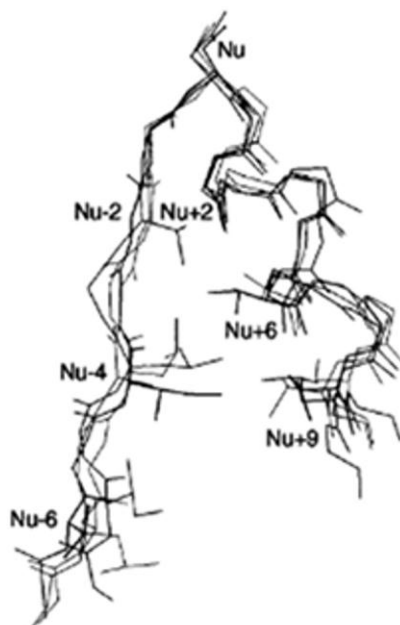


Figure 1.2. Example of the nucleophilic elbow structure

Superimposition of the nucleophilic elbow structures from four examples of the α/β hydrolase fold enzymes - *Geotrichum candidum* (*G. candidum*) lipase, dienelactone hydrolase, haloalkane dehalogenase and cutinase. Side-chains involved in the formation of the elbow are numbered in relation to the nucleophilic catalytic residue, Nu (Schrag J D and Cygler M, 1997).

The type of oxyanion hole influences the enzyme's substrate specificity. GX variants favour medium- to long-chain substrates, while GGGX variants are found in lipolytic enzymes which are inclined to hydrolyse shorter-chain substrates (Pleiss J *et al.*, 2000).

It is important to note that this nucleophilic elbow is not found in GDSL lipolytic enzymes. In these variants the catalytic serine acts as a proton donor with conserved glycine and asparagine and there is no hydrogen bond formed between the substrate-catalyst intermediate and the catalytic histidine (Akoh C *et al.*, 2004).

The order of the residues making up the catalytic triad going N to C is always nucleophile, acid and histidine, so the acid and histidine are not actually present in the nucleophilic elbow. These other two residues interact with the nucleophile residue through a hydrogen bond to each other, connecting the B7 and B8 sheets of the hydrolase fold (Schrag J D and Cygler M, 1997).

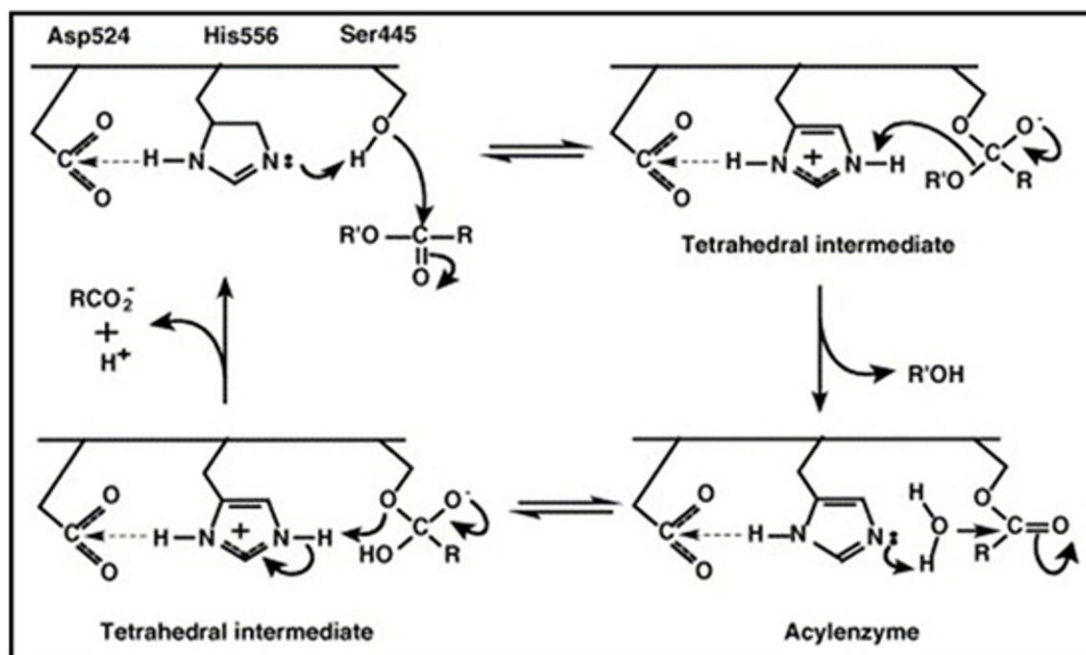


Figure 1.3. Hydrolysis of the ester bond by an esterase

An illustration of the mechanism of nucleophilic attack coupled with hydrolysis in ester bond degradation, specifically of *Aeropyrum pernix* (*A. pernix*) K1 esterase (Zhang G *et al.*, 2006).

At the GXSXG active site, the serine residue initiates a nucleophilic attack on the ester bond of the substrate which the enzyme catalyses. A tetrahedral intermediate is formed - the rate limiting step of the hydrolytic reaction - which is stabilised through hydrogen bonding within the pocket of the esterase (Juhl P B *et al.*, 2009). Specifically, a covalent bond is formed from the serine residue's hydroxyl group and the carbonyl carbon of the substrate in question. This is facilitated through proton transfer from the serine residue to the histidine residue, with further stabilisation from hydrogen bonding through the oxyanion pocket (Tyagi S and Pleiss J, 2006), i.e. the enzyme binds to the transitional state more strongly than the actual substrate itself (Pauling L, 1946), releasing the alcohol moiety of the ester and leaving an acylenzyme intermediate (see Figure 1.3). Deacetylation of the acylenzyme is achieved through hydrolytic attack of the acyl group and the imidazole group of the histidine involved in the active site. This deacetylation forms a second tetrahedral intermediate, which is vulnerable to nucleophilic attack through the histidine imidazole group. This nucleophilic attack causes the serine group to break the covalent bond to the acid moiety of the ester in favour of a hydroxyl group and the former is then ejected from the active site (Casas-Godoy L *et al.*, 2012), (see Figure 1.3.).

If the enzyme breaks down substrates with multiple ester bonds present, e.g. fats and oils, it may show regioselectivity, i.e. it breaks down certain ester bonds before others. With glycerol-backbone substrates, this regioselectivity can be either primary (*sn*-1/*sn*-3), e.g. *A. niger* and *Rhizopus delemar* (*R. delemar*) lipases, or secondary (*sn*-2), e.g. *G. candidum* lipase. Regioselectivity can be detected through partial hydrolysis of a known substrate and detecting the products of this hydrolysis (Lanser A C *et al.*, 2002).

1.5. Residue conservation in lipolytic enzymes

The triad handedness is universal in all lipolytic GX SXG enzymes and there are several residues - often located at the core of the enzyme or at the end of helices/strands and salt bridges that are highly conserved in members of this family as well, e.g. cysteine, proline and glycine - residues involved in defining the structure of the enzymes - as well as hydrophobic residues such as isoleucine, leucine and valine at the centre of these enzymes, indicating hydrophobic forces are important in the 3D structure of these proteins.

Other areas of conservation within multiple GX SXG enzymes include non-polar clusters and areas involved in hypothetical hydrogen bonding within the enzyme (Drabløs F and Petersen SB, 1997). Variable regions were either on the surface of the protein, e.g. the amphipathic $\alpha_{4,5}$ helices of *G. candidum* lipase and *Torpedo californica* (*T. californica*) acetylcholinesterase showing great variability on residues facing the surface of the protein (Variability indices ranging from 5.8-38.67) or involved in determining substrate identification/ligand binding. Residues facing the interior were usually more conserved (Variability indices ranging from 1-4.83) (Cygler, M *et al.*, 1993).

1.6. Classification system of lipolytic enzymes

For a long period of time, lipases and esterases were identified simply by the substrates they showed affinity to, with lipases showing a much wider substrate affinity than esterases in general. However, this was too vague to be used consistently, so a better segregation and identification of esterases and lipases had to be established. The most recent classification system has all lipolytic enzymes being members of one of eight different families (I-VIII), with

Family I being sub-divided into 8 further families (sub-families 1-8). The basis of compartmentalisation was on shared similar primary structure and structural properties (Arpigny J L and Jaeger K E, 1999).

While it has been proposed (Ali, Y B, et al., 2012) that lipolytic and non-lipolytic carboxylester hydrolases should be differentiated using the physico-chemical criterion to first see if the enzyme in question can catabolise a lipid, then sub-dividing these two new families through their *in vitro* activity against a wider range of substrates, the current classification method is still in use and is detailed below.

1.6.1. Family I

Family I consists solely of true lipases - defined as enzymes which show maximal activity towards insoluble long-chain triglycerides. These enzymes are subdivided thus:

Sub-family 1:

Lipases belonging to this sub-family show sequence similarity to *Pseudomonas aeruginosa* (*P. aeruginosa*) lipase and usually have a mass between 30-32kDa. These lipases require chaperone proteins identified as Lifs for expression. All members have two conserved aspartic acid residues needed for controlling Ca²⁺-binding site needed for catalytic activity and most contain an intramolecular disulphide bridge for stabilising protein folding. These features are found in close proximity to the catalytic histidine and aspartic acid residues.

Sub-family 2:

Lipases in this sub-family show sequence similarity to *Burkholderia glumae* (*B. glumae*) lipase and have a mass greater than 32 kDa (due to presence of two extra β -strands when compared to sub-family 1). Like sub-family 1, these lipases also need Lifs for expression, as well as having the two aspartic acid residues and two cysteine residues forming an internal disulphide bridge.

Sub-family 3:

Lipases from this family are found from two separate species - *Pseudomonas fluorescens* (*P. fluorescens*) and *Serratia marcescens* (*S. marcescens*). Their molecular mass is greater than sub-families 1 and 2 (50-65kDa) and they have no N-terminal signal peptide or disulphide bridge. These lipases are exported from host through type I secretion pathway using a C-terminal signalling domain.

Sub-family 4:

These are the smallest lipases known under this system, with a molecular mass of less than 20kDa. Several contain the pentapeptide sequence AXSXG instead of GX SXG. They do not require Ca^{2+} ion for catalytic activity and do not have any cysteine residues.

Sub-family 5:

All lipases in this family are from gram-positive prokaryotes, with molecular mass ~46 kDa due to a unique insertion within the α/β hydrolase fold required for zinc-binding, theorised to be behind thermal stability.

Sub-family 6:

Lipases in this family start as preproteins ~75 kDa in mass due to ~200 amino acid N-terminal domain used as a translocator signal through the cell membrane. This precursor is cleaved in the extracellular medium through specific protease activity, leaving a lipolytic domain ~46kDa (Goetz F, et al., 1998, Rosenstein R and Goetz F, 2000). Some members have shown phospholipic activity as well as lipolytic activity.

Sub-family 7:

Central region primary structure (i.e. from residues 50-150) shows significant similarity to sub-family 2. Members of this family have been found to act on a wide range of substrates, both tri- and mono-glyceride in origin, of varying fatty acid chain lengths.

Sub-family 8:

Recently identified through identification of a novel lipase - Lip1 - from *Pseudoalteromonas haloplanktis* (*P. haloplanktis*). The primary structure of this 51 kDa lipase shows little relation to any previously identified lipolytic esterases. They theoretically lack lid structures and Ca^{2+} pockets and the active site is not the expected GX SXG or equivalent pentapeptide, but instead LGG(F/L/Y)STG heptapeptide (de Pascale, et al., 2008).

1.6.2. Remaining lipolytic families

Families II to VIII are identified as carboxylesterases, capable of breaking down water-soluble ester substrates. The compartmentalising of these esterases into a further seven families was determined by the primary structure and properties of these enzymes (Arpigny J L and Jaeger K E, 1999).

Family II:

Consists of GDSL/SGNH esterases, lacking the pentapeptide GX SXG sequence and instead containing GDSL/SGNH tetrapeptide at the N-terminus. Family II esterases have five sections/blocks which contain conserved amino acid residues, with the first block containing the GDSL motif (Molgaard A, et al., 2000). As with GX SXG esterases, it is the serine residue in these GDSL/SGNH esterases which performs a nucleophilic attack on the substrate at the binding site of the esterase. However, it has been noted that in some members of this family the active site of GDSL esterases alters orientation upon the covalent binding of substrate to the protein. These alterations have been hypothesised as stabilising intermediates in hydrolytic activity (Akoh C C *et al.*, 2004).

Certain members of this family have a C-terminal domain involved in forming a pore through cell membranes for the auto-transporting of the hydrolytic domain into the extracellular medium.

Family III:

Members of this family show sequence similarity (~20%) to human platelet activating-factor acetylhydrolase (PAF-AH). However, family III esterases do not have a lid, unlike PAF-AH.

The first members were the extracellular esterases with a molecular mass of 32-35 kDa from the species *Streptomyces* and *Moraxella*. Later additions included *Acidovorax* and *Thermobifida* hydrolases, both of which are capable of degrading polyesters.

Family IV:

A series of esterases from distantly related prokaryotes that show sequence similarity to mammalian HSL (hormone-sensitive lipase) (Hemilä H *et al.*, 1994). Members of this family have three sequence domains with conserved motifs, with domains II and III containing the esterase catalytic triad. Domain I contains a consensus sequence for stabilising the oxyanion hole and promoting catalysis.

Some members can also have a 'cap' which covers the active site, regulating the hydrolytic activity, but this does not mean that members of this family are actually lipases. Unlike HSL, enzymes from this family show greatest activity on soluble, short-chain esters and show expected kinetics upon substrates.

Family V:

These esterases show homology to other, non-lipolytic hydrolases showing the α/β hydrolase fold and catalytic triad (Verschuere KH *et al.*, 1993, Misawa E *et al.*, 1998). Like Family IV, members of this family have three conserved sequence blocks with the active site residues located in blocks II and III.

Family VI:

Members of this family are among the smallest of the esterases, with sizes ranging from 23-26kDa. Like members of families IV and V, they have three conserved blocks. Family VI enzymes show ~ 40% sequence similarity to eukaryotic lysophospholipases.

Family VII:

Members of this family have a mass ~55 kDa and have four conserved sequence blocks. There are also amino acid sequence homologies to acetylcholine esterases and intestine/liver carboxylesterases (30% identity and 40% similarity).

Family VIII:

The most recent family derived in which, unlike all other carboxylesterases, members do not have the α/β hydrolase fold, but instead show greater similarity to the β -lactamases and DD-peptidases. The catalytic serine is not found in a triad arrangement, but instead is found as part of a SXXK tetrapeptide as opposed to a GX SXG pentapeptide or a GD SL/SGNH tetrapeptide. Most members have a mass ~42 kDa (Hausmann S and Jaeger KE, 2010). The serine in the SXXK tetrapeptide acts as the serine in GX SXG or GD SL/SGNH esterases (Wagner U G *et al.*, 2002)

This characterisation does not cover all known or possible future lipolytic enzymes. More esterases are being discovered which do not fit within the current definitions of the families/sub-families (Nacke H, *et al.*, 2011, Lee MH, *et al.*, 2006, Kim E, *et al.*, 2009, Jenkins J *et al.*, 2001), so this classification may require additional families/sub-families to remain useful.

1.7. Differences between lipases and esterases

All fats and oils are triglycerides; which means the easiest way for them to be degraded is through a hydrolytic reaction which breaks down the three ester bonds connecting the fatty acid moieties to the triglycerol backbone. Many are classified as EC 3.1 enzymes, according to the Enzyme Commission of the

International Union of Biochemistry (EC 3 representing all hydrolases) (Ali, Y B, et al., 2012).

1.7.1. Features of Lipases

Of all the hydrolytic esterases which are capable of breaking down ester bonds, the family which show greatest affinity towards fats and oils are lipases (EC 3.1.1.3); they favour triglycerides with long-chain acid moieties, i.e. with an aliphatic tail greater than 10 carbons. These tails need not be uniform or linear (Berger, M. and Schneider, M. P. 1991; Rogalska, E, et al., 1993) and the affinity of lipases can be altered through modifying the conditions of reaction, e.g. altering the solvent which the substrate is dissolved in can alter *Candida rugosa* (*C. rugosa*) and *Fusarium solani* (*F. solani*) substrate stereopreferences (Zandonella, G, et al., 1995). After ester hydrolysis, the fatty acid product is deprotonated which results in immediate ejection from the enzyme's active site due to the electrostatic repulsion between the two (Neves Petersen M T *et al.*, 2001). These enzymes also have a lid structure which covers the active site of the lipase. When the enzyme encounters insoluble substrate in the form of an emulsion body, the enzyme undergoes a structural change, which moves this lid away from the active site, allowing ester hydrolysis.

Lipases work best upon long-chain substrates and in aqueous solutions these substrates can be totally insoluble or poorly soluble. This is because lipases show affinity to substrate in emulsion bodies and aggregated substrates (Brockman HL, et al., 1988); the affinity of the lipase is not linked to concentration of the substrate in a reaction mixture but how concentrated the substrate is in the immediate vicinity of the enzyme, i.e. lipases work best at interfaces between themselves and these substrate bodies. At the interface, the lid moves away from the active site, permitting exposure of hydrophobic patches of the enzyme to the surrounding solvent, allowing entry of the substrate into the lipase's active site (Bornscheuer, U. T. 2006) (See Figure 1.4. for an example).

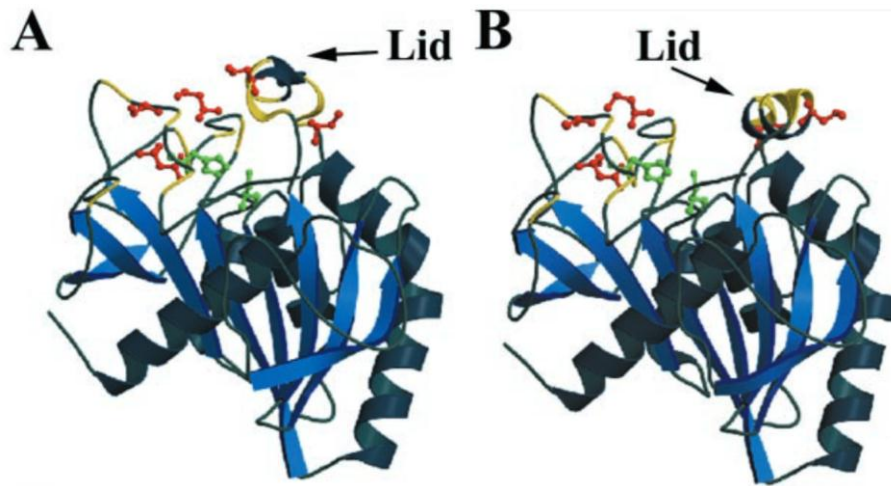


Figure 1.4. An example of how a lipase lid allows access to the active site

A 3-D image of *Humicola lanuginose* (*H. lanuginose*) lipase (HLL) showing the enzyme in its closed (A) and open (B) states, with the lid covering and exposing the catalytic triad (ball-and-stick model coloured green) when there is too little or a sufficient concentration of substrate available, respectively. Also shown are five carboxylic side-chains (ball-and-stick model coloured red) at the outskirts of a hydrophobic surface region (yellow) (Noinville S *et al.*, 2002)

Analysis of the hydrolysis of triglyceride substrate *in vitro* showed that Sn-2 monoglyceride products occupy the interface between enzyme and substrate, expelling free fatty acids, mono- and tri-glycerides. Unless there is some form of solubilising material in the reaction mixture as well, there will be a rapid accumulation of this product at the enzyme/substrate interface. This accumulation prevents access of the lipase to its substrate, reducing hydrolytic activity (Reis P M *et al.*, 2008). It has been proposed that this mechanism is also used *in vivo* as a regulating technique to control lipase activity (Reis P *et al.*, 2008).

This feature of *in vitro* reduction of lipase activity has the added complication of experiments measuring lipase activity being hard to replicate, with differences in activity being linked to how the solution in which the substrate is suspended in was mixed (Verger, R, 1998), the denaturing of some enzymes due to high interfacial tension (Verger, R, et al., 1984, Reis, P, et al., 2009). This unorthodox manner in which lipases break down their substrate is all due the lid structure present which covers the active site (Derewenda, U, et al., 1992).

Lipases' activity against substrate can be accordingly altered through modifying this lid structure - to the extent that some natural lipase isozymes

which show altered substrate specificity differ only in their lid structure (Brocca S, et al., 2003).

1.7.2. Features of Esterases

Esterases (EC 3.1.1.1) can be differentiated from lipases through a number of features. First, esterases lack a lid structure which preventing access to the active site until the enzyme is at an emulsion body, which is found in lipases. Esterases also have fewer non-polar residues making up the solvent-accessible regions on the enzyme (that is, between 50-100% accessibility to the solvent the protein is present in) than lipases.

The lack of a lid structure means that esterases are not reliant on their substrate being present in a particular format to allow access for hydrolysis. This means that esterases also show expected normal Michaelis-Menten model of activity towards substrates. The selectivity towards the esterase's substrates is usually linked to the entrance channel of the enzyme to the active site (Bencharit S, et al., 2003), that is, the chemistry of solvent accessible residues that make up the channel leading to the active site determine which substrates the esterase works best against. Also, as a general rule, esterases' optimal pH environment is lower than that of lipases (Fojan P, et al., 2000). Like lipases, they can perform the reverse reaction and perform a dehydration reaction.

The activity of esterases in their native hosts are not usually a necessity - under laboratory conditions - for cell growth/survival (Berger R *et al.*, 1998). These purposes range from cell-to-cell communication (Shinohara M, et al., 2007), providing a carbon source for the synthesis of antibiotics (Olukoshi E R and Packter N M, 1994) to detoxification (Lee W H *et al.*, 1986).

1.8. Uses of extremophilic esterases in industry

Enzymes from extremophilic origins are of industrial interest due to their ability to catalyse specific chemical reactions under conditions that may denature mesophilic enzymes or cause them to work sub-optimally. These extremophilic enzymes are isolated from organisms residing in extreme environments, e.g. the Siberian cryopeg or the Iranian hypersaline Aran-Bidgol lake which frequently reaches the salt saturation point during the dry season (Novototskaya-Vlasova K *et al.*, 2011, Bagheri M *et al.*, 2013).

The ability to catalyse particular reactions at extreme conditions made certain extremophilic enzymes sought after for their utilisation in biotechnological applications, e.g. Taq DNA polymerase (Chien A *et al.*, 1976, Kaledin A S *et al.*, 1980 Mullis K *et al.*, 1986) for orthodox PCR amplification to *Thermus* Rt41A serine protease PreTaq for purifying DNA/RNA (Vieille C and Zeikus G J, 2001). With these extremophilic enzymes, one can perform chemical reactions with a yield that would be unattainable at mesophilic conditions or with chemical reactions that do not have the enzyme present.

Extremophile lipases and esterases are no different. There have been many attempts to obtain lipases and esterases that can work in extreme environments for different applications. For example, the first commercial thermophilic lipase (Lipolase[®]) was produced by Novo Nordisk from *Thermomyces lanuginosus* for use as a part of laundry detergents (Salameh M and Wiegel J, 2007). Novozyme 435 lipase from the psychrophilic *Candida Antarctica* B is used for the acetylation of the antifungal rapamycin and its 42-ester derivatives (Gu J, et al., 2005), while similarly psychrophilic LipB68 from *Pseudomonas fluorescens* is used for transesterification of α -phenylethanol and α -phenylpropanol - both utilised for biodiesel (Luo Y *et al.*, 2006).

One example of an extremophile esterase is *Bacillus licheniformis* S-86 which is capable of synthesising isoamyl acetate at low temperatures, while at the same time demonstrating extreme stability at high pH and in the presence of detergents (Torres, S *et al.*, 2009). Another is AFEST esterase from the hyperthermophilic archaeon *Archaeoglobus fulgidus*, which is of interest to both laundry detergent and dairy industries (Manco G *et al.*, 2000, Schiraldi C *et al.*, 2002).

1.8.1. Differences and similarities between mesophilic and extremophilic esterases

Analysis of psychrophilic esterases, e.g. PhEst from *Pseudoalteromonas haloplanktis* (Aurilia, V, et al., 2008), EstO from *Pseudoalteromonas arctica* (Al Khudary, R, et al., 2010) and an esterase isolated from *Pseudoalteromas* sp. strain 643A (Cieśliński, H, et al., 2007), did not reveal any unique catalytic mechanisms by which these esterases function. These enzymes work with the same catalytic triad found in mesophilic esterases.

There are no totally unique structures found in psychrophilic esterases which are not found in their mesophilic counter-parts. It is even possible for the overall structure of a psychrophilic esterase to be similar in shape to a mesophilic esterase (See Figure 1.5. for an example).



Figure 1.5. How mesophilic and extremophilic esterases can show similarities

A superimposition of EstA (green) - an esterase isolated from the psychrophile *Pseudoalteromonas* sp. 643A - and thioesterase 1/TAP (brown) - isolated from *Escherichia coli* (*E. coli*, with the catalytic serine of both indicated by a localised inhibitor (blue). TAP was used as a search model in molecular replacement, and the only difference between the two enzymes is in the short loop fragments and the N- and C-terminal chains (Brzuszkiewicz, A, et al., 2009).

However, apart from the active sites and occasionally the structure, psychrophilic esterases can differ extensively in sequence from other members of their families, e.g. PsEst1 from *Pseudomonas* sp. strain B11-1 which shares only 15% sequence identity with other identified esterases (Suzuki, T, et al., 2003) and AEST from *Acinetobacter* sp. strain no. 6 sharing only 17% sequence identity with other identified esterases (Suzuki, T, et al., 2002). Comparisons with cold-active and mesophilic enzymes have shown a general inverse relationship between protein thermostability and the activity of the enzyme at 'cold' temperatures (Suzuki, T, et al., 2002). Research indicates that it is through different amino acids that psychrophilic enzymes are able to function at lower temperatures, not necessarily new structural motifs.

Extremophilic esterases differ from mesophilic esterases not by altered active site residues, or by unique structural features, but by a different internal structure and solvent accessible regions, e.g. more labile amino acids, i.e. amino acids' whose chemistry can be altered under the physical parameters of an extreme environment; such as arginine, aspartic acid, tryptophan, are replaced with less changeable residues in hyperthermophilic enzymes and *Alicyclobacillus acidocaldarius* (*A. acidocaldarius*) α -amylase's surface residues having a highly negative charge, granting a higher solubility and flexibility in hypersaline conditions (Robb FT and Clark DS, 1999, Matzke J *et al.*, 1997).

1.9. Aims of this project

When fats and oils stain clothes they form semi-crystalline structures (Amer M.A, et al., 1985, Ghosh S *et al.*, 2011) which lipases will not be able to degrade efficiently. Lipases show highest activity against substrate present in immiscible, dispersed, water-insoluble structures containing said substrates, i.e. emulsion bodies. Instead as there is no force provided at the interface between emulsion body and aqueous solution to force the lid covering the active site away (Bornscheuer, U. T. 2006). While analysis has shown that the effectiveness of laundry detergents in cleaning fats and oils from fabrics (Varanasi A, et al., 2001) and from individual cotton fibres (Sonesson, A W, et al., 2007) is increased when they contain lipases, this only applies at temperatures of above or equal to 40 °C. Because of this, lipases are not ideal enzymes for degrading fat and oil stains in clothes at low temperatures and are not considered further in this project.

Esterases are capable of breaking down ester bonds in substrates, though they commonly target shorter-chain acid moieties than lipases. However, esterases do not require substrates to be present in an emulsion body to perform optimally (Chahinian H, et al., 2002) - they do not have the lid structure found in lipases (Pleiss, J, et al., 1998). For this reason, this project focuses on developing a new method of measuring activity against ester substrates in a cold wash water environment with esterases. Ideally a novel, cold-active esterase, engineered to degrade long-chain esters and triglycerides at low temperatures, will be discovered. This enzyme may need to be further modified both to work well in the presence of possible additional constituents of the future laundry

detergent it would be a part of, reduce the amount of sebum produced and lower rancidity that can occur upon fat hydrolysis (Silva C *et al.*, 2012).

The overall aim of this project was to identify a novel extremophile esterase that could be utilised as a component of a laundry detergent capable of breaking down fats and oil stains on clothing efficiently in unheated washing water.

This means that the esterase chosen would have to work well in natural body washing water, e.g. in potentially hard water, that is, water containing between 120-180 mg/L of Ca^{2+} and/or Mg^{2+} ions. The esterase would also have to work without producing too much butyric acid substrate (as the odour of it is highly undesirable) and in conjunction with common laundry detergent components, e.g. Bacillus protease, sodium alkane sulphonate surfactant, sodium tripolyphosphate water softener, sodium perborate tetrahydrate oxidising agent and bleach. It would also have to work against the triglyceride components in fat and oil stains on fabric, and not when in emulsion bodies.

Firstly, an esterase would have to be identified, characterised and modified so as to show increased activity against substrate at lower temperatures.

Secondly, the theoretical new method for detecting esterase activity against substrate bound to a surface would have to be tested using esterases of known characterisation and structures.

Finally, if the method at step two works, the project will then utilise the extremophilic esterase found in the first aim with this method.

Chapter 2

Materials and Methods

2.1. General use Media and Buffers

2.1.1. Growth media methodologies

2.1.1.1. Luria-Bertani media

LB media is made by having 1g of tryptone, 0.5 g yeast extract and 1 g NaCl dissolved in 100 ml dH₂O (1.5 g agar is added if LB agar is desired). This media was autoclaved for 30 minutes at 121 °C. The resulting sterilised media was cooled to handling temperature, and any media supplements needed, e.g. antibiotics, inducing chemicals, were added under sterile conditions. Plates were poured before the agar solidified.

2.1.1.2. NZY+ Broth

NZY+ broth was made through 1 g of NZ amine, 0.5 g Yeast extract and 0.5 g NaCl all dissolved in 100ml dH₂O and autoclaved for 30 minutes at 121 °C. The resulting sterilised media was cooled to handling temperature, and any media supplements needed, e.g. antibiotics, inducing chemicals, were added under sterile conditions.

2.1.2. PAGE buffer methodologies

2.1.2.1. SDS-PAGE

4 x Resolving gel buffer was made by dissolving 36.3 g Tris with 170 ml dH₂O. pH was set to 8.8 with HCl and NaOH and volume made up to 200 ml with dH₂O.

4 x Stacking gel buffer was made by dissolving 12.1 g Tris with 170 ml dH₂O. pH was set to 6.8 with HCl and NaOH and volume made up to 200 ml with dH₂O.

SDS-PAGE gels were designed to consist of two gel layers: a stacking gel layer of a final concentration of 6% polyacrylamide to mitigate isotachopheresis on top of a resolving gel layer of a greater concentration polyacrylamide depending on the circumstances (usually 12.5%).

Resolving gel solution was the first gel to be poured into the mold, and so was made first. For 12.5% resolving gel; 2.52 ml dH₂O was mixed 3.34 ml 30% bisacrylamide with 2 ml Resolving gel buffer and 80 µl 10% SDS. Polymerisation was induced by adding 4 µl TEMED and 60 µl 10% APS. This mix was quickly poured into the mold, with isopropanol used to prevent formation of bubbles at the meniscus, and left to set.

Stacking gel solution was made like the resolving gel, but with 1.36 ml dH₂O was mixed 0.475 ml 30% bisacrylamide with 0.625 ml Stacking gel buffer and 25 µl 10% SDS. Polymerisation was induced by adding 2.5 µl TEMED and 25 µl 10% APS. This solution was poured on top of the set resolving gel, a gel comb inserted at the top of the mold and the solution was left to set (after the isopropanol was washed off).

All 20 µl protein samples were heated at 100°C for at least 4 minutes with 2 µl loading dye (2ml 4 x stacking buffer, 1.6 ml Glycerol, 3.2 ml 10% SDS, 0.8 ml 2 x β-mercaptoethanol and 0.4 ml 0.1% Bromophenol Blue) or mixed with 2 µl Non-reducing loading dye (2ml 4 x stacking buffer, 1.6 ml Glycerol, 3.2 ml 10% SDS and 0.4 ml 0.1% Bromophenol Blue). These were ran on the gel in conjunction with New England Biolab-brand Prestained Protein Marker 7-175 kDa, Broad Range in running buffer (30 g Tris, 144 g Glycine, 10 g SDS, 800 ml dH₂O, pH set to 8.3 with HCl and NaOH and volume made to 1 l for 10 x Running Buffer; useable volumes made by making 1/10 dilutions with dH₂O). Gel was run for 75 V until samples had passed through stacking gel and then 175-200V until the desired protein marker band had reached the bottom of the gel.

2.1.2.2. Native PAGE

4 x Resolving gel buffer was made by dissolving 36.3 g Tris with 170 ml dH₂O. pH was set to 8.8 with HCl and NaOH and volume made up to 200 ml with dH₂O.

4 x Stacking gel buffer was made by dissolving 14.5 g Tris with 170 ml dH₂O. pH was set to 6.8 with HCl and NaOH and volume made up to 200 ml with dH₂O.

Native PAGE gels were designed to consist of two gel layers: a stacking gel layer of a final concentration of 6% polyacrylamide to mitigate isotachopheresis on top of a resolving gel layer of a greater concentration polyacrylamide depending on the circumstances (usually 12.5%).

Resolving gel solution was the first gel to be poured into the mold, and so was made first. For 12.5% resolving gel; 2.52 ml dH₂O was mixed 3.34 ml 30% bisacrylamide with 2 ml Native resolving gel buffer. Polymerisation was induced by adding 4 µl TEMED and 60 µl 10% APS. This mix was quickly poured into the mold, with isopropanol used to prevent formation of bubbles at the meniscus, and left to set.

Stacking gel solution was made like the resolving gel, but with 1.36 ml dH₂O was mixed 0.475 ml 30% bisacrylamide and 0.625 ml Native stacking gel buffer. Polymerisation was induced by adding 2.5 µl TEMED and 25 µl 10% APS. This solution was poured on top of the set resolving gel, a gel comb inserted at the top of the mold and the solution was left to set (after the isopropanol was washed off).

All 20 µl protein samples mixed with 2 µl Non-reducing loading dye (1ml 0.5 M Tris-HCl (pH 6.8), 2 ml Glycerol, 1 ml 1% Bromophenol Blue and 4.92 ml dH₂O). These were ran on the gel in conjunction with Invitrogen brand NativeMark™ Unstained Protein Standard in running buffer (30 g Tris, 120.112 g Glycine, 800 ml dH₂O, pH set to 8.3 with HCl and NaOH and volume made to 1 l for 10 x Running Buffer; useable volumes made by making 1/10 dilutions with dH₂O). Gel was run for 75 V until samples had passed through stacking gel and then 175-200V until the desired protein marker band had reached the bottom of the gel.

2.1.3. Other buffer methodologies

2.1.3.1. Universal Buffer

2 x Universal Buffer was made by mixing 0.08 M Boric Acid, 0.08 M Phosphoric Acid and 0.08 M Acetic Acid together. When being prepared for enzyme characterisation, the pH of this mix was adjusted as desired, and the volume adjusted to 1 x concentration using water.

Universal buffer was used for reactions whereby the pH range was an adjusted condition that would go beyond the pH range of other buffers; at pH

values outside of these ranges, altering the concentration of H⁺ ion (as would happen during hydrolysis of nitrophenyl ester) could not be equilibrated by a conjugate base. Universal buffer has a pH range from 2.5 to 12, and so can maintain its pH after the release of fatty acid product from ester hydrolysis.

2.1.3.2. TAE gel

TAE gel was made by mixing 100 ml 50 X Tris Acetate EDTA solution and 1 g agarose. Agarose was melted in the TAE solution and was cooled to handling temperature before adding 10 µl 10,000 x SYBR Safe. The mix was poured into a TAE gel mold with a comb to form wells.

2.2. Kits used

- QIAprep Spin Miniprep Kit
- QIAquick PCR purification Kit
- Agilent Technologies QuikChange Lightning Directed Mutagenesis Kit
- ThermoScientific Mutation Generation System Kit
- Illustra Templiphi Kit
- Agilent Technologies GeneMorph II EZClone Domain Mutagenesis Kit
- Life Technologies pENTR/D-TOPO Cloning Kit

2.3. Primers used

Primer Name	Sequence 5'-3'	Comment
Sense E269C CalB	CTG CAA ATG ATC TGA CAC CGT GCC AGA AAG TTG CAG CAG CAG C	Second, successful attempt at introducing a PEG-binding site in CalB
Anti-sense E269C CalB	GCT GCT GCT GCA ACT TTC TGG CAC GGT GTC AGA TCA TTT GCA G	Second, successful attempt at introducing a PEG-binding site in CalB
PA3859 C14S For	CCG AAT GCC GAC GCC AGC ATC ATC TGG CTG CAC	Designed by Dr. Louise Horsfall
PA3859 C14S Rev	GTG CAG CCA GAT GAT GCT GGC GTC GGC ATT CGG	Designed by Dr. Louise Horsfall
PA3859 M37C For	GCC GAA GCC CTG CAG TGC GTC CTG CCG AGC ACC	Designed by Dr. Louise Horsfall

PA3859 M37C Rev	GGT GCT CGG CAG GAC GCA CTG CAG GGC TTC GGC	Designed by Dr. Louise Horsfall
Deactivating sense S113A PA3859	TCG CCG GTT TCG CGC AGG GCG GC	Active-site serine replaced by alanine.
Deactivating anti-sense S113A PA3859	GCC GCC CTG CGC GAA ACC GGC GA	Active-site serine replaced by alanine.
Est97 for. BamHI	<u>GCG GAT CCA</u> TGA GGC ATC AGC TGA GTT	Has BamHI restriction site
Est97 HindIII	<u>GGA AGC TTT</u> CAC TTC AAA CGC TGG TCC AG	Has HindIII restriction site
Est97 MGPR mut. For. pQE30	CCA GTA ATG ACC TCA GAA CTC CAT CTG GAT TTG TTC AGA ACG CTC GG	Mutagenesis of Est97 in pQE30
Est97 MGPR mut. Rev. pQE30	CCG AGC GTT CTG AAC AAA TCC AGA TGG AGT TCT GAG GTC ATT ACT GG	Mutagenesis of Est97 in pQE30
Est97 G53A For.	CGG CTG GTG TTG TTG GGC CAC GGC GCT ACA ACG CAC AAA AAA GTG G	Site-directed mutagenesis of G53A in Est97
Est97 G53A Rev.	CCA CTT TTT TGT GCG TTG TAG CGC CGT GGC CCA ACA ACA CCA GCC G	Site-directed mutagenesis of G53A in Est97
Est97 T231I For.	CCG GGT AAG CAC AGT GCG GTC CCA ATC TGG GAG ATG TTT GCC GGT ACG G	Site-directed mutagenesis of T231I in Est97
Est97 T231I Rev.	CCG TAC CGG CAA ACA TCT CCC AGA TTG GGA CCG CAC TGT GCT TAC CCG G	Site-directed mutagenesis of T231I in Est97
Est97 E40C For.	GTT TAC TGG TCA CCA GCC TGT GGT TCG AGC GAT CGG CTG	Introduces PEGylation site for Est97
Est97 E40C Rev.	CAG CCG ATC GCT CGA ACC ACA GGC TGG TGA CCA GTA AAC	For final attempt of PEGylating Est97 monomer

Table 2.1. Primers used in this project

A table listing the DNA sequences of all primers used in this project and notes of the utilisation of these primers

2.4. Bacterial strains used

Bacteria Strain	Use	Supplier
TOP10	Maintaining plasmid lines	Invitrogen Life Technologies
BL21-AI	Expression	Invitrogen Life Technologies
BL21 DE3 (Star)	Expression	Promega
BL21 DE3 (PLysS)	Expression	Invitrogen Life Technologies
ArcticExpress	Expression	Agilent Technologies
JM109	Expression	Sigma Aldrich
<i>E. coli</i> M15	Expression	University of Tromsø
XL10 Gold Ultracompetent	Directed Mutagenesis	Agilent Technologies

Table 2.2. Bacterial strains used in this project

A list of the bacterial strains used in this project, what they were used for. And from whom they were supplied

2.5. Plasmids used

2.5.1. pENTR-d-TOPO

pENTR-D-TOPO (2.58 kb) was a vector supplied by Invitrogen Life Technologies which has the insert site of the gene flanked by attL1 and attL2 sites. This feature means that this plasmid was used in the Gateway procedure to insert genes of interest into expression vectors through recombination (e.g. pDest17) which were used to express said gene. Confers kanamycin resistance.

2.5.2. pDest17

pDest17(6.354 kb) was an expression vector in the Invitrogen Life Technologies Gateway system (see pENTR-D-TOPO), with a ccdB and chloramphenicol resistance gene inserted between the attR1 and attR2 recombination sites - ccdB was fatal to *E. coli*, preventing the growth of any *E. coli*

containing non-recombined plasmid. Proteins expressed through this vector gain an N-terminal poly-His tag. Confers ampicillin resistance.

2.5.3. pEXP5-CT/TOPO

pEXP5-CT/TOPO (2.685 kb) was an expression vector supplied by Invitrogen Life Technologies for the expression of PCR-amplified (by Taq polymerase) genes under a T7 promoter. Proteins expressed through this vector gain a C-terminal poly-His tag. Confers ampicillin resistance.

2.5.4. pET-28a(+)

pET-28a(+) (5.369 kb) was an expression vectors supplied from Merck Millipore. pET vectors express genes under the control of a T7 promoter, has T7 epitope tag separating the MCS from the N-terminal poly-His tag. Confers kanamycin resistance.

2.5.5. pET-30a(+)

pET-30a(+) (5.422 kb) was an expression vectors supplied from Merck Millipore. pET vectors express genes under the control of a T7 promoter, has S.tag epitope separating the MCS from N-terminal poly-His tag. Confers kanamycin resistance.

2.5.6. pMAL-c2x

pMAL-c2x (6.646 kb) was an expression vector supplied from New England Biolabs used to generate proteins not readily soluble. Genes inserted into this vector were expressed under a lacIq promoter and had a cleavable N-terminal MBP tag added. Confers ampicillin resistance.

2.5.7. pQE30

pQE30 (3.5 kb) was an expression plasmid supplied by QIAGEN, but the sample obtained by this lab came from the University of Tromsø, with a gene already inserted into it. Proteins were expressed under a T5 promoter with a cleavable N-terminal poly-His tag. Confers ampicillin resistance.

2.6. Protocols used

2.6.1. Cell-specific protocols

To make glycerol stocks, transformed bacteria (See 2.6.1.1.1., 2.6.1.1.2. and 5.2.2.2.) were grown on selective agar overnight at 37°C and single colonies grown overnight in 5 ml LB media with appropriate concentration of antibiotics at 200 rpm.

850 µl of the overnight was mixed with autoclaved glycerol (150 µl) in a 2ml screw-top centrifuge tube. This can be stored permanently in a -80°C freezer, and colonies recovered through streaking samples onto LB media

2.6.1.1. Transformation protocols

2.6.1.1.1. BL21-AI transformation protocol

1 µl of vector with inserted gene and at least 15 µl competent BL21-AI (supplied by Invitrogen) were mixed and left on ice for up to 30 minutes, then subjected to heat-shock at 42°C for 30 seconds, and placed on ice for 2 minutes.

The bacteria were suspended in 500 µl LB media and grown at 37°C for 60 minutes on a shaker rotating at 200 rpm. This incubation was then grown overnight on LB agar containing appropriate antibiotics at 37°C.

2.6.1.1.2. TOP10 transformation protocol

1 µl of plasmid and at least 15 µl competent TOP10 (supplied by Invitrogen) were mixed and left on ice for up to 30 minutes, then subjected to heat-shock at 42°C for 30 seconds, and placed on ice for 2 minutes.

The bacteria were suspended in 250 µl LB media and grown at 37°C for 60 minutes on a shaker rotating at 200 rpm. This incubation was then grown overnight on LB agar containing appropriate antibiotics at 37°C.

2.6.1.2. Expression protocols

2.6.1.2.1. Small-scale expression of esterases

Successfully transformed expression bacteria hosts were re-suspended in 100 ml of LB and 1% glucose (if the protein was toxic to the transformant BL21-AI cells) and grown for 1 hour at 37°C at 200 rpm.

800 µl of this growth was then used to infect 40 ml of LB growth media with required antibiotic concentration. These separate media were grown at 37°C at 200 rpm to the desired absorbance value at OD₆₀₀ and were transferred to a range of incubation temperatures and induced with the appropriate inducing material over a range of concentrations. At specific time points, aliquots were obtained and samples of bacteria were extracted.

These bacterial samples were subjected to a chemical lysis session and run on an SDS-PAGE to determine which specific condition produced the most soluble protein of interest.

2.6.1.2.2. BL21-AI expression

Successfully transformed expression bacteria hosts (See 2.6.1.1.1.) were re-suspended in 100 ml of LB and 1% glucose and grown for 1 hour at 37°C at 200 rpm.

80/40 ml of this growth was then used to infect 4/2 l of LB growth media with required antibiotic concentration at 37°C at 200 rpm. These separate media were grown to the desired absorbance value of OD₆₀₀ (between 0.6-0.8) and were induced with required concentration of arabinose and incubated at 200 rpm at the temperature and incubation period required for highest expression of soluble protein at.

Aliquot samples were isolated to check for protein expression while the remaining bacteria were spun down for 25-30 minutes at 7500 rpm and supernatant removed. The bacterial pellet was collected and flash-frozen with liquid N₂.

2.6.2. Protein-specific protocols

2.6.2.1. SDS-PAGE/non-denaturing gel technique

To detect protein expression from bacterial grow-ups expressing protein of interest, 200 µl bacterial samples were spun down and the media supernatant

removed. This pellet was then subjected to chemical lysis using 10 x BugBuster reagent (supplied from MerckMillipore) mixed with 0.5 M Tris-HCl (pH9) with 1M NaCl to a volume 1/10th of the original aliquot volume for 10-20 minutes. The samples were spun down once more, and the supernatant isolated for checking soluble proteins.

The pellets were re-suspended for another round of BugBuster lysis for 5 minutes and were isolated as well. Pellet and supernatant samples were denatured (if needed) by heating at 100°C for 4 minutes with an appropriate volume of loading dye (see 2.1.2.).

When visualising pure protein samples, a 20 µl mix was made with protein sample, water and loading dye. This mix was denatured (if so desired) by heating at 100°C for 4 minutes.

The resulting protein mixes were run on an SDS-PAGE or a non-denaturing gel, alongside a protein marker. The gel was run (90V at -4°C for non-denaturing gels, 90V until the samples go through the stacking gel, then 200V) until the marker dye of the protein ladder reaches the edge of the gel.

The gels were submerged in InstantBlue exposure fluid for at least 20 minutes and were de-stained in dH₂O. Bands corresponding to expected target protein weight not present within non-induced control were taken as evidence of successful protein expression.

2.6.2.2. Purifying esterases through poly-His tag/Nickel immobilised metal ion affinity chromatography

When protein presence was confirmed, the remaining pellet was re-suspended in 0.05 M Tris-HCl/0.5 M NaCl/0.05 M imidazole or 0.05 M NaH₂PO₄/0.3 M NaCl/0.01 M imidazole solution for proteins expressed in BL21-AI or *E. coli* M15 cells respectively (2 l of pellet to 35 ml of solution) with 1 µl of benzonase and lysed via a French Cell Press. The lysed bacteria were spun down for 45 minutes at 14000 rpm and the supernatant stored for purifying soluble protein.

For proteins with poly-His tags, the resulting lysate was then passed through a G.E. Healthcare Chelating Sepharose Fast Flow resin-filled XK 16/20 column charged with 0.2 M NiCl₂ and then equilibrated with appropriate resuspension buffer, using an Äkta Prime pump. Non-specific proteins binding to the column

were removed by running 0.05 M Tris-HCl/0.5 M NaCl/0.05 M imidazole (for OsmC proteins, E269C CalB and C14S/M37C PA3859) or 0.05 M NaH₂PO₄/0.3 M NaCl/0.01 M imidazole (for Est97 and all variants) solution through the column. These solutions were called Wash buffers. Expressed protein was then removed from the column by running 0.05 M Tris-HCl/0.5 M NaCl/0.5 M imidazole or 0.05 M NaH₂PO₄/0.3 M NaCl/0.2 M imidazole solution through the column over an increasing gradient for 225 ml or through incremental steps at a rate of 2ml/min, with the solution passed through the charged resin being collected in 15 ml fractions. These solutions were called Elution buffers.

As buffer is passed through column, it is passed by an Optical Unit that passes UV light at 280 nm and detects how much light is absorbed by the buffer. Protein present in buffer absorbs light at 280 nm, so educated estimations can be made of which fractions contain the protein of interest. Samples were taken from the appropriate fractions and were run on a SDS-PAGE gel to confirm the weight of the protein bands. If they were of expected mass, the total fractions were dialysed twice in 0.5 M Tris-HCl/0.5 M Tris-HCl + 10% glycerol solution of an appropriate pH with an appropriate concentration of salt to prevent precipitation, for at least 4 hours which removes imidazole and permit the protein's use in assays or for chemical modification. A small aliquot (usually 100µl) of dialysed protein was used to break down a volume of nitrophenol acetate dissolved in ethanol in conjunction with a negative control consisting of an equal volume of Tris buffer to check that the dialysed sample does had esterase activity.

2.6.2.3. Bradford Assay

A series of six controls was made through diluting stock BSA (50mg/ml) (supplied from Life Technologies) with H₂O to make the following: 0 mg/ml, 0.25 mg/ml, 0.5 mg/ml, 0.75 mg/ml 1 mg/ml and 1.4 mg/ml. Samples of each of these controls (30/33 µl) were placed into separate plastic cuvettes. A sample of the test protein sample (which may be diluted with H₂O as well) was also placed in an individual cuvette.

1 ml of Bradford Reagent (supplied from Sigma Aldrich) was added to each sample at 1 minute intervals, and readings at 595nm were taken in triplicate from

each sample after a 5 minute incubation of the protein sample with the Bradford Reagent.

The readings from the six controls were made to draw up a graph, and a linear line of best fit was drawn through the points. The equation of this line was then used to calculate the concentration of the test protein sample.

2.6.5. DNA specific protocols

2.6.5.1. Vector isolation

5 ml taken from 37°C at 200 rpm overnight growths of bacteria containing vector of interest were spun down. The resulting pellets were subjected to a Spin Miniprep Kit (supplied by QIAGEN) (See 2.2.). Briefly, DNA is extracted from cell pellets through treatment with a lysing buffer, and is then precipitated out and bound to a silica membrane in a spin column. Impurities are removed by passing eluting solutions through the column, before vector DNA is removed via nuclease-free dH₂O.

2.6.5.2. DNA endonuclease cutting

Restriction enzymes for specific DNA motifs obtained from Roche or New England Biolabs;

Required mass of target DNA was mixed with the suggested units of endonuclease with appropriate endonuclease buffer to a final volume of 10µl using dH₂O. The samples were left to incubate at the suggested temperature and time for the supplier.

To check if cutting of DNA samples had been successful, an aliquot of the cut DNA was run on a 1% TAE agarose gel (See 2.6.5.9.), along with an uncut control. The resulting bands were visualised under UV light.

2.6.5.3. DNA ligation

DNA ligation first requires two or more linear DNA fragments, typically with complementary single-strand overhangs.

For simple T4 ligation, 50ng of each DNA sample were mixed with one unit of T4 Ligase and 10 x T4 Ligation buffer, made up to 20 µl with dH₂O and left overnight at 16°C, or at room temperature between 10 minutes to 2 hours.

The ligation mix was then used to transform competent cells (see 2.6.1.1.2.) which were grown overnight on selective media. Individual colonies were picked and grown overnight at 37°C at 200 rpm in 5 ml LB with relevant antibiotic. Plasmids were obtained from overnight media via QIASpin Miniprep, and were run on a TAE gel (See 2.6.5.9.) with an empty vector as a negative control to check if insertion had occurred.

2.6.5.4. Gateway System recombination

The Gateway System of expression requires DNA to be inserted into vectors through a unique set of ligation protocols. Firstly, insertion of genes of interest into TOPO vectors was different compared to other ligations, as the polymerised DNA fragments to be inserted do not have to have overhangs; ligation into TOPO vectors was blunt-ended. 2 µl PCR product were mixed with 1 µl salt solution and 1 µl TOPO 2.1 vector supplied with the kit, and dH₂O added to make up to 6 µl (See 2.2.).

The resulting mix was left for a minimum of 5 minutes at room temperature, before being used to transform TOP10 cells (See 2.6.1.1.2.), using kanamycin as the selective antibiotic.

After the gene was inserted correctly into TOPO vector, an LR Recombination reaction transfers the gene from the TOPO vector into the pDest expression vector. 3 µl TOPO vector with gene of interest inserted (50-150ng DNA) was added to 1 µl kit-supplied destination vector, TE Buffer (pH 8) to 8µl and 2 µl kit-supplied LR Clonase II enzyme mix.

The resulting mix was incubated for 25°C for 1 hour, then was treated with 1 µl Proteinase K and incubated for 37°C for 10 minutes, and was then used to transform competent TOP10 *E. coli* against appropriate antibiotics (See 2.6.1.1.2.), e.g. with pDest17, carbenicillin.

2.6.5.5. PCR primer design

15-20 nucleotide-long primers were designed to flank genes in particular plasmids, along with specific endonuclease sites if needed, as well as having melting temperatures that would not interfere with the extension temperature according to the working temperature of the polymerase used in the PCR kit.

Primers were designed *in silico* from the same company they were ordered from Eurofins MWG operon.

2.6.5.6. DNA Sequencing

Purified DNA samples were concentrated to 50-100 ng/ μ l, determined through absorbance at OD₂₆₀, and 15 μ l samples were sent to Eurofins MWG operon with primers specific for the MCS of the vector the gene is inserted in. Sequencing results were analysed *in silico*.

2.6.5.7. PCR protocols used

2.6.5.7.1. Phusion High-Fidelity DNA PCR

For general gene replication, this procedure was used to ensure low risk of mis-match replication. Template DNA were isolated and subjected to a 50 μ l PCR session with Phusion High-Fidelity DNA Polymerase with required buffers and dNTPs supplied in the kit (See 2.2.), i.e., 10 μ l 5X HF or GC Buffer (the latter is used for complex or GC-rich templates which would be inclined to be harder to denature the dsDNA) is mixed with 5 μ l 2 mM dNTP, 1 μ l of template DNA containing 50-250 ng of DNA, 5 μ l of 5 mM Forward and Reverse primers. After mixing, 0.5 μ l Phusion High-Fidelity DNA Polymerase is added and nuclease-free dH₂O is added to make a final volume of 50 μ l.

The mix is placed in a sterile PCR tube, where it was denatured for 30 seconds at 98°C, before being subjected to ~30 cycles of 98°C for 7.5 seconds (denaturing step), T_m of primers for 20 seconds (primer annealing step) and 72°C for 30 seconds/kb of gene being replicated (elongation step). The was subjected to a final extension period of 72°C for 10 minutes, before samples were run on a gel to check for PCR success.

2.6.5.7.2. GoTaq DNA PCR for DNA for insertion into TOPO vectors

1.25 μ l aliquots of template DNA were isolated and subjected to a 50 μ l PCR session with GoTaq DNA Polymerase with required buffers and dNTPs supplied in the kit, i.e., 10 μ l 5X GoTaq Reaction Buffer, 1 μ l of each 10 mM dNTP, ~0.5 μ g of template DNA, 5 μ l of 5 mM Forward and Reverse primers, and 0.5 μ l GoTaq DNA

Polymerase are all mixed, with nuclease-free dH₂O added to make up to 50 µl in a PCR tube.

The mix was incubated for 15 minutes at 72°C, purified and mixed with relevant TOPO vector (See 2.6.5.).

2.6.5.7.3. Site-directed mutagenesis PCR

Introducing single amino acid changes to proteins investigated in the project was performed using Agilent Technologies QuikChange Lightning Directed Mutagenesis kit (See 2.2.). Briefly, mutagenic primers between 25-45 bp in length are designed for the gene encoding the protein of interest - these primers do not flank the gene of interest, but instead anneal to the DNA template which is responsible for encoding the protein where the mutation is wanted to be - however, these primers are designed so as to introduce the mutant into the plasmid copies made when PCR occurs.

5 µl of supplied 10 x Reaction buffer, 25 ng of template plasmid, 125 ng of both mutagenic primers, 1 µl of dNTP mix, 1.5 µl of supplied QuikSolution are mixed, with dH₂O added to make a final volume of 50 µl. This mix is added to a PCR tube, and then 1 µl of supplied QuikChange Lightning Enzyme is added.

This mix is then incubated for 2 minutes at 95°C, before going through 18 cycles of 95°C incubation for 20 seconds for strand melting, 60°C for 10 seconds for primer annealing and 68°C for 30 seconds per kb of template plasmid length for polymerisation. After the cycles, a final polymerisation incubation takes place for 5 minutes

The original template plasmid is then digested through application of 2 µl *Dpn* I restriction enzyme for 5 minutes at 37°C. Polymerisation is checked through running on a TAE gel, and when successful PCR has occurred, 2 µl of the *Dpn* I treated PCR is used to transform kit-supplied XL10-Gold Ultracompetent cells.

2.6.5.8. PCR purification protocol

PCR DNA samples required to be purified (e.g. PCR fragments that had to be subjected to endonucleases) were subjected to a QIAquick PCR purification kit (Supplied by QIAGEN). In brief - high salt buffers bind PCR product to a silica membrane in a spin column. Contaminants are washed off of the silica through a

series of eluting solutions. PCR product is removed through incubation with nuclease free water.

2.6.5.9. TAE gel running procedure

At least 10 μ l of DNA sample were mixed with 2 μ l 6 x Orange/Blue loading dye (supplied by Promega) and were inserted into wells of 1% TAE gels (See 2.6.5.9.), along with the required DNA fragment ladder (supplied by Promega) alongside the samples, depending on expected sample mass.

The gel was suspended in TAE buffer in an electrophoresis tank, and has 50V run through it to separate out DNA fragments, until a desired time. Samples were removed from electrophoresis tanks and visualised under UV light.

2.6.5.10. Gel purification protocol

50 μ l aliquots of DNA fragments that were ran on a TAE gel (See 2.6.5.9.) could be briefly visualised on a UV trans-illuminator, and fragments of relevant size extracted using a straight-edge razor.

DNA fragments were extracted from the excised TAE gel via a Gel Extraction kit (supplied by QIAGEN) (See 2.2.).

2.6.6. On-line software for predicting surface residues

2.6.6.1. Weighted Ensemble Solvent Accessibility

An online meta-predictor software that calculates theoretical accessibility of residues in a peptide to solvents from the primary structure of said peptides through five systems; Bayesian statistics, multiple linear regression, decision tree, neural network and support vector machine. The weighted sum of the individual predictions is used to predict the probability of a residue being exposed to solvents (i.e. having a surface area over than 20% of maximum area expected of said residue)

url: <http://pipe.scs.fsu.edu/wesa.html>

(Chen H L and Zhou H X, 2005, Shan Y *et al.*, 2001)

2.6.6.2. ASA-view

A server which determines solvent accessibility of residues from proteins whose information is recorded in the PDB and displays the results in a graphical format. The DSSP algorithm is used to determine the absolute surface area for each residue; from these values, two plots are generated. The spiral plot; which categories residues according to their relative solvent accessibility values, and arranges the residues in a graphic which displays the inner-most residues in the interior of the spiral drawn in the plot, and the exposed residues in the exterior. The second plot is that bar plot, which display the solvent accessibility of each individual residue in a simple bar chart.

url: <http://www.abren.net/asaview/>

(Ahmad S *et al.*, 2004)

2.6.6.3. polyview

Like ASA-view, uses the recorded information of protein in PDB (also with primary structure or CASP format of protein as well) to display the primary structure of the peptide superimposed with graphical representations of secondary structures, solvent accessibility, relative solvent accessibility. etc.

url: <http://polyview.cchmc.org/>

(Porollo A *et al.*, 2004)

2.6.6.4. NetSurfP

A server which combines the relative surface accessibility score from residues in a primary structure with a calculation of the reliability of each prediction, and displays the results in a Z-score. While it predicts solvent accessibility of each residue, it does not predict secondary structure.

url: <http://www.cbs.dtu.dk/services/NetSurfP/>

(Petersen B, *et al.*, 2009)

2.7. Companies which supplied chemicals

Ester substrates

The Nitrophenyl esters octanoate, decanoate, dodecanoate, stearate and myristate were all supplied through Sigma Aldrich.

Nitrophenyl hexanoate was supplied from T.C.I. Chemicals.

Nitrophenyl benzoate was supplied from Alfa Aesar.

Olive Oil was supplied through Tesco and Sigma Aldrich.

Naphthyl acetate was supplied through Sigma Aldrich.

Tributylin was supplied through Acros Organics.

Chemicals for PEGylation

mm(PEG)₂₄ obtained from ThermoScientific.

TCEP.HCl obtained from Sigma Aldrich.

DMF obtained from Sigma Aldrich.

Chapter 3

Identification and characterisation of a novel family of esterases containing an OsmC domain

3.1. Introduction

3.1.1. Project aims and background.

The aim of the first stage of this project was to identify a psychrophilic esterase for use in a laundry detergent.

Lipases and esterases are enzymes which work on the same molecular mechanism, i.e. both use active site serine to perform a nucleophilic attack on the carboxyl group of the alkyl chain of an ester. Lipases work best at the interface between substrate and aqueous media when fats and oils are present in emulsion form. They contain a lid structure which moves to allow access to the lipases' active site (Brockman HL, et al., 1988, Bornscheuer U. T. 2006) (See figure 1.4.). When fats and oils are present at temperatures below their melting point, they do not form emulsion bodies but instead crystallise (Amer M.A, et al., 1985). Esterases are the focus of this project due to the fact that they lack the lid structure (Pleiss, J, et al., 1998) present on lipases, and are theoretically more capable of performing nucleophilic attack upon non-emulsified substrates than their lidded lipase counterparts.

The terms fats and oils for the purposes of this project encompass a collection of chemicals made up of a central glycerol molecule with three, aliphatic, long-chain carboxylic acid tails attached to said glycerol through ester bonds. These tails can vary in length depending on the source of the fat or oil (e.g. olive oil and butter typically have acid tails between 14 to 18 carbon atoms in length (Homapour M *et al.*, 2014; Rutkowska J and Adamska A 2011); coconut fat has acid tails primarily 12 to 14 carbon atoms in length (Appaiah P, et al., 2014). The melting point of the fats and oils are dependent on the chemistry of the fatty acid tails; long fatty acid tails increase and carbon-carbon double bonds in the aliphatic chains decreases the melting point.

3.1.2. The identification of members of a novel esterase family

While there has been a wide range of research performed on identifying, purifying and characterising low-temperature active esterases (Fu J, et al., 2012; Novototskaya-Vlasova K, et al., 2011; Cieśliński H, et al., 2007; Wei Y, et al., 2003), the aim of this project was to obtain highly active - preferably novel - monomeric esterases that work well at low temperatures for use as part of a washing powder. The new method for detecting esterase activity specifically against fat and oil stains (See 1.9. Aims of this project) requires the esterase to be in a monomer form. Novel esterases are specifically sought after due to the potential of discovering a better enzyme for industrial applications as opposed to previously characterised esterases.

Pseudomonas arctica is a psychrotolerant marine gram-negative prokaryote isolated from Spitzbergen in the arctic (Al-Khudary R, et al., 2008). In 2010, a novel esterase was cloned from this bacterium and characterised (Al-Khudary R, et al., 2010). This esterase - called EstO - had a unique domain 142 amino acids in length present at its C-terminus, attached to the esterase domain through a linker 8 amino acids in length. This domain had homology to the osmotically-induced protein OsmC found in *Escherichia coli*. At the time this paper was published, it was the most active of all novel psychrophilic esterases in scientific literature.

The OsmC domain was so named due to its similarity to the *E. coli* osmotically-induced protein of the same name. OsmC is involved in protecting bacteria from the oxidative and toxic damage by organic hydroperoxides (Lesniak J, et al., 2003). This hydroperoxidase works in a similar fashion to Ohr (Organic hydroperoxide resistance) protein, through forming an active dimer that detoxifies organic hydroperoxides using active thiol groups to reduce said substrates. Al-Khudary *et al.*, produced a truncated version of EstO (Δ EstO) which lacked the OsmC-domain, too see if the esterase activity of the remaining enzyme was influenced. It was found that Δ EstO was more active than EstO (Al-Khudary R, et al., 2010).

When compared to other recently investigated psychrophilic esterases in the literature, EstO was found to be the most active at the desired temperature range (15°C-30°C) as well as potentially monomeric. No crystal structure of the esterase had been published.

A BLAST search using the amino acid sequence of EstO found multiple alignments. In addition to having similar amino acid sequences, these homologs were also found to come from a wide range of environments, both extremophilic and mesophilic. The consistency in amino acid sequence in these esterases indicated that these could be members of a novel esterase family.

By choosing a selection of these esterases from a variety of environmental backgrounds for further analysis and characterising them, a relationship between the sequence of the esterases and their physical characteristics, e.g. activity against long-chain substrates, activity at low temperatures, could be found. Indications as to which sequences influence activity under certain conditions give potential starting points for directed mutagenesis, which could be used to generate a new esterase for use in a laundry detergent.

The EstO amino acid sequence was used by Dr. Louise Horsfall to identify five esterases using a BLAST search. When aligned, all homologs had a GX SXG pentapeptide sequence, residues that could make up the catalytic triad and a precursor GX SXG pentapeptide at very similar positions in the protein sequence (See figure 3.1.). These five esterases were chosen specifically because of their varied origins - they all came from unique environments, i.e. arctic water, thermal pools, mesophilic environments. etc.

The strains chosen; *Pseudoalteromonas arctica* (*P. arctica*) (DSM 18437), *Labrenzia aggregata* (*L. aggregata*) AKA *Stappia aggregata* (*S. aggregata*) (DSM 13394), *Roseobacter denitrificans* (*R. denitrificans*) (DSM 7001), *Catenulispora acidiphila* (*C. acidiphilia*) (DSM 44928), *Rhodothermus marinus* (*R. marinus*) (DSM 4252) and *Ensifer meliloti* (*E. meliloti*) AKA *Sinorhizobium meliloti* (*S. meliloti*) (DSM 1981) were all purchased from the DSMZ catalogue (<http://www.dsmz.de/catalogues/catalogue-microorganisms.html>), grown in the laboratory (See Table 3.2.).

Primers to amplify the genes encoding the putative esterases from extracted bacterial genomic DNA using PCR were designed by Dr. Louise Horsfall.

Because the Δ EstO variant had higher activity against nitrophenyl ester substrates than the full-length esterases (Al-Khudary R, et al., 2010), it was decided to determine if truncated versions of the homologs also had greater

activity than their wild-type forms. For convenience, the nomenclature for naming truncated versions of the esterases in this project was continued from Al-Khudary, R, et al., e.g. Proteins with OsmC domains still attached were identified as EstX, with X representing the initials of the organism it originated from, while truncated forms of the proteins are given a 'Δ' prefix.

The activity of ΔEstLA esterase was compared against its full length counterpart EstLA against several nitrophenyl substrates to see if truncation altered the activity of the esterase, and if this alteration was uniform against different substrates (See Table 3.1.). The truncated form had a higher k_{cat}/K_m value than the esterase with the OsmC group still present against all tested substrates, meaning that a greater proportion of substrate was converted into product per molecule of esterase. Removal of the OsmC domain resulted in higher activity. Since the aim of this project was to identify esterases with the highest activity, the Δ esterases were the focus of investigation.

Substrate	Esterase	K_m (mM)	k_{cat} (sec ⁻¹)	k_{cat}/K_m (mM ⁻¹ sec ⁻¹)
Nitrophenyl acetate	EstLA	4.6 ± 0.2	3.1 ± 0.1	0.67
	ΔEstLA	3.4 ± 0.3	4.4 ± 0.1	1.2
Nitrophenyl butyrate	EstLA	3.2 ± 0.4	1.8 ± 0.1	0.55
	ΔEstLA	3.3 ± 0.3	4.0 ± 0.1	1.2
Nitrophenyl benzoate	EstLA	0.098 ± 7x10 ⁻³	1.81x10 ⁻³ ± 1x10 ⁻⁴	0.019
	ΔEstLA	0.019 ± 2x10 ⁻³	9.51x10 ⁻³ ± 1x10 ⁻⁴	0.050

Table 3.1. Comparison of enzyme kinetics of EstLA and ΔEstLA against nitrophenyl substrates

Enzyme kinetics were derived for EstLA and ΔEstLA at 30 °C at pH 8.5 under conditions described by Al-Khudary R, et al., 2010. Assay results were obtained from Dr. Louise Horsfall.



Figure 3.1. Alignment of amino acid sequences of esterases identified through BLAST search

Clustal Omega alignments of the amino acid sequence of the six esterases identified by the BLAST search, namely EstO (WP_01055316), EstLA (WP_006931223), EstCA (YP_003117689), EstRM (YP_003290484.1), EstEM (YP_005717177), and EstRD (YP_682806). The C-terminal OsmC domains (outlined in red) were approximately 130 amino acids for each esterase. Research performed on EstO identified the typical GXSXG pentapeptide in which the active-site serine residue was found spanning residues 104-108, along with the remaining members of the putative catalytic triad at positions 196 and 225 (Al-Khudary R, et al., 2010). When the homologs to EstO were aligned, the GXSXG pentapeptide along with residues that theoretically fit the expected amino acids of an esterase's catalytic triad were all in similar positions as EstO (outlined in green and purple respectively for all esterases). Also found when all six were aligned as above was an earlier, unique second GXSXG pentapeptide consensus (outlined in yellow).

3.2. Materials and Methods

3.2.1. Auto-inducing media

Auto-inducing media is a form of growth media developed that induces high-level expression in *E. coli* with IPTG-inducible expression vectors without requiring monitoring of bacterial density, and was used when other inducing methods were not found to express soluble esterase.

Three different forms of ZY media were needed; ZY, 2ZY and 8ZY. ZY media was made by dissolving 0.5 g Yeast Extract and 1 g Tryptone in a final volume of 100ml dH₂O, 2ZY media was made by dissolving 1 g Yeast Extract and 2 g Tryptone in a final volume of 100ml dH₂O and 8ZY media was made by dissolving 4 g Yeast Extract and 8 g Tryptone in a final volume of 100ml dH₂O. All were autoclaved before use.

Auto-inducing trace element solution was prepared through dissolving 0.1 g FeSO₄·7H₂O, 0.88 g ZnSO₄·7H₂O, 0.04 g CuSO₄·7H₂O, 0.015 g MnSO₄·4H₂O, 0.01 g Na₂B₄O₇·10H₂O, 0.005 g (NH₄)₆MO₇O₂₄·4H₂O in 0.02 ml HCl. dH₂O was added to a final volume of 100ml and autoclaved.

50x lac solution was made by 25 g Glycerol, 2.5 g Glucose and 10 g α lactose being dissolved in 100ml dH₂O and autoclaved.

20x NPSC was produced through dissolving 5.33 g NH₄Cl, 3.228 g Na₂SO₄, 6.8 g KH₂PO₄ and 7.1 g Na₂HPO₄ in 100ml dH₂O, with pH adjusted to 6.75 with HCl and NaOH, and then autoclaved

Auto-inducing media came in six different forms, 1-6:

1 was made by mixing 9.3 ml ZY, 20 μl 1 M MgSO₄, 200 μl 40% glucose solution and 500 μl 20x NPSC solution.

2 was made by mixing 9.3 ml ZY, 20 μl 1 M MgSO₄, 200 μl 50x lac solution, 40% glucose solution and 500 μl 20x NPSC solution.

3 was made by mixing 9.3 ml 2ZY, 20 μl 1 M MgSO₄, 200 μl 50x lac solution, 40% glucose solution, 500 μl 20x NPSC solution and 10 μl Trace Elements.

4 was made by mixing 9.3 ml 2ZY, 20 µl 1 M MgSO₄, 400 µl 50x lac solution, 40% glucose solution, 500 µl 20x NPSC solution and 10 µl Trace Elements.

5 was made by mixing 9.3 ml 8ZY, 20 µl 1 M MgSO₄, 800 µl 50x lac solution, 40% glucose solution, 500 µl 20x NPSC solution and 10 µl Trace Elements.

Finally, 6 was made by mixing 9.3 ml 8ZY, 20 µl 1 M MgSO₄, 200 µl 50x lac solution, 40% glucose solution, 500 µl 20x NPSC solution, 10 µl Trace Elements and 500µl 0.5 M succinate solution.

Each 10 ml solution was inoculated with 10 µl of an overnight growth of expression host bacteria in LB and grown for 60 hours at 28°C. Expression of proteins were checked through running on an SDS-PAGE gel (See 2.1.2.1.).

3.2.2. Origins and growth temperatures of novel esterases

The esterases identified from BLAST search came from diverse organisms from a range of environmental conditions so as to see if there were any patterns sequences specific to certain conditions (See Table 3.2.).

Esterase	Organism	Condition	Growth Media	Growth temperature (°C)	References for bacteria growth conditions
EstLA	<i>L. aggregata</i> (AKA <i>S. aggregata</i>)	Psychrophile, marine	Bacto marine	28	Uchino Y, et al., 1998 Biebl H, et al., 2007
EstCA	<i>C. acidiphilia</i>	Acidophile, soil	ISP2	28	Busti, E, et al., 2006
EstRM	<i>R. marinus</i>	Halophile and thermophile, marine	Thermos 162	65	Alfredsson, G A, et al., 1988
EstEM	<i>S. meliloti</i> (AKA <i>E. Meliloti</i>)	Forms biofilm to survive without host, soil	Rhizobium	26	Rinaudi, L, et al., 2006
EstRD	<i>R. denitrificans</i>	Anyoxigenic and psychrophile, marine	Bacto marine	20	Buchan, A, et al., 2005

Table 3.2. Organisms OsmC esterase originate from

Along with the native environmental conditions the organisms grow in, and what media and temperatures were needed to grow organisms in laboratory

3.2.3. Assay for determining esterase activity

To characterise the esterases, an assay had to be used that would allow for the detection of enzyme activity under a variety of conditions.

Characterisation of esterases can be achieved by a variety of techniques, e.g. by detecting the hydrolysis of ethyl butyrate substrate through measuring how much NaOH titrant was needed to neutralise butyric acid product (Adler, A J and Kistiakowsky, G B, 1961), by detecting the hydrolysis of α -naphthyl esters by using azo coupling between the α -naphthol product and diazonium salt to produce azo dye (Johnston KJ and Ashford AE, 1980). However for this project, the assay which measures esterase activity through the hydrolysis of nitrophenyl ester was used, so as to compare activities of esterases found through BLAST with published data for EstO and Δ EstO (Al-Khudary R, et al., 2010). Nitrophenyl esters consist of fatty acids of varying lengths being attached through an ester bond to a single molecule of nitrophenol (See figure 3.2.). Nitrophenol can be measured with a spectrometer 405-410nm (Winkler UK and Stuckmann M, 1979). Since the esterases ability to hydrolyse esters was based on the fatty acid chain length, nitrophenyl esters can be used to determine activity of the esterase against a series of different fatty acid chain lengths, at different conditions of temperature, pH, metal ion concentrations, inhibitor presence etc. Nitrophenyl benzoate specifically was used as the assay substrate because its benzoic acid moiety renders it difficult to be hydrolysed under any other condition other than catalysis by an esterase.

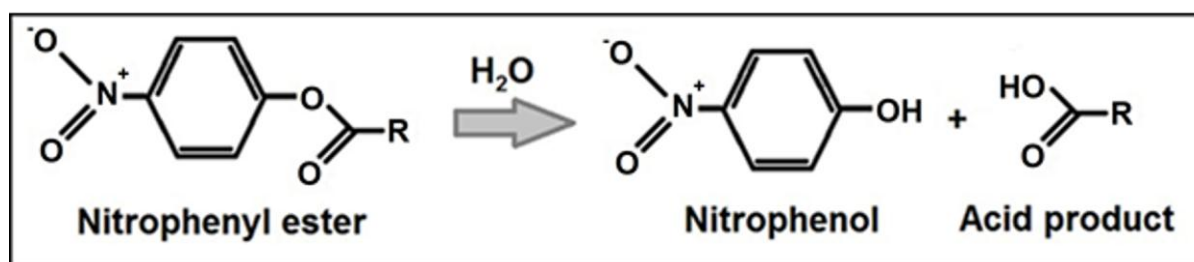


Figure 3.2. Hydrolysis of a nitrophenyl ester into nitrophenol and acid products

When a nitrophenyl ester undergoes hydrolysis, nitrophenol and acid were released. In solution, the nitrophenol gives a yellow colour, which can be measured at 405-410nm.

A stock reaction buffer was made of 25 mM Tris-HCl at pH 7 with 0.1% (w/v) gum arabic and 10% (v/v) ethanol, with 0.15 μ M nitrophenyl substrate dissolved in

ethanol (Al-Khudary R, et al., 2010). This nitrophenyl substrate/ethanol mix was made by heating in a microwave until all the substrate has been dissolved.

100 μl of esterase from one sample was mixed with 900 μl of Tris-HCl/substrate buffer in triplicate, and incubated at the desired temperature (typically 20 °C) for the desired time (typically 30 mins), they were then placed on ice for approximately 3 minutes, then reaction was halted through the addition of 100 μl of 25% NaCO_3 . The sample was then spun down for 3 minutes at 4 °C, and the reaction mixtures has their absorption measured at OD_{410} and the average value from all three reactions was calculated. The negative control for this experiment followed the same procedure, but no esterase was used. Instead, 100 μl esterase dialysis buffer was added to 900 μl of Tris-HCl/substrate buffer.

This reaction can be adjusted to work across a range of temperatures, a range of substrates, in the presence of metal chloride ions or inhibitors, or to measure activity after subjecting the esterase to a pH/temperature stability test. The activity of the esterase was measured in units, where one unit was equal to the mass of esterase required to release 1 μM of p-nitrophenol in one minute, and where $A = \epsilon cl$ (Al-Khudary R, et al., 2010).

To check activity of the enzyme in different pH conditions, the esterase and substrate were suspended in 1 x Universal Buffer (See 2.1.3.1.) instead of Tris buffer, but otherwise the reaction went ahead normally.

3.2.4. Determining esterase purification factor

One unit of esterase activity was defined as the mass of protein required to release 1 μMol of nitrophenol per minute after a 30 minute incubation of sample with Tris and nitrophenyl benzoate mix at 20 °C and pH 7 (Al-Khudary R, et al., 2010). Concentration of total nitrophenol produced from this reaction (performed in triplicate) was determined by the Beer-Lambert law, $A = \epsilon cl$. The molecular extinction coefficient of nitrophenol, ϵ , was determined to be 16000 $\text{M}^{-1} \text{cm}^{-1}$ in this lab by Dr. Louise Horsfall. Determining the concentration of nitrophenol produced in each reaction as well as the mass of protein present in each reaction allowed for the calculation of esterase activity unit for purified esterase and lysate. From this, specific activity - the esterase activity per mg of protein - can be calculated. The yield of esterase from lysate sample was derived through the

total activity, and the purification factor was determined from the ratio of purified esterase's specific activity to the lysate's specific activity.

3.3. Results

3.3.1. Purification of the esterases in this project

At the start of the project esterase genes cloned into pDest17 expression vectors by Dr. Louise Horsfall and Δ EstRD cloned into pEXP5-CT/TOPO vector by Dr Mai-Britt Jensen (See figure 3.3.). BL21-AI cells were transformed (See 2.6.1.1.1.) and the esterases expressed as described in 2.6.1.2.2. Because the genes were all expressed from pDest17 vector or pEXP5-CT/TOPO, all were translated with a poly-His tag, which meant the esterases could all be purified from their lysates via immobilised metal ion affinity chromatography (IMAC) (See 2.6.2.2.).

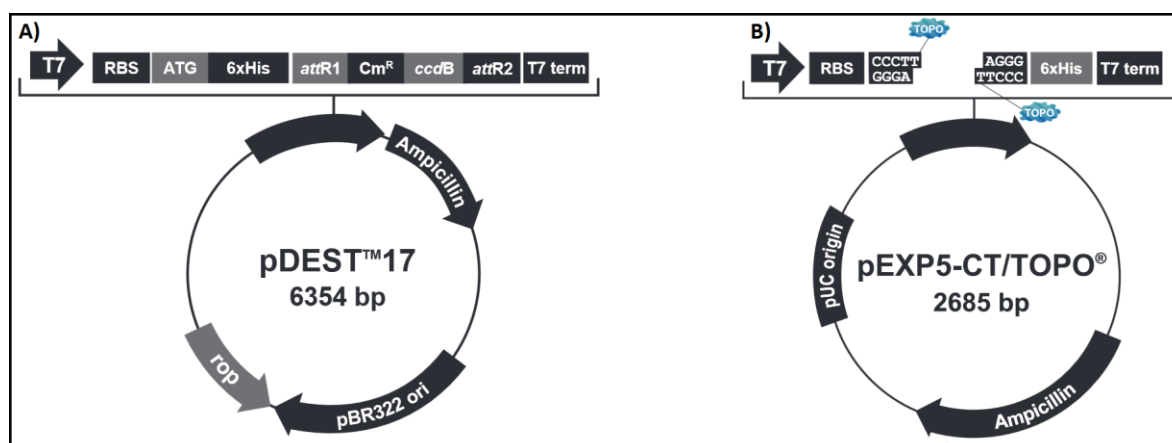


Figure 3.3. Structures of vectors used to express esterases

The physical structures and sizes of A) pDest17 and B) pEXP5-CT/TOPO, with insert sites downstream of the promoter and RBS in both highlighted. DNA is inserted into pDest17 through recombination through the *attR* sites, while in pEXP5-CT/TOPO, DNA is inserted through the Topoisomerase I binding sites. In the former, an N-terminal poly-His tag is added to the protein, in the latter, a C-terminal poly-His tag. Images modified to incorporate identifying text from Invitrogen protocols available online

(http://tools.lifetechnologies.com/content/sfs/vectors/pdest17_map.pdf and http://tools.lifetechnologies.com/content/sfs/manuals/pexp5_topo_man.pdf, accessed on 10/02/15)

3.3.2. Purification of EstLA from expression in BL21-AI

Expression of soluble EstLA was achieved with an induction with 2% filter-sterilised arabinose for a period of 4 hours at 37°C after the culture reached an absorbance value at OD₆₀₀ of 0.5 (See 2.6.1.2.2.). The protein was purified through IMAC (See 2.6.2.2.) and dialyzed to remove imidazole and was determined to be the protein of interest by it being of expected mass (47.7kDa) (See figure 3.4.) and by incubating in triplicate equal volumes of fractions containing the protein with buffer containing no protein with Tris buffer containing nitrophenyl acetate (See 3.2.3.). The protein concentration of lysate and the purified esterase was determined by a Bradford assay (See 2.6.2.3.).

Nitrophenyl benzoate was used as the assay substrate for two reasons. First it has a nitrophenol moiety which means that as it is hydrolysed, the rate of enzyme activity can be derived by measuring concentration of the nitrophenol through measurement of absorption at OD₄₁₀. Secondly its benzoic acid moiety renders it difficult to be hydrolysed under any other condition than by the action of an esterase.

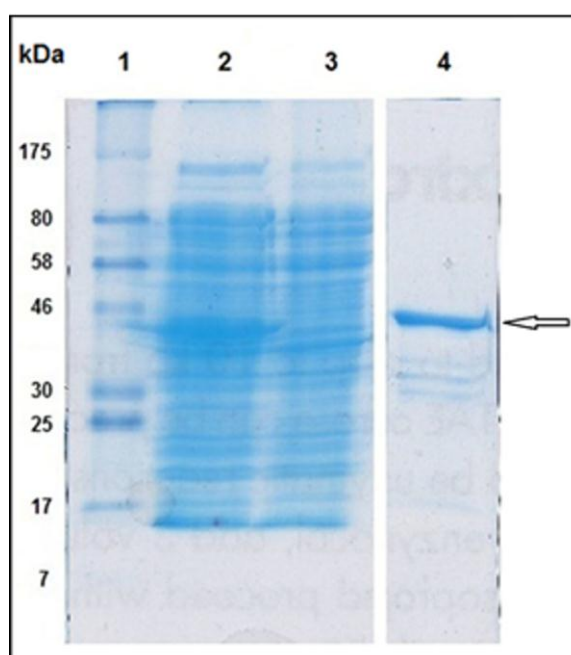


Figure 3.4. Expression and purification of soluble EstLA

SDS-PAGE analysis of soluble EstLA (47.7kDa) from BL21-AI transformants containing pDest17/EstLA that had undergone expression; samples were separated, stained and visualised on a denaturing SDS-PAGE gel. Lane 1: marker. Lane 2: bacterial lysate. Lane 3: flowthrough. Lane 4: purified EstLA (indicated by arrow)

3.3.3. Purification of Truncated Δ esterases

All Δ esterases were purified from cells that were induced under conditions as described or expressing EstLA by running bacterial lysate through an IMAC column (See 2.6.2.2.) (See figure 3.5.).

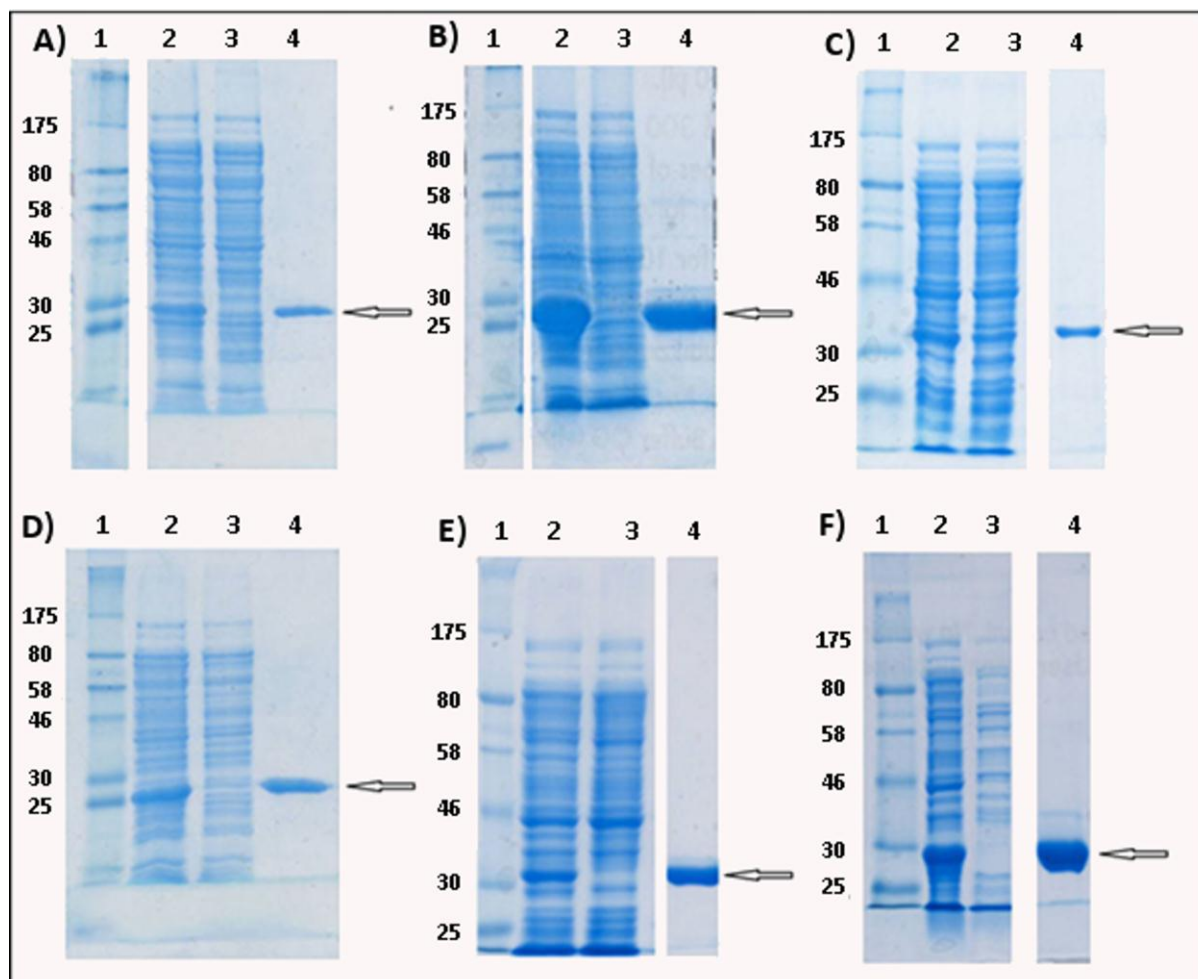


Figure 3.5. Expression and purification of soluble Δ esterase

SDS-PAGE analysis of all truncated esterases characterised in this project. Lane 1: marker. Lane 2: bacterial lysate. Lane 3: flowthrough. Lane 4: eluted protein (indicated by arrows). A) was Δ EstO (30.3 kDa), B) was Δ EstLA (31.6 kDa), C) was Δ EstCA (30.5 kDa), D) was Δ EstRD (29.8 kDa), E) was Δ EstEM (31.8 kDa) and F) was Δ EstRM (31 kDa).

Esterases were expressed from BL21-AI transformed with pDest17 vectors containing the genes coding for esterases (2.6.1.2.2.); expression was induced by the addition of 2% arabinose when culture growth reached an absorbance value at OD₆₀₀ of 0.6-0.8 and incubated for at least 4 hours at 37°C. Purification of

esterases was achieved through IMAC (See 2.6.2.2.). Fractions of collected elution buffer containing protein had samples run on an SDS-PAGE gel, and the fractions which contained protein that corresponded to the expected size of the expressed protein were dialysed.

3.3.4. Dialysis conditions for esterases in this project

The act of dialysis to remove imidazole from elution buffer containing purified protein could cause the protein to denature and become insoluble (Hamilton, S, et al. 2003). Every protein had different pH requirements and salt concentration requirements in the buffers used for elution and dialysis so as to prevent the protein from denaturing, causing it to precipitate out of solution. These conditions were determined by dialysing small volumes of protein in separate dialysis conditions and identifying what conditions resulted in the protein remaining soluble (Table 3.3.). The pH of the dialysis solution was chosen so as to maintain the buffering capability of the dialysis buffer, but to not be close to the pI of the protein. Additional components were added as they are general substances that can be used to adjust the gradient of ion movement from the buffers during dialysis.

All samples generated from this method were denatured using the SDS-PAGE protocol (See 2.1.2.1.) and were run alongside a protein marker.

Esterase	pH of buffer solutions	Additional Components
Δ EstO	8.5	N/A
EstLA/ Δ EstLA	7.2	N/A
Δ EstCA	7	0.5 M NaCl
Δ EstRM	9	0.35 M NaCl
Δ EstEM	8.5	0.5 M NaCl + 10% Glycerol
Δ EstRD	8	0.5 M NaCl

Table 3.3. Conditions required for OsmC immobilised metal ion affinity chromatography and dialysis

Compositions of dialysis buffers used to purify esterases. The presence of salt and glycerol help reduce the gradient of ion removal through dialysis, which prevents the proteins folding into an insoluble form.

3.3.5. Characterisation of the Δ esterases under a range of conditions

3.3.5.1. Characterisation of the temperature activity profiles of the Δ esterases

The temperature profile for each esterase was determined by performing an assay in triplicate (See 3.2.3.) at temperatures of 5°C-55°C in 5°C steps. Each temperature point had a negative control of substrate incubated with dialysis buffer containing no esterase. The change in absorbance per μmol of enzyme used in the assay for half an hour was calculated from the different absorption values at OD_{410} . These values were used to determine the temperature optima for each esterase. Each esterase had an individual temperature profile, although four of the six tested Δ esterases had an optimal temperature of 30°C (ΔEstO , ΔEstLA , ΔEstEM and ΔEstCA). After the optima were reached, activity dropped off, but not in a uniform fashion. ΔEstRD had a temperature optimum of 25°C (2439 $\Delta\text{Abs}/\mu\text{mole}$ enzyme in 30 min) but activity only rapidly decreases when temperature exceeded 30°C (See figure 3.6.). ΔEstRM had by far the highest activity of all tested esterases (9737 $\Delta\text{Abs}/\mu\text{mole}$ enzyme in 30 min) and the highest temperature optima at 55°C. The temperature range at which ΔEstRM was tested was increased and it was demonstrated to still have activity at 70°C.

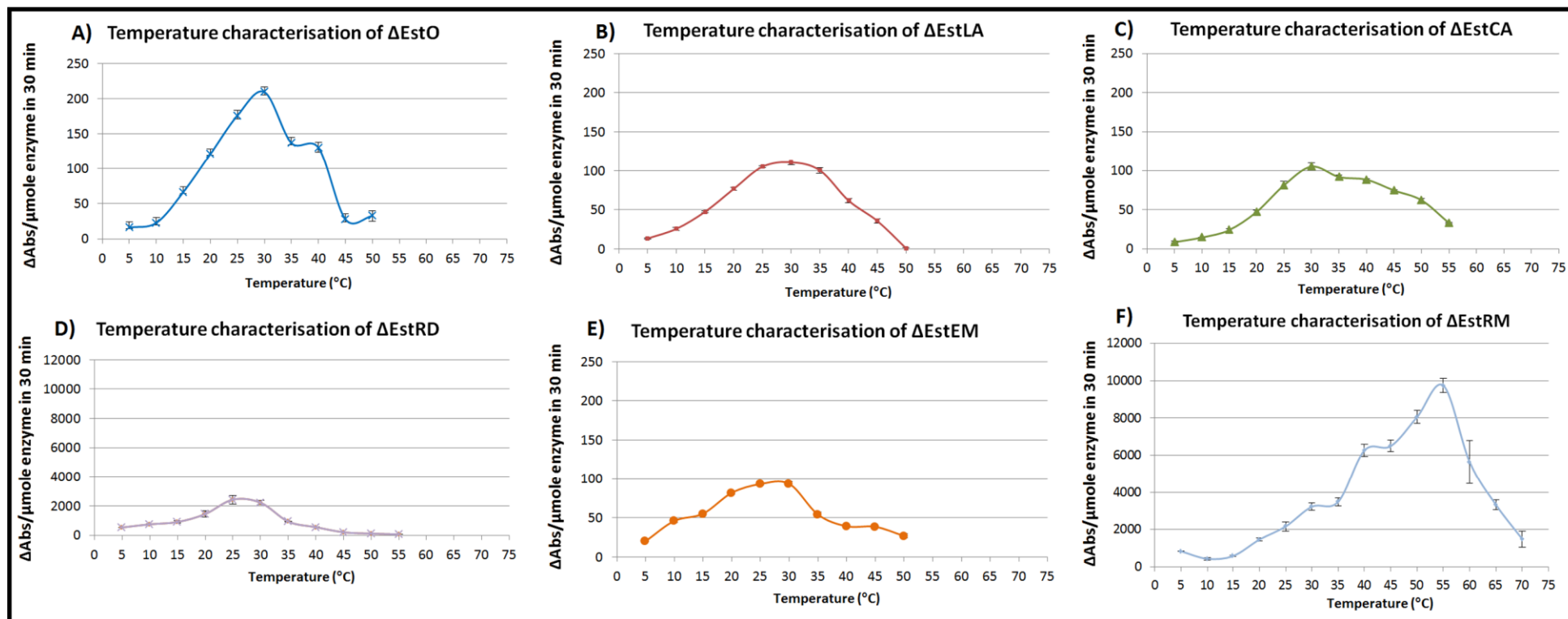


Figure 3.6. Effect of temperature on activity of Δ esterase

Protein samples were incubated with 0.15 μ M nitrophenyl benzoate as substrate at incubation temperatures which range from 5 $^{\circ}$ C to 55 $^{\circ}$ C (with the exception of Δ EstRM) through 5 degree incremental steps. Activity was measured in the change of absorbance at OD₄₁₀ per μ Mol of enzyme in each sample per 30 minutes. Experiments were performed in triplicate (See 3.2.3). Error bars correspond to standard error of the mean.

3.3.5.2. Characterisation of the pH profiles of the Δ esterases

A pH range from 4 to 10 in 0.5 pH increments was achieved using Britton-Robinson universal buffer (See 2.1.3.1.) for the reaction to occur as opposed to Tris buffer, at a constant temperature. Assays were as described in 3.2.3. (Al-Khudary R, et al., 2010).

As with determining optimal temperature conditions, each pH value had its own negative control of substrate and buffer without any enzyme present. The absorbance at OD₄₁₀ generated from these experiments were used in conjunction with the molecular extinction coefficient of nitrophenol at OD₄₁₀ to determine the concentration of nitrophenol produced. The results shown in figure 3.7. demonstrated that all the esterases characterised had optima of either pH 8.5 or pH 9. Δ EstLA, Δ EstCA and Δ EstEM had a pH optima of 8.5; Δ EstO, Δ EstRD and Δ EstRM had optima at pH 9. The esterase with the highest activity was Δ EstRM with 4223 Δ Abs/ μ mole enzyme in 30 min; the esterase which shows second highest activity at this point was Δ EstRD with 2718 Δ Abs/ μ mole enzyme in 30 min. All other esterases do not show activity above 200 Δ Abs/ μ mole enzyme in 30 min, with Δ EstCA having its optima with the comparatively lowest activity at 47 Δ Abs/ μ mole enzyme in 30 min. The pH of the environment the esterases function in influences the activity of the esterases.

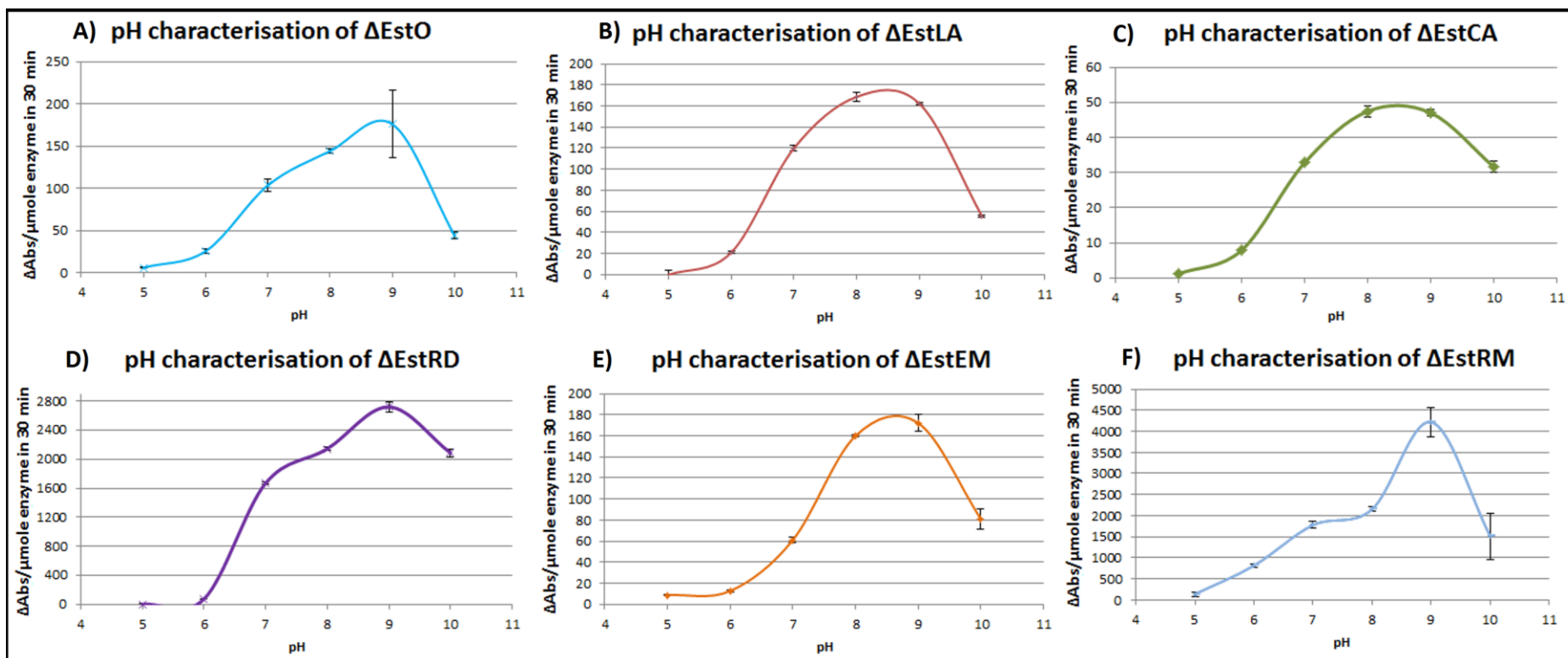


Figure 3.7. Effect of pH on activity of Δ esterase

Protein samples were incubated with 0.15 μ M nitrophenyl benzoate as substrate in Universal Buffer at separate incubation pH values 5 to 10 through incremental steps. Activity was measured in the change of absorbance values at OD₄₁₀ per μ Mol of enzyme in each sample per 30 minutes. Experiments were performed in technical triplicate. Error bars correspond to standard error of the mean.

3.3.5.3. Characterisation of Δ esterases activities with a range of substrates of varying fatty acid chain length

Experiments were undertaken to determine substrate specificity of the esterases with respect to the acid chain length and complexities. Finding esterases better at breaking down esters with long-chain alkyl groups or aromatic groups would help narrow the search for esterases that would be better at breaking down fats and oils, seeing as fats and oils contain long fatty acids.

Activity of esterases against substrates with different alkyl chain lengths and structures was investigated using the assay described in 3.2.3. (Al-Khudary R, et al., 2010). Nitrophenyl esters were chosen to investigate how activity altered with the substrate's alkyl chain length and complexities. These esters consisted of benzoate, octanoate, decanoate, dodecanoate, myristate and stearate (See Table 3.4.).

Δ EstO (See figure 3.8.A) had higher activity against nitrophenyl dodecanoate than all other substrates investigated, with 3.7 times higher activity with this substrate than nitrophenyl benzoate (774 Δ Abs/ μ mole enzyme in 30 min compared to 209 Δ Abs/ μ mole enzyme in 30 min). Activities against long chain substrates were similar to the esterases' activity against nitrophenyl benzoate. These results indicated that this esterase's active site could best accommodate a C12 acyl ester.

Results indicated that the Δ EstLA was most active against nitrophenyl octanoate, working 14 times greater against it than against nitrophenyl benzoate (3948 Δ Abs/ μ mole enzyme in 30 min to 281.21 Δ Abs/ μ mole enzyme in 30 min) (See figure 3.8. B). This enzyme also had higher activity with nitrophenyl myristate than nitrophenyl benzoate.

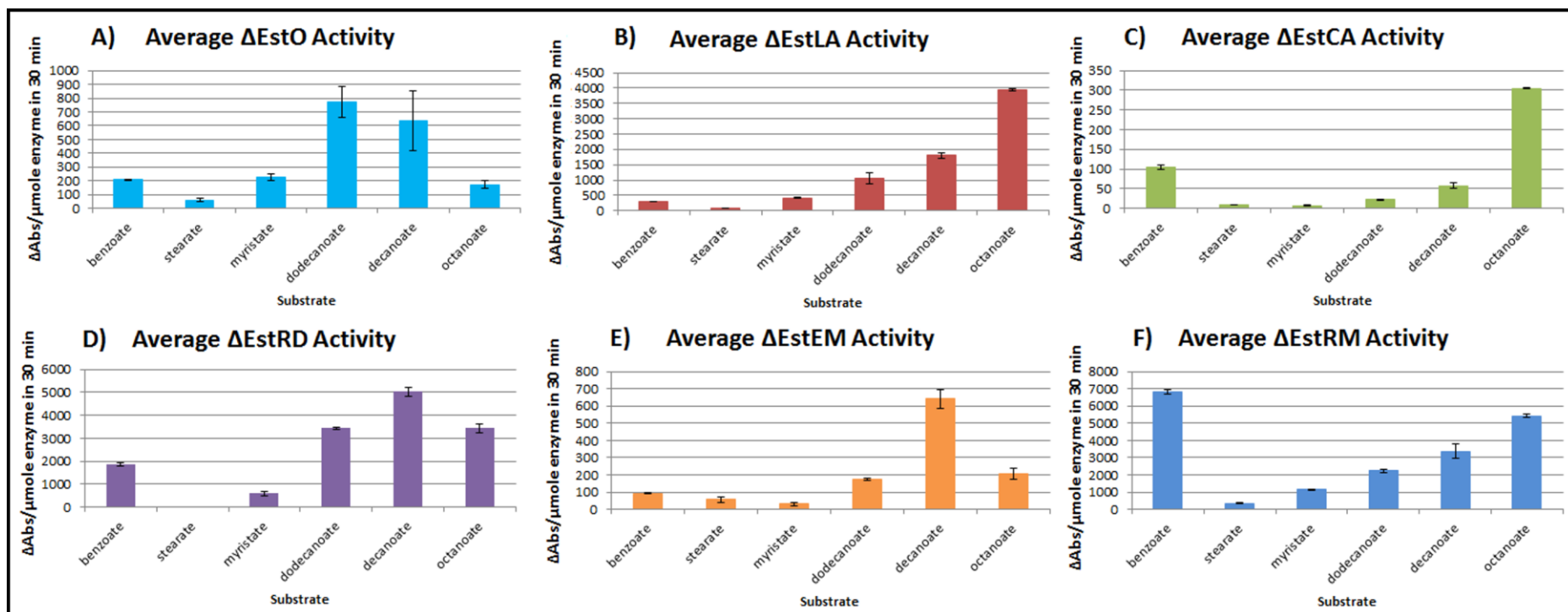


Figure 3.8. Substrate specificity of Δ esterase

Protein samples were incubated with nitrophenyl esters of varying acyl chain length as substrate, benzoate (C7) (with C6 arranged in an aromatic group), octanoate (C8), decanoate (C10), dodecanoate (C12), myristate (C14) and stearate (C18). Activity was measured in the change of absorbance values at OD₄₁₀ per μ Mol of enzyme in each sample per 30 minutes. Experiments were performed in triplicate (See 3.2.3). Error bars correspond to standard error of the mean.

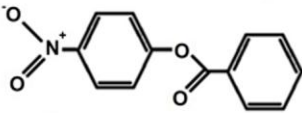
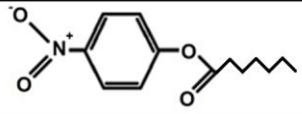
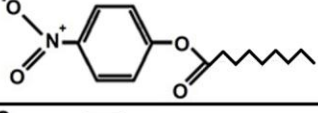
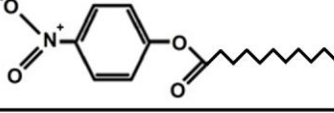
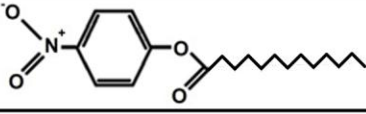
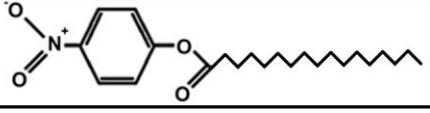
Substrate	Atomic Structure
Nitrophenyl Benzoate	
Nitrophenyl Octanoate	
Nitrophenyl Decanoate	
Nitrophenyl Dodecanoate	
Nitrophenyl Myristate	
Nitrophenyl Stearate	

Table 3.4. The chemical structure of substrates used in esterase characterisation

A comparison of the structures of all the ester substrates used in this project, detailing the differences in acid moiety chain length and structure.

Δ EstCA, was similar to Δ EstLA in that it had highest activity against nitrophenyl octanoate compared to the other substrates tested, 304.87 Δ Abs/ μ mole enzyme in 30 min compared to 105 Δ Abs/ μ mole enzyme in 30 min when hydrolysing nitrophenyl benzoate (See figure 3.8. C). Against nitrophenyl myristate and stearate, it reached only 7 and 10 Δ Abs/ μ mole enzyme in 30 min respectively.

Results showed that Δ EstRD had a higher activity against nitrophenyl decanoate than all other substrates investigated, 5021 Δ Abs/ μ mole enzyme in 30 min compared to 1837 Δ Abs/ μ mole enzyme in 30 min for nitrophenyl benzoate (See figure 3.8. D). It was less active against nitrophenyl myristate and stearate, 601 Δ Abs/ μ mole enzyme in 30 min and undetectable respectively.

Figure 3.8. E) indicated that the Δ EstEM had higher activity against nitrophenyl decanoate, 642 Δ Abs/ μ mole enzyme in 30 min compared to 93 Δ Abs/ μ mole enzyme in 30 min for nitrophenyl benzoate. Like Δ EstRD, it was less active against nitrophenyl myristate and stearate (31 and 93 Δ Abs/ μ mole enzyme in 30 min, respectively) than against nitrophenyl benzoate.

Δ EstRM had its highest activity against nitrophenyl benzoate, higher than all other substrates investigated, 6826 Δ Abs/ μ mole enzyme in 30 min (See figure 3.8. F). The next highest activity was with nitrophenyl octanoate at 5434 Δ Abs/ μ mole enzyme in 30 min. Activity against nitrophenyl myristate and stearate was relatively poor, but still higher than the other Δ esterases' (1152 and 353 Δ Abs/ μ mole enzyme in 30 min, respectively).

3.3.5.4. Investigation into effects of metal ion on activity of Δ esterases

Metal ion tolerance of the esterases was tested using the assay described in 3.2.3., but with the esterases being pre-incubated for 30 minutes with 10 mM concentrations of either K^+ , Ca^{2+} , Mg^{2+} , Co^{2+} , Zn^{2+} , Fe^{2+} or Ni^{2+} ions present (from the metal chloride salts) as well (modified from Al-Khudary R, et al., 2010). The absorbance readings at OD_{410} were converted into percentage values, with 100% value being equivalent to a reaction that had no metal ion pre-incubation. Negative controls for each tested ion consisted of reaction mixes being pre-incubated with metal ions, but having no esterase present.

The effect that these metal ions have on the esterase will give a greater understanding as to how each esterase's active site is accessed by substrate. The active site serine residue acts as a nucleophile

Δ EstO activity was increased in the presence of Ca^{2+} and Mg^{2+} , showing 146% and 120% activity respectively when pre-incubated with these metal salts. Both Co^{2+} and K^+ reduced activity to 75% and 87%. However, this esterase was most inhibited by Fe^{2+} , Ni^{2+} and Zn^{2+} , with activity being reduced to 33%, 28% and 9% respectively (See figure 3.9. A).

Δ EstLA's results indicated that hydrolytic activity was enhanced when pre-incubated with K^+ and Mg^{2+} (109% and 115%). Activity was reduced with Co^{2+} , Fe^{2+} and Ca^{2+} to 33%, 42% and 46% respectively, but Ni^{2+} and Zn^{2+} pre-incubation caused the greatest loss in activity, 1% and 6% overall (See figure 3.9. B).

Δ EstCA's characterisation revealed that in the presence of K^+ and Mg^{2+} , activity was reduced, showing 96% and 84% activities respectively. With Ca^{2+} , activity was enhanced to 113%. However, Ni^{2+} , Co^{2+} , Fe^{2+} and Zn^{2+} ions significantly

reduced activity of the esterase, resulting in 10%, 23%, no activity and 6% activities respectively (See figure 3.9. C).

Δ EstRD's characterisation showed that activity in the presence of K^+ , Mg^{2+} and Ca^{2+} was almost identical to the positive control reaction (101%, 92% and 101%). Activity was reduced to 3% with Co^{2+} , while no activity was recorded for pre-incubation with Fe^{2+} , Ni^{2+} and Zn^{2+} .

Δ EstEM's activity in the presence of Zn^{2+} , Mg^{2+} and Ca^{2+} was enhanced (112%, 121% and 144% respectively) while Fe^{2+} pre-incubation did not affect the esterase's activity (99%). Pre-incubation with K^+ reduced activity to 42% while Ni^{2+} and Co^{2+} pre-incubation resulted in a reduction to 17% activity for Ni^{2+} and no activity was recorded for Co^{2+} (See figure 3.9. E).

When Δ EstRM was characterised, results indicated K^+ pre-incubation did not change activity (104%). With Mg^{2+} , Co^{2+} and Ca^{2+} ions, esterase activity was lowered by about 15-20%; 86%, 78% and 88% respectively. Fe^{2+} , Ni^{2+} and Co^{2+} ions reduced the esterase's activity to 18%, 43% and 15% respectively (See figure 3.9. F).

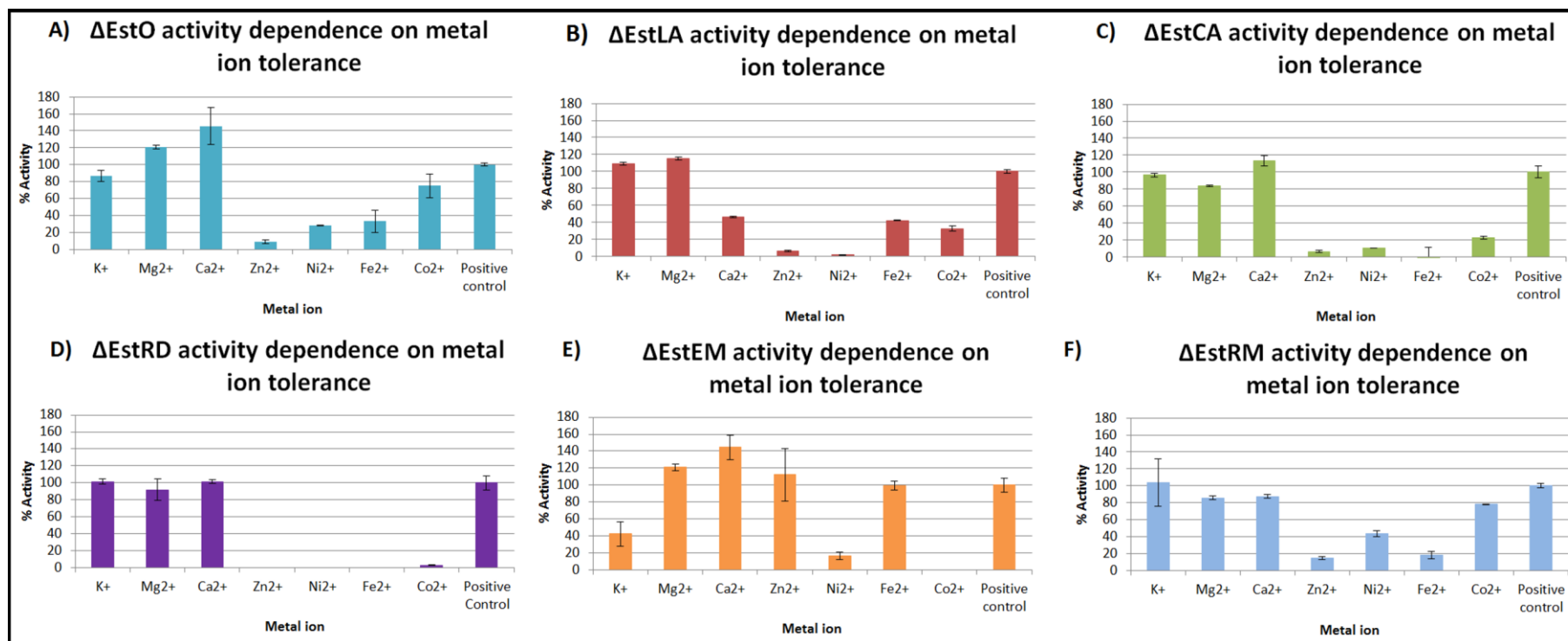


Figure 3.9. Effect of metal ions on activity of Δ esterase

Protein samples were pre-incubated for 120 minutes at 20°C with 10 mM of metal chloride salts. After pre-incubation, the proteins were incubated with 0.15 μ M nitrophenyl benzoate as substrate but with residual esterase activity shown as a percentage against the positive control with no metal salts present. Experiments were performed in triplicate (See 3.2.3). Error bars correspond to standard error of the mean.

3.3.5.5. Investigation into effects of putative inhibitors on activity of Δ esterases

Activity of the esterases in the presence of typical enzyme inhibitors was measured using the assay described in 3.2.3., but the esterases were pre-incubated in the presence of esterase inhibitors identified from the scientific literature for 1 hour before being assayed against nitrophenyl benzoate (Modified from Al-Khudary R, et al., 2010). OD₄₁₀ absorbance values were converted to percentage values, with 100% activity equating to the positive control of esterase pre-incubated without putative inhibitor. Negative controls consisted of reaction mixes pre-incubated with the potential inhibitors, but having no esterase present. The inhibitors were chosen because each could alter the activity of enzymes through different ways (See Table 3.5.)

Inhibitor	Chemistry of inhibitor and effect on enzymes
Pefabloc	Covalently binds to nucleophilic serine residues, preventing nucleophilic catalysis.
EDTA	Chelating agent that binds with great affinity to positively charged metal ions.
DTT	Reducing agent that bind to thiol residues, inhibiting their effect on protein structure.
Tween 20	Ampiphilic detergent capable of facilitating mixtures of polar and non-polar solvents.

Table 3.5. The actions of inhibition of chemicals chosen

A brief summary describing how the different chemicals chosen for characterising the esterases from this project can inhibit enzyme activity.

Figure 3.10. A) shows that Δ EstO was inhibited by all of the potential esterase inhibitors; showing the least reduction in activity with EDTA (42.37% and 92% with 10 mM and 1 mM EDTA pre-incubation). Activity was reduced by Pefabloc (15% and 29% for 4 mM and 0.4 mM). DTT pre-incubation results in the greatest reduction in activity (10% and 23% for 0.1 mM and 1 mM), 54% activity was maintained in the presence of Tween 20.

Δ EstLA was inhibited by all inhibitors tested; its activity was reduced with DTT and EDTA (4% and 37% for 1 mM and 0.1 mM DTT and 30% activity for both concentrations of EDTA). Reduction of activity was found when pre-incubated with

Pefabloc (8% and 30% for 4 mM and 0.4 mM) 56% activity was maintained in the presence of Tween 20 (See figure 3.10. B).

Δ EstCA was not inhibited by all inhibitors tested; its activity was reduced by DTT and Tween 20 pre-incubation (13% and 12% for 1 mM and 0.1 mM DTT, total activity loss for Tween 20). Pre-incubations with Pefabloc and EDTA were not as inhibitory (27% and 44% for 4 mM and 0.4 mM Pefabloc, 38% for 10mM EDTA) with a pre-incubation with 1 mM EDTA actually increasing activity (140%) (See figure 3.10. C).

Δ EstRD was inhibited by all inhibitors tested; esterase activity was most strongly reduced by DTT, Pefabloc and Tween 20, (No activities for 1 mM DTT and Tween 20, 18% for 0.1 mM DTT, 2% and 34% for 4 mM and 0.4 mM Pefabloc) (See figure 3.10. D). Activity in the presence of EDTA was reduced; 71% and 71% for 10 mM and 1 mM respectively (See figure 3.10. D).

Δ EstEM activity was inhibited by all tested inhibitors; with activity markedly reduced against DTT, EDTA and Tween 20 (14% and 39% for 1 mM and 0.1 mM DTT, inactivation with 10 mM EDTA, and 12% activity for 1 mM EDTA, while activity in the presence of Tween 20 was reduced to 14%). However, activity was not greatly reduced in presence of Pefabloc (85% and 97% activity for 4 mM and 0.4 mM pre-incubations) (See figure 3.10. E).

Δ EstRM's activity was totally removed with the pre-incubation with Tween 20 and 1 mM DTT (See figure 3.10. F), and was limited with 10 mM DTT (5%) and Pefabloc (10% and 6% for 4 mM and 0.4 mM respectively). EDTA at 10 mM also reduced activity (18%), but 1 mM EDTA did not significantly reduce activity (94%).

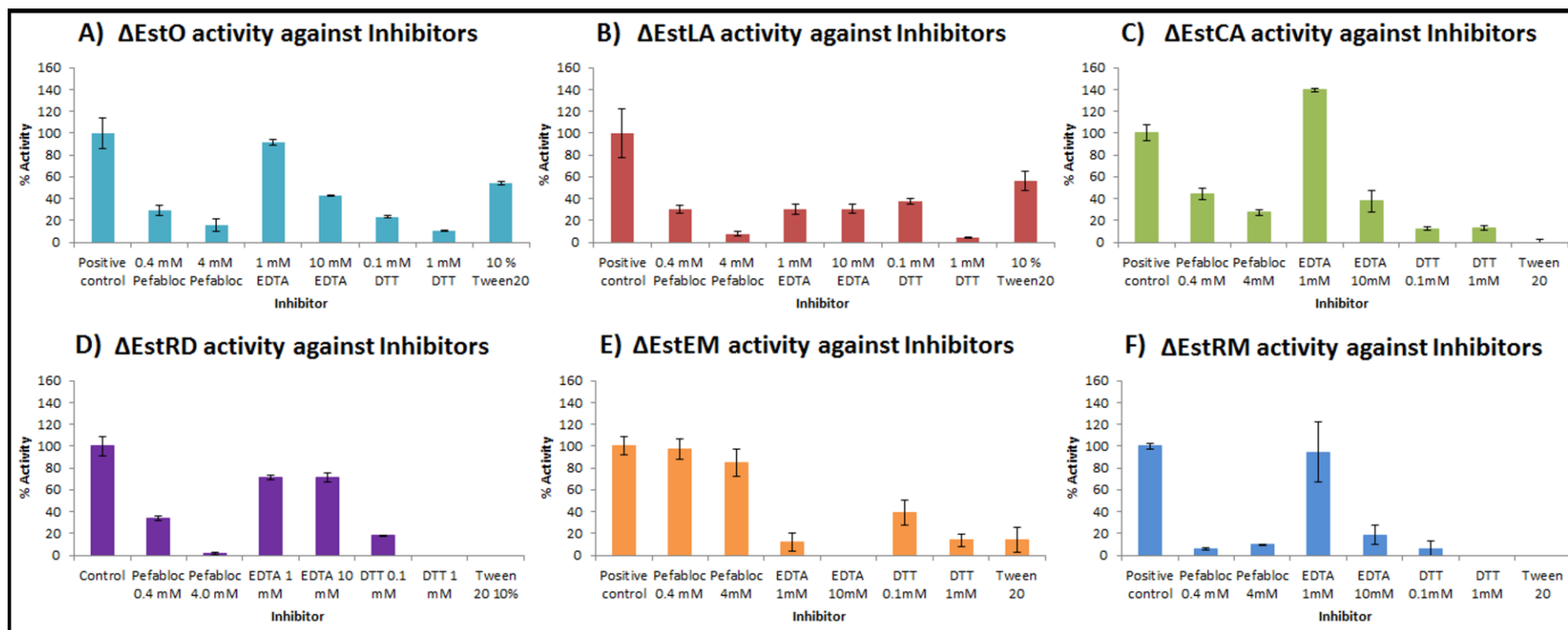


Figure 3.10. Effect of putative esterase inhibitors on activity of Δ esterase

Protein samples were pre-incubated for 60 minutes at 20°C with a selection of esterase inhibitors. After pre-incubation, the proteins were incubated with 0.15 μ M nitrophenyl benzoate as substrate (See 2.6.2., Esterase assay; Δ esterase variation), but with residual esterase activity being made as a percentage against a positive control with no inhibitor present. Experiments were performed in triplicate (See 3.2.3). Error bars correspond to standard error of the mean.

3.3.6. Multimeric state of Δ esterases

Experiments were performed to determine if any of the OsmC esterases were monomeric by running purified protein sample through a non-denaturing PAGE gel or semi-reducing SDS-PAGE gel (See 2.1.2.1.). At first, protein samples were run on an SDS-PAGE gel under either fully reduced and semi-reduced states, i.e. before being run on the gel, the samples were either suspended in loading dye containing no reducing chemicals and not heated or were suspended in loading dye with β -mercaptoethanol and boiled for 5 minutes; the fully-reduced samples showed a different banding pattern to the semi-reduced sample. Attempts were then made to run OsmC esterases through a native polyacrylamide gel, but results were poor for most esterases, only a couple of OsmC esterases showed distinct banding on native gels (See figure 3.11.). All of the OsmC esterases appeared to be in multimeric form.

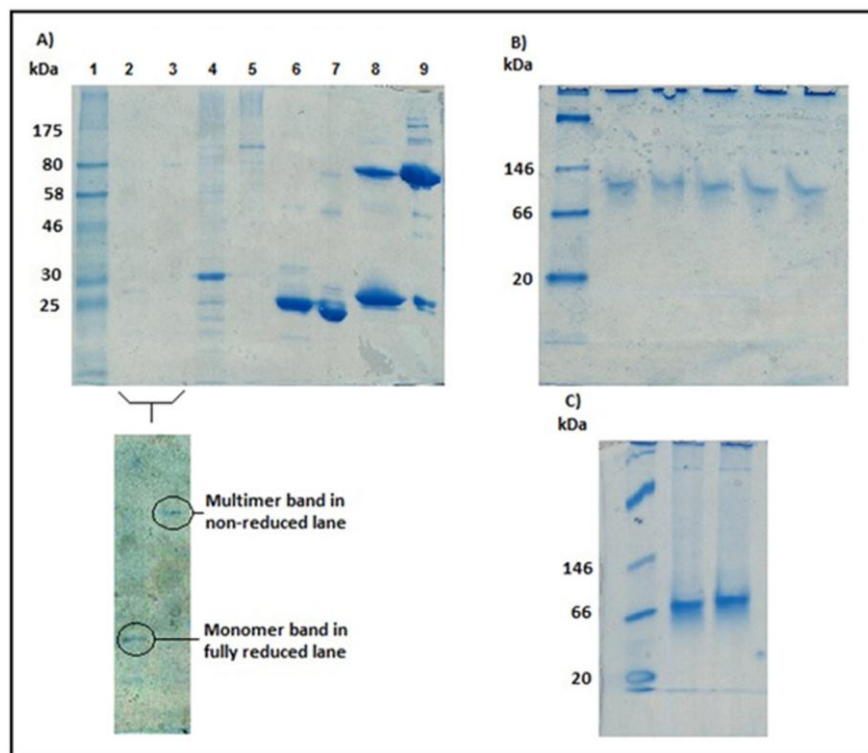


Figure 3.11. Native and semi-reductive gels demonstrating the multimeric states of OsmC esterases

A) Lane 1: marker. Lanes 2 and 3: Δ EstO. Lanes 4 and 5: Δ EstCA. Lanes 6 and 7: Δ EstRM. Lanes 8 and 9: Δ EstLA. Each enzyme was run under semi-reduced and reduced conditions respectively. Lanes 2 and 3 highlighted due to poor band intensity B) native polyacrylamide gel with five lanes of Δ EstEM run parallel to a native marker. The mass of the bands were larger than the expected monomer (43.98kDa). C) native polyacrylamide gel upon with two lanes of Δ EstRD run parallel to native marker. The mass of the bands were larger than the expected monomer (42.79kDa).

3.4. Discussion

3.4.1. Discovery of a new family of esterases

The six esterases characterised in this work constitute a new family of esterases. Al-Khudary R, et al., 2010 stated that EstO does not belong to any of the eight lipolytic families (Arpigny J L and Jaeger K E, 1999) and that EstO was the first example of an OsmC-esterase identified.

BLASTp searches of the truncated esterases characterised in this work indicated that there was homology to non-lipolytic α/β hydrolases from prokaryotes (Δ EstCA *Streptomyces violaceusniger* α/β hydrolase, Δ EstEM and Δ EstLA showing 64% and 65% homology to *Pseudovibrio* α/β hydrolase, Δ EstLA

having 58% homology to *Colwellia psychrerythraea* α/β hydrolase, Δ EstRM showing 57% homology to *Thioflavicoccus mobilis* α/β hydrolase. etc.). Members of Family V show homologies to non-lipolytic α/β hydrolases, up to 20-25% amino acid similarities (Arpigny J L and Jaeger K E, 1999). Comparing sequences of family V esterases with the sequences of esterases analysed in this project revealed that there were also shared sequence patterns, i.e. GX SXGG (Arpigny J L and Jaeger K E, 1999). From the definitions of the esterase families known, it appears that these esterases are closely related to Family V.

3.4.2. Comparison of Δ EstO with published EstO and Δ EstO activities

The purification method in this work was different to that used previously (Al-Khudary R, et al., 2010). Instead of the *E. coli* Tuner (DE3) and pLacI used by Al-Khudary R, et al., 2010, BL21-AI and pDest17 were used. Glucose was used in the media to repress expression of the araBAD promoter in BL21-AI, inhibiting expression of T7 RNA polymerase. This level of control was required to prevent cell death due to toxicity due to over-expression of esterase observed in earlier work by Dr. Louise Horsfall.

The optimal temperature for activity of Δ EstO from this work was very similar to EstO from Al-Khudary R, et al., 2010 at 25°C. However, results of this work show Δ EstO to be much more active at its optimal temperature than in published work.

This is a higher temperature than the environment *P. Arctica* is found in but this is not unusual, as there are many recorded instances of psychrophilic enzymes having temperature optima greater than that of the growth conditions experienced in their original hosts, e.g. extracellular chitinase and scleroprotease recovered from organisms residing in aphotic Antarctic sediment, protease from *Flavobacterium balustinum* P104 (Reichardt W, 1987 and Morita Y et al., 1997).

In Al-Khudary R, et al., 2010, a final concentration of 2 U/mg of EstO was used at each temperature point to determine the optima; 100% activity in the paper was equivalent to 2 μ Mols of nitrophenol produced per minute by 1 mg of EstO.

The activity of Δ EstO at optimal temperature derived in this project was higher than observed in the paper. Instead of releasing 2 μ Mols of nitrophenol

per minute at its temperature optima, EstO in this project released almost 3.5 times as much product.

Optimal pH of Δ EstO from this work was different to EstO and Δ EstO from the literature - according to the Al-Khudary R, et al., 2010, Δ EstO showed optimal activity at pH 7 and EstO showed optimal activity at pH 7.5, whereas in this work, the optimal pH of Δ EstO was determined to be pH 9.

Δ EstO from this work did not show the same substrate preferences as described in Al-Khudary R, et al., 2010, where EstO and Δ EstO work best against butyrate and activities against substrates with a chain length of twelve decrease to almost zero. However, in this work, Δ EstO had the highest activity against nitrophenyl dodecanoate of all the nitrophenyl substrates tested.

Δ EstO from this work was not identical to the pattern of activity in the presence of metal ions as described in Al-Khudary R, et al., 2010. Fe^{2+} and Co^{2+} ions had been recorded as totally or almost totally blocking activity of EstO, but Δ EstO shows 30-50% residual activity when incubated with said ions. In this project, the activity of Δ EstO with Fe^{2+} and Co^{2+} ions was 33% and 75% respectively. Work also revealed an increase in Δ EstO activity in the presence of Ca^{2+} and Mg^{2+} ions; Al-Khudary R, et al., 2010 stated that EstO or Δ EstO's activity was reduced to around 70-85%. Some esterases, namely CA, RM, RD and EM, had Na^+ present in their buffer (See Table 3.2.) so as to prevent precipitation, which could mask or alter the effect of other metal ions.

This work demonstrated that inhibition of Δ EstO activities correlated with results from Al-Khudary R, et al., 2010, with two exceptions; EDTA and Tween 20. Al-Khudary R, et al., 2010 recorded that Δ EstO retained 60% activity in the presence of 10 mM EDTA while Tween 20 reduced Δ EstO's activity to less than 10%. In this work, Δ EstO retained only 42% activity in the presence of 10 mM EDTA and approximately 50% activity was maintained with Tween 20.

The differences in activities could be due to the two versions of the esterases coming from different expression hosts - pDest17 vector was chosen in this lab to increase expression rate, but such an increase could influence how

the esterase folds. To test this, one would need to derive the structure of the esterase produced in the vector and host combination in this project, and then compare it with the structure of the esterase produced by the vector and host used by Al-Khudary R, et al., 2010.

Other factors that could alter the structure of the protein in solution would be the concentration of purified esterase; there have been records of too high a concentration of enzyme *in vitro* resulting in denaturation.

The difference in activity could also be due to the age of the esterases used. Proteins in *in vitro* environments can undergo changes which can alter their activity, e.g. tubulin and mononucleosomes accumulating isoaspartyl sites over time (Carter W G and Aswad D W, 2008, Najbauer J *et al.*, 1996). Such alterations in protein chemistry could render the esterase less stable at higher temperatures or reducing activity. However, the age of the esterase tested in the Al-Khudary R, et al., 2010 was not given - so there would be no way to accurately take such a change into account.

3.4.3. Comparing activities of all investigated Δ esterases

The esterase which showed the highest activity in most assays was Δ EstRM. Δ EstRD, the second most active esterase, had greater or equivalent activity to Δ EstRM against nitrophenyl benzoate between 20°C-25°C (Δ EstRD showed 1448 and 2430 Δ Abs/ μ mole enzyme in 30 min at each temperature point respectively and Δ EstRM showed 1458 and 2161 Δ Abs/ μ mole enzyme in 30 min at each temperature point respectively), and it had greater activity than Δ EstRM against nitrophenyl decanoate and nitrophenyl dodecanoate (Δ EstRD showed 5021 and 3431 Δ Abs/ μ mole enzyme in 30 min against each substrate respectively and Δ EstRM showed 3370 and 2230 Δ Abs/ μ mole enzyme in 30 min against each substrate respectively) (See figures 3.6. and 3.8.).

Under all other circumstances, Δ EstRM was the most active esterase, e.g. Δ EstRM showed over 10 times as much activity as Δ EstO at the latter's optimal temperature (See figure 3.12.) and almost 40 times more active than Δ EstO at their optimal pH of 8.5. (See figure 3.13.). In addition to the greater activity in general, Δ EstRM also showed activity over a larger temperature range than all other esterases, showing optimal activity at 55°C, a temperature where some investigated esterases had lost all activity.

3.4.3.1. Comparison of all Δ esterases activities across temperature range

Δ EstRM originates from *R. marinus*, a thermophilic and halophilic organism that originates from Icelandic submarine hot springs with temperatures ranging from 75-95 °C (Alfredsson GA, et al., 1988). No other esterase originated from an organism which grew in an environment as hot as *R. marinus*, so it was not surprising to find that the activity of Δ EstRM at higher temperatures was not matched by the other esterases which were not derived from a thermophile. Neither was it surprising that the peak temperature activity of Δ EstRM was not at the growth temperature of *R. marinus*. Many enzymes work at sub-optimal conditions *in vivo*; they only need to work sufficiently well to allow for the organism to survive.

Δ EstRM and Δ EstRD were the most active esterases when assayed across temperature range, showing optima at 55 °C and 25 °C respectively. The optimal temperature points were very similar for the remaining four esterases; they all had optimal activity at 30 °C.

At 20 °C, the temperature at which the ideal esterase would be put to work as a cold-water laundry detergent constituent, Δ EstO works at 58% of its optima, Δ EstLA works at 69% of its optima, Δ EstCA works at 4% of its optima, Δ EstRD works at 58% of its optima, Δ EstEM works at 86% of its optima and Δ EstRM works at 15% of its optima (See figure 3.12.). However, the activity of Δ EstRM at its optima was so much larger than any of the others that though its activity was reduced the most at 20 °C, it had greater activity at this temperature than any other OsmC esterase.

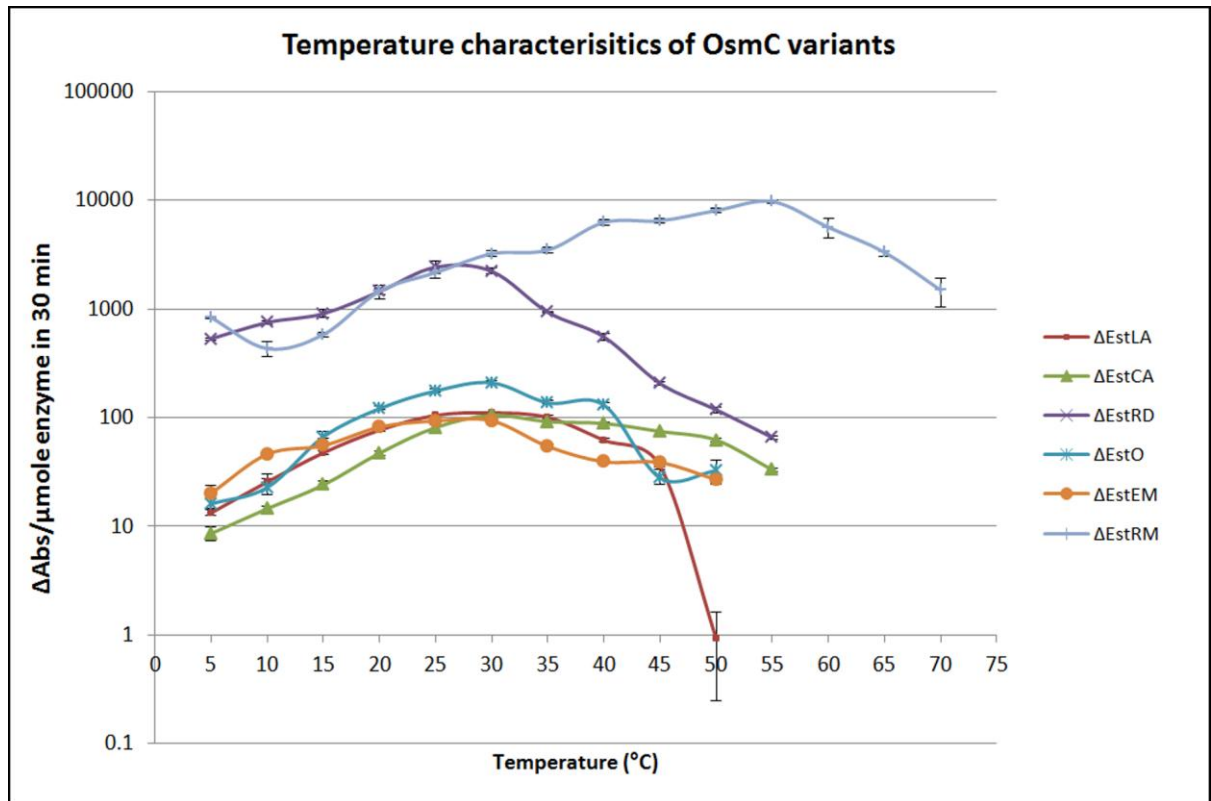


Figure 3.12. Comparison of Δ esterase activity across a range of temperatures

Each of the figures for all Δ esterase activity across temperature, i.e. Figures 3.6. A)-F) had been combined on a single graph with a logarithmic y-axis in order to easily compare their activity with one another.

3.4.3.2. Comparison of all Δ esterases activities across pH range

Results obtained from determining optimal pH conditions (See figure 3.13.) were interesting because they did not follow the patterns one might predict relating to the pH environment that the original organisms the esterases came from. All esterases had pH optima between 8.5-9, and while Δ EstRM and Δ EstRD had the two highest values at their optima (4223 and 2718 Δ Abs/ μ mole enzyme in 30 min respectively) the remaining esterases' optima were around the same value (Δ EstLA, Δ EstO and Δ EstEM having activities of 169, 172 and 176 Δ Abs/ μ mole enzyme in 30 min respectively). The only exception was Δ EstCA, which had the lowest activity at every pH point (Its optimal activity was 52 Δ Abs/ μ mole enzyme in 30 min) except at pH 5, where Δ EstLA showed no observable activity). Δ EstCA following peak pH activity pattern of other Δ esterases would indicate that this esterase does not function well in the environmental pH of *C. acidiphilia*, which is between 4.3-6.8. However, this would indicate that these esterases all function in an environment that is

alkaline; i.e. it is a distinct possibility that cellular chemistry these esterases work in is alkaline. Testing the interior pH of the native organism would confirm this hypothesis.

A feature of note in a number of these graphs of esterase activity against temperature and pH was that the line passing through all points seldom forms a smooth parabolic curve - there were points in temperature where change in activity plateaued. These anomalous results may be due to problems associated with dissolving the nitrophenol substrate in ethanol. It would also be convenient to repeat this assay with a different buffer type besides from universal buffer to see if similar activity patterns are maintained.

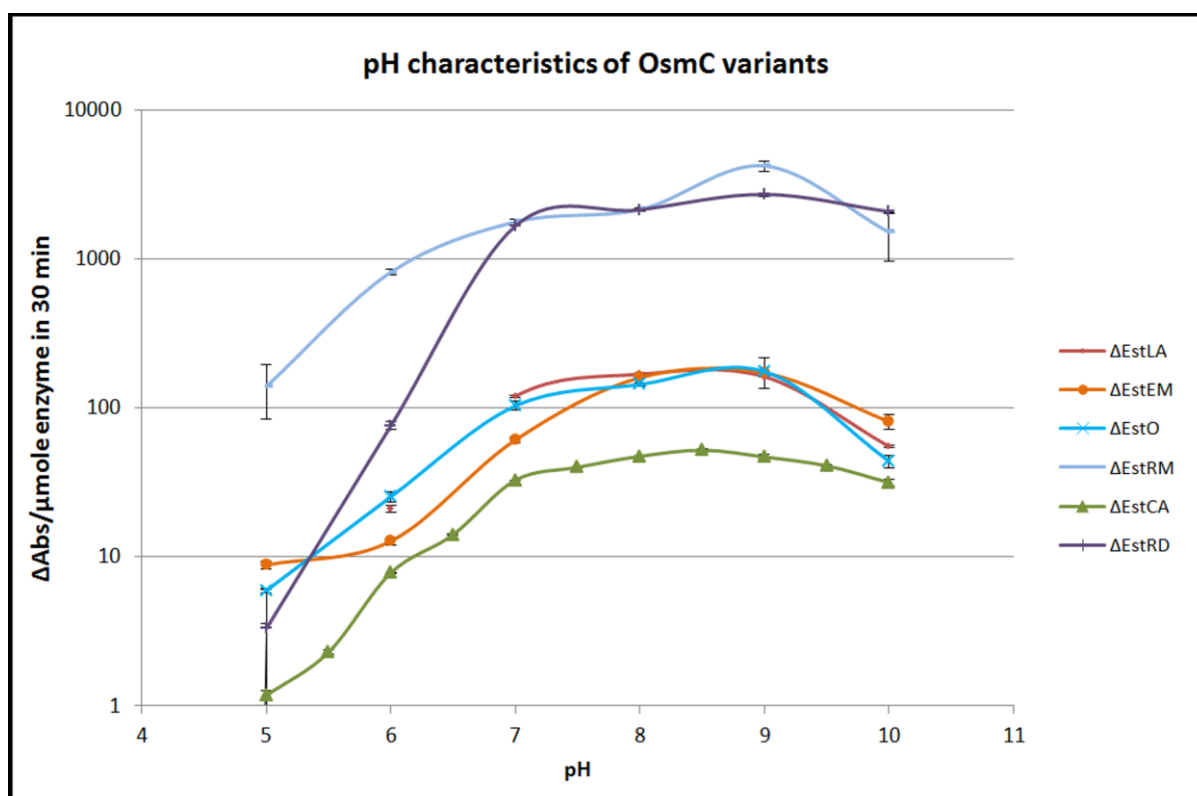


Figure 3.13. Comparison of Δ esterase activity across a range of pH

Each of the figures for all Δ esterase activity across pH, i.e. Figures 3.7. A)-F) had been combined on a graph with a logarithmic scale in order to easily compare their activity with one another.

3.4.3.3. Comparison of all Δ esterases activities against selection of substrates

Δ EstRM showed the highest activity of all tested Δ esterases against nitrophenyl benzoate - the substrate used to characterise esterase activity against changing conditions (6826 Δ Abs/ μ mole enzyme in 30 min while Δ EstRD,

the Δ esterase with nearest activity rate, shows 1873 Δ Abs/ μ mole enzyme in 30 min) (See figure 3.14.). However, Δ EstRM was not most active against all substrates; Δ EstRD showed greater activity against nitrophenyl decanoate and dodecanoate (3370 and 2230 Δ Abs/ μ mole enzyme in 30 min compared to 5021 and 3431 Δ Abs/ μ mole enzyme in 30 min respectively for both esterase and substrate).

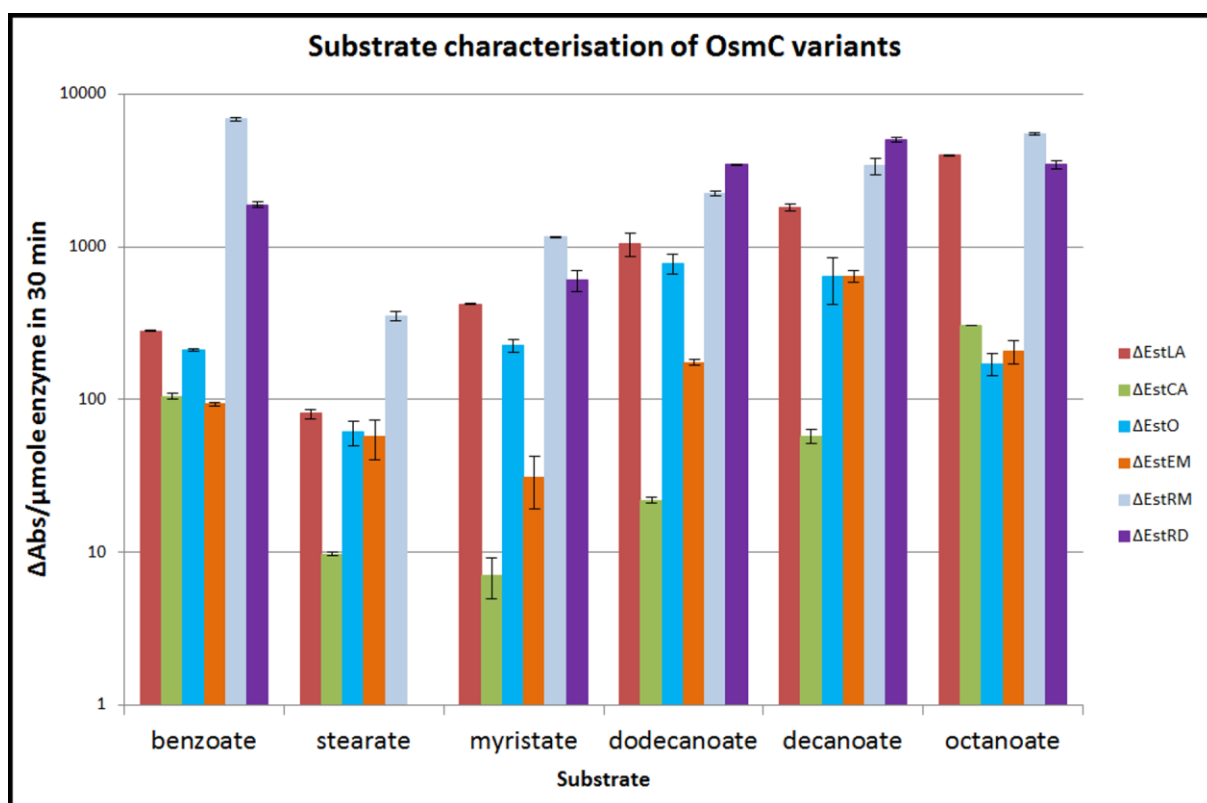


Figure 3.14. Comparison of Δ esterase activity across a range of substrates

Each of the figures for all Δ esterase activity across substrate with alkyl chain-length, i.e. Figures 3.8. A)-F) had been combined on a graph with a logarithmic scale so as to visually compare their activity with one another.

3.4.3.4. The effect of metal ions against all Δ esterases activities

With respect to esterase activity in the presence of metal ions (See figure 3.15.), general patterns emerge, e.g. K^+ , Mg^{2+} and Ca^{2+} rarely reduce activity considerably and sometimes actually increase it e.g. Δ EstLA showing increased activity after pre-incubation with K^+ (109%), Ca^{2+} increasing the activities of Δ EstEM, Δ EstCA and Δ EstO (144%, 113% and 145% respectively). Zn^{2+} , Ni^{2+} , Fe^{2+} and, to a lesser extent, Co^{2+} uniformly reduce activity. Δ EstEM does not follow this pattern; in the presence of K^+ its activity was reduced to less than 50%, but its activity was not reduced with either Zn^{2+} or Ca^{2+} .

Some esterases showing increased activity after pre-incubation with metal ions is not unusual - there have been recorded instances of this before, e.g. LipC showing optimal activity with 3 M KCl (Rao L *et al.*, 2009) and the dimethylsulphoxide-tolerant esterase from *Bacillus* sp. Showing 100% activity with an incubation with 1 M NaCl (Sana B *et al.*, 2007). In the examples given, both esterases came from halotolerant organisms.

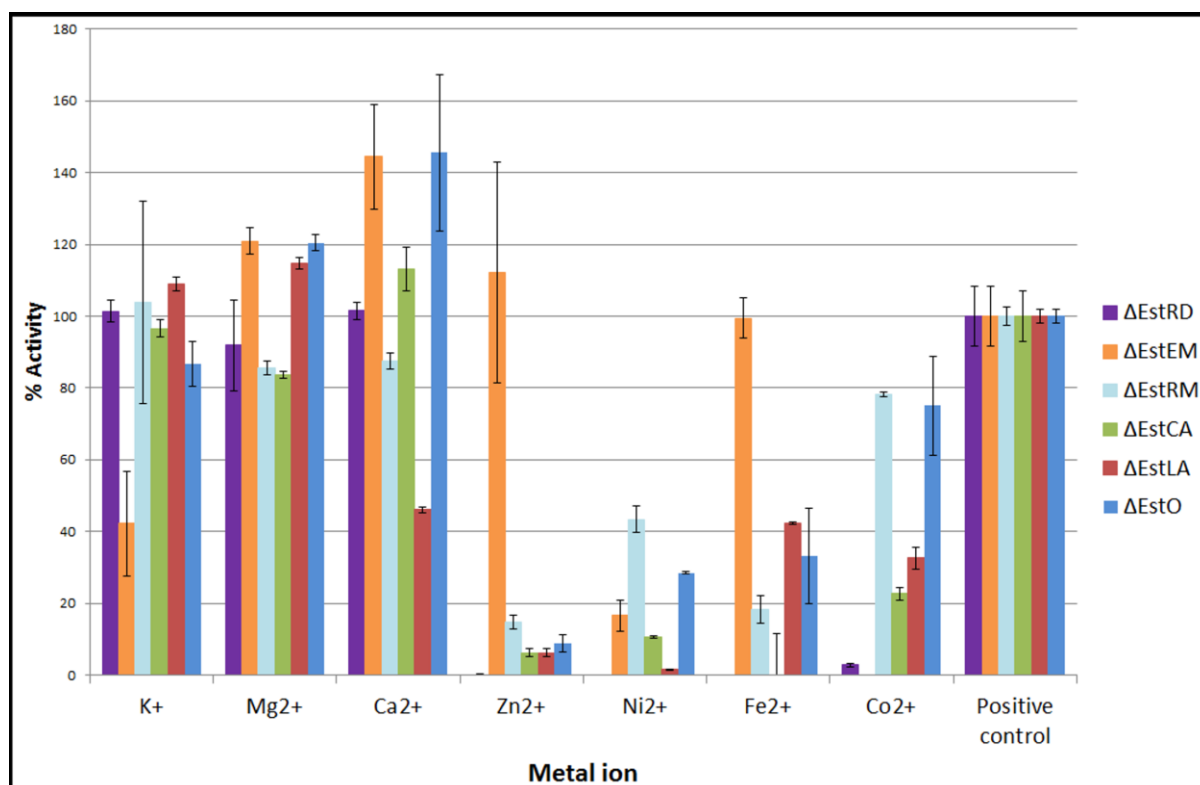


Figure 3.15. Comparison of Δ esterase activity in the presence of a selection of metal salts

Each of the figures for all Δ esterase activity with nitrophenyl benzoate after the esterases had been pre-incubated with 10 mM of metal ion, i.e. Figures 3.9. A)-F), had been combined so as to compare their activity with one another. The value generated for each esterase with every metal salt had been made a percentage with respect to the value generated from the esterase pre-incubated without a metal salt (the positive control). The value generated from the positive control was set to 100%

Δ EstEM comes from *Sinorhizobium meliloti* (*S. meliloti*), a bacterium that can grow in a biofilm in soil or within root nodules where it works as a nitrogen-fixing symbiote, converting atmospheric nitrogen to ammonia. Strains had been found that are halotolerant and metal ion tolerant; capable of growth in an environment of 684 mM NaCl (Mrabet M *et al.*, 2011) or with 200 μ g/ml of Zn (Elboutahiri N *et al.*, 2010). Calcium is also a required nutrient to maintain *S.*

meliloti growth at a low pH (Howieson JG *et al.*, 1992); so there are environmental pressures that would explain why Δ EstEM had increased metal-ion tolerance compared to other Δ esterases.

Δ EstO also shows increased activity in the presence of several metal salts, Mg^{2+} and Ca^{2+} . *P. arctica* comes from a marine environment, so there are environmental pressures with respect to metal salts, even if its environment is not considered extreme with respect to salt concentration. Other enzymes purified from *P. arctica* have shown increased activity in the presence of metal salts (Lu M *et al.*, 2010), so Δ EstO showing increased activity as well reinforces the idea that the environment of *P. arctica* induces minor halotolerance for native enzymes.

Δ EstRM also shows greater percentage activity when pre-incubated with Ni^{2+} and Co^{2+} than most other Δ esterases. Since this esterase comes from a halotolerant organism, halotolerance of the esterase was expected.

To further investigate if these esterases in question are influenced by metal ions, it might be worthwhile to investigate the proteins further, e.g. see if they have halotypical features, such as high number of aspartic and glutamic acid residues at solvent accessible regions, and fewer lysine, isoleucine and leucine residues (Graziano G and Merlino A, 2014), measuring metal ion dissociation rates using EDTA to chelate free metal ions (Hunt J A *et al* 1999), or obtaining the crystal structure of the esterases in the presence of metal ions to see how the effect the structure, where they bind and how they could influence activity (Benson L M *et al*, 2003).

3.4.3.5. Comparison of effect of inhibitors on all Δ esterases activities

The Δ esterases' sensitivities to putative inhibitors followed a general pattern; namely the higher the concentration of the inhibitor, the less active the esterase was against its substrate. There were a few exceptions; the activity of Δ EstRD after pre-incubation with 1 mM and 10 mM EDTA being identical (71%) and Δ EstRM showing greater activity with 4 mM Pefabloc than with 0.4 mM Pefabloc. However, there were some esterases that seem to show greater resistances to inhibitors than others, e.g. Δ EstEM retaining 84.5% activity in the presence of 4 mM Pefabloc, Δ EstRD retaining 71% activity after pre-incubation with EDTA (See figure 3.16.).

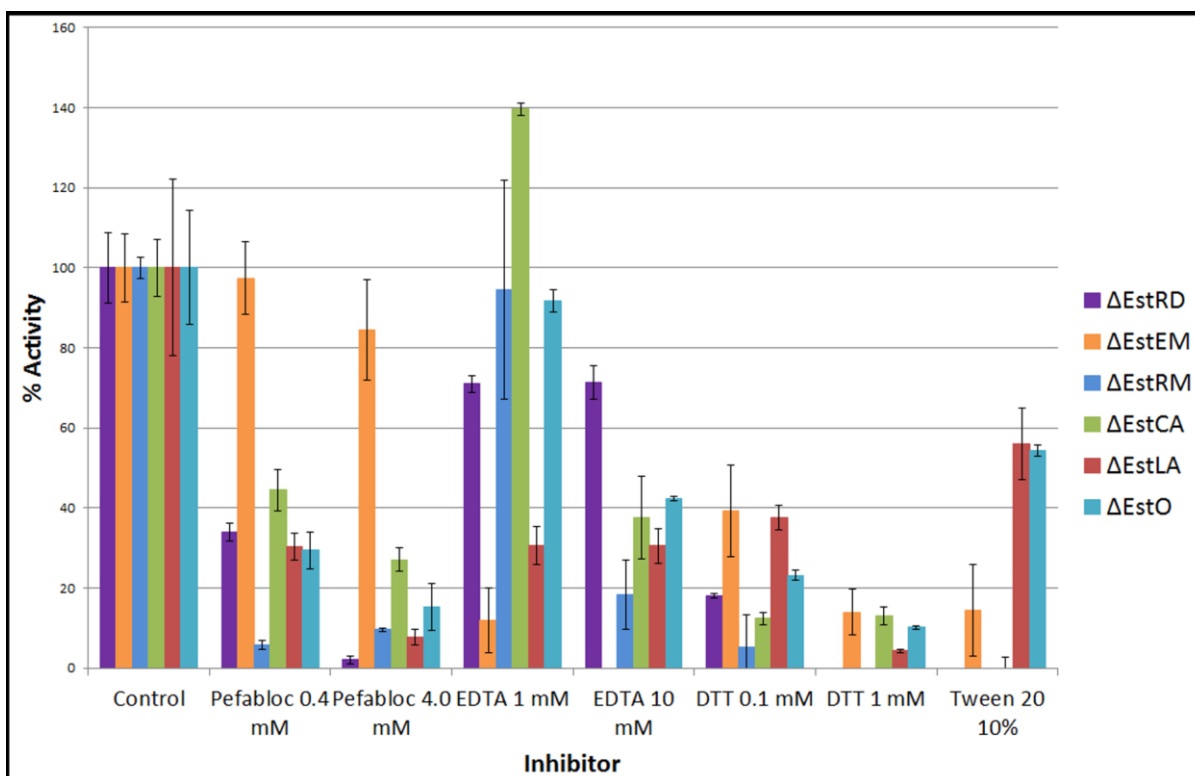


Figure 3.16. Comparison of Δ esterase activity in the presence of a selection of inhibitors

Each of the figures for all truncated esterase activity with nitrophenyl benzoate after the esterases had been pre-incubated with an inhibitor, i.e. Figures 3.10. A)-F) had been combined so as to compare their activity with one another. The value generated for each esterase with every metal salt had been made a percentage with respect to the value generated from the esterase pre-incubated without an inhibitor (the positive control). The value generated from the positive control was set to 100%

Pefabloc is a serine inhibitor which binds covalently to active-site serine through its sulphonyl group. In carboxylesterases, this covalent binding prevents the active-site serine of the esterase from performing nucleophilic attack on the ester bond of ester substrates, thus preventing any and all ester hydrolysis. It was not surprising to see that most of the Δ esterases were affected by this inhibitor, but Δ EstEM showed activity in the presence of Pefabloc. An explanation for this could be that the active site of Δ EstEM is less accessible to the Pefabloc molecules compared to other Δ esterase, effectively protecting the esterase from its effect. The structure of the esterase would have to be determined to check this hypothesis.

EDTA is a chelating agent - that is, it is a hexadentate ligand with great nucleophilic attack potential, meaning it shows high affinity as a binding agent

to metal ions. Metal ions bound to EDTA remain in solution, but have reduced reactivity. If an enzyme's activity is dependent on metal ions to perform its function, EDTA would bind the metal, inhibiting the enzyme activity. The Δ esterases did get affected by the presence of EDTA, but not at low concentrations. There was one exception, Δ EstEM which when incubated with 1 mM EDTA had its activity reduced to 12% of the positive control at 10 mM EDTA; almost all activity was lost. This implies that it was exceptionally susceptible to chelation, i.e. if there are metal ions involved in ester hydrolysis, they were not bound strongly to Δ EstEM. This was not without precedence, as there are carboxylesterases that require metal ions to catalyse ester hydrolysis, e.g. MloPLC which requires divalent cations to hydrolyse esters (Mandrach L and Manco G, 2009). One could test this through calculating the concentration of free metal ions before and after incubation of the esterases with EDTA.

DTT is a reducing agent, commonly utilised to remove disulphide bridges, a common feature formed between cysteine residues in proteins, involved in the tertiary structure and quaternary structure, i.e. they are a vital component of how the esterases fold and their catalytic ability. All the esterases show reduced activity in the presence of this reducing agent, implying that the folding of these proteins were heavily reliant on disulphide bridges. All of the tested esterases had cysteine residues present, two of them at a uniform position throughout all members. One could check if these residues are used in quaternary structure through converting them to methionine and seeing if multimerisation is maintained.

Tween 20 is a polysorbant detergent - that means it is a molecule with both hydrophilic and hydrophobic properties, capable of emulsifying normally immiscible chemicals, and can denature enzymes. Most Δ esterases were effectively rendered inactive by the presence of Tween 20, with the exception of Δ EstLA and Δ EstO, which implies that they were more capable of maintaining their structure in the presence of an emulsifier, possibly due to these proteins having little intramolecular interactions based on hydrophilic and hydrophobic residues or by being stabilised through disulphide bridges, which would fit with how much the esterases' activities were reduced in the presence of DTT.

To conclude, out of all of the Δ esterases assayed in this project, Δ EstRM shows the highest level of activity, particularly against ester substrates with long acyl chain lengths; which are common in fats and oils. It was also expressed in

the largest quantities of all of the Δ esterase, that is, it was easy to produce large yields of this esterase from bacterial lysate. If there were to be any further experimentation with respect to any Δ esterases being used as a constituent for a laundry detergent, Δ EstRM seems the most viable esterase to continue work on.

3.4.5. Comparing characterisation results to esterases used in laundry detergents

So, while Δ EstRM shows the highest overall activity in comparison to all other esterases in this project, how does it and the other esterases compare with esterases that are commonly utilised as part of laundry detergents?

To address this, the Δ esterases' activities should be compared with a carboxylesterase commonly used as a part of laundry detergents, *Humicola/Thermomyces lanuginose* lipase (TLL) also known as lipolase. This lipase was made commercially available by Novo Nordisk in 1994. TLL is well characterised and is widely utilised in a number of different applications. However, its features of high thermal stability (it will unfold at temperatures above 74°C) (Zhu K *et al.*, 2001) along with its preferences towards triglyceride substrates with acyl chain lengths between 10 and 12 carbon atoms meant that it was ideal for use as a part of laundry detergents. However, analysis of the literature reveals that TLL has not had recorded measurements of its activity against a range of nitrophenyl esters, only nitrophenyl butyrate. In fact, despite it having structure mapped, there is little in the literature about its optimal conditions or substrate preferences. A direct comparison between it and the Δ esterases cannot be achieved through the results generated in this project, without performing similar experimentation upon TLL.

TLL has been shown to have had increased activity against nitrophenyl substrates in the presence of low concentrations (i.e. approximately 2.5 mM) of detergents, but will show reduced activity upon higher detergent concentrations (Mogensen JE *et al.*, 2005). It has been suggested that there are a number of different mechanisms for this and not simply by influencing the water-lipid interface, which allows access to the active site of the lipase. The Δ esterases all showed reduced activity in the presence of Tween 20; but that was with 10% concentration of the detergent. It would be interesting to investigate more detergents effects upon the Δ esterases at lower concentrations, to see if there

was a similar pattern present with them as well. If the enzymes are to be used in a laundry detergent, commonly used chemical detergents must not compromise the enzymes' activities. This can be done in two ways; either the concentration of detergent chemical/s present in the laundry detergent must be low enough to not overtly hinder lipolytic activity, or the lipolytic enzyme must be engineered to be stable at the required concentration of detergent without losing too much of its hydrolytic capabilities.

Since TLL is a lipase; specifically a lipase with a lid structure, it shows interfacial activation upon reaching the saturation point of its substrate (Berg OG *et al.*, 1998). Two points arise from this; first the Δ esterases which lack this lid did not require the saturation point to be reached. This means that the Δ esterases should be able to work better upon a lower concentration of substrate than TLL in a wash. Secondly the point of this project was to develop an esterase to work against fats and oils at temperatures around 20°C. Literature investigating the hydrolytic activity of TLL find its optimal activity to be above 35°C (Fernandes MLM *et al.*, 2004), and requires the presence of cofactors to help hydrolyse fat and oil stains efficiently at low temperatures. The presence of the lid structure prevents the TLL from being able to hydrolyse fats when they are not in the emulsion bodies.

This inability to effectively break down fats and oils effectively at low temperatures was recognised to the extent that a variant on TLL was made, Lipolase Ultra, which increased overall esterase activity by rendering the active site more hydrophobic, and thus granting additional activity at low temperatures. However, Lipolase Ultra is not so easily produced as TLL and it still has the lid structure which hinders lipase activity against non-emulsified substrate; to determine the best lipolytic enzyme for functioning at low temperatures, esterases are still viable enzymes to investigate to work upon fats and oils at low temperatures.

Chapter 4

Assay for screening esterase affinity to fat and oil stains

4.1. Introduction

4.1.1. AFM as an assay

At 20°C many fats have been shown to be in a semi-crystalline solid form and are therefore not amenable to hydrolysis by surface active lipases. Assays used so far in the project detect ester hydrolysis when the substrate is in solution or in the form of an emulsion. There is, therefore, a driving force to develop an assay which measures affinity of the enzyme to substrate when it is not free in solution as well as substrate associated hydrolysis. There has been very limited work investigating the structure of semi-crystalline fats and this work forms part of a collaboration with the group of Dr Ashley Cadby at the University of Sheffield using Atomic Force Microscopy (AFM) to firstly investigate the surface structure of fats at cold temperatures followed by investigating the impact of various treatments including enzymatic treatment on the fats' structures and stabilities.

AFM permits microscopy on a nanometre scale by running a cantilever arm which has a miniature silicon tip over a surface with substrate bound to it. Focused on the back of the cantilever is a laser beam, whose deflection off the cantilever is detected through a photodiode. At resting point, when the cantilever does not bind to anything, the area on the photodiode where the laser rests at is the constant.

When the tip interacts with an object, forces between the tip and the slide-bound object will cause the cantilever to bend. This bending changes the position of the laser reflected off the tip, onto the photodiodes, meaning that the laser point shifts to illuminate one of the photodiodes more than the other one, resulting in a change of the difference in photocurrent. As soon as the difference in photocurrent between the two/four photodiodes changes the AFM tip is moved to reinstate the previous, constant using piezoelectric elements by a so called closed loop. The closed loop thus returns the cantilever to a position where the deflected laser was at the constant; the corrective currents used to move the AFM tip up, or down is a measure for the deflection and after calibration used to display sample height, or interaction forces. As this tip is scanned over a surface the corrective signals can be used to display e.g. surface topography.

This bending is used to derive the force interaction between tip and sample via Hooke's Law ($F = -kx$, where F = force, k = spring constant of the cantilever arm and x = bend of the cantilever). If the bending of the arm is too extreme, then the system moves the tip away from the sample; if the bending is non-existent, the system moves the tip towards the sample. This process is then repeated for the entirety of the sample slide. The amount of deflection over the entire slide can be represented through a topographic diagram, showing the exact shape and size of subject matters at a resolution of less than a nanometre. This microscopy can also be performed under a variety of different environmental conditions, e.g. different temperatures, salt concentrations, pH, etc.

Because of the physics behind the method of detection, more can be done with AFM besides nanometre scale microscopic scanning. AFM can be utilised for other measurements, e.g. nanohardness detection on metallic surfaces (Kempf M *et al.*, 1998), detecting and evaluating wear of a surface (Gahlin R and Jacobson S 1998), measuring scratch-resistance of surfaces (Sundararajan S and Bhushan B 2001) and of particular interest to this project; attaching single ligands to AFM tips through a tether (Hinterdorfer P *et al.*, 1996, Lee G U *et al.*, 1994) via a methodology called simultaneous topographical and recognition imagery, or TREC for short (See figure 4.2.).

TREC works through the adhesion force between a ligand on an AFM tip and substrate on a slide generating additional negative force upon the cantilever (See Figure 4.2.). This allows for monomolecular probing of slides which maps the pattern of substrate on the slide and maps the affinity of the ligand attached to the tip to the substrate on the slide; since the force required for the cantilever to return to its basal state after interaction of a ligand with its substrate would be greater (Stroh C M *et al.*, 2004). This technique has been used to image cell surfaces, to map the DNA binding sites of proteins and to determine the deposition of specific proteins in diseased eye tissue (Chitchevlova, L, *et al.*, 2010, Zhu R *et al.*, 2013, Creasey R *et al.*, 2011).

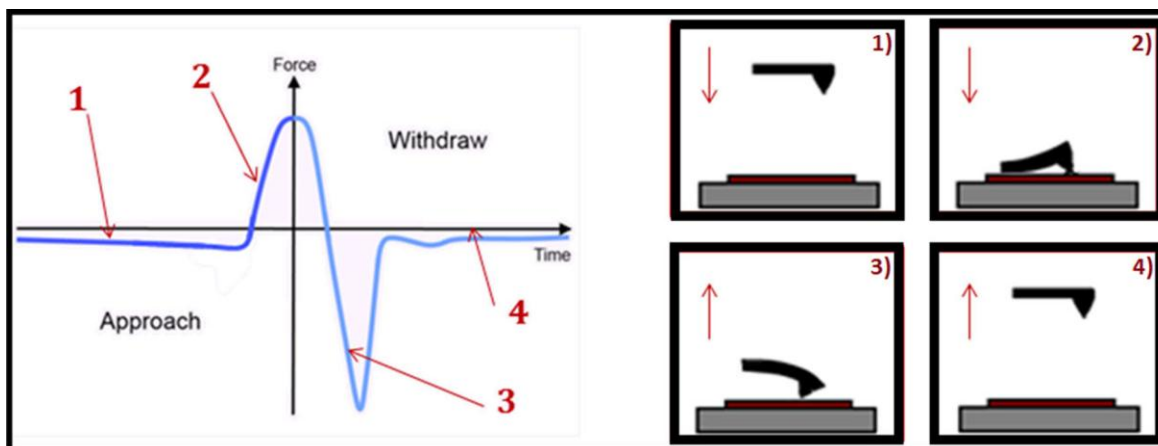


Figure 4.1. Illustrating force curves in AFM.

This is a representation of the deflection of a cantilever which corresponds to the forces an AFM tip experiences when it is first moved towards a surface for a prespecified distance (ramp), and then removed in a so called force-curve, or $V(z)$ scan. Far away from the surface (1) the cantilever is not deflected. Then it reaches the point, where the tip gets into contact with the sample (1-2) the movement of the tip further towards the surface can exert force onto the surface (2). Then the cantilever is retracted from the surface - the attraction of the tip with the surface leads to a negative force (3) which reflects how strong the binding of the tip to the surface was. After some settling the force the cantilever experiences settles to the preset values. These force-distance curves can also be used to map interactions across a surface, they are then called force-volume scans. Image modified from sample image supplied by Charlotte Nicolau of the University of Sheffield.

By scanning the sample with the ligand repeatedly over time, one could also map the degradation of substrate or creation of product due to the ligand being run over it - e.g. using AFM to detect the activity of RNA polymerase on dsDNA complexes when dNTPs are introduced through a continuously flowing system and (Kasas S *et al.*, 1997, Grandbois M *et al.*, 1998).

Since fats and oils on mica slides can be formed into crystalline structures, one could probe affinity and activity of esterases against fat and oil crystalline substrate by using the esterase as a ligand on an AFM tip. Any esterase deemed suitable to be used in this method must have a surface amino acid amenable to allow tethering to the AFM tip that would not interfere with the protein's intrinsic affinity to the substrate or the activity of the esterase. By working with our collaborators at the University of Sheffield who have expertise in performing AFM we aimed to develop an effective assay for detection of affinity between esterases and crystalline fats and oils in low-temperature, aqueous environments.

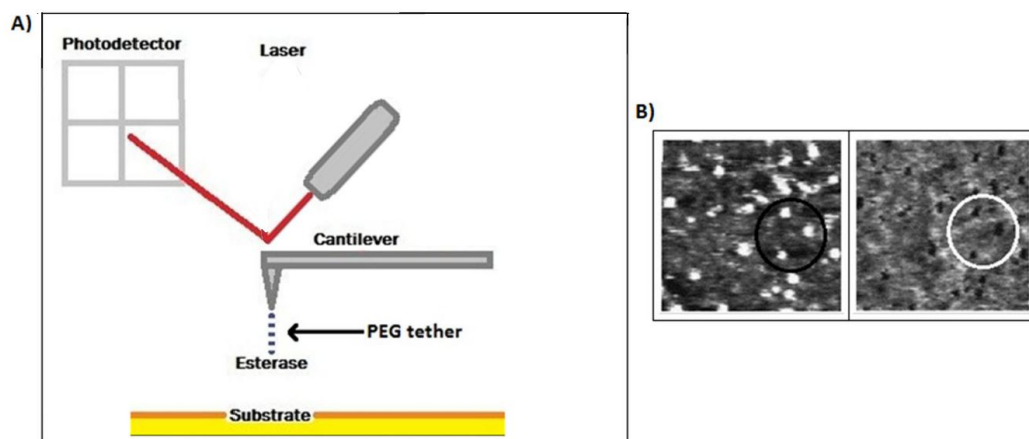


Figure 4.2. Basic methodology behind TREC imagery using AFM

How TREC would theoretically function with the esterase ligand in this project. A) The active esterase is tethered through a PEG molecule (See figure 4.4) to the AFM tip. Interaction of the esterase with substrate causes the cantilever arm to bend, which is detected through the reflection of a laser off the back of said cantilever. B) The left-most image is the topographical scan of single avidin molecules distributed on an AFM slide, the right-most image is the recognition scan of the biotin molecule attached to the AFM tip with the avidin molecules on the AFM slide. The two circles indicated good correlation between the topography and recognition scans - although not all topographical features show specific interaction as well. modified from Dupres V, et al., 2007

Before testing any members of this esterase family on AFM, the viability of using AFM as an esterase assay must first be verified using a previously well characterised esterase. TREC imagery of fats or oils substrates on mica slides would be performed initially using the AFM tip to investigate the topography of the semi-crystalline fat substrate. After the initial investigation the surface would be again explored using the enzyme-bound AFM tips and the resulting images super-imposed to see how the observed adhesion matches with topographical images. The aim would be to identify any adhesion that was due to specific interaction between the enzyme and the substrate topography.

When considering which substrates were to be tested, two features were thought a necessity; the alkyl group of the substrate had to be short enough so as to increase chances of binding affinity of the esterase's active site to the substrate and that the substrate in question had to be capable of binding to mica, but in such a way that would not prevent the accessibility of the esterase's active site to said substrate. A simple way for a chemical to bind to silicon oxide would be if said chemical had a free carboxylic acid or hydroxyl

moiety. Two substrates were identified which satisfied these criteria: 2-acetoxypropionic acid and 1-Octanoyl-*rac*-glycerol (See figure 4.3.). If this method of measuring esterase affinity to non-emulsified substrate was found to work with positive controls; that is, esterase ligands that have been well characterised and are known to work on these substrates, then this strategy could be used to more accurately determine the binding affinity of low-temperature active esterase on fats and oils on bound to a physical surface as opposed to being in an emulsion body.

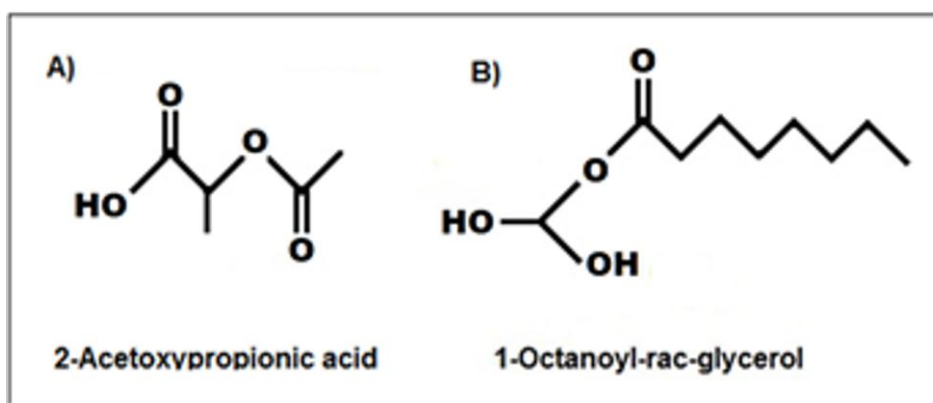


Figure 4.3. Chemical structures of substrates chosen for TREC theory

A) Is the chemical structure of 2-Acetoxypropionic acid - the free carboxylic acid moiety would allow it to bind to mica while exposing an acetate alkyl attached to the remainder of the chemical with an ester bond. B) Chemical structure of 1-Octanoyl-*rac*-glycerol. The two hydroxyl moieties would allow this chemical to bind to silicon oxide, leaving an octanoate alkyl group which an esterase is free to attack.

4.1.2. Attachment of the esterase to the AFM tip

AFM has been used before to detect enzyme activity, e.g. lysozyme activity upon oligoglycoside (Radmacher, M, et al., 1994), as well as measuring interaction between a single molecule bound to an AFM tip and substrate bound to a mica slide; to measure intramolecular forces, e.g. duplex DNA bound to the AFM tip and slide surface being pulled apart (Noy, A, et al., 1997) or intermolecular forces, e.g. the force generated through complementary DNA molecules on AFM tip and slide being detected through AFM, the binding of avidin and biotin on AFM tip and slide (Boland T. and Ratner B. D. 1995, Ebner, A, et al., 2005) and it has been used as a biosensor for antibodies interacting with specific antigens, e.g. lysozyme, avidin. etc., immobilised to a slide (Stroh, C. M, et al., 2005, Kamruzzahan, A S, et al., 2006, Wildling, L, et al., 2011).

Since AFM is capable of detecting specific molecular interactions, one should be able to probe affinity of a single enzyme against a substrate immobilised on a mica side as a form of TREC.

TREC requires there to be a single molecule on the AFM tip, but in the case of an enzyme a direct attachment may not be appropriate. Direct attachment of ligand to the AFM tip can work for complementary DNA molecules (Boland T. and Ratner B. D. 1995) or for measuring biotin-avidin interaction (Moy, V.T, et al., 1994), but with more complex protein ligands, it is not suitable. Attaching ligand to an AFM tip directly cannot guarantee the binding of a single ligand to the tip, since the whole tip would have to be treated to display a binding site for the esterase, meaning multiple esterases could bind to a single tip. There would be no guarantee that when the ligand is bound to the tip it will maintain its natural structure, so there is no guarantee the ligand will work upon its substrate. There would be limited molecular mobility for the ligand, so it could not easily interact with the substrate.

For TREC to work effectively, a single, active ligand must be attached to the AFM tip in such a way that permits the ligand to freely orient and which allows for the differentiation between specific and unspecific interactions of the ligand with the sample. To meet these requirements, linear heterobifunctional tethers are utilised, most commonly constructed from polyethylene glycol (PEG) (Hinterdorfer P, et al., 1996). Such a tether is designed to act as a bridge between the AFM tip and the ligand, and so has two separate functional groups at either end.

PEG is polymer of ethylene oxide that can be made into many different structures depending on the method of polymerisation (e.g. branched, star-shaped, linear). PEG is a highly flexible molecule that is unreactive and can be engineered to have functional groups to allow for specific binding. This chemical has been used multiple times in tethering biological ligands to AFM tips (Hinterdorfer P. and Dufrêne Y.F., 2006, Kamruzzahan, A S, et al., 2006, Wildling, L, et al., 2011, Stroh, C. M, et al., 2005) while leaving the ligand's innate activity unaffected. For these reasons, it was decided that a PEG molecule would be used to tether the esterase in question to the AFM tip. It was decided to use PEG with a maleimide functional group (See figure 4.4.) since maleimide is an unsaturated imide chemical., it is highly reactive towards thiol-groups, like the groups present on cysteine. In the presence of a solvent

accessible cysteine, maleimide will form a thioether bond which will not readily degrade.

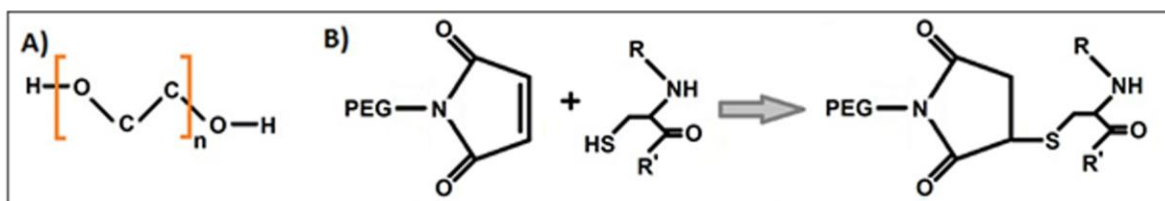


Figure 4.4. PEG and PEG maleimide

A) Is the chemical structure of linear PEG. The n-value can be varied to make the effective tether as long or as short as is needed. B) A figure illustrating the interaction between maleimide and the free sulfhydryl group on a cysteine residue.

Before attempting AFM with any of the esterases previously investigated, it was considered prudent to attempt AFM first with well-established candidate ligands first. The two esterases chosen were PA3859 - a well-studied esterase isolated from *Pseudomonas aeruginosa* (Pesaresi A. and Lamba D., 2005 and 2010), as well as Candida Antarctica Lipase B, or CalB for short, isolated from the eponymous yeast strain (Uppenberg J, et al., 1994). Both of these enzymes are known to be monomers and are known members of the α/β hydrolase fold family of lipolytic hydrolases and have their crystal 3D structures mapped (Pesaresi A and Lambda D, 2005, Uppenberg J *et al.*, 1995).

4.2. Materials and Methods

4.2.1. Synthetic gene design and synthesis

A synthetic gene was designed by converting the known primary sequence of CalB without the pre-pro-peptide domain using the Life Technologies on-line GeneOptimizer resource. The resulting DNA sequence was ordered in from EuroFins MWG Operon (See Appendix)

4.2.2. PEGylation of proteins

Analysis of the literature indicated that the most convenient way to attach PEG tether to the proteins of interest was deemed to be through an engineered cysteine residue replacing a surface residue (determined by comparing 3D-models of the protein structure along with solvent-accessibility prediction software, polyview and NetSurfP (See 2.6.6.3. and 2.6.6.4.)) of the native protein binding to a PEG molecule with a maleimide-functional group through a thioether bond with the free sulfhydryl group of the residue.

Any effects PEGylation had on the activity of esterases were determined prior to use in AFM. ThermoScientific supplied a sample of linear PEG polymers (consisting of 24 monomers) tipped with a maleimide functional group, identified by the shortened nomenclature mm(PEG)₂₄. The sample provided from ThermoScientific was dissolved to a concentration of 250 mM in filtered dimethyl sulphoxide (DMSO) or dimethylformamide (DMF) solvent so it could be mixed with ligand to a final concentration of 20-fold molar concentration greater than the ligand it was binding to.

Protein samples were first reacted with (Tris(2-carboxyethyl)phosphine hydrochloride (TCEP.HCl); which reduces natural cross-linking disulphide bridges. TCEP.HCl was used specifically over other reducing agents such as DTT or β -mercaptoethanol for two reasons: first, when it reduces the disulphide bridge, it converts both sulphur atoms into sulfhydryl groups, which maleimide binds to. Second, TCEP.HCl has no sulfhydryl group present, so any unreacted TCEP.HCl does not compete with cysteine for maleimide-binding as strongly as DTT or β -mercaptoethanol.

Effect of TCEP.HCl was compared to other known reducing agents (β -mercaptoethanol) to ensure banding pattern corresponded to a fully reduced protein sample. Optimal TCEP.HCl concentration was determined by reacting

protein samples with a gradient of TCEP.HCl concentration at room temperature or on ice for periods of 30 minutes to 2 hours, then mm(PEG)₂₄ was added at a final concentration of twenty times that of the protein's concentration. The maleimide group attached to mm(PEG)₂₄ is reactive to water, and to minimise the effect of atmospheric water, samples were taken from the stock solution in a container partially filled with liquid nitrogen. This was left to incubate for at least 2 hours on ice. To reduce the effect of oxidation on the PEG molecules by the atmosphere, aliquots were removed from PEG stock in a container that had been partially filled with liquid nitrogen. As the liquid nitrogen evolved into gaseous form, it forced out the native atmosphere, leaving an atmosphere of near-pure nitrogen. It was in this atmosphere that PEG reagent was obtained. PEGylation was verified by running samples down a 15% SDS-PAGE gel (See 2.1.2.1.) and comparing to unreduced protein samples. The PEGylated samples ran slower through the gel due to the additional mass added from the PEG tether; the attachment of mm(PEG)₂₄ would add 1.24 kDa to the overall mass of the protein.

PEGylated protein samples then had their activity compared to a sample of unPEGylated protein of equal concentration. If activity was found to be comparable, then the PEGylation was thought not to have affected the activity of the esterase.

For preparing ligands for PEGylation with collaborators at the University of Sheffield, the protein sample was treated with TCEP.HCl as before, but was then dialysed in 1 l of 20 mM Tris solution at pH 7.2, to prevent competition between binding of PEG with the binding of protein. The irreversible reduction of cross-linkers formed by disulphide bridges was checked by running samples on a 15% SDS-PAGE gel (See 2.1.2.1.). This procedure invariably results in the precipitation of some protein, but this was removed by filter-sterilisation.

4.3. Results

4.3.1. Esterase PA3859

PA3859 is an esterase from the prokaryotic *P. aeruginosa*. It can form homodimers, but exists in solution as an active monomer. PA3859 has the conserved Ser-His-Asp catalytic triad and the common GX SXG pentapeptide motif found in many carboxylesterases. A crystal structure of this esterase has been derived, which concludes that the active site of the esterase is embedded in the

middle of a cleft spanning the width of the protein (Pesaresi A and Lambda D, 2005). Said cleft has two regions; a hydrophobic sector formed through two parallel alpha-helices and a polar cavity formed through linker regions between helices and sheets. The hydrophobic sector is involved in the accommodation of the alkyl tail of substrates.

Previous work produced a variant of PA3859 in which the cysteine at position 14 was replaced with serine and a methionine at position 37 (a residue that was solvent-accessible) was replaced with cysteine through site-directed mutagenesis PCR (See 2.2.). The mutant form of the esterase was designed to show equivalent activity to the native form of the gene, while still having a solvent-accessible cysteine residue. The gene encoding the variant protein (C14S/M37C PA3859) was inserted into pDest17 vector and expressed in a BL21-AI host with the bacterial colony induced by 2% arabinose and incubated for at least 4 hours at 37° C and 200 rpm (See figure 4.5.). The bacterial pellet was re-suspended in Tris Wash buffer and purified through His-tag affinity to Nickel chloride-charged resin following the procedure in 2.6.2.2. Dialysis occurred with buffer at a pH of 7.2.

The concentration of the isolated C14S/M37C PA3859 was determined by a Bradford Assay (See 2.6.2.3.) and a small aliquot was exposed to 20-molar excess of mm(PEG)₂₄ for at least two hours on ice as per manufacturer's instructions.

4.3.2. PEGylation of C14S/M37C PA3859

Detection of PEGylation (See 4.2.2.) was performed by running an aliquot of the PEGylation sample on a SDS-PAGE gel (See 2.1.2.1.) alongside an equal concentration of C14S/M37C PA3859 that had not been exposed to mm(PEG)₂₄, without any reducing agent present in the gel or the loading buffer. If the esterase was PEGylated successfully, then two bands in the PEGylated C14S/M37C PA3859 sample were expected; one corresponding to unPEGylated C14S/M37C PA3859 at the expected mass of 26.5 kDa and the other corresponding to PEGylated C14S/M37C PA3859, which should be approximately 1 kDa heavier than unPEGylated protein.

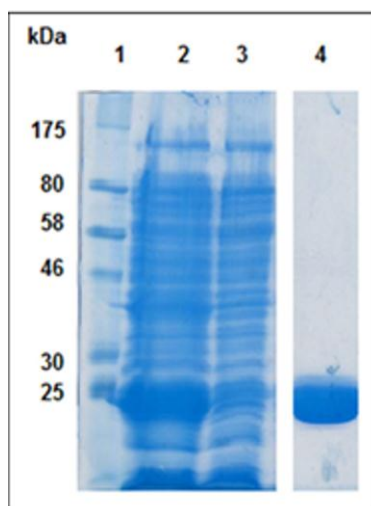


Figure 4.5. Expression and purification of soluble C14S/M37C PA3859

SDS-PAGE analysis of soluble C14S/M37C PA3859; samples were separated on a denaturing SDS-PAGE gel. Lane 1: Marker. Lane 2: bacterial lysate. Lane 3: flow-through. Lane 4: eluted protein that was dialysed and used in assays.

The first gel revealed there was little PEGylation of any C14S/M37C PA3859, and the samples of C14S/M37C PA3859, both PEGylated and unPEGylated, had a second band of protein that was approximately double the expected mass of the protein (See figure 4.6.).

This heavier band observed on the gel was probably due to a dimer forming through a disulphide bridge between solvent-accessible cysteine residues on different molecules of C14S/M37C PA3859. Reducing agents dithiotheritol or β -mercaptoethanol were not suitable to prevent dimerisation, so instead Tris(2-carboxyethyl)phosphine hydrochloride (TCEP.HCl) was used to reduce the disulphide bonds in the presence of water, leaving two thiol groups and oxidised TCEP products (See figure 4.7.).

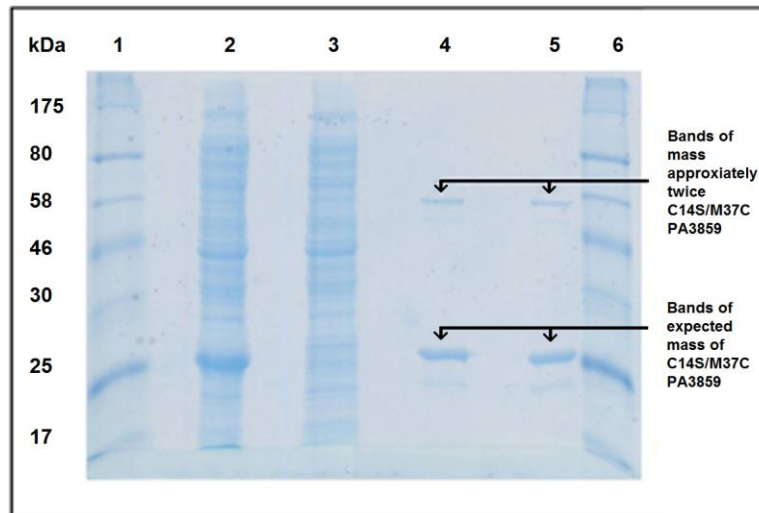


Figure 4.6. PEGylation of C14S/M37C PA3859

Samples of C14S/M37C PA3859 ran on an SDS-PAGE gel to detect PEGylation. Lanes 1 and 6: Marker, Lane 2: bacterial lysate. Lane 3: flow-through 3). Lane 4: eluted protein 4) Lane 5: PEGylated eluted protein. Both 4 and 5 had a band that was approximately twice the expected mass of C14S/M37C PA3859 (26.5 kDa)

When C14S/M37C PA3859 protein which had been incubated for at least 30 minutes with TCEP.HCl was PEGylated, results were more promising, with reduced dimer presence, and greater presence of PEGylated C14S/M37C PA3859 (See figure 4.8.). Three bands could be seen from samples in the TCEP gradient, the band of lowest mass corresponds to unPEGylated C14S/M37C PA3859, the second band corresponding to PEGylated C14S/M37C PA3859, while the heaviest band corresponded to dimerised C14S/M37C PA3859. By analysing the banding pattern from the TCEP.HCl gradient, pre-incubation with 1 mM TCEP produced the highest concentration of PEGylated C14S/M37C PA3859.

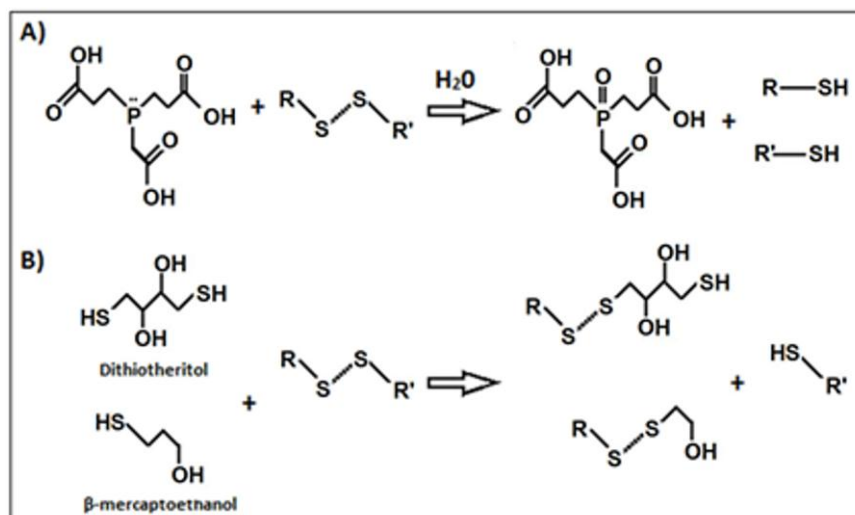


Figure 4.7. Methods of reduction of disulphide bridges.

A) Demonstrates reduction of a disulphide bridge via TCEP. B) Demonstrates reduction of a disulphide bridge by dithiothreitol (DTT) or β -mercaptoethanol. The binding of the reducing agent to the thiol group prevents chemical modification of the enzyme through that cysteine residue, and so is not sought an ideal reducing agent for PEGylation.

In order to determine if PEGylation had an impact on C14S/M37C PA3859 activity the activity of two samples (with and without PEGylation) were measured. Equal concentrations of C14S/M37C PA3859 and C14S/M37C PA3859 reacted with mm(PEG)₂₄ after a 30 minute pre-incubation with 1 mM TCEP.HCl were to be compared using assay detailed in 3.2.3., to see if the PEGylation had altered the activity of the protein. However, there was too little PEGylated C14S/M37C PA3859 to undergo a such an assay, so a different comparative reaction between C14S/M37C PA3859 that had been subjected to PEGylation and C14S/M37C PA3859 that had not been PEGylated of equal concentrations had to be designed and used. The assay designed utilised nitrophenyl substrate, but with 10 μl of enzyme being mixed with 140 μl of 0.15 μM nitrophenol acetate in Tris-buffer (See 3.2.3.). 10 μl of the enzyme was placed in a well of a 96-well microplate, in triplicate, along with a negative control of 10 μl dialysis buffer. 140 μl of 0.15 μM nitrophenol acetate in Tris-buffer was added simultaneously to all wells, and the microplate had absorbance readings at OD₄₁₀ recorded at 5 minute points for a 30 minute incubation period at room temperature because it was known that nitrophenyl acetate was an easily hydrolysed substrate. Results indicated PEGylated C14S/M37C PA3859 was not less active than unPEGylated C14S/M37C PA3859.

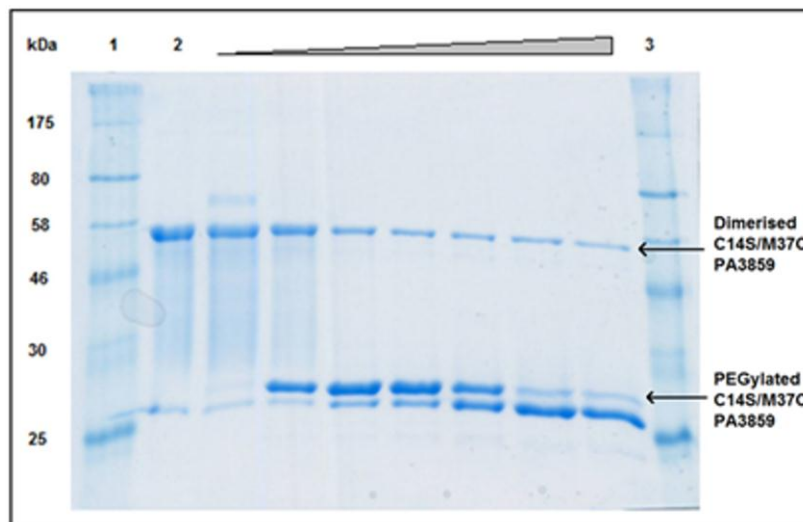


Figure 4.8. The effect of reduction of TCEP on PEGylation of C14S/M37C PA3859

Samples of purified C14S/M37C PA3859 ran on an SDS-PAGE gel to detect the effect TCEP had on PEGylation. Lanes 1 and 3: Marker. Lane 2: semi-reduced C14S/M37C PA3859. Remaining lanes were samples of C14S/M37C PA3859 reduced with an increasing gradient of TCEP concentration for 30 minutes before being incubated with mm(PEG)₂₄ for 2 hours on ice. The seven samples making up this gradient differed in TCEP concentration as follows: 0 mM, 0.5 mM, 1 mM, 5 mM, 10 mM, 15 mM and 25 mM respectively. Bands corresponding to dimerised and PEGylated C14S/M37C PA3859 were indicated.

In order to determine if TREC could be used with a catalytically inactive esterase that would not break down any substrate but would still be able to bind to substrate a variant of PA3859 was engineered that had a serine at position 113 in the active site replaced with an alanine (C14S/M37C/S113A PA3859). This should result in a mutant where hydrolytic activity of the esterase would be compromised compared to C14S/M37C PA3859, but substrate affinity should remain the same. The activity of C14S/M37C/S113A PA3859 and C14S/M37C PA3859 were tested by comparing activities using a nitrophenyl octanoate (See 3.2.2.) substrate, but with no Na₂CO₃ added. The mixes were incubated for 5 minutes at room temperature and absorbance readings measured at OD₄₁₀, along with a negative control containing the same volume of substrate, but no esterase. It was found that C14S/M37C/S113A PA3859 had average absorbance units at OD₄₁₀ of less than 0.05 no matter its concentration, while equivalent concentrations of C14S/M37C PA3859 were approximately 0.409 (See figure 4.9.)

A sample of the C14S/M37C PA3859 esterase, treated with TCEP, was sent to collaborators at the University of Sheffield for further analysis.

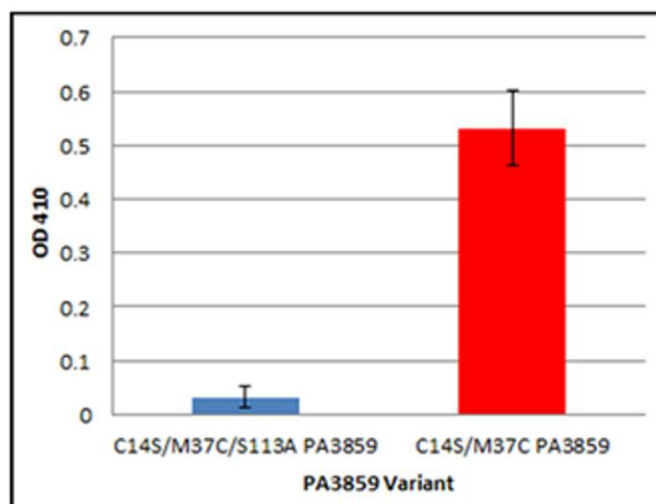


Figure 4.9. Assay of C14S/M37C/S113A PA3859 against C14S/M37C PA3859

Equal concentrations of protein were mixed with nitrophenyl octanoate as a substrate to a final volume of 1 ml and left for 5 minutes at room temperature. Results were taken in triplicate and average OD₄₁₀ absorption values along with standard errors.

4.3.3. Lipase CalB

In order to compare and contrast the activities of esterases with lipases on semi-crystalline fats surfaces using AFM the well characterised lipase CalB chosen for attachment to the AFM tip. CalB has a lid that covers the active site of the lipase that is moved away in the presence of substrate at a water interface; it also has no regio-selectivity to alkyl chains on a glycerol backbone. Its activity can be measured through most esterase activity assays - it can break down non-lipid substrates as well as fats and oils.

CalB is a eukaryotic lipase; the second lipase extracted from *Candida Antarctica* and widely used in the biotechnical industries. Though it is usually expressed in eukaryotic hosts, e.g. by the fungus *Aspergillus oryzae* and *Yarrowia lipolytica* (Emond S *et al.*, 2010), it has been expressed in prokaryotic hosts as well (Blank K, *et al.*, 2006, Jung H J, *et al.*, 2011, Larsen, M W, *et al.*, 2008, Liu D, *et al.*, 2006, Seo H S, *et al.*, 2009). An *E. coli*-optimised version of CalB was designed and synthesised (GeneArt), which omitted the *C. antarctica* secretory pathway propeptide (Blank K *et al.*, 2006), a feature that would be unnecessary for expression in *E. coli*.

The synthetic gene was designed to be flanked with EcoRI and HindIII restriction sites at its 5' and 3' ends respectively which would allow it to be inserted in frame into the MCS of pMAL-c2x expression plasmid, as well as a C-

terminal poly-His tag. pMAL-c2x was chosen specifically as it is a vector designed to express protein that is not readily expressed used in an *E coli* system. It achieves this through expressing the protein as a fusion with an N-terminal Maltose Binding Protein (MBP) domain. This MBP tag has been found to increase solubility of proteins it is fused to (Nallamsetty S and Waugh D S, 2006). This domain is attached to the expressed protein through a Factor Xa cleavage site, meaning it can be removed after protein expression.

A small-scale expression trial (2.6.1.2.1.) of CalB in pMAL-c2x vector in *E. coli* BL21-AI cells was performed with induction starting at different absorbance values at OD₆₀₀, induction periods and concentration of IPTG. Since it was suspected that CalB would not be soluble within conditions used previously, the temperature used for the induction period was 16 °C as opposed to 37 °C. Because of this, the time periods for harvesting were after 4 hours, 8 hours and an overnight incubation. The samples were induced with 1 mM or 0.3 mM IPTG and 0.2% arabinose. The samples were run on an SDS-PAGE gel (See 2.1.2.1.) and the soluble fractions were inspected for a protein band of 75.5 kDa corresponding to CalB (See figure 4.11.).

The conditions identified as being best for expressing soluble CalB protein in BL21-AI cells were an induction with 1 mM IPTG of a culture with an OD₆₀₀ between 0.6-0.8 at 16 °C with an overnight induction period (See figure 4.10.).

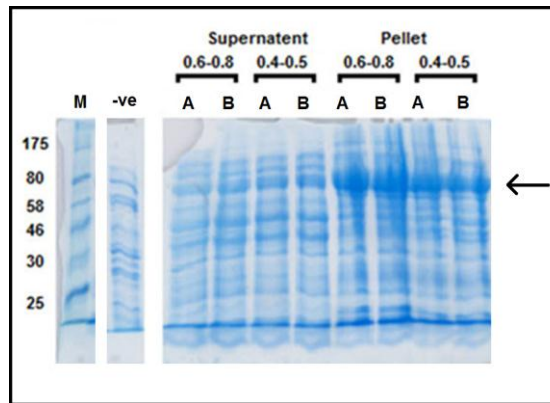


Figure 4.10. Expression trial of CalB+MBP pMAL-c2x vector in BL21-AI expression

Lanes differentiate through when induction started (either at OD_{600} absorbance values 0.4-0.5 or 0.6-0.8) and by concentration of IPTG used to begin induction (either at a final concentration of 1 mM or 0.3 mM, indicated by A or B respectively). Induction temperature was kept at a constant 16°C. Lane marked M correspond to New England Biolab Prestained Protein Marker 7-175 kDa, Broad Range. Lane marked -ve corresponds to a sample of transformed bacteria that did not have any expression of CalB+MBP in the soluble fraction. Corresponds to samples incubated for an overnight period. Expected mass of CalB+MBP tag was 75.5 kDa and indicated with an arrow.

4.3.4. Designing PEGylation site of CalB

Once it was determined that it was possible to routinely express soluble wild-type CalB, the next step was to determine which sites on the surface of the protein would be best to alter to allow for PEGylation. Through *in silico* analysis of a crystal structure of CalB (Uppenberg, J, et al., 1994) and solvent-accessibility predicting software, e.g. Weighted Ensemble Solvent Accessibility predictor and ASA-View (Chen H L and Zhou H X, 2005, Shan Y *et al.*, 2001, Ahmad S *et al.*, 2004) (See 2.6.6.1. and 2.6.6.2.) solvent-accessible residues on the surface of the protein were identified. One site on the surface of the protein which seemed sensible to be converted to a cysteine residue was glutamic acid at position 269. This residue was chosen because it was an amino acid that would in theory not greatly alter the overall activity of the protein when converted to cysteine.

Primers were designed and ordered from Eurofins genomics (See 2.6.5.5.), and site-directed mutagenesis PCR performed to replace a glutamic acid to cysteine at position 269 using QuikChange Lightning Directed Mutagenesis Kit (See 2.6.5.7.3.), using CalB in pMAL-c2x vector as a template. XL10-Gold Ultracompetent cells which were transformed by the mutated plasmids and grew

on selective media had the plasmid extracted through miniprep. These plasmids were cut with *EcoRI* and were run on a TAE gel to see if the size of the plasmid matched expected length (See 2.6.5.9.). Colonies which corresponded to the banding pattern expected through treatment with endonuclease restriction were concentrated to 50-100 ng/ μ l as determined by absorbance at OD₂₆₀ then 15 μ l sent off to Eurofins MWG for sequencing.

Expression of E269C CalB+MBP in pMAL-c2x vector in BL21-AI (See figure 4.11.) went ahead under the same conditions of CalB+MBP in pMAL-c2x vector, i.e. induction took place when absorbance values at OD₆₀₀ reached 0.6-0.8 with 1 mM IPTG and 2% arabinose at 16 °C for an overnight incubation. Proteins were purified from lysate as previously described and the concentration of purified E269C CalB+MBP was derived through a Bradford assay (See 2.6.2.3.), dialysis occurred with a buffer at pH 7.2. 100 μ l of 1.5 mg/ml E269C CalB+MBP sample was exposed overnight at 2 °C to 3 μ l of 1 mg/ml Factor Xa.

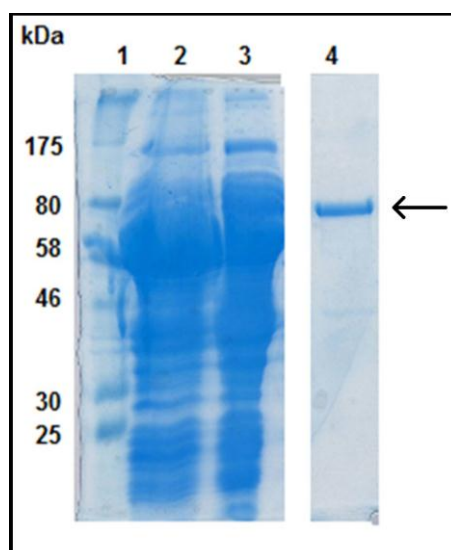


Figure 4.11. Expression and purification of soluble E269C CalB+MBP

E269C CalB was expressed through pMal-c2x vector in BL21-AI (See 2.6.1.2.2.). E269C CalB+MBP was extracted from lysate through IMAC. SDS-PAGE analysis of soluble E269C CalB+MBP; samples were separated on a denaturing SDS-PAGE gel. Lane 1: Marker. Lane 2: bacterial lysate. Sample 3: wash fraction. Sample 4: eluted protein corresponding to expected size of E269C CalB+MBP (76.9 kDa) marked with arrow. Sample 4 was dialysed and used in enzyme assays.

To determine if the E269C residue was solvent accessible, a gel was run of Factor Xa treated E269C CalB subjected to a TCEP.HCl gradient, along with negative controls of no reducing agent and a fully reduced sample (See 2.1.2.1.). A band that corresponded to the theoretical dimer mass (~68 kDa) was present in samples with no or little reducing agent (See figure 4.12.). The negative control and lowest concentration of TCEP reduced samples lack a band at the expected mass of 80 kDa in mass. Because this band could not be due to a disulphide bridge, since it was present in fully reduced control sample as well, this ~ 80 kDa band could be due to E269C CalB+MBP, which would theoretically be 76.9 kDa. As TCEP concentration increases, one band around 58 kDa in mass becomes fainter -it could correspond to an E269C CalB dimer (~68 kDa).

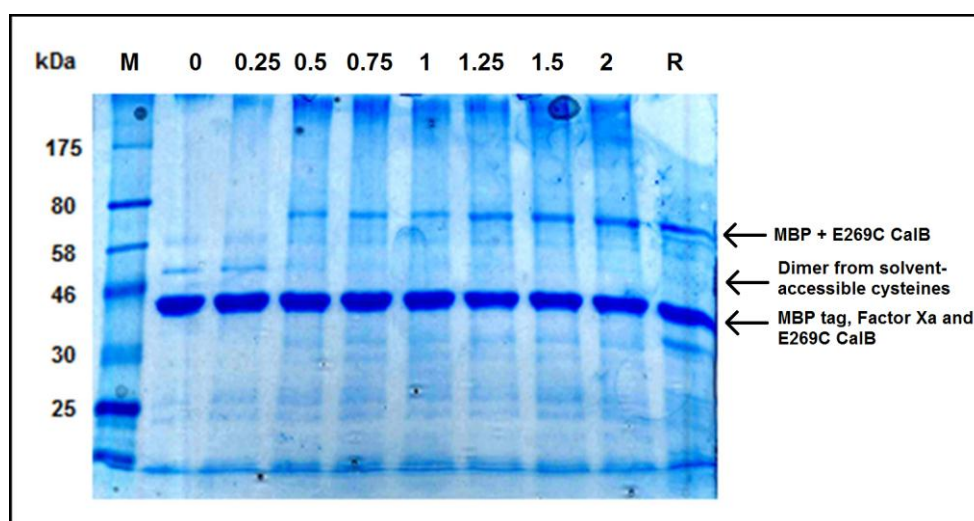


Figure 4.12. SDS-PAGE analysis showing TCEP gradient against Factor Xa-treated E269C CalB

Lane M: Marker. Remaining lanes: Factor Xa-treated E269C CalB reduced with an increasing gradient of TCEP concentration for 30 mins. TCEP concentration in gradient: 0.25 mM, 0.5 mM, 0.75 mM, 1 mM, 1.25 mM, 1.5 mM and 2 mM respectively. Lane R: fully-reduced Factor Xa-treated E269C CalB. The mass of Factor Xa = 43 kDa, mass of MBP tag = 42 kDa, mass of E269C CalB = 34 kDa (although the band will appear heavier due to protein not being fully denatured), mass of theoretical E269C CalB-MBP tag dimer = 68 kDa, mass of E269C CalB+MBP = 76.9 kDa.

The protein bands of 68 kDa in the TCEP gradient lanes of Figure 4.15. could be due to a dimerisation of E269C CalB, or due to E269C CalB+MBP. To resolve this, a second gel was run with samples of E269C CalB+MBP with reduced and unreduced controls as well (See figure 4.13.). Because there was a chance that the heavier band was due to dimerisation, some samples were PEGylated (See 4.2.2.) before being run on the gel.

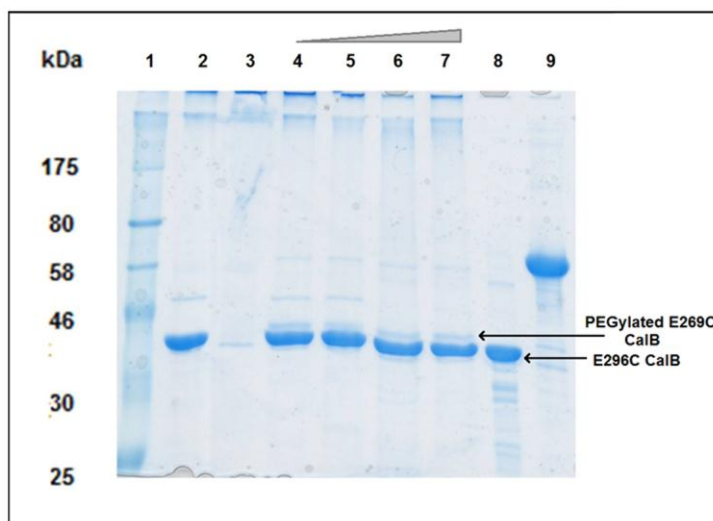


Figure 4.13. SDS-PAGE analysis showing effect of TCEP on PEGylation and reduction controls of E269C CalB

E269C CalB both cut and uncut by Factor Xa as reduced and unreduced controls were run alongside Factor Xa-treated E269C CalB reduced over a TCEP gradient and incubated with mm(PEG)₂₄. Lane 1: Marker. Lane 2: E269C CalB cut with Factor Xa, Lane 3: E269C CalB+MBP; samples in lanes 2 and 3 were unreduced. Lanes 4-7: Factor Xa-treated E269C CalB reduced with set concentrations of TCEP and incubated with mm(PEG)₂₄ (See 4.2.2.). TCEP concentrations were: 0 mM, 0.25 mM, 1 mM and 2 mM respectively. Lane 8: fully reduced E269C CalB that had been cut with Factor Xa, Lane 9: fully reduced E269C CalB+MBP. Bands corresponding to PEGylated and unPEGylated E269C CalB were indicated on figure.

The band of the E269C CalB+MBP was heavier than a potential dimer band of E269C CalB, which was what was expected (E269C CalB monomer was 34 kDa, therefore the dimer would be 68 kDa while E269C CalB+MBP was 76 kDa).

In figure 4.13., Lane 2 had a protein band slightly heavier than 46 kDa - this band could be due to the presence of Factor Xa or MBP tag, since this same band was not seen in Lane 3, which consisted of E269C CalB+MBP tag.

There was a very faint band approximately 40 kDa in Lane 3, but this does not correspond to the expected mass of E269C CalB+MBP tag (76 kDa). The lighter band could be due to minor contamination not fully removed through purification or the degradation of purified protein; multiple bands were found in the fully reduced controls of lanes 8 and 9, indicating that there may have been minor contamination. There were no bands at 76 kDa, but since lane 3 consists of unreduced E269C CalB, and the substituted residue appears to be solvent accessible, it was possible that the resulting dimer was too globular to move through the gel effectively under semi-reducing conditions.

Lanes 4-7 had two bands around 46 kDa in mass. One of these bands corresponds to E269C CalB cut with Factor Xa, the other is around 1 kDa heavier. The 1 kDa heavier band was not seen in either control which had E269C CalB cut with Factor Xa and which had not been subjected to PEGylation. Therefore, knowing that PEGylation with mm(PEG)₂₄ can lead to an increase in mass of around 1 kDa (See Figure 4.8.), this band could correspond to PEGylated E269C CalB molecule.

4.3.5. Further modification of E269C CalB

Attempts were made to further purify the E269C CalB away from Factor Xa and the cut MBP using the His tag on the protein. This proved to be unsuccessful with insufficient quantities of purified protein produced to be visualised on a gel.

It was decided to investigate if it was possible to PEGylate E269C CalB that had not had its MBP tag removed; there was no risk of PEGylation on MBP as it has no endogenous cysteine residues. PEGylation of TCEP-reduced E269C CalB+MBP was undertaken as in 4.2.2. and gels were run which contained samples of fully-reduced E269C CalB+MBP alongside fully- and partially-reduced PEGylated E269C CalB+MBP as well as E269C CalB that had been cut with Factor Xa (See figure 4.14.). The two PEGylated samples had two bands of approximately the same weight, which indicated successful PEGylation. The fact that the band did not disappear when fully reduced also indicates that the band could not be due to anything else within the protein mix besides from the binding of a PEG molecule to a cysteine residue through a thiol bond. The fully-reduced sample which was not PEGylated had only one band of the expected size of E269C CalB. This indicates that PEGylation could still occur at residue 269 while MBP tag was attached to the protein. The protein could be tethered without needing to cut it with Factor Xa and then having to subject the protein to a second round of purification.

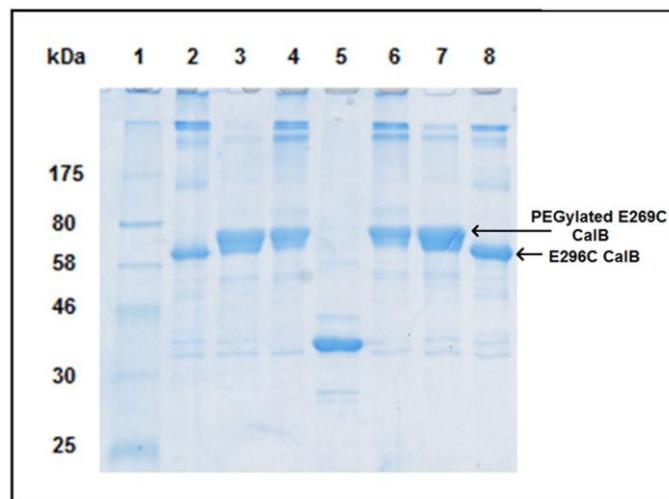


Figure 4.14. SDS-PAGE analysis showing PEGylation of E269C CalB untreated with Factor Xa
 Factor Xa-treated E269C CalB compared with E269C CalB+MBP both reduced with 1 mM TCEP with some samples incubated with 20x concentration of mm(PEG)₂₄. Lane 1: Marker. Lanes 2 and 8: reduced E269C CalB. Lanes 3 and 7: E269C CalB+MBP reduced with TCEP, PEGylated and then reduced. Lanes 4 and 6: E269C CalB+MBP reduced with TCEP and PEGylated. Lane 5: Factor Xa-treated CalB reduced with TCEP and PEGylated. By comparing Lanes 2 and 8 to lanes 3, 4, 6 and 7, one could see the effect PEGylation had on altering mass of E269C CalB.

To determine whether the act of PEGylation inhibits CalB+MBP activity, experiments were undertaken which compared the activity of equal concentrations of PEGylated E269C CalB and PEGylated E269C CalB+MBP with pre-PEGylated E269C CalB and pre-PEGylated E269C CalB+MBP. In pre-PEGylation, the proteins are incubated with the same volume of DMF (the solvent the PEG substrate was dissolved in (See 4.2.2.)) and for the same amount of time as in the case of the PEGylated proteins, but without any mm(PEG)₂₄ present in solution.

Results indicated that the activity of E269C CalB+MBP is similar regardless as to whether it has been PEGylated or pre-incubated with DMF (See figure 4.15.), i.e. the tethering of PEG to E269C CalB+MBP does not lower its activity and should not be a hindrance in the utilisation of E269C CalB+MBP as a ligand.

During the course of the project, purified samples of both C14S/M37C PA3859 and E269C CalB+MBP were reduced with TCEP and then sent down to collaborators at the University of Sheffield to use it in TREC.

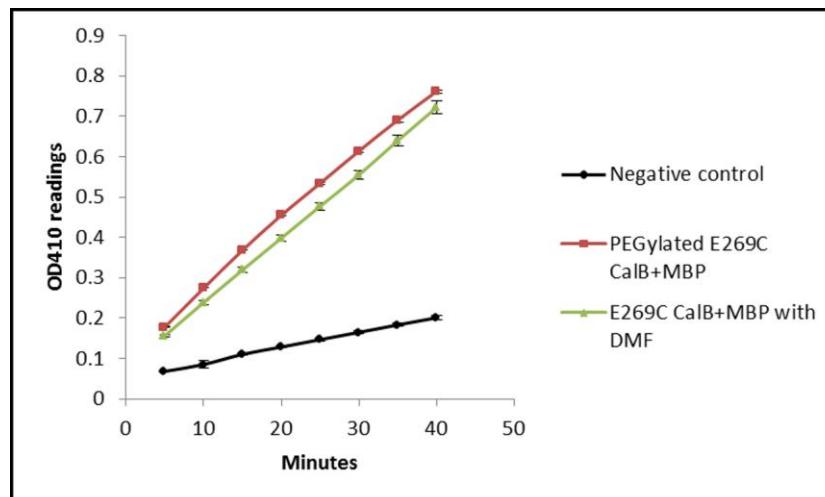


Figure 4.15. Effect of PEGylation and pre-PEGylating conditions on E269C CalB+MBP activity

Absorbance values at OD₄₁₀ obtained from incubating 5 µl of E269C CalB+MBP and incubated with DMF with mm(PEG)₂₄ (Red) compared to CalB+MBP and incubated without DMF with mm(PEG)₂₄ (Green) after both pools were incubated at room temperature with 145 µl of Tris/substrate mix (See 3.2.3.) with the substrate being nitrophenyl acetate in triplicate, along with standard error bars. Negative control consisted of the Tris/substrate mix incubated in elution buffer containing no enzyme.

4.4. AFM measurements obtained from collaborators

Purified protein which had been reduced with TCEP.HCl was sent to collaborators at the University of Sheffield. It was decided by the collaborators to perform measurements using a Bruker BioScope Catalyst AFM with Nanoscope Analysis v8.15 software used to generate the force curves. The type of AFM cantilevers used was MLCT tips of cantilever types C to F.

The protein was attached to MLCT tips that were PEGylated beforehand with linear NHS-PEG-maleimide particles 9.52 nm in length. MLCT tips were aminated through aminopropyltriethoxysilane (APTES). Amination allowed binding of PEG molecules through the NHS functional group. The PEGylated tips were exposed to 50 µl of 60 µM esterase in solution for 1 hour, resulting in the binding of the esterase particles to the maleimide functional groups of the PEGylated tips.

PEGylation of the esterase could not happen before attaching the PEG tether to the AFM tip, as the method for attaching PEG to the AFM tip would denature the esterase.

The first attempts by collaborators at the University of Sheffield at using C14S/M37C PA3859 and E269C CalB+MBP as ligands for TREC was using a quantitative nanomechanical property mapping (QNM) technique. QNM works by oscillating the cantilever as it is scanned across the sample. This means that the tip only contacts the sample surface for a small period of time, so forces that could damage ligands, e.g. forces generated by tapping of the tip on the surface and lateral forces (i.e. the cantilever partially rotating on its own axis when scanning the sample) are reduced. The cantilever vibrating means that the attached ligand is experiencing both attractive and repulsive forces to the substrate on the surface.

Preliminary attempts revealed recorded affinity of the cantilever and ligand to the sample (See figure 4.16.). However, further investigation revealed that there was no discernible difference between the results obtained for affinity between cantilever with or without ligand and the substrate. Because of these results, the collaborators decided to use force volume method instead of QNM.

Force volume method generates binding probabilities for ligand-tip and substrate interactions against naked-tip and substrate interactions by repeatedly undertaking force-distance measurements (See figure 4.1.).

Scanning with a naked AFM tip generates the binding probability of the naked AFM tip to the substrates on the mica slide. Scanning with an AFM tip with ligand bound to it generates the binding probability of the single ligand to the substrates on the mica slide. If ligand is able to interact with the substrate, the modified tips binding probability would be higher than that of the naked tip.

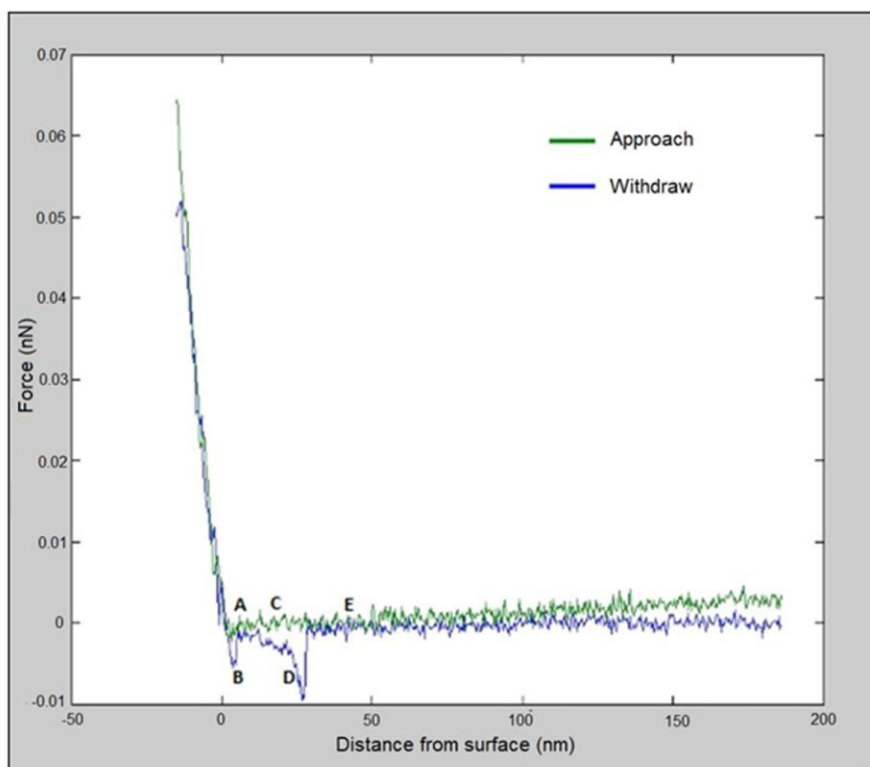


Figure 4.16. Force vs. distance graph generated with E269C CalB+MBP as a ligand in QNM AFM

E269C CalB+MBP was attached as a ligand to an AFM tip through a PEG tether. At A - the cantilever is being forced onto the surface of the slide, and the force required to return the reflected laser to the constant position goes higher. Further from the surface, at point B, the tip itself would adhere to the surface, requiring minor re-adjustment to return the reflected laser. At C, the cantilever is at a distance from the surface so that there's no interaction of the surface with either the tip or the ligand. At D, the ligand is bound to the surface, and the force required to remove the tip would have to take into account the full length of the 9.52 nm linker length as well as the ligand potentially being unfolded out as well. The stretching increases the force required to pull the tip and ligand away from the sample altogether. At point E, the ligand-cantilever is not associated with the substrate, and variations in force are due to Brownian motion as the cantilever moves away from the surface. Picture modified from Charlotte Nicolau of the University of Sheffield and generated through Gwyddion software.

Collaborators at the University of Sheffield managed to measure affinity of the negative control cantilevers along with cantilever that had tether-bound E269C CalB-PEG upon a slide with bound 2-acetoxypropionic acid (See Table 4.1.).

The binding probability of the CalB+MBP ligand against 2-acetoxypropionic acid, while low, shows significantly greater binding to sample slide than any of the other controls. It had been proposed by collaborators at the University of Sheffield that the low binding probability may be due to low substrate binding to

the mica slide, or the scanning being performed in a room temperature environment. Further research was being continued upon C14S/M37C PA3859, C14S/M37C/S113A PA3859 and E269C CalB+MBP as ligands for AFM by collaborators at the University of Sheffield.

	Binding Probability (%)	
	Mica Slide + immobilised 2-acetoxypropionic acid	Mica Slide
Naked tip	0.93	1.07
Naked tip pre-treated before PEGylation	0.24	0.81
PEG tether-tip	0.71	0.23
CalB-PEG tether-tip + unbound substrate in solution	0.85	N/A
CalB-PEG tether-tip	4.09	N/A

Table 4.1. Binding probability of CalB+MBP ligand against immobilised 2-acetoxypropionic acid

All experiments were carried out at room temperature in PBS. Each separate experiment had 8192 force curves measured, and the probability derived through affinity of the cantilever against the sample slide. The first four readings consist of the negative controls used to compare to the final reading - the test of CalB+MBP acting as a ligand. This work performed by Charlotte Nicolau at the University of Sheffield.

4.5. Discussion

4.5.1. Review of the choice of ligands

PA3859 and CalB were chosen as ligands for AFM in this project for a number of reasons. They had both been fully characterised and are known to be monomers (Pesaresi A *et al.*, 2005 and Uppenberg J *et al.*, 1994). CalB has been covalently bound to other chemicals before without losing its hydrolytic capabilities, e.g. being covalently immobilised to cyanogen bromide agar (Barbosa O *et al.*, 2012) or stabilised by binding imidazolium-functional ionic liquids through lysine residues (Jia R *et al.*, 2013). PA3859 had not been subjected to recorded chemical modification to the same scale as CalB, but the fact that it is a well characterised, monomeric esterase that had been mutagenised to have had a cysteine residue present at a solvent accessible site by Dr. Louise Horsfall meant that it was chosen alongside CalB to see if it was

possible to use AFM as a method to model esterase's ability to bind to and degrade non-emulsified fats and oils.

The monomeric aspect of these ligands is especially important as multimeric ligands are not suitable in AFM. The force of the ligand affinity to substrate combined with the force of the AFM cantilever pulling the ligand away from the substrate could overcome non-covalent forces that bind multimers together. Pulling domains of a multimeric protein apart through force enacted through AFM cantilever has been recorded (Rief M, et al., 1997) and AFM has been used to separate p53-azurin complex before (Taranta M, et al., 2008), so such concerns are not unprecedented. While quaternary interactions in a protein can be stronger than a ligand-substrate interaction, using a monomeric esterase removes the possibility of this being a problem.

Two versions of PA3859 were made, C14S/M37C PA3859 for the PEGylation of PA3859 and C14S/M37C/S113A PA3859 to test if the affinity of a ligand to a substrate through TREC was dependent on the activity of the ligand; there was insufficient time to accurately measure how less active C14S/M37C/S113A PA3859 was compared to C14S/M37C PA3859, so it was decided that once it was shown that activity of C14S/M37C/S113A PA3859 against nitrophenyl octanoate was reduced in comparison to C14S/M37C PA3859 that samples of C14S/M37C/S113A PA3859 were to be given to collaborators at the University of Sheffield. This was so as to give a greater chance of being able to generate TREC readings comparing the two forms of PA3859.

4.5.2. PEGylation for enzyme tethering

The first choice methodology had been a PEG tether which would bind to the histidine tag through a mono-sulphone functional site used to purify proteins from bacterial lysate since this method would not require any form of extra, invasive modification of the proteins to make a tether point (See figure 4.17.), however attempts to obtain this form of PEG tether were not successful. It was decided to find a different site that could be used as a tethering point for PEG which would not influence activity of esterases.

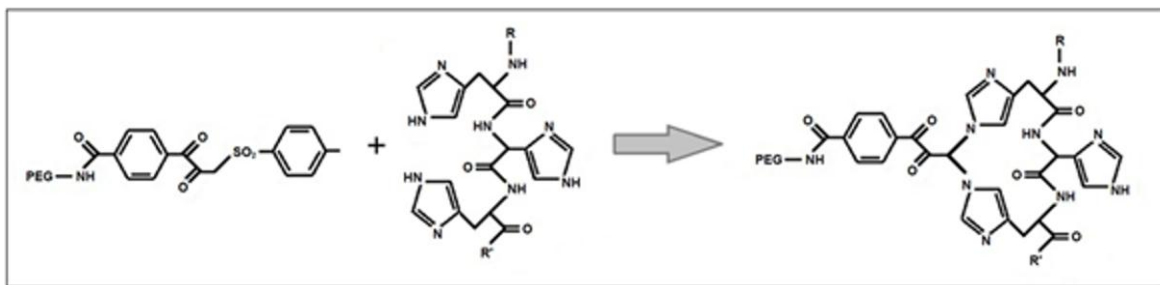


Figure 4.17. PEG molecule with mono-sulphone functional site binding to His-tag

The chemical structure of how PolyTherics advertised their PEG mono-sulphone tether binding to ligands. This technique was thought to be ideal for this project as all proteins were isolated and purified through a poly-His tag already engineered, so PEGylation through this method in theory would limit how much additional potentially activity altering modification, both pre- and post-translation, would be required to bind PEG to the ligand.

Further literature analysis indicated that the best way to tether a ligand to a PEG molecule would be through a maleimide functional group, due to how often it had been used without interfering ligand activity in previous studies. Alternative functional groups used to anchor PEG to proteins require either natural or engineered anchor points on the solvent-accessible regions of the protein, e.g. pyridyl disulphide which also requires cysteine residues or NHS esters which attach through lysine residues.

An mm(PEG)_{24} was chosen because a ligand of that size would increase the mass of a PEGylated ligand. From the results generated through SDS-PAGE gel analysis (See 2.1.2.1.) with fully reduced and semi-reduced samples of PEGylated or unPEGylated C14S/M37C PA3859, PEGylation had occurred as expected at the engineered site. To prove that this PEGylated form was viable as a ligand, and had not had its activity reduced by the attachment, mm(PEG)_{24} -treated C14S/M37C PA3859 had to be assayed and its activity contrasted with a comparable concentration of C14S/M37C PA3859 not treated with mm(PEG)_{24} . PEGylation had no negative effect on E269C CalB+MBP activity.

It would have been preferable to have used assays which compared the activity of pure PEGylated C14S/M37C PA3859 with C14S/M37C PA3859 against nitrophenyl esters, and to have compared activities not just against a single substrate at one condition but compared activities under a variety of different environmental conditions. However it would also be difficult to collect the separate pools in a high enough concentration to allow detectable assays to be performed, the protein in this pool could not be separated through purification

methods used previously, e.g. through their His-tag, as both types of protein would show equal affinity to Nickel chloride-charged resin. Neither could they be separated through the presence or absence of the PEG tether, since PEG is unreactive. Literature indicates that work has managed to purify PEGylated protein through size-exclusion chromatography which separates out products through their molecular size (Fee CJ, 2003).

CalB was expressed from the pMAL-c2x vector resulted in the MBP tag (43 kDa) being added to the protein which is theoretically removable through treating the protein with Factor Xa. To design a PEGylated version of CalB, a solvent-accessible residue would have to be converted to a cysteine. Analysis of online *in silico* methods for determining which residues were solvent accessible, leading to glutamic acid at position 269 being converted to cysteine for the PEG tether point.

As the MBP tag is joined to the expressed protein through a Factor Xa cleavage site, attempts were made to remove the tag from E269C CalB after expression and then purify E269C CalB protein. When samples of E269C CalB that had been purified after being cut with Factor Xa were run on a gel, the banding patterns were too faint to confirm that purification had been achieved. This led to attempting PEGylation of E269C CalB with the MBP tag still attached.

A full characterisation of the PEGylated E269C CalB+MBP was not necessary; just a demonstration that it was still capable of breaking down esters in a comparable way to the unPEGylated E269C CalB+MBP. By comparing the activity of the PEGylated E269C CalB+MBP with E269C CalB+MBP that had been exposed to the conditions required for the act of PEGylation, it was demonstrated that the observed reduction of activity was not probably due to the act of binding PEG tether to the protein, but was due to the presence of DMF which was used to make a solution of mm(PEG)₂₄, since both samples showed similar activities, which were lower than that of E269C CalB+MBP that had not been pre-treated with DMF. Possible ways DMF could have an effect on enzyme activity include the fact that it can exist as a positively charged resonance form; which nucleophilic serine could attack but not catalyse.

As with C14S/M37C PA3859, it would have been useful to be able to obtain pools of entirely PEGylated E269C CalB+MBP with equal concentrations of E269C CalB+MBP that had not been PEGylated and to perform assays which compared activities across a range of environmental conditions; but the quantity

of PEGylated protein to work upon was not large enough to separate out PEGylated protein from unPEGylated protein, neither was there enough protein to be able to perform more thorough assays.

With both potential ligands, it was important to measure hydrolytic activity of the enzymes after PEGylation even if it was not possible to make totally pure samples of PEGylated protein. There had been recorded instances where PEGylation causes a reduction in the function of the molecule it has chemically modified, even if the tether point is not near the active site (Kubetzko S *et al.*, 2005).

In addition to reduced activity C14S/M37C/S113 PA3859, it would have been convenient to create a version of E269C CalB+MBP which was had its activity hindered in a similar way, to see if activity loss would also remove the affinity of the ligand to substrate on an AFM slide as well.

Given more time work would have been undertaken to fully characterise the PEGylated variants of C14C/M37C PA3859, C14S/M37C/S113A PA3859 and E269C CalB+MBP against the pre-incubated with DMF variants; to see if PEGylation could alter activity of the ligands under different conditions. However, the limited assays which demonstrated activity (or lack thereof for C14S/M37C/S113A PA3859) sufficed in demonstrating the ligands were still appropriate for use in an AFM scan.

4.5.3. AFM substrate choice

The choice of substrate to be used in AFM had to balance ideals with what was practical. The most ideal substrate that would bind to a mica slide as well as display an ester bond with a short-chain aryl group would have been a substrate along the lines of hydroxybutanyl acetate - the alkyl group in the ester bond of this chemical is short enough to allow easy access the nucleophilic serine of an ester's active site. Since this was the first time research on the use of AFM to measure esterase affinity to substrate had been attempted, substrate that could bind to mica and which had the shortest available alkyl group was the most necessary feature for theoretical application, and 2-acetoxypropionic acid and 1-Octanoyl-rac-glycerol were the two substrates available which fitted that requirement.

4.5.4. Comparing PEGylation rates and procedures in this project to published results

While PEGylation could occur with the ligands designed to be probes for AFM, the rate of PEGylation should also be taken into account, not only with C14S/M37C PA3859 and E269C CalB, but with any future ligands. The higher the rate of PEGylation of a ligand means that there would be less chance of an AFM cantilever not having a ligand bound to it through the tether after the 1 hour incubation period.

The rate of PEGylation of ligand in this project was not quantified; only banding patterns generated from running samples on SDS-PAGE gels (See 2.1.2.1.) were used as evidence of PEGylation occurring. To calculate the rate of PEGylation, a variety of strategies could be applied, e.g. determining the ratio of PEGylated to unPEGylated protein by separation of proteins on an SDS-PAGE gel (Slavica A, et al., 2007), or detecting PEGylated and unPEGylated protein through high-performance reverse phase liquid chromatography (RP-HPLC) (Kunstelj M *et al.*, 2013).

A variation on PEGylation to thiol residues through maleimide-PEG is using maleimidophenyl-PEG as the tether. This form has been shown to tether to 50% of adult human haemoglobin (Ananda K, et al., 2008). Another methodology for PEGylation is a strategy reliant on binding the enzyme in question to a PEG molecule through a native disulphide bridge by using a functional group that breaks and then re-makes the bridge with itself as an integral part of the bridge without altering the tertiary structure of the enzyme. This could only work with the CalB variants and not with PA3859 due to the latter not having endogenous cysteine residues and this would only be possible if any of the former's endogenous disulphide bridges were solvent accessible.

PEG-monosulphone (See Figure 4.20) have been shown to result in a higher ratio of PEGylated protein to unPEGylated protein, e.g. experiments with interferon (INF) α -2b gave yields of 65% PEGylated INF when using PEG-monosulphone (Balan S *et al.*, 2007). Such strategies had also been used in antibody fragments (Shaunak S *et al.*, 2006) and leptin, and so such a strategy could be considered as an alternative for PEGylation, if PEGylation through a maleimide functional group does not produce enough PEGylated product.

Chapter 5

Directed evolution of an esterase for increased activity at lower temperatures

5.1. Introduction

5.1.1. Directed evolution

The other desirable characteristic of an esterase for use in a washing detergent in addition to hydrolytic activity at low temperature is a high affinity for long-chain substrates; a feature not frequently seen in esterases, but more commonly seen in lipases. However, as was stated earlier, lipases show affinity to fats and oils in emulsion bodies, using the lid structure which covers the active site as the determining feature to allow access of the substrate to the active site. At lower temperatures, fats and oils are present in semi-crystalline forms, so the lipase lid could not be moved to allow access to the active site. It was deemed more sensible to instead attempt to generate esterases, whose accessibilities to the active sites are not determined by physical structures of the enzyme, to break down long-chain substrates at low temperatures. To bring about these features in candidate esterases, a directed evolution strategy was undertaken.

Directed evolution consists of the DNA of the target genes being subjected to mutagenesis and the resulting mutant library screened for the desired phenotypic features (See figure 5.1.).

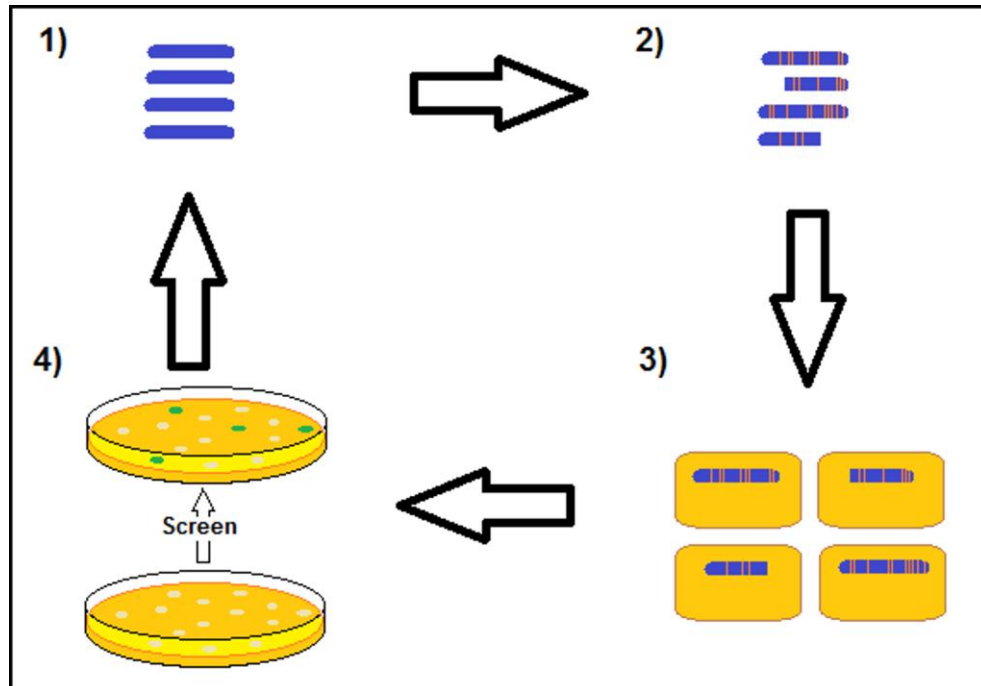


Figure 5.1. A diagram illustrating the four stages of any random mutagenesis technique.

Step 1) Several copies of the gene of interest were isolated. Step 2) The genes were subjected to random mutagenesis, generating a library of mutants. Step 3) The library of mutants was placed into an environment which allows expression, most commonly the mutant library is used to transform bacterial expression hosts. Step 4) The variants with the desired phenotype were isolated, characterised and subjected to another round of mutagenesis.

There are a wide variety of mutagenesis methods for generating a mutant library. Early methods involved subjecting the host organism containing the target gene to mutagenic conditions. Examples include using N-methyl-N'-nitro-N-nitrosoguanidine (MNNG) and ethylmethane sulphate (EMS) which are alkylating agents that generate transitions at guanidine-cytosine sites (Kohalimi S E and Kunz B A, 1989). Alternatively, subjecting host organisms to UV light (a wavelength of 254 nm) will introduce transitions, transversions and thymine-thymine cross-linker dimers (Kunz B A *et al.*, 1987 and Lee G S *et al.*, 1988). These methods are no longer used when mutagenising a target gene because targeting the host organisms with the mutagen mutates the entire organism and not just the target gene. The effects of the mutagens on the host organism can interfere with the screen, thus preventing an accurate measurement of any mutants of the target gene.

Biological methods were also used on the host organisms, such as bacteriophage Mu transposon to insert randomly in DNA vectors (Pajunen M I *et*

al., 2005) or by inserting vectors containing the target gene into bacterial hosts which are genetically altered to promote an increased number of mutations into vector DNA, like the XL1-Red competent cell line, engineered to be deficient in the DNA repair pathway enzymes, *mutS*, *mutD* and *mutT* (Cox E C, 1976, Scheuermann R *et al.*, 1983). However, these methods have limited accuracy in where introduced mutations will occur; even Mu transposon mutagenesis against the vector cannot guarantee that insertional mutations will occur within the expressed gene. To get the highest ratio of mutations that affect the activity of the protein, the mutagenic method must be directed against the gene of interest only.

More direct techniques for making a mutant library through mutagenising target genes have been developed. These techniques can change specific nucleotides in the target gene so the encoded protein's amino acid is altered into a new, known form, e.g. through site-specific mutagenesis (Braman J *et al.*, 1996) and inserting the mutant target gene into an expression vector to transform competent bacteria. However this form of mutagenesis requires knowledge of what effects are likely to occur through the directed mutagenesis, it would be too labour intensive to fully saturate a gene through site-specific mutagenesis.

Another way to mutagenise a target gene is to do so randomly - e.g. altering the QuikChange protocol to generate mutant target genes via low-fidelity PCR, and then using the multiple mutant versions of the gene as megaprimers to replicate the expression vector from which the original target gene arose (Miyazaki K and Takenouchi M, 2002, Miyazaki K, 2003). The end result would be a library of expression vectors containing random target genes which can be used to transform competent bacteria.

The approach using mutagenic libraries has been used to find lipolytic mutant enzymes for increase enantioselectivity towards a substrate (Horsman G P *et al.*, 2003), increasing esterase activity towards lipid and long-chain substrates (Reyes-Duarte D *et al.*, 2005, Höst G *et al.* 2006), increasing stability towards substrate oxidation (Di Lorenzo M *et al.*, 2007), generating thermostability in a p-nitrobenzyl esterase (Gershenson A *et al.*, 2010). etc. These mutants can be used to inform an understanding of how alterations in the primary structure affects the enzyme's 3-dimensional structure, catalytic activity, stability and performance under different environmental conditions. In

addition directed evolution has been used for the engineering of industrially-relevant and biotechnologically exploitable tools e.g. *Rhodobacter sphaeroides* esterase being altered to show greater substrate selectivity (Ma J *et al.*, 2012) improving activity of *Aeropyrum pernix* esterase against long-chain substrates (Chang L *et al.*, 2011)

5.1.2. Mutant library screening

In order to identify a mutant with a desired phenotype an appropriate screen must be available. This screen must be able to directly compare the activities of multiple gene products in tandem, and must be able to discriminate which of the variants have the desired phenotype, i.e. it must be a quick, sensitive and high-throughput screen. Such screens can be *in vivo*, *in vitro* or *in silico*, if the mutant library of the target gene is saturated (Menda N *et al.*, 2004). Any screen which does not accurately use the desired features of the gene product as the only form of differentiating one mutant from another will delay isolation and further characterisation of a suitable enzyme.

This does not mean that if one is trying to generate a mutant that shows a change in multiple features that a screen has to be made for each feature. *In vivo* screens can be designed to detect altered features of mutagenesis of the target gene at once, e.g. adding a soft-agar overlay of 0.1% CMC and 0.2 mM IPTG, which measures endoglucanase activity through zone clearing around bacteria expressing genes with endoglucanase activity to bacterial colonies containing mutant library of endoglucanase III that have been plated on LB agar plates which contain 0.05% OBR-HEC which measures endoglucanase activity through zones of clearing (Nakazawa H *et al.*, 2009).

Other screens require the mutant variants to show activity in order to survive, which is convenient for removing any null mutants that would be generated through random mutagenesis, e.g. growing variants on minimal media where carbon can only be sourced through desired activity (Chaloupka J A *et al.*, 2006) or by exposure to a chemical that would cause cell death or growth retardation unless gene function is obtained or removed (Müller-Hill B *et al.*, 1964, Wang L *et al.*, 2008). The mutagenesis may need to be undertaken several times to obtain the ideal mutant enzyme - the chances of getting the best result

from one round of mutagenesis and screening is poor. This technique has been utilised, e.g. to engineer superior esterases for applications in the pharmaceutical industry (Bornscheuer U T *et al.*, 1998, Moore JC and Arnold FH. 1996).

5.1.3. Screens for esterase activity

Screens developed for the high-throughput *in vivo* detection of lipolytic activity are inherently linked to a product being produced or a substrate being degraded through ester hydrolysis, giving off a detectable change in the environment of the expression host.

These changes can be detected through a colour change of an indicator within the agar as product is made from ester hydrolysis, e.g. hydrolysis of naphthyl esters releasing a naphthoxide moiety to form an azo compound with diazonium salt bringing about colour change (Böttcher, D *et al.*, 2010), detection of bacterial host's lipolytic activity on tributyrin or olive oil with Rhodamine b and illuminated with ultraviolet light (Bhavani M *et al.*, 2012, Leonov S L 2010), using ester substrates with an ethanoic acid moiety and measuring rate of NADH production made with said acid moiety reacting with oxaloacetate to produce citrate which can be measured through change in OD₃₄₀ (Baumann, M *et al.*, 2001), etc.

Another way of detecting esterase activity is through formation of a halo indicating substrate degradation, e.g. bacterial esterase activity on tributyrin agar produces clear halos around the colonies, (Mourey A and Kilbertus G 1975), the degradation of Tween 20 or Tween 80 on agar plates produces measurable halos formed through the resulting precipitate (Kumar D *et al.*, 2012).

5.2. Materials and Methods

5.2.1. Media for detecting esterase activity

5.2.1.1. Tributyrin agar

Tributyrin media was made through sonicating 5 g gum Arabic, 5 ml tributyrin and dH₂O to 15 ml for 45 minutes, before being added to the remainder of the tributyrin agar constituents (A suspension of 0.5 g tryptone, 1 g yeast extract, 0.5 g NaCl and 1.5 g Agar). The media was made up to 90 ml with dH₂O and its pH was adjusted to 7.5. This was then made up to 100 ml and autoclaved at 121 °C for 15 minutes, agitated violently while cooling so as to promote uniform emulsification. The resulting sterilised media was cooled to handling temperature, and any media supplements needed, e.g. antibiotics, inducing chemicals, were added under sterile conditions. Method was supplied by Arne Wehling of iGEM group at TU Darmstadt.

Individual colonies were streaked onto these plates and left to grow at 15-20 °C. Esterase activity was indicated by formation of clear halos around colonies.

5.2.1.2. Novel soft agar overlay

Novel soft agar indicator overlay was made by melting 0.01g agar in 9 ml 25 mM Tris-HCl at pH 8. 0.15 µM nitrophenyl substrate is dissolved in 1 ml ethanol and substrate/ethanol mix and bromocresol purple indicator dye dissolved in water is added at a final concentration of 0.01% once the overlay has cooled to handling temperature. The overlay was mixed to promote uniform substrate distribution and poured on top of LB agar plates which had bacterial colonies expressing esterase of interest grown under inducing conditions. Esterase activity of colonies underneath the overlay was seen through the colonies changing colour from white to yellow.

5.2.1.3. Rhodamine B lipolytic detection agar

Rhodamine B lipolytic detection agar is made by mixing 0.5 g peptone, 0.3 g yeast extract and 1.5 g agar with 100ml dH₂O. This is autoclaved for 30 minutes at 121 °C. The resulting sterilised media was cooled to handling temperature, and 1ml of olive oil or tributyrin, filter-sterilised Rhodamine B solution to a final concentration of 0.001% and any media supplements needed,

e.g. antibiotics, inducing chemicals, were added under sterile conditions before pouring the plates

The positive control used to test plaque formation on plates was *Thermomyces lanuginosus* lipase from Sigma-Aldrich. After incubation and digestion of substrate for at least 48 hours at room temperature, lipolytic activity of colonies was observed by illuminating plates with UV light. Lipolytic/esterase activity was visualised by a fluorescent halo.

This procedure can be altered to replace the olive oil with any other substrate containing an acid moiety that gets released upon enzymatic activity, e.g. 0.15 μM nitrophenyl substrate dissolved in ethanol volume 1/10th of total media volume.

5.2.1.4. Bromocresol purple and ester substrate Tris agar

Bromocresol purple/ester substrate plate assay was made by melting 0.5 g agar in 100ml 25 mM Tris-HCl (pH 8). 0.15 μM nitrophenyl substrate or 1% oil or 1% tributyrin is dissolved in 1 ml ethanol and substrate/ethanol mix and bromocresol purple indicator dye dissolved in water is to a final concentration of 0.01% is added along with other media supplements e.g., antibiotics, inducing chemicals. etc., under sterile conditions once the media has cooled to handling temperature. Colonies are streaked onto agar and left to grow at room temperature. Esterase activity of colonies grown on plates was seen through the colonies changing colour from white to yellow.

5.2.1.5. Fast Blue and naphthyl substrate agar

0.025 g agar is melted in 5 ml dH₂O. When cooled to handling temperature, 80 μl of 20mg/ml of naphthyl acetate dissolved in NN-DMF and 80 μl of 80 mg/ml of Fast Blue dissolved in DMSO were added to the agar overlay under sterile conditions. The overlay was poured on top of LB agar plates which had bacterial colonies expressing esterase of interest grown under inducing conditions, with esterase activity indicated through colonies turning brown.

5.2.1.6. Tween 20 agar

Tween 20 *in vitro* esterase assay agar was made by mixing 1 g Peptone, 0.5 g NaCl, 0.01 g CaCl₂.2H₂O, 2 g agar and 1 ml Tween 20 in 100ml dH₂O. The mix was autoclaved and was cooled to handling temperature with any media

supplements needed, e.g. antibiotics, inducing chemicals, added under sterile conditions.

Lipolytic activity in this pate was indicated through precipitation of calcium salt of fatty acids released from Tween 20 hydrolysis.

5.2.1.7. Minimal media agar

Minimal media trace element mix was made by first adding 2.5 g Na₂EDTA to 400 ml with dH₂O and pH is set to 7. To this, 0.25 g FeCl₃·(6H₂O), 0.025 g ZnCl₂, 0.005 g CaCl₂, 0.005 g CoCl₂·(6H₂O), 0.005 g H₃BO₃ and 0.8 g MnCl₂·(6H₂O) is added, while pH was re-set to 7 after the addition of each element. Media was autoclaved at 121 °C for 30 minutes and stored at 4 °C.

5 x M9 solution was made by dissolving 3.389 g Na₂HPO₄, 1.5 g KH₂PO₄, 0.25 g NaCl and 0.5 g NH₄Cl to 100 ml dH₂O. Resulting mixture was autoclaved at 121 °C for 30 minutes.

Minimal media agar was made through mixing 10ml 5 x M9 solution, 0.2 ml 1M MgSO₄, 10 µl 1M CaCl, 2 ml Trace Element solution and 1 ml Olive oil/Tributyrin or 0.15 µM ester substrate. This is made up to 100ml with dH₂O containing 1.5 g agarose. Resulting mix is autoclaved at 121 °C for 30 minutes.

The resulting media was cooled to handling temperature, and any media supplements needed, e.g. antibiotics, inducing chemicals, were added under sterile conditions, and plates poured. Esterase activity indicated through colony growth.

5.2.2. *E. coli* M15 cell line maintenance, transformation and expression protocols

5.2.2.1. Production of competent *E. coli* M15 protocol

E. coli M15 cells containing pREP4 plasmid (supplied from QIAGEN) were spread out on kanamycin-selective LB plates (25 µg/ml) from the supplied one-stab culture tube and grown overnight at 37 °C.

A single colony from this plate was isolated and grown for a further night in 10 ml of LB with kanamycin to an absorbance value between 0.6-0.8 at OD₆₀₀ at 37 °C at 200 rpm.

1 ml of this incubation was used to inoculate 100 ml of pre-warmed LB with kanamycin, and was grown at 37°C at 200 rpm until an absorbance value at OD₆₀₀ of 0.5 was reached.

The growth was spun down in ice-cooled 50ml centrifuge tubes at 4000 rpm for 5 minutes at 4°C. The supernatant was removed and the cells re-suspended in ice-cold TFB1 (30 ml for 100 ml of bacteria).

The re-suspension was kept on ice for 90 minutes, and was then spun down for a further 5 minutes at 4000 rpm at 4°C. Again the supernatant was removed, and the cells re-suspended in ice-cold TFB2 (4 ml for 100 ml of bacteria).

100-200 µl of cells were transferred into 1.5 ml centrifuge tubes, and then immediately flash-frozen in liquid nitrogen before being stored at -70°C. These aliquots were used for transformation.

5.2.2.2. *E. coli* M15 transformation protocol

1 µl of plasmid and at least 100 µl competent *E. coli* M15 cells were mixed and left on ice for up to 20 minutes, then subjected to heat-shock at 42°C for 90 seconds.

The bacteria were suspended in 250 µl LB media and grown at 37°C for 60-90 minutes on a shaker rotating at 200 rpm. This incubation was then grown overnight on LB agar containing appropriate antibiotics at 37°C.

5.2.2.3. *E. coli* M15 expression

Successfully transformed *E. coli* M15 bacteria (See 5.2.2.2.) were re-suspended in 100 ml of LB and grown for 1 hour at 37°C at 200 rpm.

80 or 40 ml of this growth was then used to infect 4 or 2 l of LB growth media with required antibiotic concentration at 37°C at 200 rpm respectively. These were grown to the desired absorbance value at OD₆₀₀ of 0.5, whereupon they were induced by 0.1 mM IPTG. The induced media was then incubated at 12°C at 200 rpm over-night for expression of soluble protein.

Aliquot samples were isolated for checking protein expression while the remaining bacteria were spun down for 25-30 minutes at 7500 rpm and supernatant removed. The bacterial pellet was collected and flash-frozen with liquid N₂.

5.2.3. Assay methodology

5.2.3.1. Esterase assay Est97 variation

A stock reaction buffer was made of 50 mM Tris-HCl at pH 7.5 with 1% acetonitrile, with 0.1 mM nitrophenyl substrate dissolved in said acetonitrile. A separate stock of esterase to a desired concentration was made up and kept on ice. A 100 μ l of esterase stock - along with a separate negative control made with 100 μ l esterase dialysis buffer - was mixed with 900 μ l of 50 mM Tris-HCl/substrate buffer, and incubated at the desired temperature for the desired time. After incubation, the samples were removed from the water bath, kept on ice and the OD quickly read at 405 nm.

For assays involving altering pH, the substrate and enzyme were mixed with 50 mM Tris-HCl for pH 7-9.5 and 50 mM phosphate buffer for pH 6-8.

Assays for determining the V_{max} , K_m and k_{cat} were performed by having a set concentration of Est97 catalyse a nitrophenyl hexanoate as a substrate over a range of concentrations from 0.01 mM to 0.15 mM for 2 minutes at 25°C, with the resulting values being used to generate Michaelis-Menten and Lineweaver-Burke graphs.

In all esterase assays involving measuring nitrophenol product concentration through optical density, if the results for a set mass of esterase gave readings in excess of 1, the experiments were repeated, but with less esterase so as to get a value less than 1. This was because, according to the Beer-Lambert law, $T = I/I_0 = e^{-(\alpha \ln(10))l} = e^{-\sigma l N}$, a value of 1 means that 90% of the light at said wavelength has been absorbed; any values in excess of 1 cannot be measured accurately.

5.2.3.2. Molar extinction coefficient (ϵ) nitrophenol determination

A set stock of nitrophenol solution was made (using buffer of experiment). From this stock, a dilution series of 50, 25, 12.5, 6.25 and 3.125 μ M nitrophenol buffer was made.

The absorbance value of each dilution series was recorded in triplicate, and the average value taken and used to determine ϵ when $\epsilon = \text{Absorbance value} / \text{Concentration of product (M)} * \text{path length of cuvette (cm)}$.

Average ϵ from all dilution series taken to equal the general molar extinction coefficient under the specific conditions.

5.2.4. Mutagenic PCR protocols

5.2.4.1. Directed Mutagenesis PCR

Primers designed to incorporate the desired change for the gene were made (See 2.6.5.5.), and the DNA was subjected to the QuikChange mutagenesis kit (See 2.2.).

The hemimethylated DNA product was digested at 37°C using *DpnI* endonuclease, which removes the methylated, non-mutated parent strand. The remaining DNA was then used to transform XL1-Blue supercompetent cells, in conjunction with NZY+ broth at pH 7.5, supplemented with 12.5 mM MgCl₂, 12.5 mM MgSO₄ and 20 mM glucose, and the calls were plated on LB plates containing relevant antibiotic. Plasmids were isolated from individual colonies were sequenced to confirm mutagenesis has occurred as planned.

Mutagenesis of the DNA can be done in such a way so as to introduce a restriction site into the gene as well as new amino acids. With the experiments in which this happened, the plasmid DNA underwent endonuclease digestion (See 2.6.5.2.), and the fragments were run on TAE gel (See 2.6.5.9.). Only the fragments which correspond to the site-directed mutagenesis would be sent off for sequencing to Eurofins MWG.

5.2.4.2. Random Mutagenic PCR

5.2.4.2.1. Rolling mutagenesis PCR

0.5 µl of 30 pM template DNA mixed with 5 µl sample buffer. This mixture heated at 95°C for 3 minutes to denature plasmid and cooled immediately by placing on ice to promote hexamer annealing. To this, a premix made of 5 µl reaction buffer, 0.2 µl enzyme mix and 1µl 15 mM MnCl₂ was added and the reaction incubated for 24 hours at 30°C. The reaction was halted by heating at 65°C for 10 minutes, and the DNA can be used to transform TOP10 cells (see 2.6.1.1.2.). Reagents supplied from Illustra Templiphi kit (See 2.2.)

5.2.4.2.2. Mu Transposon mutagenesis

DNA samples were subjected to the ThermoScientific Mutation Generation System Kit (See 2.2.). Briefly, samples of target plasmid DNA are reacted with MuA Transposase and Entranceposon; which cause random insertions of

transposons into the vector. These can then be treated again with *NotI* endonuclease (See 2.6.5.2.) to remove the transposon, but leave a 15 bp insert in the vector.

5.2.4.2.3. GeneMorph II EZClone Domain Mutagenesis

Following the procedures in the GeneMorph II EZClone Domain Mutagenesis kit (See 2.2.), primers which flanked the WT gene of interest were used to generate a collection of mutant copies of the gene of interest from an original pool of 100 ng WT gene in vector so as to generate the highest rate of mutations through the error-prone PCR provided by this kit. At the same time as this was done, a control was made using kit-supplied materials to mutagenise *lacZ* in pUC18 vector. These mutant gene copies were isolated from the PCR mix and purified.

These mutant copies were used as megaprimers to replicate the entire vector from which it originally came, and the resulting mix was digested with *DpnI* endonuclease (See 2.6.5.2.) so as to remove vector containing WT gene from the mix.

The resulting mixes of random mutant gene inserted in vector were used to transform expression hosts (See 5.2.2.2.). Mutagenised pUC18 vector was used to transform XL10-Gold ultracompetent cells which were plated on LB agar plates containing 80 µg/ml X-gal and 20 mM IPTG. Resulting bacteria that grew from the transformation were screened as appropriate.

5.2.4.2.4. Low GTP nucleotide mutagenesis.

This methodology follows typical 50 µl Phusion polymerisation procedure (See 2.6.5.7.1.), but instead of using 2 µl of 10 mM GTP as like the other dNTPs, only 0.6 µl 10 mM GTP was used. A low concentration of GTP in a PCR procedure promotes mis-matches during the process of polymerisation.

5.2.4.2.5. MnCl₂ mutagenesis.

This methodology follows typical 50 µl Phusion polymerisation procedure (See 2.6.5.7.1.), but was performed in the presence of 2 µl 2.5 mM MnCl₂. MnCl₂ encourages mis-insertion of nucleotides through the polymerase enzyme.

5.3. Results

5.3.1. Analysis of a psychrophilic monomeric esterase

As stated previously (See 5.1.) the novel esterases were not monomeric and were therefore not appropriate for attachment to the AFM tip. We therefore decided to investigate the use of an alternative esterase, Est97, which was expressed from a DNA sequence originally isolated from a metagenomic sample of an Arctic intertidal sediment (Fu J, et al., 2012) that could form a dimer in solution but could also function as a monomer.

A copy of the gene inserted in pQE30 expression vector in *E. coli* M15 bacteria in a glycerol suspension was generously donated by the Norwegian College of Fishery Science of the University of Tromsø, the lab which had managed to characterise Est97.

The pQE30 expression vector has a MCS downstream of a poly-His tag preceded immediately by a Factor Xa protease recognition peptide sequence. pQE30 contains a T5 promoter, which is recognised by *E. coli*'s endogenous RNA polymerase. M15 is a strain of *E. coli* developed to regulate expression of genes inserted into pQE vectors through the presence of the pREP4 plasmid which constitutively expresses in trans lac repressor, which would prevent *E. coli* RNAP access to T5 promoter on pQE30. The repressor's effect can be removed through the addition of IPTG; thus permitting control of gene expression.

Colonies were grown from transformed bacteria in glycerol suspension plated onto LB plates with carbenicillin antibiotic selection. Individual colonies were grown overnight in selective media and plasmid DNA purified (See 2.6.5.1.). These plasmids were digested with *HindIII* to ensure there was a gene of the expected size within the vector. The positive plasmids were then sequenced to confirm the identity and correct sequence of the est97 gene.

5.3.2. Purification of Est97

5.3.2.1. Alterations to established method for expression and purification

Expression trial methodology was based on that described in the original paper that characterised Est97 (Fu J, et al., 2012) (See 5.2.2.2. and 5.2.2.3.). Expression of the protein was detected by running soluble and insoluble protein

fractions on a SDS-PAGE gel (See 2.1.2.1.) and seeing if a protein band of expected mass was present (29.6 kDa) (See figure 5.2.).

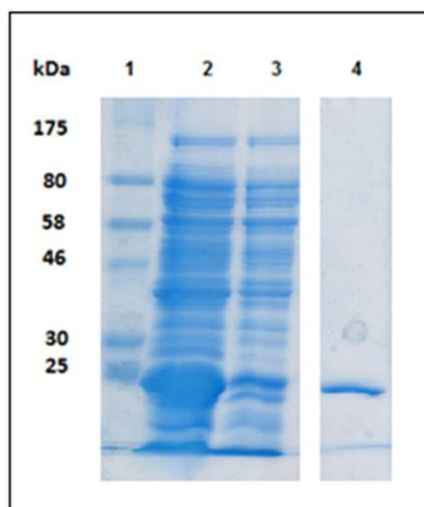


Figure 5.2. Expression and purification of soluble Est97

SDS-PAGE gel Lane 1: Marker. Lane 2: bacterial lysate. Lane 3: flow-through. Lane 4: eluted protein that was dialysed and used in assays.

When trials produced eluted protein at the expected masses, purification on a larger scale was undertaken. Induced bacterial pellets from 3 litres of media were lysed using a French press. The lysed bacteria were then subjected to an IMAC (See 2.6.2.2.), but suspended in 0.05 M NaH_2PO_4 /0.3 M NaCl buffer at pH 8, with the stated concentrations of imidazole. First attempts to elute Est97 from nickel-charged resin column following published procedure was unsuccessful as no protein of the expected size came off when running elution buffer through the column. Instead, the protein was eluted with buffer containing twice as much imidazole than as suggested by Fu J *et al.*, 2012, (See 2.6.2.2.), i.e. with 200 mM imidazole instead of 100 mM, and resulted in very pure samples of Est97 (See figure 5.2.). The eluted protein was dialysed in 0.05 M Tris-HCl at pH 8 with 10% glycerol so as to remain soluble in solution.

Est97 purified protein was run on a gel under native conditions or semi-reduced conditions (See figure 5.3.) to check the multimeric state of the esterase. The native gel indicated that the mass of Est97 was greater than 66 kDa. However, authors of Fu J *et al.*, 2012, confirmed by personal communication that Est97 also formed an active monomer.

In order to verify if Est97 is present as a monomer, purified Est97 was concentrated through a Millipore Amicon centrifuge filter unit with an MWCO of 30 kDa, which has an advertised 100% integrity. Est97 monomer (26.8kDa) should pass through the filter into the flowthrough but not any multimers. The flowthrough was concentrated in a second filter unit, this time of MWCO of 10 kDa. Any monomeric Est97 would be concentrated enough to check esterase activity. The esterase activity of this fraction was detected by comparing a negative control of dialysis buffer with 145 μ l of 25 mM Tris with 0.15 μ M nitrophenyl octanoate at pH 7 to an equal volume of protein fraction subjected to concentration with 145 μ l of 25 mM Tris with 0.15 μ M nitrophenyl octanoate at pH 7 (See 3.2.3.). The concentrated protein that could only be monomeric Est97 was found to have hydrolytic activity.

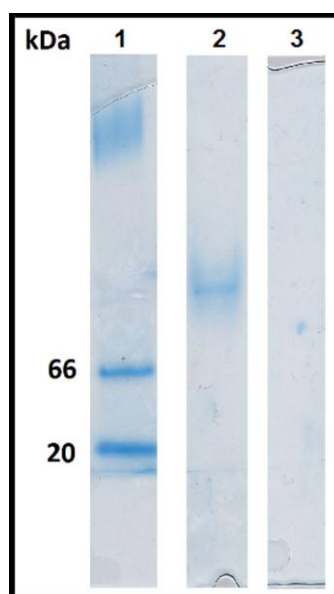


Figure 5.3. Native gel run of Est97

A native PAGE where non-boiled Est97 samples were run in sample buffer without beta-mercaptoethanol. Lane 1: marker, Lane 2: Est97, Lane 3: boiled Est97. The boiled sample did not show a band in the same mass range as unboiled Est97; with it being totally denatured it was thought to have run fully though the gel.

5.3.3. Measuring Est97 activity

To compare K_m and k_{cat} values of Est97 with the published data the assay in Fu J, et al., 2012 was followed (See 5.2.3.1.). The substrate used to determine activity was nitrophenyl hexanoate. After incubation at 25 °C for 2

minutes, the nitrophenol concentration from the reaction mix was derived from taking absorption readings at OD₄₀₅.

A Lineweaver-Burke graph was plotted; 100 µl 0.5 mg/ml Est97 (derived through a Bradford assay (2.6.2.3.) from a single purified batch was assayed against a range of nitrophenyl hexanoate concentrations in triplicate. The range of nitrophenyl hexanoate concentrations consisted of 0.01, 0.0111, 0.0125, 0.014286, 0.0167, 0.02, 0.025, 0.0333, 0.05 and 0.15 mM, and the activity at each concentration derived. K_m and k_{cat} were elucidated from the line of best fit (See Table 5.2.).

k_{cat} values were lower by approximately 1/10th of the k_{cat} values extrapolated from Fu J *et al.*, 2012 which first characterises Est97, (3.99 sec^{-1} , compared to 25.8 sec^{-1}) though the K_m values were almost identical (37.32 µM compared to 39 µM). Repeated kinetics of Est97 in this lab indicated that this was not due to a one-off problem linked to user error or by protein aging.

Attempts were also made to determine the temperature profile of the Est97 variants. Reactions were performed at different temperatures as described in 5.2.3., but with a range of temperatures from 5 °C to 55 °C in 5 °C incremental steps (See Figure 5.4.).

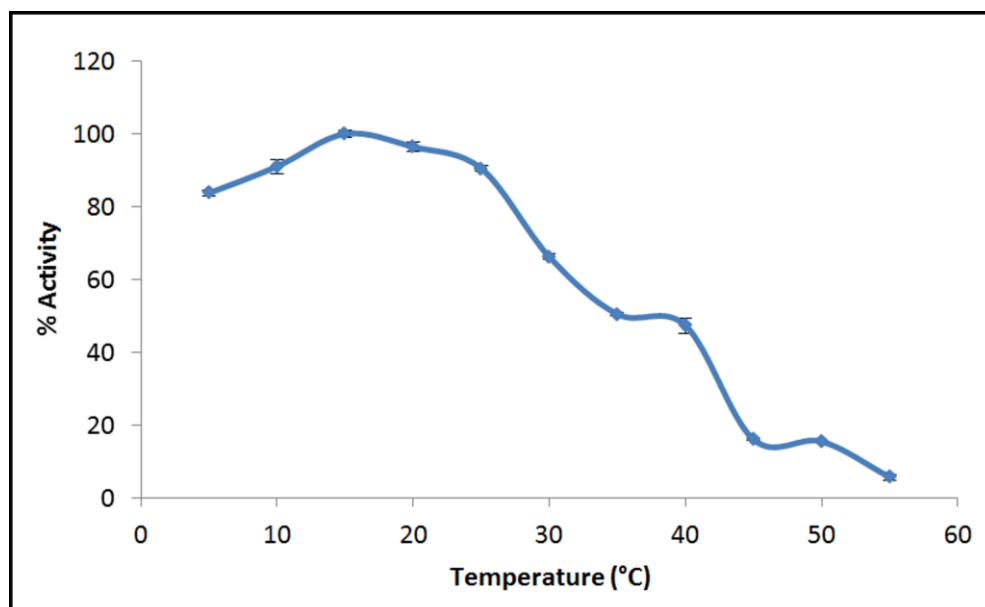


Figure 5.4. Activity of Est97 across temperature range

Establishing the Est97 temperature range from a single purification against nitrophenyl hexanoate following the procedure for establishing Est97's temperature range in the literature (Fu J, et al. 2012).

The temperature range of Est97 in this project did not correspond to earlier published results. In this experiment, showed 100% activity of 30.7 units/mg of protein at an optimal temperature of 15°C, whereas earlier published results have the optimal temperature of Est97 at 35°C with 100% activity, determined to be 10.7 units/mg of protein (Fu J *et al.*, 2012).

5.3.4. Directed evolution and its application in this project

5.3.4.1. Screening techniques employed in this project

Minimal media plates (See 5.2.1.7.) with Rhodamine B dye as an indicator and olive oil as the carbon source with 0.2% arabinose and 1 mM IPTG as an inducer of gene expression were tested as a screen for esterase activity (See 5.2.1.3.). When free fatty acids generated from lipid hydrolysis react with Rhodamine B embedded in the agar, a fluorescent dye forms that can be seen upon illumination with UV light. In theory this technique should allow the screening of a library against fats and oils at low temperatures. Variants were made which were minimal media, but also lacked the Rhodamine B dye - the theory behind these plates was that as the substrate was degraded, clear halos would form around lipolytically active colonies.

A variant on this type of plate was made which had tributyrin as the sole carbon source instead of olive oil. Tributyrin is a chemical that consists of three molecules of butyric acid bound through an ester bond to a glycerol backbone. This substrate is easily hydrolysed by esters and when used in agar, it can detect *in vivo* esterase activity through formation of clear halos around colonies with esterase activity.

Nitrophenyl substrate and bromocresol purple Tris agar plates were made (See 5.2.1.4.); the presence of esterase in bacteria grown on these plates would break down the nitrophenyl substrate, releasing acid which would react with the bromocresol purple, theoretically forming yellow halos. In theory this technique should allow the screening of a library against long chain substrates at low temperatures.

Naphthyl esters and Fast blue soft agar overlay was made to pour over bacteria grown under expressive conditions (See 5.2.1.5.); the idea being that the naphthol product made from the hydrolysis of naphthyl ester coupling to the Fast Blue RR salt to make a brown diazo dye over active colonies. In theory this technique should allow the screening of a library against long chain substrates at low temperatures.

Tween 20 plates were made which had $\text{CaCl}_2 \cdot 2\text{H}_2\text{O}$ present in the agar (See 5.2.1.6.). Upon the breakdown of Tween 20, halos of calcium salt crystals should form around bacterial colonies that show esterase activity due to the calcium reacting with the acid produced upon esterase hydrolysis. In theory this technique should allow screening of esterase activity at low temperatures.

5.3.4.2. Mutagenic techniques employed in this project

The gene encoding the Est97 esterase was subjected to random mutagenesis to generate potential variants that showed greater activity towards long-chain ester substrates and triglycerides at temperatures of 20°C.

It was decided against using a mutagenic bacterial strain which is engineered to have a high mutation rate, e.g. XL1-Red *E. coli*, due to inaccuracy of the mutagenesis. Attempts were made using error-prone PCR where primers

were made flanking the gene of interest, including appropriate endonuclease (See 2.6.5.2.) restriction sites 5' and 3' of the gene so as to allow re-insertion into the original vector the gene was replicated from. Problems arose with the re-ligating of the PCR product into the appropriate vector, in that re-formation of the vector was not seen.

Analysis of the literature for cases where the plasmid was mutagenised *in vitro* without DNA restriction and ligation revealed two possibilities; random Mu transposon insertion mutagenesis and rolling mutagenesis plasmid duplication (Pajunen MI, et al., 2005, Fujii R, et al., 2004, Fujii R, et al., 2006 and Huovinen T, et al., 2011). Further analysis also revealed that one could utilise QuikChange site-directed mutagenesis kit's inherent properties to perform random mutagenesis by performing the whole plasmid PCR in the presence of MnCl₂, resulting in multiple mutations throughout the whole plasmid as well as the gene of interest (Koyanagi T, et al., 2008). Finally, also considered was GeneMorph II EZClone Domain Mutagenesis kit to generate mutant versions of the target gene (under conditions to generate the highest number of mutants per polymerisation session, i.e. with a starting DNA mass of 0.1-100ng, which produces 9-16 mutations/kb of DNA). The collection of mutant target genes are then used as megaprimers, in that they were annealed to original donor plasmid and, through a high-fidelity enzyme mix, were extended to re-form the plasmid from which they were originally copied from. *DpnI* was then used to remove donor plasmid, and the plasmids containing mutant genes were used to transform X-10 Gold Ultracompetent cells (See 5.2.4.).

5.3.4.3. Creation of mutant esterase libraries

Mutagenic PCR using rolling mutagenesis PCR, Mu transposon mutagenesis and GeneMorph II EZClone Domain mutagenesis went ahead (See 5.2.4.2.) (See Table 2.1. for primers used). Plasmids generated from these techniques were used to transform relevant competent cells and grown on selective media; GeneMorph II EZClone Domain mutagenesis (See 5.2.4.2.3.) was used to mutate Est97 (See Table 2.1. for primers used) and kit-supplied *lacZ* control. The mutant libraries were used to transform XL10-Gold ultracompetent cells which were grown overnight on selective media containing IPTG and X-gal.

Transformations from DNA made through GeneMorph II EZClone Domain mutagenesis kit generated the highest number of colonies. There was evidence through the control gene of *lacZ* that mutagenesis had occurred; colonies that turned a blue colour had a functioning *lacZ* gene and thus functioning β -galactosidase activity, whereas white colonies had the *lacZ* function removed and no β -galactosidase activity; evidence that mutagenesis of *lacZ* had occurred. Mutations in the control were indicative of the process working.

The results generated through GeneMorph II EZClone mutagenesis meant attempts to generate mutants through the other two techniques were dropped; both could not guarantee that the mutations that did occur would occur within the target gene only, and Mu transposon mutagenesis could only generate insertional mutants.

5.3.4.4. Results of screening mutagenic library

The aim of the mutagenesis was to select for enzymes that showed increased activity at 20°C towards long-chain substrates. Using the GeneMorph II EZClone Domain mutagenesis kit to theoretically introduce the highest number of mis-match mutations within the *Est97* gene (i.e. using 100 ng of template DNA so as to introduce 9-16 mutations per 1000 base pairs, seeing as *Est97* is 758 base pairs in length, this means that there should be up to 6-12 mutations in the produced mutants), a library of random mutant *Est97* genes in pQE30 vector was made to be inserted into *E. coli* M15 cells. A variety of screens were attempted to determine differences in activities between members within the library (See table 5.1.).

Screen Type	Evidence of hydrolysis	Observed results
Minimal media	Growth of colonies	Limited growth
Minimal media + Rhodamine B dye	Growth of colonies + fluorescence halos around colonies showing activity	Limited growth, no fluorescence.
Nitrophenyl substrates + bromocresol purple dye	Colonies showing increased ester hydrolysis colonies should turn yellow	No growth
Naphthyl substrates + Fast Blue dye	Colonies showing increased ester hydrolysis colonies should turn brown	Limited growth, no noticeable colour change
Tween 20 + CaCl ₂ .2H ₂ O	Colonies showing increased ester hydrolysis colonies generate crystalline halos	No halo generation
Tributyryn agar plates	Colonies showing increased ester hydrolysis colonies generate clear halos	Discernible activity found

Table 5.1. *In vivo* assays attempted in this project

A list of the assays used in this project with the observed results when plated with bacteria containing esterases grown under inducing conditions, and what results were found. Only tributyrin agar assay generated results.

Colonies expressing esterase grown on minimal media both with and without rhodamine B indicator, e.g. BL21-AI containing Δ EstRM in pDest17 and BL21-AI containing CalB expressed in pMal-c2x were found to glow and negative control colonies, BL21-AI with poly (ADP-ribose) glycohydrolase (pARG) in pDest17 (pARG catabolises poly (ADP-ribose) chain and does not hydrolyse ester bonds) did not. However, there were no halos generated around any colony, even though application of pure lipase as a positive control (*Thermomyces lanuginose* lipase) generated a halo. Even though there was a difference between negative control bacteria and test bacteria, the lack of a generated halo meant that this procedure was abandoned in favour of other techniques.

All further *in vivo* assays were tested through the plating of *E. coli* M15 expressing Est97 in pQE30 by adding 0.1 mM IPTG to the growth agar, which promoted expression of the esterases. No positive controls were added, because it was not known what bacteria could be plated that would result in a positive control.

E. coli M15 cells expressing Est97 through pQE30 were tested on Tris agar plates with nitrophenyl substrate and bromocresol purple indicator dye, on plates overlaid with agar containing naphthyl ester substrate and Fast Blue indicator dye and Tween 20 plates were made which had CaCl₂.2H₂O present in

the agar. However, none of these techniques produced definitive results; no growth was seen using the nitrophenyl substrate method, no detectable results could be found with naphthyl ester substrate or with Tween 20 plate assay.

Tributylin agar (See 5.2.1.1.) with inducing material mixed was made up and bacteria expressing the esterase were plated onto them. This technique was found to work, with negative and positive controls showing definitively different, repeatable results. However, this screen didn't test esterase activity against long chain substrates, so more techniques were investigated.

None of these *in vivo* expression tests were found to show results that could definitively demonstrate activity of an expressed esterase against long-chain ester substrate in this project. It was therefore decided to develop a novel assay (See 5.2.1.2.)

5.3.5. Preliminary assay development for observation of tributyrin hydrolysis via colour change through bromocresol purple indicator dye

A previous assay which was tried, but not found to be successful, was using Tris agar made to a pH of 7.5, containing an ester substrate and bromocresol purple dye. As the substrate in the Tris agar was broken down by esterase, the acid moiety was released, lowering the pH of the surrounding Tris agar. As the pH decreases, the colour of the Tris agar goes from purple to yellow; the faster the breakdown of ester substrate, the faster the release of acid product and the faster the colour change (See 5.2.1.4.). However, when this assay was tried in this project, there was not enough bacterial growth to produce definitive pH change.

To test if this assay could work against bacteria used in this work, colonies of Est97 esterase-expressing *E. coli* M15 bacteria grown on media containing inducing material, along with a negative control of *E. coli* M15 bacteria with no Est97 were re-suspended in 20 µl of Tris buffer (pH 7.5) with 1% tributyrin and 0.01% bromocresol purple indicator dye (See figure 5.5.). The induced colony that expresses the Est97 changes the solution's colour faster than

the colony that had not been transformed with esterase - the indicator buffer could be used to detect the presence of esterase activity from bacterial hosts without the influence of endogenous esterases in the host.

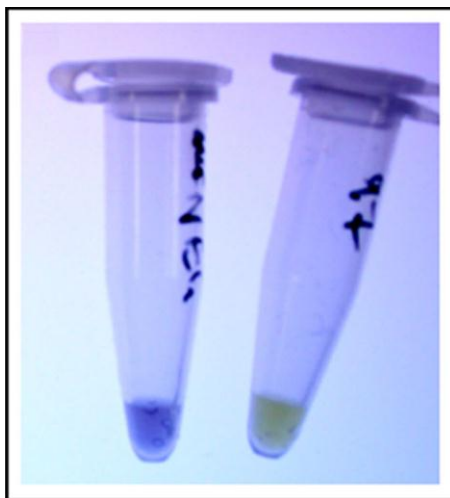


Figure 5.5. Re-suspending induced expression vector in indicator buffer

Left centrifuge tube contains a single *E. coli* M15 colony containing empty pQE30 vector grown overnight on inducing LB agar plate suspended in 20 μ l of Tris buffer (pH 7.5) with 1% tributyrin and 0.01% bromocresol purple indicator dye and the right centrifuge tube including a single *E. coli* M15 colony containing Est97/pQE30 vector grown overnight on selective LB agar plate with 0.1 mM IPTG suspended in 20 μ l of Tris buffer (pH 7.5) with 1% tributyrin and 0.01% bromocresol purple indicator dye. After 5 minute incubation at room temperature, the photograph was taken.

5.3.6. Novel esterase assay development

To overcome this limitation the chemistry of bromocresol purple pH indication was combined with an overlay procedure the mutant library was grown on 1.5% agar under inducing conditions, and then a soft-agar overlay was applied containing 0.15 μ M substrate and 0.01% indicator. An advantage with this technique over that of the earlier, established naphthyl-ester assay was that when using bromocresol purple, the substrate the esterase catalyses doesn't need to be a naphthyl-ester; it could be any form of ester or fat. It was also be easily modified to occur at different temperatures, pH values (although not below 5.2, as that was the pH at which the dye changes colour) and other environmental conditions. Finally, because it was an overlay technique, growth of the bacterial colonies were not dependent on long-chain substrates as the

sole carbon source, which could retard their growth and prevent detectable *in vivo* assaying.

Earliest attempts of this assay demonstrated that colonies that grew closer together tended to turn yellow faster than colonies less densely packed (See figure 5.6.). Dilution series could control how many colonies grew on a plate, but this could not control where on the plate they would grow, so attempts to visualise a large library of mutants through this technique required a transfer of individual mutant colonies grown overnight at 20°C to inducing LB agar plate at regularly spaced intervals.

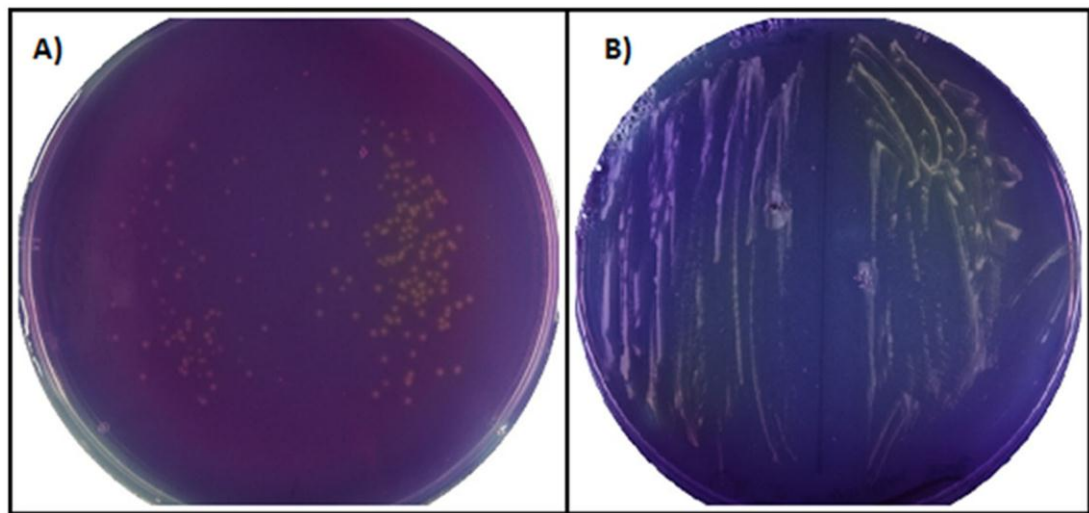


Figure 5.6. Plates illustrating novel esterase assay

A) Tris and nitrophenyl myristate and bromocresol purple overlay working on BL21-AI containing C14S/M37C/S113A PA3859 inserted into pDest17 (positive control) and BL21-AI containing pARG inserted into pDest17 (negative control). B) Tris and nitrophenyl octanoate and bromocresol purple overlay working on BL21-AI containing C14S/M37C/S113A PA3859 inserted into pDest17 (positive control) and BL21-AI containing pARG inserted into pDest17 (negative control). In both cases, the positive control was on the right half of the plate, the negative on the left.

Because detection through the novel esterase assay had been achieved with BL21-AI expressing C14S/M37C PA3859, attempts were made to compare the novel assay probing the activities of BL21-AI bacteria expressing C14S/M37C PA3859 esterase and BL21-AI cells expressing pARG with tributyrin plates BL21-AI bacteria expressing C14S/M37C PA3859 esterase and BL21-AI cells expressing pARG. BL21-AI expressing C14S/M37C PA3859 in pDest17 was shown to hydrolyse tributyrin through measuring activity via the bromocresol purple overlay method (See figure 5.7. A)). However, when plating out individual colonies of BL21-AI

expressing PA3859 on tributyrin plates, no halos were found around the esterase-expressing bacteria (See figure 5.7. B)). The evidence of hydrolytic activity against tributyrin detected by the novel assay could not be verified by the established *in vivo* esterase assay.

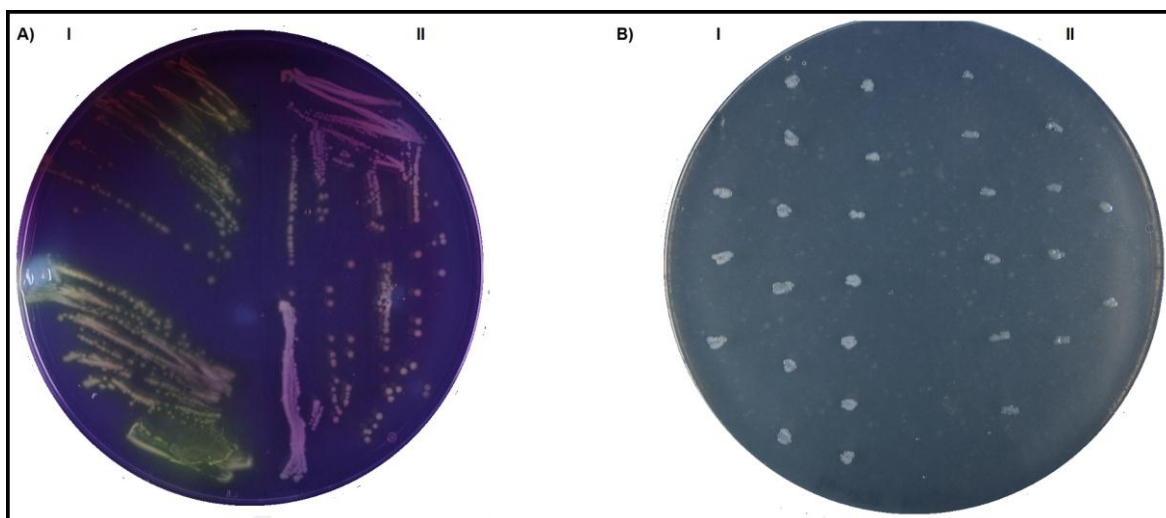


Figure 5.7. Inconsistencies with *in vivo* detection of esterase activity of BL21-AI expressing C14S/M37C PA3859

Plate A) Tris-tributyrin indicator buffer overlay on a streak of BL21-AI cells transformed with C14S/M37C PA3859/pDest17 or PARG/pDest17, sections I and II respectively. Plate B) tributyrin assay of multiple, individual BL21-AI colonies transferred through streaking, transformed with C14S/M37C PA3859/pDest17 or PARG/pDest17, sections I and II respectively.

Attempts were made to combine the tributyrin hydrolysis media with Tris-substrate overlay agar with the aim of identifying mutants that had ester hydrolysis activity at 20° C as well as the ability to hydrolyse long chain substrate, e.g. olive oil. The exact experiment involved streaking colonies of *E. coli* M15 transformed with a mutant library of Est97 in pQE30, with a positive control of *E. coli* M15 transformed with Est97 in pQE30 and a negative control of *E. coli* M15 transformed with empty pQE30 vector. The results demonstrated that the size of the bacterial colony influenced the rate of acid production in the overlay; so a large colony that was not shown to generate a clear halo on tributyrin media could turn yellow faster than a smaller negative control colony, or smaller colonies which did show activity on tributyrin (See figure 5.8.). This could possibly be due to butyric acid, a product of tributyrin hydrolysis, being toxic to *E. coli* growth, preventing cells which show positive activity on a tributyrin assay plate from breaking down the same substrate in a soft agar overlay faster than colonies which showed less activity in the tributyrin agar, but would have a greater concentration of endogenous esterases.

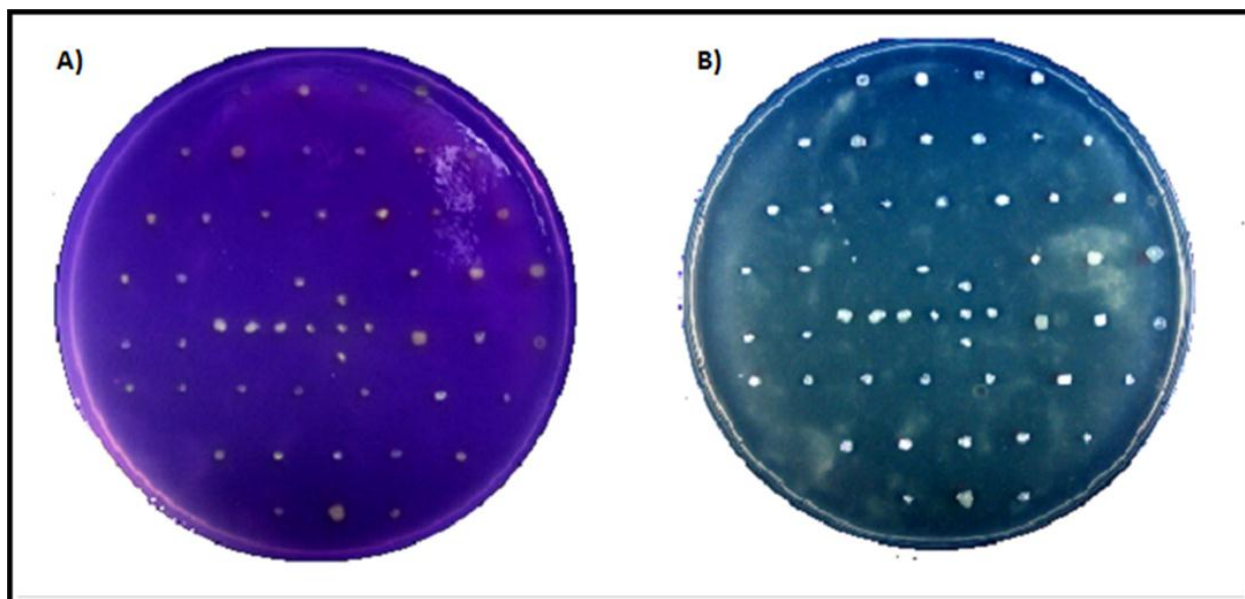


Figure 5.8. Comparing tributyrin plate assay with Tris-overlay assay

A side-by-side comparison of a tributyrin plate assay of a mutagenic library of Est97/pQE30 in *E. coli* M15 expression host with the same pattern of scraped of Est97/pQE30 in *E. coli* M15 expression host on a tributyrin plate assay overlaid with Tris indicator soft agar containing tributyrin as the substrate. In both plates, the positive control consists of five separate *E. coli* M15 transformed with WT Est97/pQE30 plated in a '+' pattern in the centre of the plate. The negative control were three *E. coli* M15 transformed with pQE30 vector plated in a '-' pattern to the immediate left of the positive control cells. Yellow colouration of the colonies in A) was not as definitive as the size of the halos produced in B). Larger colonies with no clear halo appeared to have equal or greater intensity of yellow as smaller colonies with halos.

5.3.7. Screen of mutant library of Est97

Because of the inability to obtain repeatable results in the novel esterase assay, it was decided that it would be better to utilise the established tributyrin assay as a screen. The tributyrin assay had been avoided previously because it only demonstrated esterase activity against small chain substrates and not long chain substrates, but since the reliability of the assay could not be guaranteed, it was the only *in vivo* assay that gave definitive results. During the screening process, different colonies had their copy of Est97 sequenced to verify the rate of mutagenesis. The mutagenic PCR had been designed to give the theoretically maximum number of mutations, i.e. 6-12 base pair mutations in Est97. However, upon sequencing 30 different colonies generated from transformation of *E. coli*

M15 with the mutagenic library, the highest number of base pair changes in any one mutant was only 4, the mutation rate was much lower than expected.

After screening over a thousand colonies, one colony showed greater activity upon tributyrin at low temperature (i.e. the plates were left to grow at 20°C overnight) in comparison to WT Est97. This colony was cultured and the vector (See 2.6.5.1.). The vector was then used to transform new *E. coli* M15 competent cells on a fresh batch of tributyrin agar (See 5.2.1.1.) to ensure that the higher activity was through the mutated version of Est97 and not by an anomaly of the original bacterial host or the original tributyrin plate. The mutant still showed increased activity when compared to WT Est97 (See figure 5.9.).

When the vector was isolated from bacteria and the Est97 gene sequenced, the mutant was found to contain two mutations, the first being a glycine residue replaced with an alanine residue at position 53, the second being a threonine replaced with isoleucine at 231. Hence, this variant was named G53A/T231I Est97.

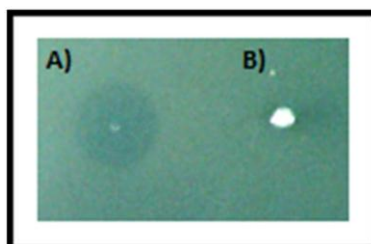


Figure 5.9. Comparison of the halos generated by G53A/T231I Est97 and WT Est97 on a tributyrin agar plate at 15°C

Where A) was G53A/T231I Est97 demonstrating increased halo generation over B) WT Est97. Also note that the colony growth of G53A/T231I had been severely curtailed, probably due to high concentration of butyric acid in immediate surrounding which is toxic to *E. coli*.

5.3.7.1. Mutants of Est97 isolated and assayed

Since the double mutant showed increased activity *in vivo* against tributyrin compared to WT Est97, two other variants were made - G53A and T231I, using a site-directed mutagenesis kit (See 2.6.5.7.3.), to see if only one of the substitutions increased esterase activity. These were used to transform *E. coli* M15 bacteria (See 5.2.2.2.) and were grown on tributyrin plates along with two strains of *E. coli* M15, one expressing WT Est97 and one expressing G53A/T231I Est97 (See figure 5.10 A)). Results shown in these plates showed

that all of the three mutants showed better activity than WT Est97, but G53A showed least improvement, while T231I showed largest halo generation.

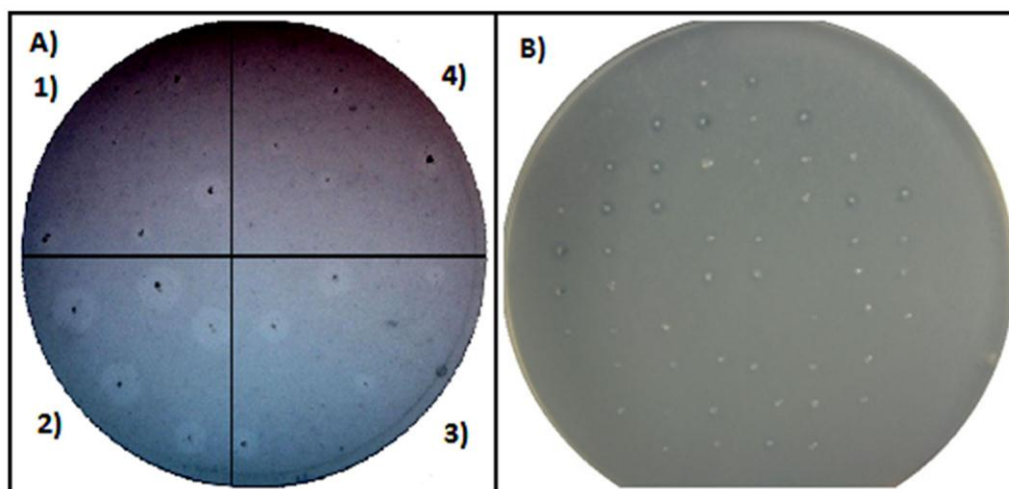


Figure 5.10. Tributyrin agar used to probe *E. coli* M15 Est97/pQE30 variants

A) Tributyrin agar plate assay comparing WT Est97 inserted into pQE30 vector and grown in *E. coli* M15 expression cells (quadrant 3)) with the three variants behind increased activity, with G53A/T231I double mutant in quadrant 2), G53A in quadrant 1) and T231I in quadrant 4) B) A Tributyrin assay plate of a mutagenic library generated from G53A/T231I Est97, inserted into pQE30 vector and grown in *E. coli* M15 cells. Centre 4 colonies were G53A/T231I Est97 control colonies.

Since G53A, T231I and G53A/T231I variants were seen to have higher activity than WT Est97 *in vivo*, the proteins were expressed (See figure 5.11.) (See 5.2.2.3.) and the kinetics for all three proteins were measured (See figure 5.12.) and calculated (Table 5.2.).

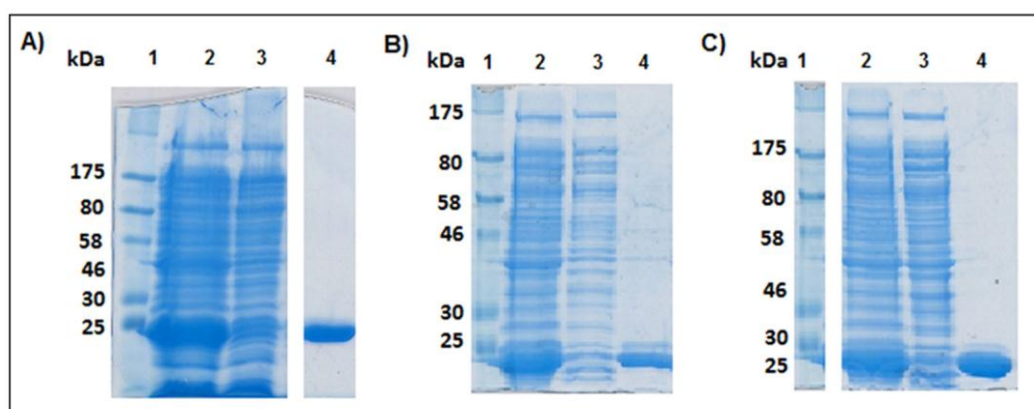


Figure 5.11. Expression and purification of soluble G53A/T231I Est97, G53A Est97 and T231I Est97

SDS-PAGE analysis of soluble Est97; A) G53A/T231I Est97, B) G53A Est97 and C) T231I Est97. Samples were separated on a denaturing SDS-PAGE gel. Lane 1: Marker. Lane 2 was bacterial lysate. Lane 3 was flowthrough. Lane 4 was purified protein used in assays.

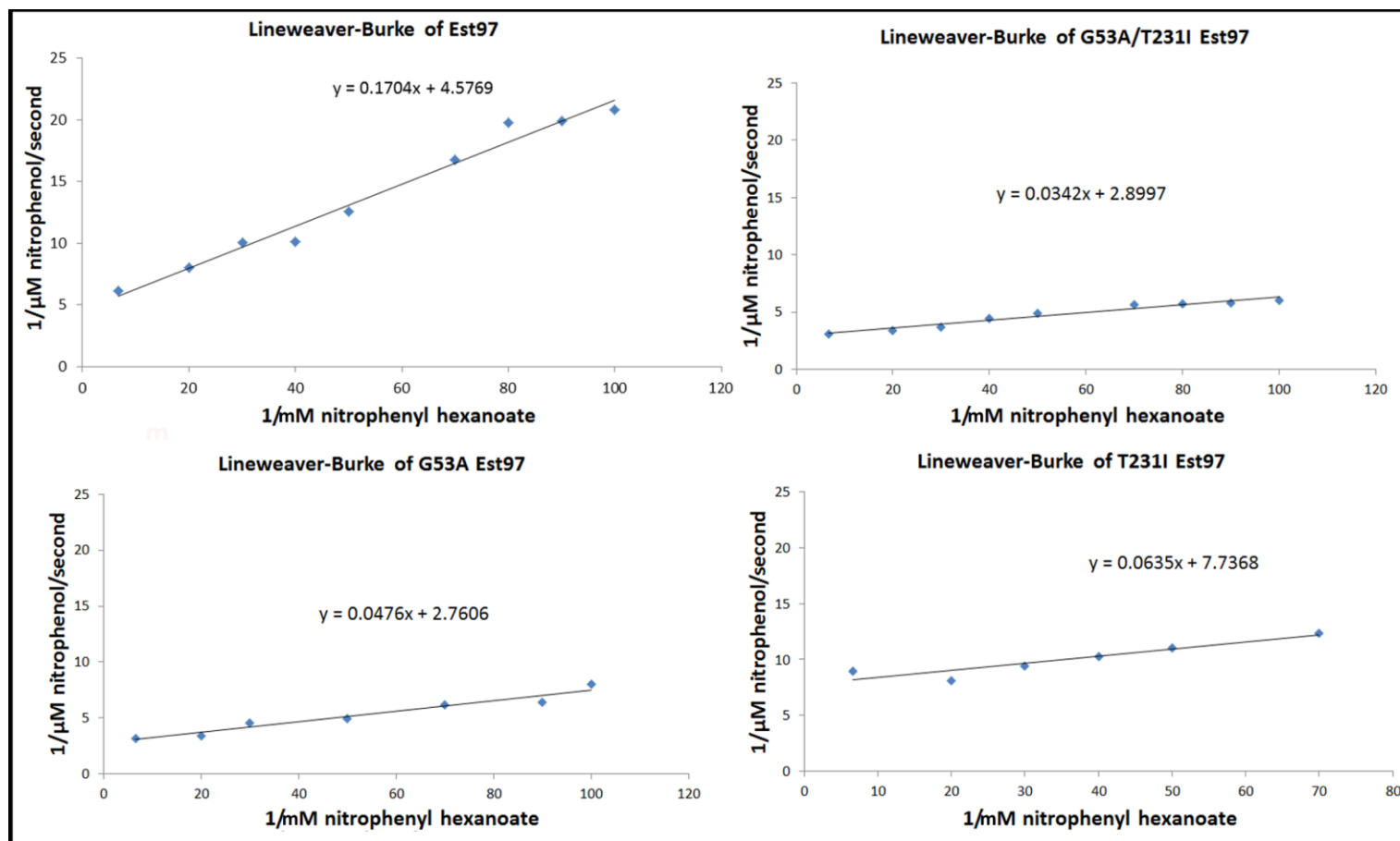


Figure 5.12. Lineweaver-Burke graphs comparing Est97 to G53A, T231I and G53A/T231I variants of Est97

The activity of a set concentration of each protein was measured against nitrophenyl hexanoate at set concentrations which would allow for the calculation of the inverse values of the activity of these esterases against the inverse concentration of the substrate (See 5.2.3.1.). The calculated value for the gradient of the line of best fit was used to derive $1/K_m$ and $1/v_{max}$. From these values it was possible to derive K_{cat} and then K_{cat}/K_m .

Comparing the K_m and k_{cat} values at 25°C from Table 5.2. revealed that all of the mutant versions of Est97 had lower K_m values and higher k_{cat} values than WT Est97.

Est97 variant	V_{max} ($\mu\text{M}/\text{sec}$)	K_m (μM)	k_{cat} (sec^{-1})	k_{cat}/K_m ($\text{sec}^{-1}\mu\text{M}^{-1}$)
WT	0.22	37.23	2.57	0.07
G53A	0.36	4.02	17.24	4.29
T231I	0.13	1.43	8.2	5.73
G53A/T231I	0.34	3.83	11.79	3.08

Table 5.2. Enzyme kinetics of wild-type and mutant variants of Est97 found through screen
 K_m and k_{cat} were derived for G53A Est97, T231I Est97 and G53A/T231I Est97 through plotting out the Lineweaver-Burke graphs against nitrophenyl hexanoate (See figure 5.12.) and compared against WT Est97 K_m and k_{cat} values.

The results also show that the increase in k_{cat} from the individual residue changes of G53A and T231I were not cumulative, but the decrease in K_m may be; i.e. G53A/T231I, G35A and T231I had higher k_{cat} values than WT Est97, but the double mutant did not show greater k_{cat} values than G53A (11.79 sec^{-1} compared to 17.24 sec^{-1}). The double mutant didn't have a K_m value lower than both single mutants - T231I in this case had lower K_m values than G53A/T231I Est97 (1.43 μM to 3.83 μM).

Since versions of Est97 had been discovered using the mutagenic screen that were more active than the wild type form, the next logical step would be to identify what other changes there are in these mutants by performing a full characterisation.

5.4. PEGylation of Est97

Later work in the project involved investigating the use of Est97 esterase as another ligand for use in AFM. *In silico* analysis (using online programs polyview and NetSurfP (Porollo A, et al., 2004 and Petersen B, et al., 2009) (See 2.6.6.3. and 2.6.6.4.)) of the solvent accessibility of the residues of Est97 indicated that an ideal PEGylation site would be E40, as it was a glutamic acid residue and had a high a relative solvent accessibility score (80-90% according to polyview; 0.753, with an absolute surface accessibility score of 131.584 according to NetSurfP).

From these *in silico* results, primers were designed to alter the residue to cysteine (See 2.3). Attempts to generate mutant genes through QuikChange Directed mutagenesis kits were not successful - either there was no vector produced, or the bacteria that did grow did not grow well. Mutagenesis was instead performed using QuikChange Lightning Directed mutagenesis kit (See 2.2.). When the sequence of the E40C variant of Est97 had been confirmed, protein was expressed from the pQE30 vector in which it was contained. Expression of E40C Est97 followed the general protocol for expression within an *E. coli* M15 host (See 5.2.2.2. and 5.2.2.3.).

Soluble E40C Est97 was obtained following *E. coli* M15 expression protocol (See 5.2.2.3.) (See figure 5.14.). The kinetics of E40C Est97 were compared with WT Est97; its K_m and k_{cat} values were marginally higher than the WT version of Est97 (37.3 μ M compared to 37.2 μ M and 3.99/sec compared to 2.57/sec respectively), (See figure 5.13. A) and B), see Table 5.3. Experiment A). Though k_{cat} values were much lower than the published values for this esterase, kinetic values did not change between Est97 and E40C Est97, and so the latter was used for further PEGylation experimentation.

A TCEP.HCl reduction gradient was made with 1ml of 0.05 mg/ml of E40C Est97 which was left for 30 minutes on ice, which was then reacted with mm(PEG)₂₄ in DMSO in a ratio of 1:40 for 2 hours on ice (See 4.2.2.). With no TCEP present, a dimer was formed, corresponding to the expected disulphide bridge forming between two solvent-accessible cysteine residues. Results from an SDS-gel indicated that 0.25 mM TCEP.HCl allowed for the highest ratio of PEGylated E40C to unPEGylated E40C (See figure 5.15.).

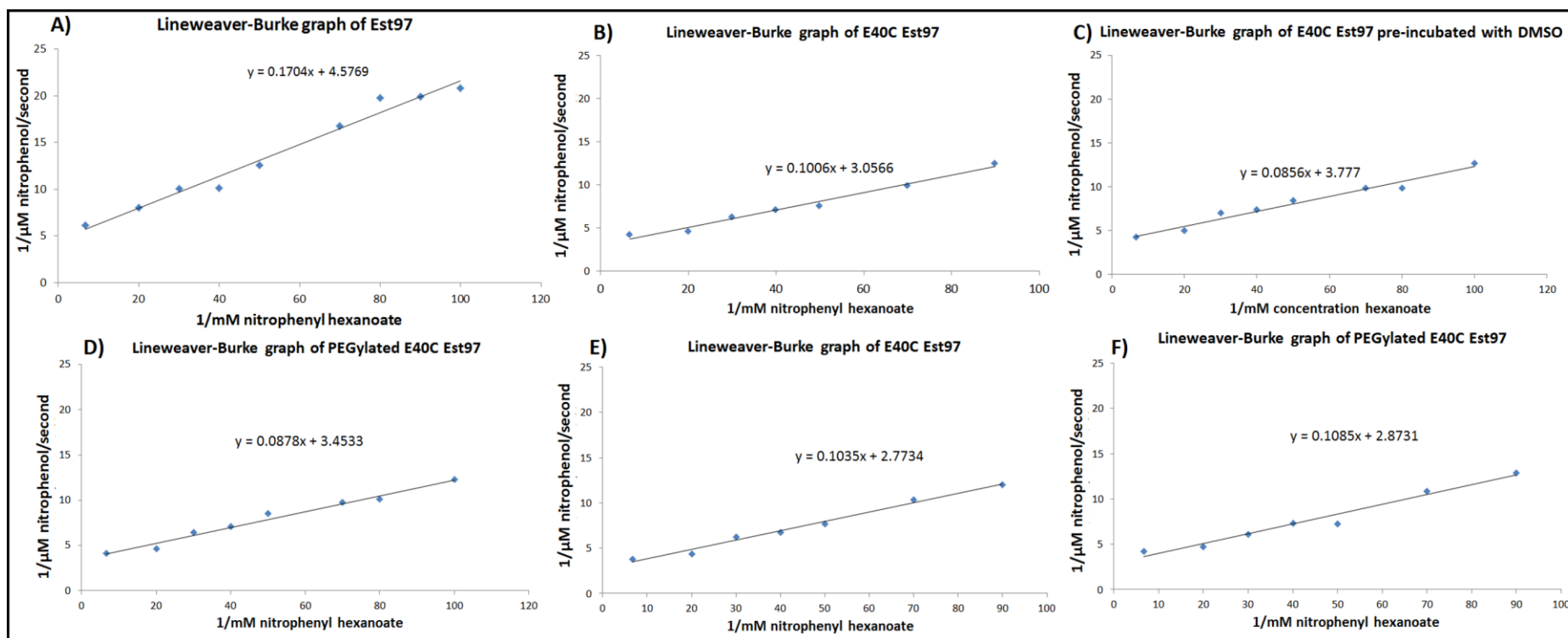


Figure 5.13. Lineweaver-Burke graphs comparing Est97 to E40C Est97 without any modification, with pre-incubation with DMSO and when PEGylated

The activity of a set concentration of each protein was measured against nitrophenyl hexanoate at set concentrations which would allow for the calculation of the inverse values of the activity of these esterases against the inverse concentration of the substrate (See 5.2.3.1.). The calculated value for the gradient of the line of best fit was used to derive $1/K_m$ and $1/v_{max}$. From these values it was possible to derive K_{cat} and then K_{cat}/K_m . Graphs A) and B) generated the values for experiment A in Table 5.3, Graphs C) and D) generated the values for experiment B in Table 5.3 while Graphs E) and F) generated the values for experiment C in Table 5.3

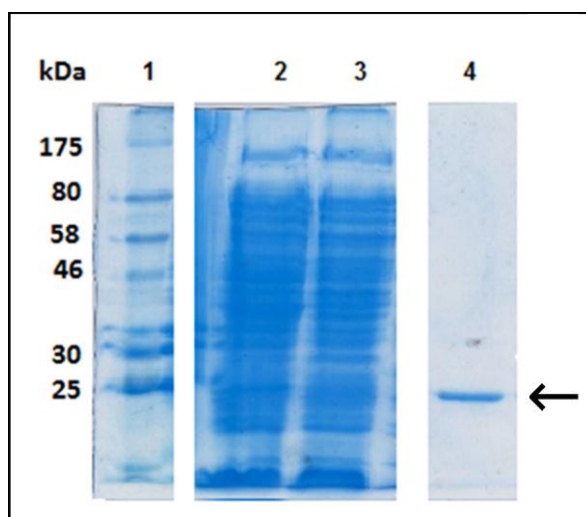


Figure 5.14. Expression and purification of soluble E40C Est97

SDS-PAGE analyses of soluble Est97 from large grow-up expression; samples were separated on a denaturing SDS-PAGE gel. Lane 1: Marker. Lane 2: bacterial lysate. Lane 3: flow-through. Lane 4: eluted protein of the expected mass of E40C Est97 (29.6 kDa) that was dialysed and used in assays (indicated by arrow).

Experiment	Est97 variant	V_{max} ($\mu\text{M}/\text{sec}$)	K_m (μM)	k_{cat} (sec^{-1})	k_{cat}/K_m ($\text{sec}^{-1}\mu\text{M}^{-1}$)
A	Est97	0.22	37.23	2.57	0.07
	E40C Est97	0.33	32.91	3.62	0.11
B	Pre-incubated with DMSO E40C Est97	0.26	22.66	2.93	0.12
	PEGylated E40C Est97	0.28	24.85	3.13	0.13
C	E40C Est97	0.36	37.32	3.99	0.11
	PEGylated E40C Est97	0.35	37.76	3.85	0.10

Table 5.3. Comparison kinetics of Est97 and PEGylated Est97 variants generated in this project

K_m and k_{cat} values of Est97 and E40C Est97 variants both PEGylated and pre-incubated with DMSO were calculated through Lineweaver Burke graphs generated from activity of the esterase against nitrophenyl hexanoate (See figure 5.13.).

In order to determine what influence of the presence of DMSO has on E40C Est97 activity, a sample of E40C Est97 was PEGylated as described in 4.2.2., along with a sample of E40C Est97 that was subjected to the same chemical treatment as the PEGylated E40C Est97, but without mm(PEG)₂₄, i.e. it was exposed to TCEP.HCl and DMSO, but no PEGylation could occur; it was pre-incubated with DMSO. Kinetics of these two samples revealed reduced K_m and k_{cat} values compared to un-altered E40C Est97 and WT Est97. However, their values of K_m and k_{cat} were nearly identical ($K_m = 22.6 \mu\text{M}$ and $k_{cat} = 2.931/\text{sec}$ for

unPEGylated E40C Est97, $K_m = 24.9 \mu\text{M}$ and $k_{\text{cat}} = 3.134/\text{sec}$ for PEGylated Est97) (See figure 5.13. C) and D), see Table 5.3. Experiment B). PEGylation in itself didn't reduce activity, the method of PEGylation *in vitro* i.e. exposure to DMSO and TCEP.HCl, could. However, because attaching this ligand to PEG molecules already attached to an AFM tip does not require the presence of DMSO. DMSO is only used to make a solution of $\text{mm}(\text{PEG})_{24}$, so what reduction in activity seen with the PEGylated E40C Est97 was not thought to be problematic.

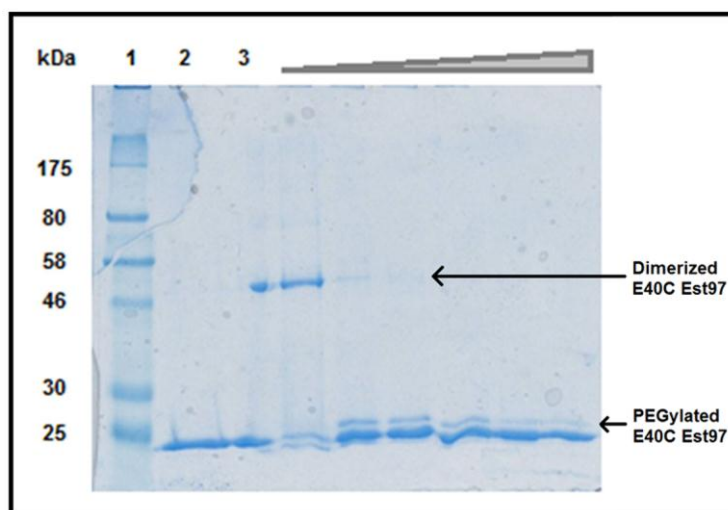


Figure 5.15. The effect of a TCEP gradient on PEGylation of E40C Est97

1ml samples of 0.05 mg/ml of E40C were PEGylated (See 4.2.2.) were run on an SDS-PAGE gel. Lane 1: Marker. Lane 2: fully reduced E40C Est97. Lane 3: semi-reduced E40C Est97. Remaining: samples of E40C Est97 reduced with an increasing gradient of TCEP concentration for 30 minutes then incubated with $\text{mm}(\text{PEG})_{24}$ 40 times the concentrated of protein for 2 hours on ice. TCEP concentrations of the gradient were: 0, 0.25, 0.5, 0.75, 1 and 2.5 mM.

To verify if this alteration in activity was due to chemical exposure and not, say, protein degradation, a comparison was made between a fresh sample of Est97 untreated with TCEP and DMSO, and one that was PEGylated as before (See figure 5.13. E) and F), see Table 5.3. Experiment C). Both k_{cat} and K_m values were similar ($K_m = 37.319 \mu\text{M}$ and $k_{\text{cat}} = 3.992/\text{sec}$ for untreated protein, $K_m = 37.764 \mu\text{M}$ and $k_{\text{cat}} = 3.854$ for the PEGylated protein).

5.5. Discussion

5.5.1. Methodology employed in this project for obtaining and assaying Est97

It was decided to detect the monomeric state of Est97 using centrifugation through MWCO falcon tubes, and then assaying the concentrated sample from the falcon tubes with nitrophenyl octanoate. This method was thought to be more accurate than using native gels in that it detects the presence of an esterase of expected mass as opposed to detecting only proteins of expected mass. However, there could also be a possibility that the protein could re-form into multimers after being passed through the MWCO filter; further investigation would be required to determine whether this is the case.

Fu J *et al.*, 2012 used K_m and k_{cat} values to quantify esterase activity, therefore in this project the same technique was utilised for all forms of Est97 in order to permit the results generated in this project to be compared to published results. Alternative methods of measuring esterase activity could involve full characterisation of the Est97 variants utilised in this project, as was done with the OsmC esterases earlier in the project.

5.5.2. Reviewing the generation of the mutant library

Methods to create random mutagenic libraries were reviewed and a number of procedures found which matched the criteria of generating mis-match mutations in random areas within a gene of interest, specifically the GeneMorph II EZClone Domain Mutagenesis kit which generated mis-match mutations in the gene of interest through low-fidelity PCR.

Mis-match mutagenesis was favoured over other potential choices as it would bring about the highest number of random amino acid substitutions. Deletion and insertion mutagenesis could alter the reading frame of the gene or drastically alter the secondary and tertiary structure of the protein that the ratio of inactive variants against active variants would be skewed towards non-functioning enzymes.

As a large number of mutants were desired - this meant XL1-Red *E. coli* strain was not used, since it would take many days to generate mutant vectors, the inherent mutagenic qualities of the strain would eventually result in the destruction of individual colonies, meaning that repeated transformation

attempts would have to be made to make a large mutant library through this method and it could not be guaranteed the mutations would be located in the Est97 gene.

All the procedures that would produce a large number of mutants quickly were attempted to see if any of them could be successfully adopted. GeneMorph II EZClone Domain mutagenesis produced multiple colonies on selective media. Though other attempts also generated colonies, e.g. Mu transposon insertion, these techniques were only attempted in the first place as a precaution against the GeneMorph II EZClone Domain mutagenesis failing. When the GeneMorph II EZClone Domain mutagenesis was found to work, all other attempts at mutagenesis were abandoned in favour of it.

5.5.3. Reviewing the screening of the mutant library

Tributylin agar made via the method suggested Arne Wehling (See 5.2.1.1.) was the best technique for screening the colonies grown from GeneMorph II EZClone Domain mutagenesis for higher activity against an ester substrate at low temperatures, seeing as it did accurately represent increased activity (through the size of the clear halo generated) and could be performed at low temperatures (by simply incubating the plate at a low temperature). It didn't work on the principle of selecting against colonies which were unable to break down ester substrate which would have preferred for spotting the most active colonies generated from transformation with the mutant library, i.e. it was not a screen that when a colony was found to be incapable of performing the desired reaction, resulted in the death of said colony. The fact that butyric acid is toxic to *E. coli* effectively meant that the most active colonies generated were often the smallest in size; which did mean that the halos generated were much easier to spot, but that there was a greater risk of not being able to grow up enough bacteria from a colony to successfully attempt a miniprep plasmid isolation (See 2.6.5.1.).

It would have been interesting to see how improvements could have been made on the novel overlay assay to use it to screen the colonies against long chain substrates at 20° C, but a number of difficulties arose, which meant refining this assay while assaying the mutagenic library using more orthodox means was not possible.

The overlay technique required a set volume of soft agar to be made that needed to have indicator dye and substrate mixed in equally, and then poured on when the overlay was cool enough to not kill the bacterial colonies, but at the same time was warm enough that the agar did not set before it had been poured; if the bottom layer of agar was uneven; the soft agar couldn't be applied evenly onto the whole plate, which meant the overlay had areas which were uneven in colour, the pH of the Tris agar had to be high enough to ensure that when first poured it was dark purple, but not so high so as to kill the bacterial colonies. Colour change of colonies happened relatively quickly, even at low temperatures. The size of the colonies also seemed to have an effect on the rate of colour change, which didn't match with results made from duplicate streaks made on tributyrin agar plates. It would have been convenient to attempt to measure the change in colouration quantifiably, which would detect colour change, e.g. through OD₄₁₀, over time through some type of a colorimeter which would remove the necessity of human error.

Tributyrin agar (See 5.2.1.1.) made it much easier to find variants with higher activity than the novel screen - the differentiation between colonies was much slower with the tributyrin screen than with the overlay assay and wasn't reliant on a subtle colour change of the colonies themselves. As it happened, at least one variant was isolated through this technique which was found to show greater activity than the wild-type Est97 made earlier, so the screen did succeed in its purpose, even if it was not working against a long-alkyl chain substrate.

G53A/T231I Est97 had lower K_m and higher k_{cat} values over Est97 produced in this project; and G53A and T231I Est97 variants also had lower K_m and higher k_{cat} values over Est97 as well (although none of them had higher k_{cat} values given for Est97 in the paper by Fu J *et al.*, 2012).

The lower K_m values indicated that less substrate was required for the mutated variants of Est97 to be half saturated and that these variants show a higher affinity towards the substrate used in the assay. The higher k_{cat} values meant that there were a greater number of reactions being carried out per mole of protein in these *in vivo* higher activity Est97 variants than in either WT Est97 or E40C Est97. These results indicated that these mutant Est97 variants were more active by themselves, and not by any additional factors brought in by the host it was expressed in or variations in the environment it was assayed at. These mutants did show higher activity than Est97 - with the lowest change in

the kinetics meaning an affinity increased by nine-fold and k_{cat} value being almost quadrupled. The fact that these kinetic values were calculated using nitrophenyl hexanoate as opposed to tributyrin indicates that the increase in activity of these variants of Est97 was not limited to tributyrin.

G53A/T231I Est97 did not have a k_{cat} value higher than G53A Est97 and T231I Est97; G53A Est97 had a higher k_{cat} value. Neither did G53A/T231I Est97 have a K_m value lower than both G53A Est97 and T231I Est97; T231I Est97 had a lower K_m value. This indicates that the increased activities brought about from these single amino acid substitutions were not cumulative; that both of them on their own allow the esterase to have higher activity, but when both residues were altered, they could work against each other. However, they did not completely hinder each other's effect, seeing as G53A/T231I Est97 was still much more active than Est97.

The possible reasons behind why replacing the natural amino acids with these different forms were not immediately clear. Glycine and alanine are the shortest and second shortest amino acid respectively of all 21 amino acids (the molecular weights being 75.07 and 89.1 respectively), so the probability that the alteration in activity being due to a change brought about by the size of the side-chains is unlikely.

The major difference between the two residues is in their chemistries; glycine can act as both a hydrophile and a hydrophobe, whereas alanine is strictly hydrophobic due to its methyl side-chain.

Threonine and isoleucine are also similar in size (molecular weights being 119.12 and 131.18 respectively, a difference less than that between glycine and alanine), but the former is a strict hydrophile while the latter is a strict hydrophobe.

It seemed as if these changes in amino acids change the chemistries but not the actual space taken up by the amino acid side-chains. Neither of the two were part of the catalytic triad of Est97; so this change probably does not influence the activity Est97's active site directly. The alteration in the chemistries would have to change of the esterase's tertiary structure.

Glycine at position 53 is part of a structure dubbed a disordered loop, found adjacent to the active site of the esterase, whereas threonine at position 231 is the first residue making up the final alpha-helix and is in close proximity

to a residue known to associate with zinc ions (glutamic acid at position 233). Zinc has been found to strongly inhibit Est97 activity (Fu J, *et al.* 2012).

It would make sense if these changes altered the chemistry of the entrance channel to the active site of the esterase; which would especially hold true for G53A, considering residue 53 is part of the disordered loop adjacent to the active site. To test what effect these amino acid substitutions had on the shape of the esterase, the crystal structures of both the single mutants as well as the double mutant would have to be made. Had there been more time in this project probing the effects these amino acid residue substitutions had on the esterases would have been investigated, as well as the crystal structure formed from a zinc soak - to see if the residue association with zinc ions is maintained with T231I.

Had time for the mutagenic library of Est97 been available, a second round of mutagenesis on the G53A, T231I and G53A/T231I Est97 variants would have been desired, to see if there were any more clones that showed even activity greater than them on tributyrin agar at 20°C. This could have revealed more combinations of mis-matched residues that could increase activity on substrate at 20°C over the original Est97 variant; and also give a better background on why the changes result in better activities as well.

It would have been good to make E40C/G53A Est97 and E40C/G53A/T231I Est97 variants, time permitting. That way, PEGylation of these variants and characterisation of PEGylated versions of these variants compared to unPEGylated variants could be achieved. Following the logic from E40C Est97, reduction in activity would not be expected. These variants could then be sent for use as a high-active psychrophilic esterase ligand in AFM for the collaborators at the University of Sheffield, alongside E40C Est97 as well. That way, one could see if the differences in activity between these variants are at all detected through AFM.

5.5.4. Reasoning for the mutagenesis and alteration in residues in this project

The random mutagenesis used in this project managed to generate at least two amino acid alterations which resulted in an increased esterase activity, G53A and T231I. This was after screening at least a thousand different colonies

produced through transformation with a mutagenic library of Est97. How do these results compare with others from different projects?

Directed evolution has been used to generate mutant esterases with many different characteristics from the progenitor. Esterases have been made to have had a greater enantioselectivity against substrates (Ma J *et al.*, 2012 and Musidłowska-Persson A and Bornscheuer U T, 2003), improving acylation (Ye L *et al.*, 2013), thermostability (Jochens H *et al.*, 2010) and altering esterase affinity to long-chain substrates (Chang L *et al.*, 2011) have been achieved as well as generating alternatives that show enhanced enzymatic activity in general. In the examples given, these alterations were brought about by either one or two amino acid substitutions, much like in this project. Most examples given required analysis of over one thousand colonies at least, with one study requiring the analysis of 4,000-6,000 colonies (Ma J *et al.*, 2012); so the fact that this project was able to find a viable mutant displaying desired characteristics after screening approximately one thousand colonies was unexpected, since the directed evolution utilised in this project was achieved through random mutagenesis.

Screening methods used to discover variants of enzymes that work better at low temperatures were based on the same principles utilised in this project - growing colonies from the library produced, then screening individual colonies against the desired substrate at temperatures considered low for the catalysed reaction (Sriprapundh D *et al.*, 2003, Lebbink JH *et al.*, 2000, Pulido MA *et al.*, 2007). The logic behind the screen in this project is sound.

5.5.5. Alternative strategies to random mutagenesis in generating cold-active variants

Random mutagenesis is not the only technique available when performing directed evolution. Alternatives include site-directed mutagenesis (See 2.6.5.7.3.); either of specific amino acid residues or distinct areas within the protein known to encode particular structures of the protein that could generate the desired feature wanted if subjected to changes (e.g. deletion, truncation, saturation. etc.). Such strategies have been used multiple times for enzymes in general, but also in esterases, e.g. altering enantioselectivity of pig liver esterase (PLE) (Musidłowska-Persson A and Bornscheuer U T, 2003) and compensating for the trade-off of higher enantioselectivity for lower hydrolytic

activity in a mutant version of *Rhodobacter sphaeroides* esterase (Guo F *et al.*, 2013).

Site-directed mutagenesis' advantages over completely random mutagenesis of the entire gene include being able to generate more mutants probable to have desired features - there would be a much lower chance of generating null mutants in this strategy. In the same line of thinking, there are fewer chances of mutations working against each other, masking features that could be desired. Because of this, the act of screening the mutant libraries made would also be quicker, because there would be fewer variants generated through this strategy.

In the case of Est97, the chances of any directed mutagenesis being performed to generate variants that could work better than the wild type at lower temperatures was low. To use such a strategy would require knowledge of exact relation of amino acid sequence to feature of the protein in question; which for Est97 was not possible, at least not with how much is known about it so far. The chances of an educated guess of which residues should be changed to increase low-temperature activity would be low; certainly lower than any random mutagenesis performed. Also, though directed mutagenesis would lower the chances of developing null mutants as opposed to random mutagenesis of the whole gene, directed evolution also loses the chance of discovering an unexpected mutation having a hand in generating a desired feature in a region that would not be expected otherwise.

Had there been more time and more knowledge of the relationship between primary structure and esterase function, directed mutagenesis could have been attempted upon Est97 to investigate further mutations capable of producing increased activity at a lower temperature.

5.5.6. PEGylation strategy of Est97

Designing an mm(PEG) binding site on Est97 followed the procedure for developing a site of CalB, i.e. *in silico* calculations of the primary structure of the most solvent-accessible residues that could be altered into a cysteine site without risking destabilisation of the protein. This procedure was successful; engineering a PEG-binding site onto Est97 through E40C did not reduce Est97 activity. PEGylation of Est97 could occur through this site and PEGylation did not seem to alter the kinetics of the esterase, either. As could be seen from the gel

to visualise PEGylation, the ratio of PEGylated E40C Est97 to unPEGylated E40C Est97 was not as great as PEGylated C14S/M37C PA3859 to unPEGylated C14S/M37C PA3859 (See figures 4.19. and 4.8.); determining a ratio of TCEP:protein reaction mix that would have given the most PEGylated E40C Est97 would have been preferable, but there was not enough time to do so.

When the activities of PEGylated E40C Est97 and pre-incubated with DMSO E40C Est97 were compared to E40C Est97, both showed lower K_m and k_{cat} values compared to the unmodified E40C Est97. This indicated that chemical modification of E40C Est97 would reduce activity. By making a fresh set of E40C Est97 to PEGylate and then comparing the kinetics of PEGylated and unPEGylated E40C Est97 from this fresh batch revealed almost identical values, ($K_m = 37.319 \mu\text{M}$ and $k_{cat} = 3.992/\text{sec}$ for untreated protein, $K_m = 37.764 \mu\text{M}$ and $k_{cat} = 3.854/\text{sec}$) (See 5.16). Variation in activity observed earlier were probably is not due to chemical alteration, but due to the age of the protein. PEGylating E40C didn't alter activity - it was an ideal ligand for AFM TREC.

The values for the kinetics of Est97 and E40C Est97 obtained here were unusual in that the k_{cat} values were lower by approximately a factor of 10 than the k_{cat} values extrapolated from Fu J *et al.*, 2012 which first characterises Est97, (3.99 sec^{-1} and 3.85 sec^{-1} respectively, compared to 25.8 sec^{-1}) though the K_m values were almost identical ($37.32 \mu\text{M}$ and $37.76 \mu\text{M}$ compared to $39 \mu\text{M}$). Repeated kinetics of these two Est97 pools in this lab indicated that this was not due to a one-off problem e.g., linked to protein aging. Looking over Fu J *et al.*, 2012 again revealed that two different values of k_{cat} for Est97 working against nitrophenyl hexanoate were given (under Abstract section, Paragraph 1, K_m and k_{cat} values were given as $39 \mu\text{M}$ and 25.8 sec^{-1} , respectively, while under Enzyme characteristics of rEst97, Paragraph 2, K_m and k_{cat} values against nitrophenyl hexanoate were given as $39\mu\text{M}$ and 26.8 sec^{-1} (Fu J *et al.*, 2012). There may be a writing error with the paper in question, and that the Est97 variants made in this project do not have reduced k_{cat} values. Alternatively it could be that the method of increasing the yield of esterase produced caused mis-folding which resulted in a loss of activity.

Chapter 6

Discussion

6.1. Introduction

A problem inherent in washing oil and fats off of clothes with laundry detergent is having the washing water at a temperature to promote the optimal breakdown of typical edible oil and fats, e.g. butter, olive oil, margarines, sunflower oil, etc. Heating washing water is not always viable, due to a lack of resources. Lowering the optimal temperature of the constituents responsible for catalysing these soils so that they would show practical hydrolytic activity against substrates at 20°C would remove this problem, and thus make washing clothes less expensive both in respect to labour and resources. The application of psychrophilic esterases as constituents of a low-temperature laundry detergent is a potential way of lowering the optimal temperature of said detergent against fats and oils.

The aims of this study was to provide preliminary characterisation of little-researched esterases to see if there are any that could be used as such a constituent, along with the research into how one could assay an esterase against fats and oils at a low temperature and also seeing if there were any ways in which the activity of the little-researched esterases could have their activity improved upon substrates at lower temperatures.

While a number of aims were met in this project, there were some areas that could have been expanded upon. This final chapter details what was discovered in the project, as well as what future research could be directed to from results obtained during in this project.

6.2. Summarising the OsmC characterisation

Six members of a new family of esterases were identified through a BLASTp search, the encoding DNA cloned from their original hosts and transformed into an expression vector system. The expression vectors containing the esterases genes were used to transform competent cells so as to be induced and obtain purified esterase. Results indicated that of these esterases, Δ EstRM showed highest overall activity against nitrophenyl benzoate as well as against most long-chain substrates. Its optimal temperature was well over 20°C, its activity was so large at the lower temperatures, that it was superior over almost all other OsmC esterases.

When taking into account that Δ EstRM showed the highest activity against nitrophenyl myristate and stearate, as well as greater stability against metal ions and several esterase inhibitors compared to Δ EstRD, it would seem valid to conclude that Δ EstRM shows the greatest potential for use as, if not as a ligand in TREC, then a component in biotechnological applications involving long-chain substrate hydrolysis.

6.3. Summarising PEGylating esterases for use in TREC

To measure affinity of an esterase to fat and oil at low temperatures on a fabric surface (and so forming a semi-crystalline structure), TREC through AFM was considered to be the best option, and so research into how esterases could be used as a ligand in this method was performed. It was concluded that the ideal esterase in such an assay would have to be a monomer and also bind to an AFM tip through a linear mm(PEG) molecule.

None of the OsmC esterases were deemed suitable for use as an AFM ligand because repeated native gel runs indicated that all were multimers. It would have been convenient to double check these findings through passing esterases MWCO centrifuge tubes of relevant size exclusion sieve and seeing if protein is present in fractions that correspond to monomer or multimer sizes as was done with Est97 (See 5.3.2.1.), as results from native gel runs were not definitive.

The two monomeric esterases chosen to be tested by AFM, PA3859 and CalB, were altered by site-directed mutagenesis to permit PEGylation, changing a solvent-accessible residue to a cysteine to permit binding of a PEG molecule through maleimide. Success in finding appropriate residues was determined by running samples of each protein which had been subjected to PEGylating methodology through a PAGE gel in semi-reducing conditions along with samples of the same proteins at the same concentration that had not been subjected to PEGylation. If the PEGylated samples had two bands or thicker bands at the expected weight of the monomer in comparison to the unPEGylated form, this was deemed as evidence that the protein had been PEGylated.

To test if the act of PEGylation affected esterase activity, a nitrophenyl substrate was incubated with equal volumes and concentrations of PEGylated

and unPEGylated were allowed to react with a nitrophenyl substrate and the absorption readings at OD₄₁₀ was measured over time. The only reduction in activity was found to be due to the pre-PEGylating conditions that the enzymes had been exposed to, and not the actual PEGylation itself. Because of these results, these enzymes were considered suitable ligands for use in AFM, and were sent to collaborators at the University of Sheffield accordingly to begin preliminary investigation into TREC with them as ligands against substrates bound to mica. There they were used and found to bind to substrate.

6.4. Summarising the development of an esterase for use in AFM

Although CalB and PA3859 had variants made that could be PEGylated and thus used in AFM, a less well-characterised ligand was wanted to be investigated for this project, and so literature was analysed to find a monomeric, psychrophilic esterase.

Est97 was found to be an appropriate ligand for AFM application, in that it was both monomeric and psychrophilic. Binding sites for PEGylation were determined *in silico*, and PEGylation methodology went ahead, and was found to work. At the same time, Est97 was also subjected to directed evolution which investigated ester hydrolysis of mutants generated through error-prone PCR at low temperature *in vivo*.

After several rounds, a mutant was found which showed improved activity compared to a colony expressing wild type protein. After double-checking the activity of the enzymes *in vivo*, the activity of the mutant was compared *in vitro* with wild type Est97, and its sequence was derived. The mutant, which had two amino acid substitutions (glycine residue at position 53 replaced by alanine and threonine at position 231 was replaced by isoleucine) was found to be much more active than the wild type.

Investigations into the activities of mutants made which had only one residue mutated were compared with the double mutant and the wild type, and the activities compared. Results indicated that showed that all the mutants had a greater affinity for substrate and, at 20°C, catalysed more molecules of substrate per second than the wild type Est97. It also revealed that there may have been an error in the paper published that originally investigated Est97,

seeing as the k_{cat} values for Est97 made in this project were almost uniformly $1/10^{\text{th}}$ of that listed in the paper and that the mutant's k_{cat} values one half of the paper's k_{cat} values for Est97, and also because the paper gives two different values for k_{cat} itself.

Attempts to characterise the activity of the Est97 variants had to be abandoned due to lack of time. However, contemporary directed mutagenesis studies have been able to generate new versions of enzymes which are shown to have greater activity at lower temperatures; there would be no reason to suppose that there would be no variants of Est97 that would have better activity at lower temperatures and against long-chain substrates.

It would have also been convenient to test TREC using the E40C Est97 variant made in this project, but since AFM results had only been accomplished with E269C CalB, it was thought better to let the collaborators check TREC using remaining, well characterised ligands first.

6.5. Were preliminary goals of project reached?

When looking over the original aims laid out in the introduction, some of the desired goals were reached; characterisation of novel extremophile esterases in a new family had been accomplished, preparing and making a methodology for using esterases for AFM has been achieved and generated a novel monomeric cold-active esterase through directed evolution had been achieved, but some goals were not accomplished.

Selection for a more active esterase mutant at low temperatures was only achieved against tributyrin and not the long-chain triglyceride substrates commonly found within fats and oils. Results from assays that used long-chain substrates were not definitive, either through the novel assay (See 5.2.1.2.) not having been optimised enough or by it being unsuitable altogether. These strategies were abandoned in favour of being able to detect increased ester hydrolysis activity at low temperatures in general.

Secondly, there was not enough time to select for mutants that would not generate butyric acid in the presence of multiple general oil stains. Butyric acid is not desired when cleaning clothes of fats and oils due to the fact that it gives off a rancid smell. Tributyrin plate assays were adopted well knowing that the hydrolysis of the product produces butyric acid, but only because other assays used were unsuccessful. Also, as later analysis of G53A Est97, T231I Est97 and

G53A/T231I Est97 revealed, tributyrin plate assays were convenient for detecting an increase in general esterase activity; not just against tributyrin.

Finally, no more AFM scans beyond the data given (See Figure 4.17.) were generated using the ligands made specifically to break down substrates at low temperature from this project. However, this data was generated from collaborators at the University of Sheffield; who had the hardware needed to perform AFM. What data was obtained only gave promising but not definitive results.

6.6. Future direction of work from this project

Beyond completing the goals set out at the start of this project and completing characterisation of mutant esterases, the most obvious direction to take would be to begin design of the laundry detergent the esterase would be a component of. This could involve designing an inactive superstructure scaffold that could bind the esterase and other components together in such a way that would allow them to clean stains and lowering the chances of the components working against each other, e.g. proteases working against protein components and detergents denaturing biological agents within the laundry detergent. The scaffold would have to be easy to construct and polymerise, but at the same time be inert. PEG, seeing as it has all of these features present, could be an ideal component for this scaffold.

The scaffold would have to be designed to not hinder the cleaning constituents from accessing the stains. Long string structures, where each active functional component is placed one after the other on a linear scaffold chain, would not be a good choice as it would limit the components working within clothing fibres. A hypothetical structure would have to be smaller, e.g. where a scaffold core is studded with the components. This strategy would reduce the laundry detergent components working against each other, thus improving its affectivity in wash and its shelf-life.

Also, the esterases would have to be altered to allow attachment to such a scaffold without hindering activity. It could also involve further mutagenising the esterase to work effectively against fats and oils at low temperatures in the presence of detergents and other chemicals present in the laundry detergent.

If the esterases do not work well in a laundry detergent application, i.e. they are unable to work effectively against substrate not in an emulsion body,

there are still other ways they can be utilised; specifically degrading lipid-based pollution in the environment. Bioremediation of contaminated sites can be a labour and resource-intensive task, with some situations requiring physical removal of parts of the environment to be able to remove impurities. Methods of bioremediation capable of treating the environment with as little application of outside material as possible and with tools that would not result in further damage to the environment are ideal. An esterase that works at low temperatures and can work on lipid substrate would be ideal for removing fat deposits in soil or water and would at the same time not cause any additional damage to the environment; so long as the resulting lowering of pH caused by the production of fatty acids was taken into account.

Even though none of the Δ esterases were suitable for use as a ligand in AFM for probing affinity against substrate, there are other applications for the novel esterases in biochemical industries. One possibility relies on the ability of esterases to perform dehydration synthesis, i.e. the reverse of their natural function, resulting in specific ester manufacturing. Specific synthesis and degradation, particularly at low temperatures, is of particular scientific and financial interest for pharmaceutical industries as they can be used for developing new and improved medical compounds. Other industries that are interested in ester's ability to perform ester synthesis and degradation at low temperatures include food industries and biodiesel manufacture. The exact conditions to promote dehydration synthesis would have to be determined; probably through adjusting the esterases' environment.

One area of the project which showed the development of an entirely new method of analysis which should be further investigated was the development of the novel *in vivo* ester assay. It has the potential to be a valuable method of probing mutagenic libraries for not just ester hydrolysis, but any catalytic reaction which results in a change in pH. Its advantages over other *in vivo* methods of measuring esterase activity are several - but primarily it can work on any ester substrate. Other *in vivo* esterase assays are dependent on the substrate degradation to release a product that reacts with an indicator also present, e.g. the release naphthoxide from a naphthoxy ester reacting with azo dye, or precipitation resulting from the degradation of Tween 20. The colour

change of the indicator in the developed assay is brought about by the pH lowering upon the release of acid from ester hydrolysis. That meant that this assay could be used to check activity directly against substrates that are wanted to be hydrolysed by the esterase; if one wanted to check lipase activity of an enzyme, it would be preferable to check the activity against a long chain triglyceride and not just tributyrin.

Because the indicator chemical is supplied to the *in vivo* mutagenic library post growing phase through a soft-agar overlay, components that could influence enzyme activity but could not be added to the basal agar for fear of retarding cell growth, e.g. growing on tributyrin agar can produce butyric acid which is toxic to *E. coli*, could be added. For example, the novel assay could add tributyrin to the soft agar overlay, allowing all the colonies to grow at an equal rate first before having them hydrolyse tributyrin as a substrate.

The only condition it would be unsuitable to take into account would be pH, seeing as it is the pH change which causes the change in colouration; by altering the pH of the soft agar too far beyond pH 7 could cause too little or too much colour change too quickly, reducing the ease in spotting active clones from a mutagenic library.

There are other applications for the esterases and techniques described in this thesis, but the validity of suggesting them is reliant on results from experiments yet to be performed. Nevertheless, this list of potential routes that could be taken from this project illustrates that there a number of different directions research could be taken in from what results and conclusions have been found. Not only in the original field (of generating low temperature active esterases for use as a part of laundry detergents), but in a wide variety of biotechnological applications. There is a lot of promise from what this project discovered.

Appendix

DNA sequences:

EstO+N-terminal poly-His:

ATGTCGTA CTACTACCATCACCATCACCATCACCTCGAATCAACAAGTTTGTACAAAAAAGCA
GGCTNNCGACAAAAAGTATCTTTTAAAAGCGGCGATTTAGAACTTGCCGGCCAACTTGAA
CTTCCCTCTGGTGACGTTAAGTTTTACGCGCTATTTGCACACTGCTTTACCTGCGGTAAA
GACATTGCAGCAGCCACTCGTATTAGCCGAGCTTTAACACAACAAGGCATTGCCGTACTA
CGTTTCGACTTTACCGGTTTAGGTAATAGCGATGGCGACTTTGCTAACAGTAACTTTTCA
TCAAACATTCAAGATTTAGTATCTGCGGCAAATCATTTACGTGAGCATTTTTCGCGGCCG
CAACTACTCATTGGCCACAGTTTAGGCGGGGCTGCCGTTCTTGCTGCTGCGGAGCATAT
TCTTGAAGTATCGGCTATTACAACCATTGGTGCACCGTCAGATGCGCAGCACGTAGCGC
ATAATTTTGAAGCACACCTTGATGAAATTAACGCAGCAGGTGAAGCTAAAGTAACTTAG
CCGGCCGTGAATTTACCATTA AAAAGCAATTTATTGACGATATAGCCAAGTACGATAAAA
GCCACATAAGTAACTTAAGCGCGCATTATTAGTAATGCACTCCCCTATTGATGCGACGG
TAAATATTAGTGAAGCTGAAAAAATTTATGCATCAGCCAAGCATCCTAAAAGCTTTATTA
GCCTAGATAACGCCGATCACCTTTTAAACAATAAAAACGATGCCGACTACGCAGCACAAA
TAATTGCAACGTGGGCAAACCGTTATGTTAAGTACGACAAAATAAATACACGGCAAGTT
TAACGGGTGGCAATGTACTCGTTGAAGAAAAAGACCATGTATTTACTCAGCACGTAAGTA
CAAAAGATCATACTTGGCTTGCAGATGAGCCAATAAAAAGTAGGTGGTAAAACTTAGGTC
CTGATCCGTATCATCACTTATTAGCGGGGCTTGGTGCCTGTACGGCCATGCACTGCGT
ATGTACGCTACACGTAAAACTTACCACTGGAGCATGTAAAAGTAGAGCTTGATCACACT
CGCGATTACAACAAGATTGCGACGATTGTGAGCAAACAGGTAACCTTGAAGCAATTACC
CGTAAAATCACCTTACGTGGCGACTTAACAGAGCCACAACGCCAGCGTTTACTCGAAATA
GCCGACAAATGCCCTGTGCATAAAACACTACATAATAACCCAGTTATTGTAAGTGAAGTG
GTAGAATAATGA

ΔEstO+N-terminal poly-His:

ATGTCGTA CTACTACCATCACCATCACCATCACCTCGAATCAACAAGTTTGTACAAAAAAGCA
GGCTNNCGACAAAAAGTATCTTTTAAAAGCGGCGATTTAGAACTTGCCGGCCAACTTGAA
CTTCCCTCTGGTGACGTTAAGTTTTACGCGCTATTTGCACACTGCTTTACCTGCGGTAAA
GACATTGCAGCAGCCACTCGTATTAGCCGAGCTTTAACACAACAAGGCATTGCCGTACTA
CGTTTCGACTTTACCGGTTTAGGTAATAGCGATGGCGACTTTGCTAACAGTAACTTTTCA
TCAAACATTCAAGATTTAGTATCTGCGGCAAATCATTTACGTGAGCATTTTTCGCGGCCG

CAACTACTCATTGGCCACAGTTTAGGCGGGGCTGCCGTTCTTGCTGCTGCGGAGCATAT
TCTTGAAGTATCGGCTATTACAACCATTGGTGCACCGTCAGATGCGCAGCACGTAGCGC
ATAATTTTGAAGCACACCTTGATGAAATTAACGCAGCAGGTGAAGCTAAAGTAACTTAG
CCGGCCGTGAATTTACCATTA AAAAGCAATTTATTGACGATATAGCCAAGTACGATAAAA
GCCACATAAGTAACTTAAGCGCGCATTATTAGTAATGCACTCCCCTATTGATGCGACGG
TAAATATTAGTGAAGCTGAAAAAATTTATGCATCAGCCAAGCATCCTAAAAGCTTTATTA
GCCTAGATAACGCCGATCACCTTTTAACAAATAAAAACGATGCCGACTACGCAGCACAAA
TAATTGCAACGTGGGCAAACCGTTATGTTAAGTACGACATGA

EstLA+N-terminal poly-His:

ATGTCGTA CTACCATCACCATCACCATCACCTCGAATCAACAAGTTTGTACAAAAAAGCA
GGCTNNGGACAGCACCCGCTGAACTGGAATTTGACGGAGCGCACGAGGCAAGCCTCG
CCGCCCCGGCTGGACTTGCCTTCTGGCAACATCAGGGCGTTTGCCTGTTTGCGCACTGC
TTTACCTGCTCGAAGGACATCGCTGCTGCTCGCCATATCGCCAGCGCGCTTTCGCAGGA
AGGCATCGCCGTGCTCCGTTTCGATTTACCGGCCCTTGGCGGCAGTGGCGGTGATTTTC
GCCTCGACCGGCTTTTCTCCAATGTCGAGGACCTGAAACGGGCTGCAGACTACCTGCG
CCGGA ACTATCAGGCCCCACAGTTGTTGATCGGACACTCGCTCGGCGGAGCCGCCGTTTC
TGTCGGTTGCCGCCGACATTCCCGAAGTGCGGGCCGTCGTGACGATTGGGGCGCCCTC
GGACGCAGATCACGTCATCCACAGCTTCAAGGGTGAGGAAGACACGATCCGCCAGCAGG
GCCAGGGCGAAGTCTGTCTCGAAGGGCGCAGCTTACCATCCGCAAGGAGTTTCTGGAG
GATCTGGA AACCAGTCCGTTCCGGACAAGGTCGCAAGTCTCGGCAAGGCGCTTCTGGT
GATGCACGCCCGCTTGATGAAGTTGTCGGCATCGACAACGCCACCAGCATTTTTCGTGC
CCGCAAAGCATCCCAAAGCTTCGTCTCTCTGGATACGGCGGATCATCTTCTGTGAAAA
GCCAGGACGCCGCTATGCGGCCCGCGTGATTGCGGGCTGGGTTGGACGCTATCTCGA
TCCCGTGGAGGAGAGCGCCGACGACGAGGTGAAGGACGGCGTTGAGGTGGTTGAGACC
GGGCAGGGCAAGTTTCAGGTCATGGTCAACAGCGGCAAGCACCGCATGATCGCCGACGA
ACCAAGGGACGTCGGCGGTATCGACAGCGGCCCGTCGCCCTATGGCTTTCTGTCCGCCG
CTCTTGGCGCCTGCACAGTGATGACATTGCGTATGTACGCCGAACGCAAGGGGCTCGAC
GTCGACCGGATCGGCACGCGGTTCTGCACGGCAAGGTGCATGCTGACGATTGCAAAGA
GTGTTCTGAAAGCGTGAAGTCGAGAGGGCGGCAAGATCGACCGTTTCGAGCGCATGATC
ACGCTGGAAGGAAACCTGGACGAAGCGACGCGGACCCGGATGCTTGAAATCGCCGACAA
ATGTCCCGTGCATCGTACCCTGGAAGCAGGCGCGGCCGTGGTGACGCGGGAAGTGCCG
TCCGGCACACCGGAGGCGTGA

ΔEstLA+N-terminal poly-His:

ATGTCGTA
CTACCAT
CACCAT
CACCAT
CACCT
CGAAT
CAACA
AGTTT
GTACA
AAAAA
AGCA
GGCTN
GGACAG
CACCC
GCTGA
AACT
GGAAT
TTGAC
GGAG
CGCAC
GAGG
CAAGC
CTCG
CCGCCC
GGCT
GGACT
TGCCT
TCTGG
CAAC
ATCAG
GGCG
TTTGC
CCTGT
TTTGC
GCACT
GCTGC
AGGA
AGGC
ATCGC
CGTG
CTCCG
GTTCG
ATTT
CACCG
GCCT
TGGCG
GCAG
TGGC
GGTG
ATTT
CGCT
CGAC
CTGCG
GAGG
CAAGC
CTCG
GACT
ACCT
GCG
CCGGA
ACTAT
CAGG
CCCC
ACAG
TTGTT
GATCG
GACACT
CGCT
CGGCG
GAGCC
GCCG
TTC
TGTCC
GTTGCC
GCCG
ACATT
CCCC
GAAG
TGCGG
GCCG
TCTCG
TGAC
GATT
GGGG
GCGCC
CTC
GGACG
CAGAT
CACGT
CATCC
ACAG
CTTCA
AGGG
TGAG
GAAG
ACAC
GATCC
GCCAG
CAGG
GCCAG
GGCG
GAAG
TCTGT
CTCGA
AGGG
CGCAG
CTTCA
CCAT
CCGCA
AGGAG
TTTCT
GGAG
GATCT
GGAA
ACCC
AGTCC
GTTCC
GGGACA
AGGT
CGCA
AGTCT
CGGCA
AGGCG
CTTCT
GGT
GATGC
ACGCCC
GCTT
GATGA
AGTT
GTCGG
CATCG
ACAAC
GCCACC
AGCAT
TTTT
CGTCG
CCGCA
AAGCA
TCCCAA
AGCTT
CGTCT
CTCTG
GATAC
GCGCG
GATCAT
CTTCT
GTGCA
AAAA
GCCAG
GACGCC
GCTAT
GCGGCC
CGGT
GATTG
CGGG
CTGGG
TTGG
ACGCT
ATCTCGA

ΔEstRD+C-terminal poly-His:

ATGCCA
ACAGA
ACGA
ATTGC
CTTTG
CCGGG
CATGAT
GGCGG
ACAG
CTTG
CCGCG
CGGG
CTTG
ATTTG
CGCG
CATT
GCTT
CACCT
GCG
GCAAG
GACAT
CCCGG
CCGCG
CGCC
GGATT
GCTG
CGCG
CCTT
GCGG
CATT
GGGG
ATTGC
GGTG
CTGCG
GTTT
GATTT
ACCGG
GCTGG
GACAT
TCGG
ATGGG
GAGTT
TGCGA
ATACG
TCGTT
CACAT
CAAAT
GTGG
ACGAT
CTGAT
CGCAG
CGCAT
CGTT
ATCT
GTCA
GAGA
ACAAC
AAGAC
ACCGT
CGCT
GATCAT
CGGCC
ATTC
GCTCG
GGGG
GCGCT
GCGGT
ACTG
AAAG
CCCG
AGCCG
CGCTT
GACAG
CATCA
AGGCG
GTCT
GACCAT
CGGGG
CGCC
TTT
GATCC
CCGG
TCA
CGTCA
CACACA
AACT
TTGCG
CAGG
CCTT
GCCC
GAGAT
CAAAT
CGAGG
GGCG
TGGCC
GAA
GTCAG
CCTT
GGCGG
GCGG
CCTT
CCAG
ATCAG
CAAGG
CATT
TGTGG
ACGAT
GTGCG
CGCA
GACCG
AACT
GGAAG
AGAG
TGTGG
CCAAT
CTGA
ATGC
AGCT
TTT
GCTGG
TGTG
CATG
CGC
CGCT
GGAC
GATATT
GTGCG
GATT
GAGA
ACGC
AGGT
CAGAT
TTTT
CAGC
GCCG
CGAA
CAC
CCAAG
AGCTT
CATCAC
GCTT
GACGG
GCGG
ATCAT
CTGGT
CAGC
GCCG
CGGCG
GATGC
GGAGT
ATGTG
GCCAG
CCTG
ATCGA
ACAT
GGTCT
GCGCG
CTAT
CTGG
ATAT
CGCAC
GCC
CGGCC
CCGCT
CCCG
GTGCG
CCCGA
AGGCG
TGCT
GCGCG
TGGC
GGAG
GCGG
ACCC
GAA
GGGG
TTCA
AGGG
TCAT
CATC
ACCAT
CATCA
CTGA

ΔEstRM+N-terminal poly-His:

ATGTCGTA
CTACCATC
ACCATCAC
CTCGAAT
CAACAAG
TTTGTAC
AAAAAAG
CAGCA
GGCTNN
CAGATCA
AAAACCG
TTACGTT
TGGAAA
ACAACCG
CGGGGAG
CGCCTG
GCCGCCC
G
TCTGGAT
CTGCCGG
TCGATACC
CAGCCC
GTCGCTT
ACGCGCT
GTTTGC
CCACTG
CTTTA
CCTGCT
CGAAAA
CCTGAA
AGCCGTT
ACGACG
ATCAGTC
GAGCGCT
GACAAC
TCAGGG
C
TATGCG
GTGTTG
CGCTTC
GATTTT
ACCGGG
CTGGGAG
AAAGCG
AAGGAG
ATTTTCC
GAG
GACCAC
CTTTGCC
ACCAAT
TTTTGA
AGATCTT
CGCGCAG
CCTGCC
GTTTTCT
CAGTGC
GCA
GTATGAG
CCGCTG
CTCTGCT
GATCGG
CCACTC
GCTGGG
TGGAGC
GGCTGT
GCTGGCC
G
GTTGCG
GGCGAG
TTCCCC
GAAGTAA
AAGCCGT
GGCCACC
ATCGGT
GCGCCCT
GCGATCC
G
GGCGCAC
GTGCGG
CATCTG
CTGCGT
CCGGCG
CTGGATA
CCATCAA
AACGGT
TGGCGAG
G
GCGGTGG
TGATCT
GGGCGG
AAGGCC
TTTCCG
GATCAAAA
AAGCAAT
TTTCTC
GAAGAG
CT
GGAGCG
CGTCAAT
CTGGAG
GATCAAG
TCCGCAC
GATGCGT
CGTCCG
TTATTG
CTTTTCC
C
ATTCAC
CTACCG
ATCAGAT
TGTGGG
CATCGA
GAACGCT
GCCTGC
CTGTTTC
CAGGCAG
CC
CGTCAT
CCGAAG
AGCTTC
GTGTGCT
GGACCAG
GCCGAT
CATCTG
CTGAGCA
ACTCGGA
G
CGATGCT
GCGTTC
GTGGGG
GAGGTG
CTGGGCG
CCTGGG
CGCGGG
CGTTAC
GTGGGAC
G
TCGTTGA

ΔEstEM+N-terminal poly-His:

ATGTCGTA
CTACCATC
ACCATCAC
CTCGAAT
CAACAAG
TTTGTAC
AAAAAAG
CAGCA
GGCTNN
GCATTCA
ATACGCA
ACGGCT
CCAATTT
TCCGGG
CATTCC
GGCGCG
ACGCTTAG
G
CGCCCG
CCTCGAT
CTGCCAA
ATGGGCC
ATTGCG
CGCCTAC
GCGCTTT
TTTGC
CCATTGCT
T
TCACCT
GTTCCAG
GGATCT
GGCGGC
AGCACG
CCAGATT
GGGGCG
GAGCTT
GCGCGTGA
G
AGGCAT
CGCTGTC
CTGCGT
TTTTGAT
TTCACG
GGGCTGG
GATCGAG
CGAAGG
CGAATTCG
C
CTTCGAC
AAATTT
CTCCTCC
AACGTT
GCCGAC
CTTCTTT
CAGCCG
CGGACT
ATTTGCG
CC
ACCACT
ATCAGG
CACCCG
CGGTGCT
GATCGG
CCATTC
GCTCGG
CGGGCG
CAGCGG
TCCTC
G
GCCGTC
GCCGGG
GAAATT
CCGGAAG
TGCGCG
CCGTAG
CCACCAT
CGGCGCG
CCGGCTG
G
ATGTCG
GCCACG
TGTTGA
AGAACT
TCGGAG
CGAGCCT
CGAGGAG
ATCGACA
AGAACGG
T
GAGGCC
GACGTG
ATCTCG
CGGGGCG
CACGTT
CCTTAT
CAGAAAG
CAATTT
GTTCGAG
GA
CACGCG
TGCGACC
GCATTA
AAGGAT
GCTGTT
GGGAG
ATTGAAG
AAGCCA
ATCCTC
ATCC
TTCACG
CGCCGCT
GGACC
ATACGGT
AGGGAT
CGAGAAC
GCCACC
GAAATCT
TCGTGCG
G
GCCAGG
CATCCG
AAAAGCT
TCATCT
CGCTGG
ACAAGG
CCGACC
ACCTGCT
CACCGACC
C
TGAGGAC
GCAGCCT
TTGCCG
GACGGAT
CATTTCC
GGAATGG
CTGACAC
GCTATCT
TTGCCG
C
CTGACAC
GCCGCA
AGGCGC
AGGCCCG
ATCGAAC
ATGTCC
ACGTGAG
GTGA

ΔEstCA+N-terminal poly-His:

ATGGGACAGCACCCGCTGAAACTGGAATTTGACGGAGCGCACGAGGCAAGCCTCGCCGC
CCGGCTGGACTTGCCTTCTGGCAACTCCACCTCGCTCAAGGTCACCTTTCCCGGCGGTG
GCGGCGTCGCCCTCGCCGCTCGGCTGGAGCTGCCCCACGGCGCCGCGCCCCGGGCGTA
CGCGATCTTCGCCACTGCTTCACGTGCGGCAAGGACGCCGTCGCCGCTCGCGGATCG
CCCGCGCGCTGACCGACCACGGCATCGCGGTGCTGCGCTTCGACTTCACCGGCCTGGGC
CAGTCCGACGGCGACTTCGGGAACACCGGCTTCACCTCCAACGTGGAGGACCTGGTCGC
GGCGGCGGACCACCTGCGCACCGAGTACGGCGCGCCGAGCCTGCTCATCGGCCACTCCC
TCGGCGGCGCCGCGGTCCTGGCCGCCCGCCACGGCATCCCCGAGGTGCGCGCCGTGGT
GACGATCGGGGCACCGGCGGACCCCTCCACATCGCCACCTGCTCAGCGAAGCCCGCG
ACACCATCGAGCGCGACGGCGAGGCGACGGTGACGCTGGGCGGGCGCGACTTCTGCGT
CCGCAGCAGTTTCTGGCCGACATAGCGGATCAGCCGCAGGCCGAACGCATCCACGACC
TGAAGGCCGCCCTGCTGGTCATGCACTCCCCGACGAGACGGTCGGCGTCGACAAC
GCCCCGACAGATCTTCGACGCGCGCGCCACCCGAAGTCCTTCGTGTCGCTGGACGGCGC
CGACCACCTGCTCACCCGGCGGCGCGACGCGGAGTACGCCGCGACGGTCCTGGCCGCG
TGGGTCAGCCGCTATCTTCCCGAGCCCGAGCCCTCCACGGTGTGA

Synthetic CalB gene:

GAATTCCTGCCGAGCGGTAGCGATCCGGCATTAGCCAGCCGAAAAGCGTTCTGGATGC
CGGTCTGACCTGTCAGGGTGCAAGCCCCGAGCAGCGTTAGCAAACCGATTCTGCTGGTTC
CGGGTACAGGCACCACCGGTCCGCAGAGCTTTGATAGCAATTGGATTCCGCTGAGCACA
CAGCTGGGTTATACCCCGTGTTGGATTAGTCCGCCTCCGTTTATGCTGAATGATACCCA
GGTTAATACCGAGTATATGGTGAATGCAATTACCGCACTGTATGCAGGTAGCGGTAATA
ACAAACTGCCGTTCTGACATGGTACAGGGTGGTCTGGTTGCACAGTGGGGTCTGACA
TTTTTTCCGAGCATTCTGAGCAAAGTTGATCGTCTGATGGCATTTCACCCGATTATAAA
GGCACCATTCTGGCAGGTCCGCTGGATGCACTGGCAGTTAGCGCACCGAGCGTTTGGC
AGCAGACCACCGGTAGCGCACTGACCACCGCACTGCGTAATGCCGGTGGCTGACCAG
ATTGTTCCGACCACCAATCTGTATAGCGCAACCGATGAAATTGTTAGCCGCAGGTTAGC
AATTCACCGCTGGATAGCAGCTACCTGTTTAATGGTAAAAATGTTAGGCACAGGCCGTT
TGTGGTCCGCTGTTTGTGATTGATCATGCGGGTAGCCTGACCAGCCAGTTTAGCTATGT
TGTTGGTCGTAGTGCCCTGCGTAGCACCACAGGTCAGGCACGTAGCGCAGATTATGGTA
TTACCGATTGTAATCCGCTGCCTGCAAATGATCTGACACCCGGAACAGAAAGTTGCAGCAG
CAGCACTGCTGGCACCAGGCGAGCAGCCGCAATTGTTGCAGGTCCGAAACAGAATTGTGAA
CCGGATCTGATGCCGTATGCACGTCCGTTTGCAGTTGGTAAACGTACCTGTAGCGGTAT
TGTTACACCGGGATCC**CATCACCATCACCATCACTAAGGTACCAAGCTT**

Where EcoRI restriction site was in red, C-terminal poly-His tag was in blue, KpnI was in orange and HindIII was in green.

E269C mutCalB:

GAATTCCTGCCGAGCGGTAGCGATCCGGCATTAGCCAGCCGAAAAGCGTTCTGGATGC
CGGTCTGACCTGTCAGGGTGAAGCCCGTCAAGCGTTAGCAAACCGATTCTGCTGGTTC
CGGGTACAGGCACCACCGGTCCGCAGAGCTTTGATAGCAATTGGATTCCGCTGAGCACA
CAGCTGGGTTATACCCCGTGTTGGATTAGTCCGCCTCCGTTTATGCTGAATGATACCCA
GGTTAATACCGAGTATATGGTGAATGCAATTACCGCACTGTATGCAGGTAGCGGTAATA
ACAACTGCCGGTTCTGACATGGTCACAGGGTGGTCTGGTTGCACAGTGGGGTCTGACA
TTTTTTCCGAGCATTTCGTAGCAAAGTTGATCGTCTGATGGCATTTCACCCGATTATAAA
GGCACCGTTCTGGCAGGTCCGCTGGATGCACTGGCAGTTAGCGCACCCGAGCGTTTGGC
AGCAGACCACCGGTAGCGCACTGACCACCGCACTGCGTAATGCCGGTGGCCTGACCCAG
ATTGTTCCGACCACCAATCTGTATAGCGCAACCGATGAAATTGTGCAGCCGCAGGTTAGC
AATTCACCGCTGGATAGCAGCTACCTGTTAATGGTAAAAATGTTGAGGCACAGGCCGTT
TGTGGTCCGCTGTTTGTGATTGATCATGCGGGTAGCCTGACCAGCCAGTTTAGCTATGT
TGTTGGTCGTAGTGCCCTGCGTAGCACCACAGGTCAGGCACGTAGCGCAGATTATGGTA
TTACCGATTGTAATCCGCTGCCTGCAAATGATCTGACACCGTGCCAGAAAGTTGCAGCAG
CAGCACTGCTGGCACCCGGCAGCAGCCGCAATTGTTGCAGGTCCGAAACAGAATTGTGAA
CCGGATCTGATGCCGTATGCACGTCCGTTTGCAGTTGGTAAACGTACCTGTAGCGGTAT
TGTTACACCGGGATCCCATCACCATCACCATCACTAAGGTACCAAGCTT

PA3859:

ATGAGCGAACCCTGATCCTCGATGCCCCGAATGCCGACGCCTGTATCATCTGGCTGCA
CGGCCTGGGCGCCGACCGTACCGACTTCAAACCGGTGGCCGAAGCCCTGCAGATGGTCC
TGCCGAGCACCCGCTTCATCCTCCCCAGGCGCCGAGCCAGGCGGTGACGGTCAATGGC
GGCTGGGTCATGCCGAGCTGGTACGACATCCTTGCCTTCAGTCCGGCGCGGGCCATCGA
CGAAGACCAGTTGAACGCCTCCGCCGACCAGGTCATCGCTCTCATCGATGAACAGCGCG
CCAAGGGCATCGCCGCCGAGCGGATCATCCTCGCCGTTTCTCGCAGGGCGGCGCGGT
GGTCCTGCATACCGCCTTCGCCGCTACGCCAGCCGCTCGGCGGGGTGCTGGCGCTAT
CCACCTACGCGCCGACCTTCGACGACCTGGCGCTGGACGAGCGCCACAAGCGGATTCCG
GTCCTGCACCTGCACGGCAGCCAGGACGACGTGGTCGACCCGCGCTTGGCCGCGCGG
CCCATGACGCCTTGCAGGCGCAGGGCGTGGAGGTGGGCTGGCACGACTACCCGATGGG
CCACGAGGTGTCCCTGGAGGAAATCCACGACATCGGCGCCTGGCTGCGCAAGCGCCTCT
GA

C14S/M37C PA3859:

ATGAGCGAACCCCTGATCCTCGATGCCCCGAATGCCGACGCCAGCATCATCTGGCTGCA
CGGCCTGGGCGCCGACCGTACCGACTTCAAACCGGTGGCCGAAGCCCTGCAGTGCGTCC
TGCCGAGCACCCGCTTCATCCTCCCCAGGCGCCGAGCCAGGCGGTGACGGTCAATGGC
GGCTGGGTCATGCCGAGCTGGTACGACATCCTTGCCTTCAGTCCGGCGCGGGCCATCGA
CGAAGACCAGTTGAACGCCTCCGCCGACCAGGTCATCGCTCTCATCGATGAACAGCGCG
CCAAGGGCATCGCCGCCGAGCGGATCATCCTCGCCGGTTTCTCGCAGGGCGGCGCGGT
GGTCCTGCATAACCGCCTTCCGCCGCTACGCCAGCCGCTCGGCGGGGTGCTGGCGCTAT
CCACCTACGCGCCGACCTTCGACGACCTGGCGCTGGACGAGCGCCACAAGCGGATTCCG
GTCCTGCACCTGCACGGCAGCCAGGACGACGTGGTTCGACCCGGCGCTTGGCCGCGCGG
CCCATGACGCCTTGCAGGCGCAGGGCGTGGAGGTGGGCTGGCACGACTACCCGATGGG
CCACGAGGTGTCCCTGGAGGAAATCCACGACATCGGCGCCTGGCTGCGCAAGCGCCTCT
GA

C14S/M37C/S113A PA3859:

ATGAGCGAACCCCTGATCCTCGATGCCCCGAATGCCGACGCCAGCATCATCTGGCTGCA
CGGCCTGGGCGCCGACCGTACCGACTTCAAACCGGTGGCCGAAGCCCTGCAGTGCGTCC
TGCCGAGCACCCGCTTCATCCTCCCCAGGCGCCGAGCCAGGCGGTGACGGTCAATGGC
GGCTGGGTCATGCCGAGCTGGTACGACATCCTTGCCTTCAGTCCGGCGCGGGCCATCGA
CGAAGACCAGTTGAACGCCTCCGCCGACCAGGTCATCGCTCTCATCGATGAACAGCGCG
CCAAGGGCATCGCCGCCGAGCGGATCATCCTCGCCGGTTTTCGCGCAGGGCGGCGCGGT
GGTCCTGCATAACCGCCTTCCGCCGCTACGCCAGCCGCTCGGCGGGGTGCTGGCGCTAT
CCACCTACGCGCCGACCTTCGACGACCTGGCGCTGGACGAGCGCCACAAGCGGATTCCG
GTCCTGCACCTGCACGGCAGCCAGGACGACGTGGTTCGACCCGGCGCTTGGCCGCGCGG
CCCATGACGCCTTGCAGGCGCAGGGCGTGGAGGTGGGCTGGCACGACTACCCGATGGG
CCACGAGGTGTCCCTGGAGGAAATCCACGACATCGGCGCCTGGCTGCGCAAGCGCCTCT
GA

Est97:

ATGAGGCATCAGATGAGTTGGAACGGTAAAGACGAACGCAAGCTGAGCGTGCAGGAAC
GGGGATTCTCGCTGGAGGTCGACGGCAGAACGGTGCCCGGCGTTTACTGGTCACCAGC
CGAAGGTTTCGAGCGATCGGCTGGTGTGTTGGGCCACGGCGGTACAACGCACAAAAA
GTGGAGTACATCGAGCAGGTTGCCAAGCTGCTGGTGGGTCGCGGAATATCAGCCATGG
CCATTGACGGACCAGGGCATGGCGAGCGAGCGAGTGTGCAGGCAGGTCGCGAACCTAC

GGACGTTGTTGGTTTGGATGCCTTTCCCCGCATGTGGCATGAAGGGGGCGGCACCGCT
GCCGTGATTGCGGACTGGGCTGCCGCCCTCGACTTTATAGAAGCCGAAGAAGGCCCTCG
ACCGACGGGTTGGTGGGGCTTGTCCATGGGCACCATGATGGGGCTTCCCGTCACTGCG
TCGGATAAACGCATCAAGGTGGCCTTGCTTGGTTTGTATGGGCGTCGAGGGGGTGAACG
GAGAAGACCTGGTCAGGCTCGCTCCGCAGGTCACATGCCCGGTGCGTTATTTATTGCAA
TGGGATGATGAGCTGGTGTCCCTGCAGTCGGGGCTCGAACTGTTCCGGCAAACCTGGGGA
CAAAGCAAAAACACTGCACGTGAATCCGGGTAAGCACAGTGCCGGTCCCAACCTGGGAG
ATGTTTGCCGGTACGGTTGACTATCTGGACCAGCGTTTGAAGTGA

E40C Est97:

ATGAGGCATCAGATGAGTTGGAACGGTAAAGACGAACGCAAGCTGAGCGTGCAGGAAC
GGGGATTCTCGCTGGAGGTCGACGGCAGAACGGTGCCCGGCGTTTACTGGTCACCAGC
CTGTGGTTTCGAGCGATCGGCTGGTGTGTTGGGCCACGGCGGTACAACGCACAAAAAA
GTGGAGTACATCGAGCAGTTGCCAAGCTGCTGGTGGGTCGCGGAATATCAGCCATGG
CCATTGACGGACCAGGGCATGGCGAGCGAGCGAGTGTGCAGGCAGGTCGCGAACCTAC
GGACGTTGTTGGTTTGGATGCCTTTCCCCGCATGTGGCATGAAGGGGGCGGCACCGCT
GCCGTGATTGCGGACTGGGCTGCCGCCCTCGACTTTATAGAAGCCGAAGAAGGCCCTCG
ACCGACGGGTTGGTGGGGCTTGTCCATGGGCACCATGATGGGGCTTCCCGTCACTGCG
TCGGATAAACGCATCAAGGTGGCCTTGCTTGGTTTGTATGGGCGTCGAGGGGGTGAACG
GAGAAGACCTGGTCAGGCTCGCTCCGCAGGTCACATGCCCGGTGCGTTATTTATTGCAA
TGGGATGATGAGCTGGTGTCCCTGCAGTCGGGGCTCGAACTGTTCCGGCAAACCTGGGGA
CAAAGCAAAAACACTGCACGTGAATCCGGGTAAGCACAGTGCCGGTCCCAACCTGGGAG
ATGTTTGCCGGTACGGTTGACTATCTGGACCAGCGTTTGAAGTGA

G53A Est97:

ATGAGGCATCAGATGAGTTGGAACGGTAAAGACGAACGCAAGCTGAGCGTGCAGGAAC
GGGGATTCTCGCTGGAGGTCGACGGCAGAACGGTGCCCGGCGTTTACTGGTCACCAGC
CGAAGGTTTCGAGCGATCGGCTGGTGTGTTGGGCCACGGCGCTACAACGCACAAAAAAG
TGGAGTACATCGAGCAGTTGCCAAGCTGCTGGTGGGTCGCGGAATATCAGCCATGGC
CATTGACGGACCAGGGCATGGCGAGCGAGCGAGTGTGCAGGCAGGTCGCGAACCTACG
GACGTTGTTGGTTTGGATGCCTTTCCCCGCATGTGGCATGAAGGGGGCGGCACCGCTG
CCGTGATTGCGGACTGGGCTGCCGCCCTCGACTTTATAGAAGCCGAAGAAGGCCCTCGA
CCGACGGGTTGGTGGGGCTTGTCCATGGGCACCATGATGGGGCTTCCCGTCACTGCGT
CGGATAAACGCATCAAGGTGGCCTTGCTTGGTTTGTATGGGCGTCGAGGGGGTGAACGG
AGAAGACCTGGTCAGGCTCGCTCCGCAGGTCACATGCCCGGTGCGTTATTTATTGCAAT

GGGATGATGAGCTGGTGTCCCTGCAGTCGGGGCTCGAACTGTTTCGGCAAACCTGGGGAC
AAAGCAAAAAACACTGCACGTGAATCCGGGTAAGCACAGTGCGGTCCCAACCTGGGAGA
TGTTTGCCGGTACGGTTGACTATCTGGACCAGCGTTTGAAGTGA

T231I Est97:

ATGAGGCATCAGATGAGTTGGAACGGTAAAGACGAACGCAAGCTGAGCGTGCAGGAAC
GGGGATTCTCGCTGGAGGTCGACGGCAGAACGGTGCCCGGCGTTTACTGGTCACCAGC
CGAAGGTTTCGAGCGATCGGCTGGTGTGTTGGGCCACGGCGGTACAACGCACAAAAAA
GTGGAGTACATCGAGCAGGTTGCCAAGCTGCTGGTGGGTCGCGGAATATCAGCCATGG
CCATTGACGGACCAGGGCATGGCGAGCGAGCGAGTGTGCAGGCAGGTCGCGAACCTAC
GGACGTTGTTGGTTTGGATGCCTTTCCCGCATGTGGCATGAAGGGGGCGGCACCGCT
GCCGTGATTGCGGACTGGGCTGCCGCCCTCGACTTTATAGAAGCCGAAGAAGGCCCTCG
ACCGACGGGTTGGTGGGGCTTGTCCATGGGCACCATGATGGGGCTTCCCGTCACTGCG
TCGGATAAACGCATCAAGGTGGCCTTGCTTGGTTTGTATGGGCGTCGAGGGGGTGAACG
GAGAAGACCTGGTCAGGCTCGCTCCGCAGGTCACATGCCCGGTGCGTTATTTATTGCAA
TGGGATGATGAGCTGGTGTCCCTGCAGTCGGGGCTCGAACTGTTTCGGCAAACCTGGGGA
CAAAGCAAAAAACACTGCACGTGAATCCGGGTAAGCACAGTGCGGTCCCAATCTGGGAG
ATGTTTGCCGGTACGGTTGACTATCTGGACCAGCGTTTGAAGTGA

G53A/T231I Est97:

ATGAGGCATCAGATGAGTTGGAACGGTAAAGACGAACGCAAGCTGAGCGTGCAGGAAC
GGGGATTCTCGCTGGAGGTCGACGGCAGAACGGTGCCCGGCGTTTACTGGTCACCAGC
CGAAGGTTTCGAGCGATCGGCTGGTGTGTTGGGCCACGGCGCTACAACGCACAAAAAAG
TGGAGTACATCGAGCAGGTTGCCAAGCTGCTGGTGGGTCGCGGAATATCAGCCATGGC
CATTGACGGACCAGGGCATGGCGAGCGAGCGAGTGTGCAGGCAGGTCGCGAACCTACG
GACGTTGTTGGTTTGGATGCCTTTCCCGCATGTGGCATGAAGGGGGCGGCACCGCTG
CCGTGATTGCGGACTGGGCTGCCGCCCTCGACTTTATAGAAGCCGAAGAAGGCCCTCGA
CCGACGGGTTGGTGGGGCTTGTCCATGGGCACCATGATGGGGCTTCCCGTCACTGCGT
CGGATAAACGCATCAAGGTGGCCTTGCTTGGTTTGTATGGGCGTCGAGGGGGTGAACGG
AGAAGACCTGGTCAGGCTCGCTCCGCAGGTCACATGCCCGGTGCGTTATTTATTGCAAT
GGGATGATGAGCTGGTGTCCCTGCAGTCGGGGCTCGAACTGTTTCGGCAAACCTGGGGAC
AAAGCAAAAAACACTGCACGTGAATCCGGGTAAGCACAGTGCGGTCCCAATCTGGGAGA
TGTTTGCCGGTACGGTTGACTATCTGGACCAGCGTTTGAAGTGA

Amino acid sequences:

EstO+N-terminal poly-His:

MSYYHHHHHHLESTSLYKKAGSAAAPFGRRQKVSFKSGDLELAGQLELPSGDVKFYALFAHCF
TCGKDIAAATRISRALTQQGIAVLRFDFTGLGNSDGDGFANSNFSSNIQDLVSAANHLREHFAAP
QLLIGHSLGGAAVLAAAHEHILEVSAITTIGAPSDAQHVAHNFEAHLDEINAAGEAKVNLAGREFT
IKKQFIDDI AKYDKSHISLKRALLVMHSPIDATVNISEAEKIYASAKHPKSFISLDNADHLLTNKN
DADYAAQIIATWANRYVKYDKTKYTASLTGGNVLVEEKDHFVFTQHVSTKDHTWLADEPIKVG
GKNLGPDPYHHLLAGLGACTAMTLRMYATRKNLPLEHVKVELDHTRDYKDCDDCEQTGNL
EAITRKITLRGDLTEPQRQRLLLEIADKCPVHKTLHNNPVIVSELVE

ΔEstO+N-terminal poly-His:

MSYYHHHHHHLESTSLYKKAGSAAAPFGRRQKVSFKSGDLELAGQLELPSGDVKFYALFAHCF
TCGKDIAAATRISRALTQQGIAVLRFDFTGLGNSDGDGFANSNFSSNIQDLVSAANHLREHFAAP
QLLIGHSLGGAAVLAAAHEHILEVSAITTIGAPSDAQHVAHNFEAHLDEINAAGEAKVNLAGREFT
IKKQFIDDI AKYDKSHISLKRALLVMHSPIDATVNISEAEKIYASAKHPKSFISLDNADHLLTNKN
DADYAAQIIATWANRYVKY

EstLA+N-terminal poly-His:

MSYYHHHHHHLESTSLYKKAGSAAAPFGRGQHPLKLEFDGAHEASLAARLDLPSGNIRAFALF
AHCFTCSKDIAAARHIASALSQEGIAVLRFDFTGLGGSGGDFASTGFSSNVEDLKRAADYLRN
YQAPQLLIGHSLGGAAVLSVAADIPEVRVVITIGAPSDADHVIHSFKGEEDTIRQQGQGEVCL
GRSFTIRKEFLEDLETQSVRDKVASLGKALLVMHAPLDEVVIGIDNATSIFVAAKHPKSFVSLDTA
DHLLSKSQDAAYAARVIAGWVGRYLDPVEESADDEVKDGVEVVETGQGKFQVMVNSGKHRMI
ADEPRDVGIDSGSPYGFLSAALGACTVMTLRMYAERKGLDVDRIGTRVLHGKVHADDCKEC
SESVKSRGGKIDRFERMITLEGNLDEATRTRMLEIADKCPVHRTLEAGAAVVTREVPSGTPEA

ΔEstLA+N-terminal poly-His:

MSYYHHHHHHLESTSLYKKAGSAAAPFGRGQHPLKLEFDGAHEASLAARLDLPSGNIRAFALF
AHCFTCSKDIAAARHIASALSQEGIAVLRFDFTGLGGSGGDFASTGFSSNVEDLKRAADYLRN
YQAPQLLIGHSLGGAAVLSVAADIPEVRVVITIGAPSDADHVIHSFKGEEDTIRQQGQGEVCL
GRSFTIRKEFLEDLETQSVRDKVASLGKALLVMHAPLDEVVIGIDNATSIFVAAKHPKSFVSLDTA
DHLLSKSQDAAYAARVIAGWVGRYLDPVEESADDEVKD

ΔEstRD+C-terminal poly-His:

MPTERIAFAGHDGGQLAARLDLPQGPLVATAIFAHCFTCGKDIPAARRIARLAALGIAVLRFD
FTGLGHSDGEFANTSFTSNVDDLIAAHRYLSENNKTPSLIIGHSLGGAAVLKAAAALDSIKAVVTI
GAPFDPGHVTHNFAQALPEIKSRGVAEVS LGGRPFQJSAFVDDVAQTELEESVANLNAALLVL
HAPLDDIVGIENAGQIFSAAKHPKSFITLDGADHLVSAAADA EYVASLIATWSARYLDIARPAPP
GAPEGVLRVAEADPKGFKGHHHHHH

ΔEstEM+N-terminal poly-His:

MSYYHHHHHHLESTSLYKKAGSAAAPFGAFNTQRLQFSGHSGATLSARLDLPNGPLRAYALFA
HCFTCSKDLAAARQIGAELAREGIAVLRFDFTGLGSSEGEFASTNFSSNVADLLSAADYLRHHY
QAPAVLIGHSLGGAAVLAVAGEIPEVRVAVATIGAPADVGHVLKNFGASLEEIDKGEADVLAGR
TFLIRKQFVEDTRAHRIKDAVGRLKKPILILHAPLDHTVGIENATEIFVAARHPKSFVSLDKADHL
LTDPEDAAFAGRIISEWLTRYLAADTPQGAGPIEHVHVR

ΔEstRM+N-terminal poly-His:

MSYYHHHHHHLESTSLYKKAGSAAAPFGQIKTVTFENNRGERLAARLDLPVDTQPVAYALFAH
CFTCSKLNKAVTTISRALTTQGYAVLRFDFTGLGESEGEFSETTFATNFEDLRAACRFLSAQYE
PPALLIGHSLGGAAVLAVAGEFPEVKAVATIGAPCDPAHVRHLLRPALDTIKTVGEAVVDLGGR
PFRIKKQFLEELERNLEDQVRTMRRPLLLFHSPTDQIVGIENAA CLFQAARHPKSFVSLDQADH
LLSNSDDAAFVGEVLGAWARRYVGRR

ΔEstCA+N-terminal poly-His:

MSYYHHHHHHLESTSLYKKAGSAAAPFGSTSLKVTFPGGGGVALAARLELPDGAAPRAYAIFA
HCFTCGKDAVAASRIARALTDHGIAVLRFDFTGLGQSDGDFGNTGFTSNVEDLVAAADHLRTE
YGAPSLIGHSLGGAAVLAARHG IPEVRVAVVTIGAPADPSHIAHLLSEARDTIERDGEATVTLGG
RDFCVRSSFLADIADQPQAERIHDLKAALLVMHSPQDETVGVDNARQIFDAARHPKSFVSLDGA
DHLLTRRRDAEYAATVLAAWVSRYLPEPEPSTV

MBP+CalB:

MKIEEGKLVIIWINGDKGYNGLAEVGGKFEKDTGIKVTVEHPDKLEEKFPQVAATGDGPDIIIFWA
HDRFGGYAQSGLLAEITPKAFQDKLYPFTWDAVRYNGKLIAYPIAVEALS LIYNKDLLPNPPKT
WEEIPALDKELKAKGKSALMFNLQEPYFTWPLIAADGGYAFKYENGYDIKDVGVNAGAKAG
LTFLVDLIKNKHMNADTDYSIAEAAFNKGETAMTINGPWAWSNIDTSKVNYGVTVLPTFKGQP
SKPFVGVLSAGINAASPNKELAKEFLENYLLTDEGLEAVNKDKPLGAVALKS YEELAKDPRIAA

TMENAQKGEIMPNIQMSAFWYAVRTAVINAASGRQTVDEALKDAQTNSSSNNNNNNNNNNL
GIEGRISEFLPSGSDPAFSQPKSVLDAGLTCQGASPSSVSKPILLVPGTGTTGPQSFDSNWIP
LSTQLGYTPCWISPPPFMLNDTQVNTEYMVNAITALYAGSGNNKLPVLTWSQGGLVAQWGLTFF
PSIRSKVDRLMAFAPDYKGTVLGAGPLDALAVSAPSVWQQTGSALTTALRNAGGLTQIVPTTN
LYSATDEIVQPQVSNPLDSSYLFNGKNVQAQAVCGPLFVIDHAGSLTSQFSYVVGRSALRSTT
GQARSADYGITDCNPLPANDLTPEQKVAAAALLAPAAAAIVAGPKQNCEPDLMPYARPFVAVGK
RTCSGIVTPGSHHHHHH

MBP+E269C CalB:

MKIEEGKLVWINGDKGYNGLAEVGGKFEKDTGIKVTVEHPDKLEEKFPQVAATGDGPDIIFWA
HDRFGGYAQSGLLAEITPDKAFQDKLYPFTWDAVRYNGKLIAYPIAVEALSIIYNKDLLPNPPKT
WEEIPALDKELKAKGKSALMFNLQEPYFTWPLIAADGGYAFKYENGGYDIKDVGVNAGAKAG
LTFLVDLIKNKHMNADTDYSIAEAAFNKGETAMTINGPWAWSNIDTSKVNYGVTVLPTFKGQP
SKPFVGVLSAGINAASPNKELAKEFLENYLLTDEGLEAVNKDKPLGAVALKSYYEELAKDPRIAA
TMENAQKGEIMPNIQMSAFWYAVRTAVINAASGRQTVDEALKDAQTNSSSNNNNNNNNNNL
GIEGRISEFLPSGSDPAFSQPKSVLDAGLTCQGASPSSVSKPILLVPGTGTTGPQSFDSNWIP
LSTQLGYTPCWISPPPFMLNDTQVNTEYMVNAITALYAGSGNNKLPVLTWSQGGLVAQWGLTFF
PSIRSKVDRLMAFAPDYKGTVLGAGPLDALAVSAPSVWQQTGSALTTALRNAGGLTQIVPTTN
LYSATDEIVQPQVSNPLDSSYLFNGKNVQAQAVCGPLFVIDHAGSLTSQFSYVVGRSALRSTT
GQARSADYGITDCNPLPANDLTPCQKVAAAALLAPAAAAIVAGPKQNCEPDLMPYARPFVAVGK
RTCSGIVTPGSHHHHHH

PA3859 + N-terminal poly-His:

MSYYHHHHHHLESTSLYKKAGSAAAPFGRSEPLILDAPNADACIIWLHGLGADRTDFKPVAEAL
QMVLPPSTRFILPQAPSQAVTVNGGWMPWSYDILAFSPARAIDEDQLNASADQVIALIDEQRAK
GIAAERIILAGFSQGGAVVLHTAFRRYAQPLGGVLALSTYAPTFFDLALDERHKRIPVLHLHGS
QDDVVDPALGRAAHDALQAQGVVEGWHDYPMGHEVSLEEIH DIGAWLRKRL

C14S/M37C PA3859+N-terminal poly-His:

MSYYHHHHHHLESTSLYKKAGSAAAPFGRSEPLILDAPNADASIIWLHGLGADRTDFKPVAEAL
QCVLPSTRFILPQAPSQAVTVNGGWMPWSYDILAFSPARAIDEDQLNASADQVIALIDEQRAK
GIAAERIILAGFSQGGAVVLHTAFRRYAQPLGGVLALSTYAPTFFDLALDERHKRIPVLHLHGS
QDDVVDPALGRAAHDALQAQGVVEGWHDYPMGHEVSLEEIH DIGAWLRKRL

C14S/M37C/S113A PA3859 + N-terminal poly-His:

MSYYHHHHHLESTSLYKKAGSAAAPFGRSEPLILDAPNADASIWLHGLGADRTDFKPVAEAL
QCVPSTRFILPQAPSQAVTVNGGWVMP SWYDILAFSPARAIDEDQLNASADQVIALIDEQRAK
GIAAERIILAGFAQGGAVVLHTAFRRYAQPLGGVLALSTYAPTFFDDLALDERHKRIPVLHLHGS
QDDVVDPALGRAAHDALQAQGVVEVGHWDYPMGHEVSLEEIHDIGAWLRKRL

Est97 + N-terminal poly-His:

MRGSHHHHHHGSGSGSGIEGRPYNGTMRHQMSWNGKDERKLSVQERGFSLVDGRTVPGVY
WSPAEGSSDRLVLLGHGGTTHKKVEYIEQVAKLLVGRGISAMAIDGPGHGERASVQAGREPTD
VVGLDAFPRMWHEGGGTA AVIADWAAALDFIEAEEGPRPTGWWGLSMGTMMGLPVTASDK
RIKVALLGLMGVEGVNGEDLVRLAPQVTCVRYLLQWDELVSLQSGLELFGKLGTKQKTLHV
NPGKHSAPPTWEMFAGTVDYLDQRLK

E40C Est97 + N-terminal poly-His:

MRGSHHHHHHGSGSGSGIEGRPYNGTMRHQMSWNGKDERKLSVQERGFSLVDGRTVPGVY
WSPACGSSDRLVLLGHGGTTHKKVEYIEQVAKLLVGRGISAMAIDGPGHGERASVQAGREPTD
VVGLDAFPRMWHEGGGTA AVIADWAAALDFIEAEEGPRPTGWWGLSMGTMMGLPVTASDK
RIKVALLGLMGVEGVNGEDLVRLAPQVTCVRYLLQWDELVSLQSGLELFGKLGTKQKTLHV
NPGKHSAPPTWEMFAGTVDYLDQRLK

G53A Est97 + N-terminal poly-His:

MRGSHHHHHHGSGSGSGIEGRPYNGTMRHQMSWNGKDERKLSVQERGFSLVDGRTVPGVY
WSPAEGSSDRLVLLGHGATTHKKVEYIEQVAKLLVGRGISAMAIDGPGHGERASVQAGREPTD
VVGLDAFPRMWHEGGGTA AVIADWAAALDFIEAEEGPRPTGWWGLSMGTMMGLPVTASDK
RIKVALLGLMGVEGVNGEDLVRLAPQVTCVRYLLQWDELVSLQSGLELFGKLGTKQKTLHV
NPGKHSAPPTWEMFAGTVDYLDQRLK

T231I Est97 + N-terminal poly-His:

MRGSHHHHHHGSGSGSGIEGRPYNGTMRHQMSWNGKDERKLSVQERGFSLVDGRTVPGVY
WSPAEGSSDRLVLLGHGGTTHKKVEYIEQVAKLLVGRGISAMAIDGPGHGERASVQAGREPTD
VVGLDAFPRMWHEGGGTA AVIADWAAALDFIEAEEGPRPTGWWGLSMGTMMGLPVTASDK
RIKVALLGLMGVEGVNGEDLVRLAPQVTCVRYLLQWDELVSLQSGLELFGKLGTKQKTLHV
NPGKHSAPPIWEMFAGTVDYLDQRLK

G53A/T231I Est97 + N-terminal poly-His:

MRGSHHHHHHGSGSGSIEGRPYNGTMRHQMSWNGKDERKLSVQERGFSLVDGRTVPGVY
WSPAEGSSDRLVLLGHGATTHKKVEYIEQVAKLLVGRGISAMAIDGPGHGERASVQAGREPTD
VVGLDAFPRMWHEGGTA AVIADWAAALDFIEAEEGPRPTGWWGLSMGTMMGLPVTASDK
RIKVALLGLMGVEGVNGEDLVRLAPQVTCPVRYLLQWDELVSLSGLELFGKLGTKQKTLHV
NPGKHSAPWIWEMFAGTVDYLDQRLK

Bibliography

- Adler AJ, Kistiakowsky GB, 1961, Isolation and properties of pig liver esterase., *Journal of Biological Chemistry*, Vol. 236, no. 12, p3240-3245
- Ahmad S, Gromiha M M, Fawareh H, Sarai A, 2004, ASAView: Database and tool for solvent accessibility representation in proteins. *BMC Bioinformatics*, Vol 5 no.51, p1-5
- Akoh CC, Lee GC, Liaw YC, Huang TH, Shaw JF., 2004, GDSL family of serine esterases/lipases., *Prog Lipid Res.*, Vol. 43, no.6, p534-552
- Alfredsson GA, Kristjansson JK, Hjorleifsdottir S, Stetter KO,1988, *Rhodothermus marinus*, gen nov, sp nov, a thermophilic, halophilic bacterium from submarine hot springs in Iceland., *J Gen Microbiol*, Vol. 134, no.2, p299-306
- Ali YB, Verger R, Abousalham A, 2012, Lipases or esterases: does it really matter? Toward a new bio-physico-chemical classification., *Methods in Molecular Biology*, Vol. 861, p31-51
- Al-Khudary R., Stösser NI, Qoura F, Antranikian G, 2008, *Pseudoalteromonas arctica* sp. nov., an aerobic, psychrotolerant, marine bacterium isolated from Spitzbergen, *Int J Syst Evol Microbiol*, Vol 58, no. 9, p2018-2024
- Al-Khudary R., Venkatachalam R, Katzer M, Elleuche S, Antranikian G, 2010, A cold-adapted esterase of a novel marine isolate, *Pseudoalteromonas arctica*: gene cloning, enzyme purification and characterization, *Extremophiles*, Vol 14, no. 3, p273-285
- Amer MA, Kupranycz DB, Baker BE, 1985, Physical and chemical characteristics of butterfat fractions obtained by crystallization from molten fat., *Journal of the American oil chemists society*, Vol. 62, no. 11, 1551-1557
- Ananda K, Nacharaju P, Smith PK, Acharya SA, Manjula BN., 2008, Analysis of functionalization of methoxy-PEG as maleimide-PEG., *Anal Biochem*, Vol. 374, no. 2, p231-234
- Appaiah P, Sunil L, Kumar PKP, Krishna AGG., 2014, Composition of Coconut Testa, Coconut Kernel and its Oil., *Journal of the American oil chemists society*, Vol. 91, no. 6, p917-924

Arpigny JL, Jaeger KE., 1999, Bacterial lipolytic enzymes: classification and properties., *Biochem J*, Vol. 343, no. 1, p177-183

Asther M, Haon M, Roussos S, Record E, Delattre M, Lesage-Meessen L, Labat M, Asther M, 2002, Feruloyl esterase from *Aspergillus niger* a comparison of the production in solid state and submerged fermentation. *Process Biochem* Vol. 38, p685-691

Athawale, V., Manjrekar, N., Athawale, M., 2001, Enzymatic synthesis of chiral menthyl methacrylate monomer by *Pseudomonas cepacia* lipase catalysed resolution of (\pm)-menthol, *J of Mol Catalysis*, Vol. 16, no. 3-4, p169-173

Aurilia, V., Parracino, A. and D'Auria, S., 2008 Microbial carbohydrate esterases in cold adapted environments. *Institute of Protein Biochemistry*, Vol. 2, p234-240

Aydemir S, Akin N, Koçak C, 2007, Effect of Lipase Enzyme on the Ripening of White Pickled Cheese., *Journal of Food Lipids*, Vol. 8, no. 3, p205-213

Bagheri M, Amoozegar MA, Didari M, Makhdoumi-Kakhki A, Schumann P, Spröer C, Sánchez-Porro C, Ventosa A., 2013, *Marinobacter persicus* sp. nov., a moderately halophilic bacterium from a saline lake in Iran., *Antonie Van Leeuwenhoek*, Vol. 104, no. 1, p47-54

Balan S, Choi JW, Godwin A, Teo I, Laborde CM, Heidelberger S, Zloh M, Shaunak S, Brocchini S., 2007, Site-specific PEGylation of protein disulphide bonds using a three-carbon bridge., *Bioconjug Chem*, Vol. 18, no. 1, p61-76.

Barbosa O, Ruiz M, Oritz C, Fernandez M, Torres R, Fernandez-Lafuente R, 2012, Modulation of the properties of immobilised CALB by chemical modification with 2,3,4-trinitrobenzenesulfonate or ethylenediamine. Advantages of using adsorbed lipases on hydrophobic supports., *Process Biochem*, Vol. 47, no. 5 p867-876

Barron LJ, Hernández I, Bilbao A, Flanagan CE, Nájera AI, Virto M, Pérez-Elortondo FJ, Albisu M, de Renobales M., 2004, Changes in lipid fractions and sensory properties of Idiazabal cheese induced by lipase addition. *J Dairy Res*, Vol. 71, no. 3, p372-379

Baumann, M., Stürmer R. and Bornscheuer, U. T., 2001, A High-Throughput-Screening Method for the Identification of Active and Enantioselective Hydrolases. *Angewandte Chemie* Vol. 40 p4201-4204

Bencharit S, Morton CL, Xue Y, Potter PM, Redinbo MR., 2003, Structural basis of heroin and cocaine metabolism by a promiscuous human drug-processing enzyme., *Nat Struct Biol*, Vol. 10, no. 5, p349-356

Benson LM, Kumar R, Cavanagh J, Naylor S., 2003, Protein-metal ion interactions, stoichiometries and relative affinities determined by on-line size exclusion gel filtration mass spectrometry., *Rapid Commun. Mass. Spectrom.*, Vol. 17, no. 4, p267-271

Berg OG, Cajal Y, Butterfoss GL, Grey RL, Alsina MA, Yu BZ, Jain MK., 1998, Interfacial activation of triglyceride lipase from *Thermomyces (Humicola) lanuginosa*: kinetic parameters and a basis for control of the lid., *Biochemistry*, Vol. 37, no. 19 p6615-6627

Berger, M and Schneider M. P., 1991, Lipases in organic solvents: The fatty acid chain length profile. *Biotechnology Letters*, 13: 641-645

Berger R, Hoffmann M, Keller U, 1998, Molecular analysis of a gene encoding a cell-bound esterase from *Streptomyces chrysomallus*, *J. Bacteriol*, Vol. 180, p6396-6399

Bhavani M, Chowdary G V, David M, Archana G, 2012, Screening, Isolation and Biochemical Characterization of Novel Lipase Producing Bacteria from Soil Samples, *Int J of Biol Engineering*, Vol 2., no. 2, p18-22

Biebl H, Pukall R, Lünsdorf H, Schulz S, Allgaier M, Tindall BJ, Wagner-Döbler I, 2007, Description of *Labrenzia alexandrii* gen. nov., sp. nov., a novel alphaproteobacterium containing bacteriochlorophyll a, and a proposal for reclassification of *Stappia aggregata* as *Labrenzia aggregata* comb. nov., of *Stappia marina* as *Labrenzia marina* comb. nov. and of *Stappia alba* as *Labrenzia alba* comb. nov., and emended descriptions of the genera *Pannonibacter*, *Stappia* and *Roseibium*, and of the species *Roseibium denhamense* and *Roseibium hamelinense*., *Int J Syst Evol Microbiol*, Vol. 57, no.5, p1095-1107

Blank K, Morfill J, Gump H, Gaub HE, 2006, Functional expression of *Candida antarctica* lipase B in *Escherichia coli*, *J Biotechnol*, Vol. 125, no. 4, p474-483

Blow DM, Birktoft JJ, Hartley BS., 1969, Role of a buried acid group in the mechanism of action of chymotrypsin., *Nature*, Vol. 221, no. 5178, p337-340

Boland T, Ratner BD, 1995, Direct measurement of hydrogen bonding in DNA Nucleotide bases by atomic force microscopy., *Proc Natl Acad Sci USA*, Vol. 92, no. 12, p5297-5301

Bornscheuer UT, Altenbuchner J, Meyer HH. 1998, Directed evolution of an esterase for the stereoselective resolution of a key intermediate in the synthesis of epothilones., *Biotechnol Bioeng.*, Vol. 58, no. 5, p554-559

Bornscheuer, U. T., 2006, Microbial carboxyl esterases: classification, properties and application in biocatalysis. *FEMS Microbiology Reviews*, 26: 73-81

Braman, J, Papworth, C, Greener, A, 1996, Site-directed mutagenesis using double-stranded plasmid DNA templates., *Methods in Mol Biol*, Vol. 57, p31-44

Brocca S, Secundo F, Ossola M, Alberghina L, Carrea G, Lotti M., 2003, Sequence of the lid affects activity and specificity of *Candida rugosa* lipase isoenzymes., *Prote Sci.*, Vol. 12, no. 10, p2312-2319

Brockman HL, Momsen WE, Tsujita T., 1988, Lipid-lipid complexes: Properties and effects on lipase binding to surfaces. *Journal of the American Oil Chemist's Society*, Vol. 65, no. 6, p891-896

Brzuszkiewicz, A., Nowak, E., Dauter, Z., Dauter, M., Cieśliński, H., Długotecka, A., Kur, J., 2009, Structure of EstA esterase from psychrotrophic *Pseudoalteromonas* sp. 643A covalently inhibited by monoethylphosphonate. *Acta Crystallogr Sect F Struct Biol Cryst Commun* 65: 862-865

Buchan A, Gonzalez J, Moran M A, 2005, Overview of the marine *Roseobacter* lineage. *Appl. Environ. Microbiol.* Vol.71, no.10, p5665-5677

Busti E, Cavaletti L, Monciardini P, Schumann P, Rohde M, Sosio M, Donadio S., 2006, *Catenulispora acidiphila* gen. nov., sp. nov., a novel, mycelium-forming actinomycete, and proposal of *Catenulisporaceae* fam. nov., *Int J Syst Evol Microbiol*, Vol. 56, no. 8, p1741-1746

Böttcher, D., Schmidt, M., and Bornscheuer, U. T., 2010, Screens for Active and Stereoselective Hydrolytic Enzymes. *Methods Mol. Biol.* Vol. 668 p169-176

Cammarota MC, Rosa DR, Duarte IC, Saavedra NK, Varesche MB, Zaiat M, Freire DM., 2013, The effect of enzymatic pre-hydrolysis of dairy wastewater on the granular and immobilised microbial community in anaerobic bioreactors., *Environ Technol*, Vol. 34, no.1-4, p417-428

Carter WG, Aswad DW., 2008, Formation, Localization, and Repair of L-Isoaspartyl Sites in Histones H2A and H2B in Nucleosomes from Rat Liver and Chicken Erythrocytes., *Biochemistry*, Vol. 47, no. 40, p10757-10764

Casas-Godoy L, Duquesne S, Bordes F, Sandoval G, Marty A., 2012, Lipases: an overview., *Method Mol. Biol.*, Vol. 861, p3-30

Chahinian, H., Nini, L., Boitard, E., Dubès, J. P., Comeau, L. C. and Sarda, L. 2002 Distinction between esterases and lipases: a kinetic study with vinyl esters and TAG. *Lipids*, 37: 653-6

Chaloupka JA, Bullock SA, Iourgenko V, Levin LR, Buck J., 2006, Autoinhibitory regulation of soluble adenylyl cyclase., *Mol Reprod Dev*, Vol. 73, no. 3, p361-368

Chang L, Guo-he T, Bai-song Z, Zuo-ming Z, Yan F., 2011, Improvement of Substrate Selectivity of Hyperthermophilic Esterase to Long-chain Acyl Ester by Directed Evolution., *Chinese Journal of Biol*, Vol. 24, no. 12, p1400-1404

Chen, H-L, Zhou, H-X., 2005, Prediction of solvent accessibility and sites of deleterious mutations from protein sequence. *Nucl. Acids Res*. Vol. 33, p3193-3199

Chien A, Edgar DB, Trela JM., 1976, Deoxyribonucleic acid polymerase from the extreme thermophile *Thermus aquaticus*., *J. Bacteriol*, Vol. 127, no. 3, p1550-1557

Choi GS, Kim JY, Kim JH, Ryu YW, Kim GJ., 2003, Construction and characterization of a recombinant esterase with high activity and enantioselectivity to (S)-ketoprofen ethyl ester., *Protein Expr Purif.*, Vol. 29, no. 1, p85-93

Choi YJ, Lee BH., 2001, Culture conditions for the production of esterase from *Lactobacillus casei* CL 96., *Bioprocess Biosyst Eng.*, Vol. 24, p59-63

Choo, W. S., Birch, E. J. and Stewart, I., 2009 Radical scavenging activity of lipophilized products from transesterification of flaxseed oil with cinnamic acid or ferulic acid. *Lipids*, Vol. 44, no.9, p807-815

Chtcheglova LA, Wildling L, Waschke J, Drenckhahn D, Hinterdorfer P., 2010, AFM functional imaging on vascular endothelial cells, *J Mol Recognit.*, Vol. 23, no. 6, p589-596

Cieśliński H, Białkowska AM, Długotecka A, Daroch M, Tkaczuk KL, Kalinowska H, Kur J, Turkiewicz M., 2007, A cold-adapted esterase from psychrotrophic *Pseudoalteromonas* sp. strain 643A, *Arch Microbiol*, Vol 188, no. 1, p27-36

Cox E C, 1976, Bacterial mutator genes and the control of spontaneous mutation., *Annu Rev Genet.*, Vol. 10, p135-156

Creasey R, Sharma S, Gibson CT, Craig JE, Ebner A, Becker T, Hinterdorfer P, Voelcker NH., Atomic force microscopy-based antibody recognition imaging of proteins in the pathological deposits in pseudoexfoliation syndrome., *Ultramicroscopy*, Vol. 111, no. 8, p1055-1061

Cygler M, Schrag JD, Sussman JL, Harel M, Silman I, Gentry MK, Doctor BP., 1993, Relationship between sequence conservation and three-dimensional structure in a large family of esterases, lipases, and related proteins., *Protein Sci*, Vol. 2, no. 3, p366-382

Dalrymple BP, Cybinski DH, Layton I, McSweeney CS, Xue GP, Swadling YJ, Lowry JB., 1997, Three *Neocallimastix patriciarum* esterases associated with the degradation of complex polysaccharides are members of a new family of hydrolases., *Microbiology*, Vol. 143, part 8, p2605-2614

de Pascale D, Cusano AM, Autore F, Parrilli E, di Prisco G, Marino G, Tutino ML, 2008, The cold-active Lip1 lipase from the antarctic bacterium *Pseudoalteromonas haloplanktis TAC125* is a member of a new bacterial lipolytic enzyme family., *Extremophiles*, Vol. 12, p311-323

Derewenda, U., Brzozowski, A. M., Lawson, D. M. and Derewenda Z.S.,(1992) Catalysis at the interface: the anatomy of a conformational change in a triglyceride lipase. *Biochemistry*, 5: 1532-1541

Dharmsthiti S, Kuhasuntisuk B, 1998, Lipase from *Pseudomonas aeruginosa* LP602: biochemical properties and application for wastewater treatment., *J Industr Microbiol Biotechnol*, Vol. 21, p75-80

Dherbécourt J, Falentin H, Jardin J, Maillard MB, Baglinière F, Barloy-Hubler F, Thierry A., 2010, Identification of a secreted lipolytic esterase in *Propionibacterium freudenreichii*, a ripening process bacterium involved in Emmental cheese lipolysis., *Appl Environ Microbiol.*, Vol. 76, no. 4, p1181-1188

Di Lorenzo M, Hidalgo A, Molina R, Hermoso JA, Pirozzi D, Bornscheuer UT, 2007, Enhancement of the stability of a prolipase from *Rhizopus oryzae* toward aldehydes by saturation mutagenesis. *Appl Environ Microbiol*, Vol. 73, p7291-7299.

Dordick, J. S., 1989, Enzymatic catalysis in monophasic organic solvents, *Enzyme and Microbial Technology*, Vol. 4,p 192-211

Drabløs F, Petersen SB., 1997, Identification of conserved residues in family of esterase and lipase sequences., *Methods Enzymology*, Vol. 284, p28-61

- Dupres V, Verbelen C, Dufrêne YF, 2007, Probing molecular recognition sites on biosurfaces using AFM., *Biomaterials*, Vol. 28, no. 15, p2393-2402
- Ebner A, Kienberger F, Kada G, Strohm CM, Geretschlager M, Kamruzzahan AS, Wildling L, Johnson WT, Ashcroft B, Nelson J, Lindsay SM, Gruber HJ, Hinterdorfer P, 2005, Localization of single avidin-biotin interactions using simultaneous topography and molecular recognition imaging., *Chemphyschem*, Vol. 6, no. 5, p897-900
- Elboutahiri N, Thami-Alami I, Udupa SM., 2010, Phenotypic and genetic diversity in *Sinorhizobium meliloti* and *S. medicae* from drought and salt affected regions of Morocco., *BMC Microbiol*, Vol. 10, no. 15.
- Emond S, Montanier C, Nicaud JM, Marty A, Monsan P, André I, Remaud-Siméon M., 2010, New efficient recombinant expression system to engineer *Candida antarctica* lipase B., *Appl Environ Microbiol*, Vol. 76, no. 8, p2684-2687
- Fee CJ, 2003, Size-exclusion reaction chromatography (SERC): a new technique for protein PEGylation., *Biotechnol Bioeng*, Vol. 82, no. 2, p200-206
- Fernandes MLM, Krieger N, Baron AM, Zamora PP, Ramos LP, Mitchell DA, 2004, Hydrolysis and synthesis reactions catalysed by *Thermomyces lanuginosa* lipase in the AOT/Isooctane reversed micellar system. *J. of Molecular Catalysis B: Enzymatic*, Vol. 30, no. 1, p43-49
- Fischer M, Thai QK, Grieb M, Pleiss J., 2006, DWARF--a data warehouse system for analyzing protein families., *BMC Bioinformatics*, Vol. 7, no. 495
- Fojan P, Jonson PH, Petersen MT, Petersen SB., 2000, What distinguishes an esterase from a lipase: a novel structural approach., *Biochimie*, Vol. 82, no. 11, p1033-1041
- Fu J, Leiros HK, de Pascale D, Johnson KA, Blencke HM, Landfald B., 2012, Functional and structural studies of a novel cold-adapted esterase from an Arctic intertidal metagenomic library., *Appl Microbiol Biotechnol*, DOI 10.1007/s00253-012-4276-9
- Fujii R, Kitaoka M, Hayashi K., 2004, One-step random mutagenesis by error-prone rolling circle amplification., *Nucleic Acid Res.*, Vol 32, no. 19, e145
- Fujii R, Kitaoka M, Hayashi K., 2006, Error-prone rolling circle amplification: the simplest random mutagenesis protocol., *Nat Protoc*, Vol. 1, no.5, p2493-2497
- Gahlin R Jacobson S, 1998, Novel method to map and quantify wear on a micro-scale, *Wear*, Vol. 222, no. 2, p93-102

Gershenson A, Schauerte JA, Giver L, Arnold FH., 2010, Tryptophan phosphorescence study of enzyme flexibility and unfolding in laboratory-evolved thermostable esterases., *Biochemistry*, Vol. 39, no. 16, p4658-4665

Ghosh S, Rousseau D, 2011, Fat crystals and water-in-oil emulsion stability, *Current Opinion in Colloid and Interface Science*, Vol. 16, no.5, p421-431

Godinho LF, Reis CR, Tepper PG, Poelarends GJ, Quax WJ., 2011, Discovery of an Escherichia coli esterase with high activity and enantioselectivity toward 1,2-O-isopropylidenglycerol esters., *Appl Environ Microbiol.*, Vo. 77, no.17, p6094-6099

Goetz F, Verheij HM, Rosenstein R, 1998, Staphylococcal lipases: molecular characterisation, secretion, and processing. *Chem Phys Lipids* Vol. 93, p15-25

Grandbois M, Clausen-Schaumann H, Gaub H., 1998, Atomic force microscope imaging of phospholipid bilayer degradation by phospholipase A₂., *Biophys J*, Vol. 74, no. 5, p2398-2404

Graziano G, Merlino A, 2014, Molecular bases of protein halotolerance., *Biochim Biophys Acta*, Vol. 1844, no. 4, p850-858

Gu, J., Ruppen, M.E., Cai, P., 2005, Lipase-catalyzed regioselective esterification of rapamycin: Synthesis of temsirolimus (CCI-779), *Organic Letters*, Vol. 7, no. 18, p3945-3948

Guglielmetti, S., Noni, I. D., Caracciolo, F., Molinari, F., Parini, C. and Mora, D. (2007) Bacterial Cinnamoyl Esterase Activity Screening for the Production of a Novel Functional Food Product. *Appl Environ Microbiol.* Vol. 74, no.4, p1284-1288

Guo F, Xu H, Xu H, Yu H., 2013, Compensation of the enantioselectivity-activity trade-off in the directed evolution of an esterase from Rhodobacter sphaeroides by site-directed saturation mutagenesis., *Appl Microbiol Biotechnol*, Vol. 97, no. 8, p3355-3362

Güler Z, 2007, Changes in salted yoghurt during storage, *International Journal of Food Science & Technology*, Vol. 42, no. 2, p235-245

Hamilton S, Odili J, Pacifico MD, Wilson GD, Kupsch JM, 2003, Effect of imidazole on the solubility of a his-tagged antibody fragment., *Hybrid Hybridomics*, Vol. 22, no. 6, p347-355

Hasan F, Shah A A, Hameed A, 2006, Industrial applications of microbial lipases, *Enzyme and Microbial Technology*, Vol. 39, no. 2, p235-251

Hausmann S, Jaeger KE, 2010, Lipolytic enzymes from bacteria. *Handbook of Hydrocarbon and Lipid Microbiology*, Vol. 2 (TimmisKN, ed), p1099-1126. Springer, Berlin

Hemilä H, Koivula TT, Palva I., 1994, Hormone-sensitive lipase is closely related to several bacterial proteins, and distantly related to acetylcholinesterase and lipoprotein lipase: identification of a superfamily of esterases and lipases., *Biochem Biophys Acta*, Vol. 1210, no. 2, p249-253

Hinterdorfer P, Baumgartner W, Gruber HJ, Schilcher K, Schindler H., 1996, Detection and localization of individual antibody-antigen recognition events by atomic force microscopy., *Proc Natl Acad Sci USA*, Vol. 93, no. 8, p3477-3481

Hinterdorfer P, Dufrêne YF., 2006, Detection and localization of single molecular recognition events using atomic force microscopy. *Nat Methods*, Vol. 3, no. 5, p347-355

Homapour M, Hamed M, Moslehishad M, Safafar H., 2014, Physical and chemical properties of olive oil extracted from olive cultivars grown in Shiraz and Kazeroon., *Iranian Journal of Nutrition Sciences & Food Technology*, Vol. 9, no. 1, p121-130

Hunt JA, Ahmed M, Fierke CA., 1999, Metal binding specificity in carbonic anhydrase is influenced by conserved hydrophobic core residues., *Biochemistry*, Vol. 38, no. 28, p9054-9062

Horsman GP, Liu AM, Henke E, Bornscheuer UT, Kazlauskas RJ., 2003, Mutations in distant residues moderately increase the enantioselectivity of *Pseudomonas fluorescens* esterase towards methyl 3-bromo-2-methylpropanoate and ethyl 3-phenylbutyrate., *Chemistry*, Vol. 9, no. 9, p1933-1939

Howieson JG, Robson AD, Abbott LK, 1992, Calcium modifies pH effects on the growth of acid-tolerant and acid-sensitive *Rhizobium meliloti*, *Australian Journal of Agricultural Research*, Vol. 43, no. 3, p765-772

Huovinen T, Julin M, Sanmark H, Lamminmäki U., 2011, Enhanced error-prone RCA mutagenesis by concatemer resolution., *Plasmid*, Vol. 66, no. 1, p47-51

Höst G, Mårtensson LG, Jonsson BH., 2006, Redesign of human carbonic anhydrase II for increased esterase activity and specificity towards esters with long acyl chains., *Biochem Biophys Acta.*, Vol. 1764, no. 10, p1601-1606

Imandoust SB, Gadam SN., 2007, Are people willing to pay for river water quality, contingent valuation., *Int. J. of Environ. Sci. and Tech.*, Vol. 4, no. 2, p401-408

Jaeger KE, Dijkstra BW, Reetz MT., 1999, Bacterial biocatalysts: molecular biology, three-dimensional structures, and biotechnological applications of lipases., *Annu Rev Microbiol*, Vol 53, no 315-351

Jahangir R, McCloskey CB, Mc Clung WG, Labow RS, Brash JL, Santerre JP., 2003, The influence of protein adsorption and surface modifying macromolecules on the hydrolytic degradation of a poly(ether-urethane) by cholesterol esterase., *Biomaterials*, Vol. 24, no. 1, p121-130

Jenkins J, Mayans O, Smith D, Worboys K, Pickersgill RW., 2001, Three-dimensional structure of *Erwinia chrysanthemi* pectin methylesterase reveals a novel esterase active site., *J Mol Biol*, Vol. 305, no. 4, p951-960

Jia R, Hu Y, Liu L, Jiang L, Huang H., 2013, Chemical modification for improving activity and stability of lipase B from *Candida antarctica* with imidazolium-functional ionic liquids., *Org Biomol Chem*, Vol. 11 no. 41, p7192-7198

Jochens H, Aerts D, Bornscheuer UT., 2010, Thermostabilisation of an esterase by alignment-guided focussed directed evolution., *Protein Eng Des Sel*, Vol. 23, no. 12, p903-909

Johnston KJ, Ashford AE, 1980, A simultaneous-coupling azo dye method for the quantitative assay of esterase using alpha-naphthyl acetate as substrate., *Histochem J.*, Vol. 12, no.2, p221-234

Juhl PB, Trodler P, Tyagi S, Pleiss J., 2009, Modelling substrate specificity and enantioselectivity for lipases and esterases by substrate-imprinted docking., *BMC Struct Biol*, vol. 9, no. 39

Jung HC, Kwon SJ, Pan JG., 2006, Display of a thermostable lipase on the surface of a solvent-resistant bacterium, *Pseudomonas putida* GM730, and its applications in whole-cell biocatalysis., *BMC Biotechnol.*, Vol. 6, no. 23

Jung HJ, Kim SK, Min WK, Lee SS, Park K, Park YC, Seo JH., 2011, Polycationic amino acid tags enhance soluble expression of *Candida antarctica*

lipase B in recombinant *Escherichia coli.*, *Bioprocess Biosyst Eng*, Vol. 34, no. 7, p833-839

Kaledin A S, Sliusarenko AG, Gorodetskii S I, 1980, Isolation and properties of DNA polymerase from extreme thermophilic bacteria *Thermus aquaticus* YT-1 *Biokhimiya* Vol. 45, p644-651

Kamruzzahan AS, Ebner A, Wildling L, Kienberger F, Riener CK, Hahn CD, Pollheimer PD, Winklehner P, Hölzl M, Lackner B, Schörkl DM, Hinterdorfer P, Gruber HJ., 2006, Antibody linking to atomic force microscope tips via disulphide bond formation., *Bioconjug Chem.*, Vol. 16, no. 6, p1473-1481

Kasas S, Thomson NH, Smith BL, Hansma HG, Zhu X, Guthold M, Bustamante C, Kool ET, Kashlev M, Hansma PK., 1997, *Escherichia coli* RNA polymerase activity observed using atomic force microscopy., *Biochemistry*, Vol. 36, no. 3, p461-468

Kempf M, Göken M, Vehoff H, 1998, Nanohardness measurements for studying local mechanical properties of metals, *Applied Physics A*, Vol. 66, no. 1, pS843 -S846

Kilcawley K N, Wilkinson M G, Fox P F, 1998, Enzyme-modified cheese, *Int. Dairy Journ.* Vol. 8, no. 1, p1-10

Kim GJ, Choi GS, Kim JY, Lee JB, Jo DH, Ryu YW (2002) Screening, production and properties of a stereo specific esterase from pseudomonas species-34 with high selectivity to (S)-ketoprofen ethyl ester. *J Mol Catal B*, Vol. 17, p29-38

Kim E, Oh K, Lee M, Kang C, Oh T, Yoon J, 2009, Novel cold-adapted alkaline lipase from an intertidal flat metagenome and proposal for a new family of bacterial lipases. *Appl Environ Microb* Vol. 75, p257-260

Kohalmi SE, Kunz BA., 1988, Role of neighbouring bases and assessment of strand specificity in ethylmethanesulphonate and N-methyl-N'-nitro-N-nitrosoguanidine mutagenesis in the SUP4-o gene of *Saccharomyces cerevisiae.*, Vol. 204, no. 3, p561-568

Koyanagi T, Yoshida E, Minami H, Katayama T, Kumagai H., 2008, A rapid, simple, and effective method of constructing a randomly mutagenised plasmid library free from ligation., *Biosci Biotechnol Biochem*, Vol. 72, no. 4, p1134-1137

Kubetzko S, Sarkar CA, Plückthun A., 2005, Protein PEGylation decreases observed target association rates via a dual blocking mechanism., *Mol Pharmacol*, Vol. 68, no. 5, p1439-1454.

- Kumar D, Kumar L, Nagar S, Raina C, Parshad R, Gupta V K., 2012, Screening, isolation and production of lipase/esterase producing *Bacillus* sp. strain DVL2 and its potential evaluation in esterification and resolution reactions., *Archives of Applied Science Research*, Vol. 4, no. 4, p1763-1770
- Kunstelj M, Fidler K, Skrajnar S, Kenig M, Smilović V, Kusterle M, Caserman S, Zore I, Porekar VG, Jevševar S., 2013, Cysteine-specific PEGylation of rhG-CSF via selenylsulphide bond., *Bioconjug Chem*, Vol. 24, no. 6, p889-896
- Kunz BA, Pierce MK, Mis JR, Giroux CN., 1987, DNA sequence analysis of the mutational specificity of u.v. light in the SUP4-o gene of yeast., *Mutagenesis*, Vol. 2, no. 6, p445-453
- Kynclova E, Hartig A, Schalkhammer T., 1995, Oligonucleotide labelled lipase as a new sensitive hybridization probe and its use in bio-assays and biosensors., *J Mol Recognit*, Vol. 8, no. 1-2, p139-145
- Lanser AC, Manthey LK, Hou CT., 2001, Regioselectivity of new bacterial lipases determined by hydrolysis of triolein., *Curr. Microbiol.*, Vol. 44, no. 5, p336-340
- Larsen MW, Bornscheuer UT, Hult K., 2008, Expression of *Candida antarctica* lipase B in *Pichia pastoris* and various *Escherichia coli* systems., *Protein Expr Purif*, Vol. 62, no. 1, p90-97
- Lebbink JH, Kaper T, Bron P, van der Oost J, de Vos WM., 2000, Improving Low-Temperature Catalysis in the Hyperthermostable *Pyrococcus furiosus* β -Glucosidase CelB by Directed Evolution., *Biochemistry*, Vol. 39, no. 13, p3656-3665
- Lee GS, Savage EA, Ritzel RG, von Borstel RC., 1988, The base-alteration spectrum of spontaneous and ultraviolet radiation-induced forward mutations in the URA3 locus of *Saccharomyces cerevisiae*., *Mol Gen Genet*, Vol. 214, no. 3, p396-404
- Lee, G U, Kidwell D A, Colton R J., 1994, Sensing discrete streptavidin-biotin interaction with the atomic force microscope., *Langmuir*, Vol. 10 p354-357
- Lee MH, Lee CH, Oh TK, Song JK, Yoon JH, 2006, Isolation and characterization of a novel lipase from a metagenomic library of tidal flat sediments: evidence for a new family of bacterial lipases., *Appl Environ Microbiol*, Vol. 72, no. 11, p7406-7409

- Lee WH, Wheatley W, Benedict WF, Huang CM, Lee EY., 1986, Purification, biochemical characterization, and biological function of human esterase D., *Proc Natl Acad Sci U S A*, Vol. 83, no. 18, p6790-6794
- Lefkowitz, L. J., Kupina, J. M., Hirth, N. L., Henry, R. M., Noland, G. Y., Barbee, J. Y. Jr., Zhou, J. Y. and Weese, C. B., 2007, Intraindividual stability of human erythrocyte cholinesterase activity. *Clin. Chem.* Vol.53, no.7, p1358-1363
- Leonov S L, 2010, Screening for novel cold-active lipases from wild-type bacterial isolates, *Inn. Romanian Food Biotechnol*, Vol. 6, p12-17
- Lesniak J, Barton WA, Nikolov DB., 2003, Structural and functional features of the Escherichia coli hydroperoxide resistance protein OsmC., *Protein Sci*, Vol. 12, no. 12, p2838-2843
- Lin J, Iyer M, 2007, Cold or hot wash: Technological choices, cultural change, and their impact on clothes-washing energy use in China, *Energy Policy*, Vol. 35, no. 5, p3046-3052
- Liu D, Schmid RD, Rusnak M., 2006, Functional expression of Candida antarctica lipase B in the Escherichia coli cytoplasm—a screening system for a frequently used biocatalyst, *Appl Microbiol Biotechnol*, Vol. 72, no. 5, p1024-1032
- Lu M, Wang S, Fang Y, Li H, Liu S, Liu H., 2010, Cloning, expression, purification, and characterization of cold-adapted α -amylase from *Pseudoalteromonas arctica* GS230., *Protein J.*, Vol. 29, no. 8, p591-697
- Luo Y, Zheng Y, Jiang Z, Ma Y, Wei D, 2006, A novel psychrophilic lipase from *Pseudomonas fluorescens* with unique property in chiral resolution and biodiesel production via transesterification., *Appl Microbiol and Biotechnol*, Vol. 73, no. 2, p349-355
- Ma J, Wu L, Guo F, Gu J, Tang X, Jiang L, Liu J, Zhou J, Yu H., 2012, Enhanced enantioselectivity of a carboxyl esterase from *Rhodobacter sphaeroides* by directed evolution., *Appl Microbiol Biotechnol*, Vol. 97, no. 11, p4897-4906
- Manco G, Giosuè E, D'Auria S, Herman P, Carrea G, Rossi M., 2000, Cloning, overexpression, and properties of a new thermophilic and thermostable esterase with sequence similarity to hormone-sensitive lipase subfamily from the archaeon *Archaeoglobus fulgidus*., *Arch Biochem Biophys*, Vol. 373, no. 1, p182-192

Mandrich L, Menchise V, Alterio V, De Simone G, Pedone C, Rossi M, Manco G., 2008, Functional and structural features of the oxyanion hole in a thermophilic esterase from *Alicyclobacillus acidocaldarius*., *Proteins*, Vol. 71, no. 4, p1721-1731

Mandrich L, Manco G, 2009, Evolution in the amidohydrolase superfamily: substrate-assisted gain of function in the E183K mutant of a phosphotriesterase-like metal-carboxylesterase., *Biochemistry*, Vol. 48, no. 24, p5602-5612

Martínez-Cuesta M C, de Palencia P F, Requena T, Peláez C, 2001, Enzymatic ability of *Lactobacillus casei* subsp. *casei* IFPL731 for flavour development in cheese., *Int. Dairy Journ*, Vol. 11, p577-585

Matsumae H, Furui M, Shibatani T, 1993, Lipase-catalyzed asymmetric hydrolysis of 3-phenylglycidic acid ester, the key intermediate in the synthesis of diltiazem hydrochloride, *Journal of Fermentation and Bioengineering*, Vol. 75, no. 2, p93-98

Matzke J, Schwermann B, Bakker EP., 1997, Acidostable and acidophilic proteins: the example of the alpha-amylase from *Alicyclobacillus acidocaldarius*., *Comp Biochem Physiol A Physiol*, Vol. 118, no. 3, p475-479

Menda N, Semel Y, Peled D, Eshed Y, Zamir D., 2004, *In silico* screening of a saturated mutation library of tomato., *Plant J.*, Vol. 38, no. 5, p861-872

Misawa E, Chan Kwo Chion CK, Archer IV, Woodland MP, Zhou NY, Carter SF, Widdowson DA, Leak DJ., 1998, Characterisation of a catabolic epoxide hydrolase from a *Corynebacterium* sp. *Eur J Biochem*, Vol. 253, no. 1, p173-183

Miyazaki K, Takenouchi M, 2002, Creating random mutagenesis libraries using megaprimer PCR of whole plasmid, *Biotechniques*, Vol. 33, no. 5, 1033-1034, 1036-1038

Miyazaki K, 2003, Creating random mutagenesis libraries by megaprimer PCR of whole plasmid (MEGAWHOP)., *Methods in Mol. Biol.*, Vol. 231, p23-28

Mogensen JE, Sehgal P, Otzen DE., 2005, Activation, inhibition, and destabilisation of *Thermomyces lanuginosus* lipase by detergents., *Biochemistry*, Vol. 44, no. 5, p1719-1730

Molgaard A, Kauppinen S, Larsen S, 2000, Rhamnogalacturonan acetyl esterase elucidates the structure and function of a new family of hydrolases, *Structure*, Vol. 8, p373-383

Moore JC, Arnold FH., 1996, Directed evolution of a para-nitrobenzyl esterase for aqueous-organic solvents., *Nat Biotech*, Vol. 14, no. 4, p458-467

Morita Y, Nakamura T, Hasan Q, Murakami Y, Yokoyama K, and Tamiya E, (1997) Cold-active enzymes from cold-adapted bacteria. *J Am Oil Chem Soc* 74 p441-444

Mourey A, Kilbertus G., 1975, Simple media containing stabilised tributyrin for demonstrating lipolytic bacteria in foods and soils., *J Appl Bacteriol*, Vol. 40, no. 1, p47-51

Moy VT, Florin EL, Gaub HE., 1994, Intermolecular forces and energies between ligands and receptors., *Science*, Vol. 266, no. 5183, p257-259

Mrabet M, Zribi K, Mhadhbi H, Djéballi N, Mhamdi R, Aouani M E, Nakamura K., 2011, Salt tolerance of a *Sinorhizobium meliloti* strain isolated from dry lands: growth capacity and protein profile changes., *Ann Microbiol*, Vol. 61, p361-369

Mullis K, Faloona F, Scharf S, Saiki R, Horn G, Erlich H., 1986, Specific enzymatic amplification of DNA *in vitro*: the polymerase chain reaction., *Cold Spring Harb Symp Quant Biol.*, Vol. 51, no. 1, p263-273

Munoz A, Katerndahl D A, 2000, Diagnosis and management of acute pancreatitis, *Am Fam Physician* Vol. 62, p164-174

Musidlowska-Persson A, Bornscheuer U T, 2003, Site directed mutagenesis of recombinant pig liver esterase yields mutants with altered enantioselectivity., *Tetrahedron: Asymmetry*, Vol. 14, no. 10, p1341-1344

Muthukumar N, Dhar S C, 1982, Comparative studies on the degreasing of skins using acid lipase and solvent with reference to the quality of finished leathers, *Leather Sci*, Vol. 29, p417-424

Müller-Hill B, Crapo L, Gilbert W., 1968, Mutants that make more lac repressor., *Proc Natl Acad Sci USA*, Vol. 59, no. 4, p1259-1264

Nacke H, Will C, Herzog S, Nowka B, Engelhaupt M, Daniel R., 2011, Identification of novel lipolytic genes and gene families by screening of metagenomic libraries derived from soil samples of the German Biodiversity Exploratories. *FEMS Microbiol Ecol*, Vol. 78, no. 1, p188-201

Najbauer J, Orpiszewski J, Aswad DW., 1996, Molecular aging of tubulin: accumulation of isoaspartyl sites *in vitro* and *in vivo*., *Biochemistry*, Vol. 35, no. 16, p5183-5190

Nakazawa H, Okada K, Onodera T, Ogasawara W, Okada H, Morikawa Y., 2009, Directed evolution of endoglucanase III (Cel12A) from *Trichoderma reesei*., *Appl Microbiol Biotechnol*, Vol. 83, no. 4, p649-657

Nallamsetty S, Waugh DS., 2006, Solubility-enhancing proteins MBP and NusA play a passive role in the folding of their fusion partners., *Protein Expr Purif*, Vol. 45, no. 1, p175-182

Neves Petersen MT, Fojan P, Petersen SB., 2001, How do lipases and esterases work: the electrostatic contribution., *J Biotechnol* Vol. 85, no. 2, p115-147

Niazi JH, Prasad DT, Karegoudar TB., 2001, Initial degradation of dimethylphthalate by esterases from *Bacillus* species., *FEMS Microbiol. Lett.*, Vol. 196, no. 2, p201-205

Nidumolu R, Prahalad CK, & Rangaswami MR., 2009, Why sustainability is now the key driver of innovation. *Harvard Business Review*, Vol. 87, no. 9, p56-64

Noinville S, Revault M, Baron MH, Tiss A, Yapoudjian S, Ivanova M, Verger R., 2002, Conformational changes and orientation of *Humicola lanuginosa* lipase on a solid hydrophobic surface: an in situ interface Fourier transform infrared-attenuated total reflection study., *Biophys J*, Vol. 82, no. 5, p2709-2719

Novototskaya-Vlasova K, Petrovskaya L, Yakimov S, Gilichinsky D., 2011, Cloning, purification, and characterization of a cold-adapted esterase produced by *Psychrobacter cryohalolentis* K5T from Siberian cryopeg., *FEMS Microbiol Ecol.*, Vol 82, no. 2, p367-375

Noy A, Vezenov DV, Kayyem JF, Meade TJ, Lieber CM., 1997, Stretching and breaking duplex DNA by chemical force microscopy., *Chem Biol*, Vol. 4, no. 7, p519-527

Oei HH, van der Meer IM, Hofman A, Koudstaal PJ, Stijnen T, Breteler MM, Witteman JC., 2005, Lipoprotein-associated phospholipase A2 activity is associated with risk of coronary heart disease and ischemic stroke: the Rotterdam Study., *Circulation*, Vol. 111, no. 5, p570-575

Olukoshi ER, Packter NM, 1994, Importance of stored triacylglycerols in *Streptomyces*: possible carbon source for antibiotics., *Microbiology*, Vol. 140, no. 4, p931-943

Ollis DL, Cheah E, Cygler M, Dijkstra B, Frolov F, Franken SM, Harel M, Remington SJ, Silman I, Schrag J, Sussman J L, Verschueren K H G, Goldman A, 1992, The α/β hydrolase fold, *Protein Eng*, Vol. 5, no. 3, p197-211

Pajunen MI, Pulliainen AT, Finne J, Savilahti H., 2005, Generation of transposon insertion mutant libraries for Gram-positive bacteria by

electroporation of phage Mu DNA transposition complexes., *Microbiology*, Vol 151, part 4, p1209-1218

Pakula C, Stamminger R., 2010, Electricity and water consumption for laundry washing by washing machine worldwide, *Energy Efficiency*, Vol. 3, no. 4, p365-382

Palmeira DJ, Abreu JC, Andrade LH., 2011, Lipase-catalyzed kinetic resolution of aryltrimethylsilyl chiral alcohols., *Molecules*, Vol. 16, no. 11, p9697-9713

Pauling L, 1946, Molecular architecture and biological reactions., *Chem Engineering News*, Vol. 24, p1375-1377

Pesaresi A, Devescovi G, Lamba D, Venturi V, Degrassi G., 2005, Isolation, characterization, and heterologous expression of a carboxylesterase of *Pseudomonas aeruginosa* PAO1., *Curr Microbiol*, Vol. 50, no. 2, p102-109

Pesaresi A, Lamba D., 2005, Crystallization, X-ray diffraction analysis and phasing of carboxylesterase PA3859 from *Pseudomonas aeruginosa*., *Biochim Biophys Acta*, Vol. 1752, no. 2, p197-201

Pesaresi A, Lamba D., 2010, Insights into the fatty acid chain length specificity of the carboxylesterase PA3859 from *Pseudomonas aeruginosa*: A combined structural, biochemical and computational study., *Biochimie*, Vol. 92, no. 12, p1787-1792

Petersen B, Petersen TN, Andersen P, Nielsen M, Lundegaard C., 2009, A generic method for assignment of reliability scores applied to solvent accessibility predictions., *BMC Struct Biol*, Vol. 9, no. 51

Petkewich R, 2005, Cold-water laundry detergent is a hot idea., *Environmental Science and Technology A-Page*, 39, 478A

Pleiss, J., Fischer, M., Schmid, R. D., 1998, Anatomy of lipase binding sites: the scissile fatty acid binding site. *Chemistry and Physics of Lipids*, 93: 67-80

Pleiss, J, Fischer M, Peiker M, Thiele C, Schmid R D, 2000, Lipase engineering database: Understanding and exploiting sequence-structure-function relationships, *J of Mol Cat B*, Vol. 10, no. 5, p491-508

Porollo, A, Adamczak, R, Meller J, (2004) POLYVIEW: A Flexible Visualization Tool for Structural and Functional Annotations of Proteins, *Bioinformatics*, Vol. 20, p2460-2462.

Pulido MA, Koga Y, Takano K, Kanaya S., 2007, Directed evolution of Tk-subtilisin from a hyperthermophilic archaeon: identification of a single amino acid substitution responsible for low-temperature adaptation., *Protein Eng Des Sel*, Vol. 20, no. 3, p143-153

Radmacher M, Fritz M, Hansma HG, Hansma PK., 1994, Direct observation of enzyme activity with the atomic force microscope., *Science*, Vol. 265, no. 5178, p1577-1579

Rao L, Zhao X, Pan F, Li Y, Xue Y, Ma Y, Lu JR., 2009, Solution behavior and activity of a halophilic esterase under high salt concentration. *PLoS One*, Vol. 4, no. 9, p1-10

Record, E., Asther, M., Sigiollot, C., Pages, S., Punt, P. J., Delattre, M., Haon, M., van der Hondel, C. A. M. J. J., Sigiollot, J.-C., Lesage-Meessen, L. Asther M, 2003, Overproduction of the *Aspergillus niger* feruloyl esterase for pulp bleaching application. *Acta Biochim Biophys Sin (Shanghai)*, Vol. 39, no. 11, p811-828

Reichardt, W. (1987) Differential temperature effects on the efficiency of carbon pathways in Antarctic marine benthos. *Mar Ecol Prog Ser*, Vol. 40, p127-135.

Rief M, Gautel M, Oesterhelt F, Fernandez JM, Gaub HE., 1997, Reversible unfolding of individual titin immunoglobulin domains by AFM., *Science*, Vol. 276, no. 5315, p1109-1112

Reis P, Holmberg K, Miller R, Krägel J, Grigoriev DO, Leser ME, Watzke HJ., 2008, Competition between lipases and monoglycerides at interfaces., *Langmuir*, Vol. 24, no. 14, p7400-7407

Reis P M, Raab T W, Chuat J Y, Leser M E, Miller R, Watzke H J, Holmberg K, 2008, Influence of Surfactants on Lipase Fat Digestion in a Model Gastro-intestinal System., *Food Biophys*, Vol. 3, no. 4, p370-381

Reis, P., Holmberg, K., Watzke, H., Leser, M. E. and Miller, R., 2009, Lipases at interfaces: a review. *Adv Colloid Interface Sci.*, 147-148: 237-250

Reyes-Duarte D, Polaina J, López-Cortés N, Alcalde M, Plou FJ, Elborough K, Ballesteros A, Timmis KN, Golyshin PN, Ferrer M., 2005, Conversion of a carboxylesterase into a triacylglycerol lipase by a random mutation., *Angew Chem Int Ed Engl*, Vol. 44, no. 46, p7553-7557

Rinaudi L, Fujishige NA, Hirsch AM, Banchio E, Zorreguieta A, Giordano W., 2006, Effects of nutritional and environmental conditions on *Sinorhizobium meliloti* biofilm formation, *Res Microbiol*, Vol. 157, no.9, p867-875

Robb FT, Clark DS, 1999, Adaptation of proteins from hyperthermophiles to high pressure and high temperature., *J Mol Microbiol Biotechnol*, Vol. 1, no. 1, p101-105

Robertson DL, Hilton S, Wong KR, Koepke A, Buckley JT., 1994, Influence of active site and tyrosine modification on the secretion and activity of the *Aeromonas hydrophila* lipase/acyltransferase., *J Biol Chem*, Vol. 269, no. 3, p2146-2150

Rogalska, E., Cudrey, C., Ferrato, F. Verger, R, 1993, Stereoselective hydrolysis of triglycerides by animal and microbial lipases. *Chirality*, 5: 24-30.

Rosenstein R, Goetz F, 2000, Staphylococcal lipases: biochemical and molecular characterization. *Biochimie* Vol. 82 p1005-1014.

Rutkowska J, Adamska A, 2011, Fatty Acid Composition of Butter Originated from North-Eastern Region of Poland, *Polish Journal of Food and Nutrition Sciences*, Vol. 61, no. 3, p187-193

Sack RB, Siddique AK, Longini IM Jr, Nizam A, Yunus M, Islam MS, Morris JG Jr, Ali A, Huq A, Nair GB, Qadri F, Faruque SM, Sack DA, Colwell RR., 2003, A 4-year study of the epidemiology of *Vibrio cholerae* in four rural areas of Bangladesh., *J Infect Dis*, Vol. 187, no.1, p96-101

Salameh M, Wiegel J., 2007, Lipases from extremophiles and potential for industrial applications., *Adv Appl Microbiol*, Vol. 61, p253-283

San Sebastián M, Armstrong B, Córdoba JA, Stephens C., 2001, Exposures and cancer incidence near oil fields in the Amazon basin of Ecuador, *Occup. Environ. Med.*, Vol. 58, no. 8, p517-522

Sana B, Ghosh D, Saha M, Mukherjee J., 2007, Purification and characterization of an extremely dimethylsulfoxide tolerant esterase from a salt-tolerant *Bacillus* species isolated from the marine environment of the Sundarbans, *Process Biochemistry*, Vol. 42, no. 12, p1571-1578

Scheuermann R, Tam S, Burgers PM, Lu C, Echols H., 1983, Identification of the epsilon-subunit of *Escherichia coli* DNA polymerase III holoenzyme as the dnaQ gene product: a fidelity subunit for DNA replication., *Proc Natl Acad Sci USA*, Vol. 80, no. 23, p7085-7089.

- Schiraldi C, Giuliano M, De Rosa M., 2002, Perspectives on biotechnological applications of archaea., *Archaea*, Vol. 1, no. 2, p75-86
- Schrag JD, Cygler M., 1997, Lipases and alpha/beta hydrolase fold., *Methods Enzymology*, Vol. 284, p85-107
- Schulze H, Schmid RD, Bachmann TT., 2002, Rapid detection of neurotoxic insecticides in food using disposable acetylcholinesterase-biosensors and simple solvent extraction., *Anal Bioanal Chem*, Vol. 372, no. 2, p268-272
- Seo HS, Kim SE, Han KY, Park JS, Kim YH, Sim SJ, Lee J., 2009, Functional fusion mutant of *Candida antarctica* lipase B (CalB) expressed in *Escherichia coli*., *Biochim Biophys Acta*, Vol. 1794, no. 3, p519-525
- Shan, Y, Wang, G, Zhou, H X, 2001, Fold recognition and accurate query-template alignment by a combination of PSI-BLAST and threading. *Proteins* Vol. 42, p23-37
- Shaunak S, Godwin A, Choi JW, Balan S, Pedone E, Vijayarangam D, Heidelberger S, Teo I, Zloh M, Brocchini S., 2006, Site-specific PEGylation of native disulphide bonds in therapeutic proteins., *Nat Chem Biol*, Vol. 2, no.6, p312-313
- Shaw JF, Chang RC, Chuang KH, Yen YT, Wang YJ, Wang FG., 1994, Nucleotide sequence of a novel arylesterase gene from *Vibrio mimicus* and characterization of the enzyme expressed in *Escherichia coli*., *Biochem J*, Vol. 298, part 3, p675-680
- Shen D, Xu J-H, Wu H-Y, L Y-Y., 2002, Significantly improved esterase activity of *Trichosporon brassicae* cells for ketoprofen resolution by 2-propanol treatment., *J Mol Catal.*, Vol. 18, no. 4-6, p219-224
- Shinohara M, Nakajima N, Uehara Y, 2007, Purification and characterization of a novel esterase (beta-hydroxypalmitate methyl ester hydrolase) and prevention of the expression of virulence by *Ralstonia solanacearum*, *J. Applied Microbiol*, Vo. 103, p152-162
- Silva C, Azoia NG, Martins M, Matamá T, Wu J, Cavaco-Paulo A., 2012, Molecular recognition of esterase plays a major role on the removal of fatty soils during detergency., *J Biotechnol*, Vol. 161, no. 3, p228-234
- Simister J, 2012, Time spent on paid and unpaid work: findings from 'Work, Attitudes and Spending' surveys, *WAS research paper* -01/1

Singh S, Chaubey A, Malhotra B D, 2004, Amperometric cholesterol biosensor based on immobilised cholesterol esterase and cholesterol oxidase on conducting polypyrrole films, *Analytica Chimica Acta*, Vol. 502, no. 2, p229-234

Slavica A, Dib I, Nidetzky B., 2007, Selective modification of surface-exposed thiol groups in *Trigonopsis variabilis* D-amino acid oxidase using poly(ethylene glycol) maleimide and its effect on activity and stability of the enzyme., *Biotechnol Bioeng*, Vol. 96, no. 1, p9-17

Sonesson AW, Callisen TH, Elofsson UM, Brismar H., 2007, Imaging the Detergency of Single Cotton Fibers with Confocal Microscopy: the Effect of Surfactants and Lipases., *Journal of Surfactants and Detergents*, Vol. 10, no.4, p211-218

Sriprapundh D, Vieille C, Zeikus JG., 2003, Directed evolution of *Thermotoga neapolitana* xylose isomerase: high activity on glucose at low temperature and low pH, *Protein Eng*, Vol. 16, no. 9, p683-690

Stroh CM, Ebner A, Geretschläger M, Freudenthaler G, Kienberger F, Kamruzzahan AS, Smith-Gill SJ, Gruber HJ, Hinterdorfer P., 2004, Simultaneous topography and recognition imaging using force microscopy., *Biophys*, Vol. 87, no. 3, p1981-1990

Sundararajan S, Bhushan B, 2001, Development of a continuous microscratch technique in an atomic force microscope and its application to study scratch resistance of ultrathin hard amorphous carbon coatings, *J Mater Res*, Vol. 16, no. 2, p437-445

Suzuki, T., Nakayama, T., Kurihara, T., Nishino, T., Esaki, N, 2002, Primary structure and catalytic properties of a cold-active esterase from a psychrotroph, *Acinetobacter* sp. strain No. 6. isolated from Siberian soil. *Biosci Biotechnol Biochem* 66: 1682-1690

Suzuki, T., Nakayama, T., Choo, D. W., Hirano, Y., Kurihara, T., Nishino, T. Esaki, N., 2003, Cloning, heterologous expression, renaturation, and characterization of a cold-adapted esterase with unique primary structure from a psychrotroph *Pseudomonas* sp. strain B11-1. *Protein Expr Purif* 30: 171-17

Tanaka, K., Yoshida, K., Sasaki, C., Osano, Y.T., 2002, Practical asymmetric synthesis of the herbicide (S)-indanofan via lipase-catalyzed kinetic resolution of a diol and stereoselective acid-catalyzed hydrolysis of a chiral epoxide, *J. of Org Chemistry*, Vol. 67, no. 9, p3131-3133

Taranta M, Bizzarri AR, Cannistraro S., 2008, Probing the interaction between p53 and the bacterial protein azurin by single molecule force spectroscopy., *J Mol Recognit*, Vol. 21, no. 1, p63-70

Thomas R L, Murtagh K, 2006, Characterization of Tannase Activity on Tea Extracts, *Journal of Food Science*, Vol. 50, no. 4, p1126-1129

Torres S, Baigori M D, Swathy S L, Pandry A, Castro G R, 2009, Enzymatic synthesis of banana flavour (isoamyl acetate) by *Bacillus licheniformis* S-86 esterase., *Food Research Intrntl*, Vol. 42, no. 4, p454-460

Tyagi S, Pleiss J, 2006, Biochemical profiling *in silico*—Predicting substrate specificities of large enzyme families, *J of Biotech*, Vol. 124, no. 1, p108-116

Uchino Y, Hirata A, Yokota A, Sugiyama J., 1998, Reclassification of marine *Agrobacterium* species: Proposals of *Stappia stellulata* gen. nov., comb. nov., *Stappia aggregata* sp. nov., nom. rev., *Ruegeria atlantica* gen. nov., comb. nov., *Ruegeria gelatinovora* comb. nov., *Ruegeria algicola* comb. nov., and *Ahrensia kieliense* gen. nov., sp. nov., nom. rev., *J Gen Appl Microbiol*, Vol. 44, no. 3, 201-210

Uno T, Itoh A, Miyamoto T, Kubo M, Kanamaru K, Yamagata H, Yasufuku Y, Imaishi H, 2012, Ferulic Acid Production in the Brewing of Rice Wine (Sake), *Journal of the Institute of Brewing*, Vol. 115, no. 2, p116-121

Uppenberg J, Hansen MT, Patkar S, Jones TA., 1994, The sequence, crystal structure determination and refinement of two crystal forms of lipase B from *Candida Antarctica*., *Structure*., Vol. 2, No. 4, p293-308

Upton C, Buckley JT., 1995, A new family of lipolytic enzymes?, *Trends Biochem Sci.*, Vol. 20, no. 5, p178-179

Varanasi A, Obendorf SK, Pedersen LS, Mejldal R., 2001, Lipid distribution on textiles in relation to washing with lipases., *Journal of Surfactants and Detergents*, Vol. 4, no.2, p135-146

Vath GM, Earhart CA, Monie DD, landolo JJ, Schlievert PM, Ohlendorf DH., 1999, The crystal structure of exfoliative toxin B: a superantigen with enzymatic activity., *Biochemistry*, Vol. 38, no. 32, p10239-10246

Vieille C, Zeikus GJ., 2001, Hyperthermophilic enzymes: sources, uses, and molecular mechanisms for thermostability., *Microbiol Mol Biol Rev*, Vol. 65, no. 1, p1-43

Verger R, Pattus F, Pieroni G, Riviere C, Ferrato F, Leonardi J, Dargent B., 1984, Regulation by the “Interfacial Quality” of some Biological Activities., *Colloids and Surfaces*, Vol. 10, p163-180

Verger R., 1998, Interfacial Activation of lipases: facts and artifacts., *Tibtech.*, Vol.15, p32-38

Verschueren KH, Seljée F, Rozeboom HJ, Kalk KH, Dijkstra BW., 1993, Crystallographic analysis of the catalytic mechanism of haloalkane dehalogenase., *Nature*, Vol. 363, no. 6431, p693-698

Vijayalakshmi A, Tarunashree Y, Baruwati B, Manorama SV, Narayana BL, Johnson RE, Rao NM, 2008, Enzyme field effect transistor (ENFET) for estimation of triglycerides using magnetic nanoparticles., *Biosens Bioelectron.*, Vol. 23, no. 11, p1708-1714

Vitecek J, Petrlova J, Adam V, Havel L, Kramer KJ, Babula P, Kizek R., 2007, A Fluorimetric Sensor for Detection of One Living Cell., *Sensors*, Vol. 7, p222-238

Vujaklija D, Schröder W, Abramić M, Zou P, Lescić I, Franke P, Pigac J., 2002, A novel streptomycete lipase: cloning, sequencing and high-level expression of the *Streptomyces rimosus* GDS(L)-lipase gene. *Arch Microbiol*, Vol. 178, no. 2, p124-130

Wagner UG, Petersen EI, Schwab H, Kratky C., 2002, EstB from *Burkholderia gladioli*: a novel esterase with a beta-lactamase fold reveals steric factors to discriminate between esterolytic and beta-lactam cleaving activity., *Protein Sci*, Vol. 11, no. 3, p467-478

Wang L, Evans J, Andrews HK, Beckstead RB, Thummel CS, Bashirullah A., 2008, A genetic screen identifies new regulators of steroid-triggered programmed cell death in *Drosophila*., *Genetics*, Vol. 180, no. 1, p269-281

Wei Y, Schottel JL, Derewenda U, Swenson L, Patkar S, Derewenda ZS., 1995, A novel variant of the catalytic triad in the *Streptomyces scabies* esterase. *Nat Structural Biol*, Vol. 2, no. 3, p218-223

Wildling L, Unterauer B, Zhu R, Rupprecht A, Haselgrübler T, Rankl C, Ebner A, Vater D, Pollheimer P, Pohl E E, Hinterdorfer P, Gruber H J., 2011, Linking of sensor molecules with amino groups to amino-functionalized AFM tips. *Bioconjug. Chem.*, Vol. 22, no. 6, p1239-1248

Winkler UK, Stuckmann M, 1979, Glycogen, hyaluronate, and some other polysaccharides greatly enhance the formation of exolipase by *Serratia marcescens*. *J. Bacteriol*, Vol. 138, p663-670

Wright A J, Fishwick M J, 1978, Lipid degradation during manufacture of black tea, *Phytochem* Vol. 18, p1511-1513

Ye L, Xu H, Yu H., 2013, Enhanced acylation activity of esterase BioH from *Escherichia coli* by directed evolution towards improved hydrolysis activity, *Biochem Engineer Jour*, Vol. 79, p182-186

Yilmaz G, Ayar A, Akin N, 2005, The effect of microbial lipase on the lipolysis during the ripening of Tulum cheese, *Journal of Food Engineering*, Vol. 69, no. 3, p269-274

Zandonella, G., Haalck, L., Spener, F., Faber, K., Paltauf, F., Hermetter, A., 1995, Inversion of Lipase Stereospecificity for Fluorogenic Alkyldiacyl Glycerols. *European Journal of Biochemistry*, Vol 231, p50-55

Zhang G, Gao R, Zheng L, Zhang A, Wang Y, Wang Q, Feng Y, Cao S, 2006, Study on the relationship between structure and enantioselectivity of a hyperthermophilic esterase from archaeon *Aeropyrum pernix* K1, *J of Mol Catalysis B: Enzymatic*, Vol. 38, no3-6, p148-153

Zhu K, Jutila A, Tuominen EK, Patkar SA, Svendsen A, Kinnunen PK., 2001, Impact of the tryptophan residues of *Humicola lanuginosa* lipase on its thermal stability., *Biochim Biophys Acta*, Vol. 1547, no. 2, p329-338

Zhu R, Rupprecht A, Ebner A, Haselgrübler T, Gruber HJ, Hinterdorfer P, Pohl EE., 2013, Mapping the nucleotide binding site of uncoupling protein 1 using atomic force microscopy., *J Am Chem Society*, Vol.135, no. 9, p3640-3646